ROČNÍK/*VOL.* **LXVI**
ROK/*YEAR* **2013**
7

Hutnické listy

METALLURGICAL JOURNAL

ODBORNÝ ČASOPIS PRO METALURGII A MATERIÁLOVÉ INŽENÝRSTVÍ
PROFESSIONAL PERIODICAL FOR METALLURGY AND MATERIAL ENGINEERING

WWW.HUTNICKELISTY.CZ
ISSN 0018-8069

mimořádné vydání
special edition

Trenčianska univerzita Alexandra Dubčeka v Trenčíne
Fakulta priemyselných technológií v Púchove

Vydavatel
OCELOT s.r.o.
Pohraniční 693/31
706 02 Ostrava-Vítkovice
IČO 49245848, DIČ CZ49245848
Registrace v obchodním rejstříku Krajského soudu v Ostravě, oddíl C, vložka 30879

Redakce, kontaktní adresa
OCELOT s.r.o.
Redakce časopisu Hutnické listy
areál VŠB – TU Ostrava, A 534
17. listopadu 15/2127
708 33 Ostrava-Poruba
www.hutnickelisty.cz
www.metallurgicaljournal.eu

Vedoucí redaktor
Ing. Jan Počta, CSc.
☎ 596995156
e-mail: redakce@hutnickelisty.cz
j.pocta@seznam.cz

Redaktorka
Jaroslava Pindorová
e-mail: jaroslava.pindorova@seznam.cz

Redakční rada
Předseda:
Prof.Ing. Ľudovít Dobrovský, CSc., Dr.h.c., VŠB-TU Ostrava
Členové:
Ing. Michal Baštinský, EVRAZ VÍTKOVICE STEEL, a.s.
Ing. Karol Hala, U.S. Steel Košice, s.r.o.
Prof. dr. hab. inž. Leszek Blacha, Politechnika Šląska
Prof. dr. hab. inž. Henryk Dyja, Politechnika Częstochowska
Prof. Ing. Vojtěch Hrubý, CSc. Univerzita obrany
Ing. Henryk Huczala, TŘINECKÉ ŽELEZÁRNY, a.s.
Prof. Ing. František Kavička, CSc., VUT v Brně
Ing. Ludvík Martínek, Ph.D., ŽĎAS, a.s.
Prof. Ing. Karel Matocha, CSc., MATERIÁLOVÝ A METALURGICKÝ VÝZKUM s.r.o.
Ing. Radim Pachlopník, ArcelorMittal Ostrava, a.s.
Prof. Ing. Ľudovít Pariľák, CSc., ŽP VVC s.r.o.
Ing. Jiří Petržela, Ph.D., VÍTKOVICE HEAVY MACHINERY, a.s.
Ing. Jaroslav Pindor, Ph.D., MATERIÁLOVÝ A METALURGICKÝ VÝZKUM s.r.o.
Ing. Vladimír Toman, Hutnictví železa, a.s.
Prof. Ing. Karel Tomášek, CSc., TU v Košiciach

Grafika záhlaví a podkladu na titulní straně
Miroslav Juřica,
e-mail: grafik@konstrukce.cz
a red.

Tisk
T-print s.r.o., Průmyslová 1003, 739 65 Třinec

Registrační číslo
MK ČR E 18087

Mezinárodní standardní číslo
ISSN 0018-8069

O b s a h

prof. Ing. Ján Vavro, PhD. **5**
úvodní slovo

neželezné kovy a slitiny

Ing. Dana Bakošová, PhD. **6**
Štúdium zliatin hliníka použitím elektronickej speckle interferometrie ESPI
Ing. Natália Luptáková, PhD., prof. Ing. Františka Pešlová, PhD., Mgr. Evgenyi Anisimov, PhD. **10**
Analýza trosky pri výrobe oxidu zinočnatého

materiálové inženýrství

14
doc. RNDr. Ján Bezecný, CSc., Ing. Andrej Dubec, Ing. Róbert Vavrík
Vodíkové skrehnutie vysokopevných ocelí
Ing. Adriána Pavúčková, Ing. Michaela Fedorová, prof. Ing. Františka Pešlová, PhD. **17**
Degradačné procesy materiálov zaťažených teplotnými šokmi
Ing. Petra Kováčiková, prof. Ing. Ján Vavro, PhD., Ing. Rudolf Valášek, Ing. Ján Vavro jn., PhD. **22**
Únava konštrukčnej ocele pri cyklickom zaťažení
Ing. Lenka Hazuchová, doc. Ing. Jan Krmela, PhD. **25**
Použitie lamelových bŕzd z hľadiska materiálov
Ing. Zuzana Harmatová, prof. Ing. Eugen Jóna, DrSc., Ing. Jana Medvecká, PhD. **28**
Biologicky významné materiály s Cu^{2+} iónmi a heterocyklickými zlúčeninami a ich termické vlastnosti
doc. Mgr. Ivan Kopal, Ph.D. **31**
Výpočet aktivačnej energie relaxačných prechodov polymérnych materiálov
Ing. Karol Kováč, doc. Mgr. Ivan Kopal, PhD. **35**
Zisťovanie primárnych a sekundárnych relaxačných prechodov tvrdeného polyuretánu pomocou dvoch rôznych metód
doc. Ing. Petra Skalková, PhD., Ing. Róbert Janík, PhD., Ing. Monika Štrbáková **38**
Dynamicko mechanické vlastnosti zmesí NR/polysacharid
Ing. Lenka Špániková, prof. Ing. Darina Ondrušová, PhD., Ing. Slavomíra Domčeková, Ing. Katarína Holcová, Ing. Michaela Ďurčeková **41**
Štúdium vulkanizačných charakteristík kaučukových zmesí s obsahom plnív na báze prírodného a syntetického zeolitu
Ing. Monika Struharňanská, doc. Ing. Jan Krmela, PhD., Ing. Peter Vido **44**
Vyhodnocovanie experimentálnych výsledkov vybraných materiálových charakteristík gumárenských zmesí pred a po zostarnutiu
Ing. Vladimíra Krmelová, PhD., Ing. Ladislav Janek, PhD., doc. Ing. Iva Sroková, PhD., RNDr. Vlasta Sasinková, Mgr. Agáta Laurenčíková, PhD. **48**
Nové plnivá gumárenských zmesí: organicky modifikovaný montmorilonit a škrob
prof. RNDr. Mariana Pajtášová, PhD., Ing. Andrea Feriancová, PhD., Ing. Zuzana Jankurová, PhD., Ing. Katarína Holcová, Ing. Janka Paliesková **51**
Vplyv plniva Cu^{2+} kaolínu na termické a štruktúrne charakteristiky gumárenských zložiek
Ing. Michal Dubovský, doc. Ing. Milan Olšovský, PhD., doc. Ing. Pavel Švanda, PhD. **55**
Degradácia vlastností gumárenských zmesí v biopalivách
doc. Ing. Pavol Lizák, PhD. **59**
Vplyv štruktúry pletenín na priepustnosť vzduchu
Ing. Vladimíra Krmelová, PhD., doc. Ing. Iva Sroková, PhD., Dr inž. Iwona Stachurek, RNDr. Vlasta Sasinková **63**
Cinamáty karboxymetylcelulózy – príprava a charakterizácia
Ing. Vladimíra Krmelová, PhD., Ing. Alena Bielaková **67**
Modifikovaný 4-O-glukuronoxylán: príprava a povrchovo-aktívne vlastnosti

koroze, povrchová úprava

Ing. Marián Božek, doc. Ing. Milan Olšovský, PhD. **71**
Nové potenciálne adhézne činidlá gumárenských nánosových zmesí
prof. RNDr. Mariana Pajtášová, PhD., Ing. Zuzana Jankurová, PhD., Ing. Andrea Feriancová, PhD., Ing. Janka Palieskova, Ing. Katarína Holcová **75**
Modifikované ílové materiály a ich vplyv na vlastnosti polymérnych materiálov
doc. Ing. Marta Kianicová, PhD., Ing. Jaroslav Trník, Ing. Ján Kafrík, Ing. Ondřej Dvořáček **78**
Odolnosť difúznych ochranných SiAl povlakov deponovaných CVD procesom na Ni-superzliatinách
doc. Ing. Marta Kianicová, PhD., Ing. Ján Kafrík, Ing. Jaroslav Trník, Ing. Ondřej Dvořáček **82**
Štúdium koróznej odolnosti Ni-superzliatin s difúznymi povlakmi za vysokých teplôt
doc. Mgr. Ivan Kopal, PhD., Ing. Leoš Polka, prof. Ing. Lubomír Lapčík, PhD. **86**
Vplyv teploty žíhania/dĺženia na štruktúru polypropylenového filmu

strojírenské dohotovení hutních výrobků

Ing. Lenka Hazuchová, doc. Ing. Jan Krmela, PhD. **89**
Grafický návrh podvozkovej lamelovej brzdy pre bezpilotné vzdušné prostriedky
Ing. Jozefína Panáčková, Ing. Peter Vido, doc. Ing. Jan Krmela, Ph.D. **92**
Mikrolokalita kritických častí plášťa pneumatík

Hlavní články v časopisu jsou uváděny v českém, slovenském nebo anglickém jazyce.

Časopis vychází 6x ročně. Cena jednotlivého čísla 200,-- Kč. K ceně se připočítává DPH. Roční předplatné základní 1190,- Kč, studentské 20 % sleva proti potvrzení o studiu. Předplatné se zvyšuje o poštovné vycházející z dodávek každému odběrateli. Předplatné se automaticky prodlužuje na další období, pokud je odběratel jeden měsíc před uplynutím abonentního období písemně nezruší. Objednávky na předplatné přijímá redakce. Informace o podmínkách publikace, inzerce a reklamy podává redakce.

Za původnost příspěvků, jejich věcnou a jazykovou správnost odpovídají autoři. Podklady k tisku redakce přijímá v elektronické podobě. Recenzní posudky jsou uloženy v redakci. Žádná část publikovaného čísla nesmí být reprodukována, kopírována nebo elektronicky šířena bez písemného souhlasu vydavatele.

© OCELOT s.r.o., 2013
ISSN 0018-8069

Časopis byl v r. 2008 zařazen Radou vlády ČR pro výzkum a vývoj do seznamu recenzovaných neimpaktovaných periodik vydávaných v ČR.

Hlavní články jsou evidovány v mezinárodní databázi METADEX a ILLUSTRATA TECHNOLOGY, obě spravované firmou ProQuest, USA.

Abstrakty hlavních článků jsou evidovány v české, slovenské a anglické verzi na webových stránkách Hutnických listů.

ekologie, recyklace, druhotné zpracování materiálu

Ing. Slavomíra Domčeková, prof. Ing. Darina Ondrušová, PhD., Ing. Lenka Špániková, Ing. Zuzana Jankurová, PhD. **95**
Stužujúci účinok prachu zo sklárskej výroby v kaučukových zmesiach
Ing. Veronika Janíková, Ing. Róbert Janík, PhD., prof. Ing. Eugen Jóna, DrSc. **99**
Použitie monoiónovej formy montmorillonitu na odstránenie toxických organických zlúčenín

zkušebnictví, měřictví, laboratorní metody

Ing. Jela Legerská, PhD. **102**
Hodnotenie prestupu tepla a vlhkosti u vybraného sortimentu bielizňových textílií
Ing. Jela Legerská, PhD., Ing. Matej Drobný **106**
Hodnotenie úplného ohmatu textílií
Ing. Jela Legerská, PhD., doc. Mgr. Ivan Kopal, PhD. **110**
Meranie tepelných vlastností autopoťahov pulznou prechodovou metódou
Ing. Michal Pastorek, doc. Ing. Jan Krmela, Ph.D. **114**
Stanovenie dynamických a statických materiálových parametrov rôzne starých behúňov plášťov pneumatík
Ing. Ján Vavro, jr., PhD., prof. Ing. Ján Vavro, PhD., Ing. Alena Vavrová, Ing. Petra Kováčiková, Ing. Radka Bezdedová **118**
Experimentálna a numerická modálna analýza dosky uhlíkového kompozitu
Ing. Ján Vavro, jr., PhD., prof. Ing. Ján Vavro, PhD., Ing. Alena Vavrová, Ing. Petra Kováčiková, Ing. Radka Bezdedová **122**
Experimentálna a numerická modálna analýza dosky skleneného kompozitu
Ing. Ján Vavro, jr., PhD., prof. Ing. Ján Vavro, PhD., Ing. Alena Vavrová, Ing. Petra Kováčiková, Ing. Radka Bezdedová **126**
Experimentálna a numerická modálna analýza dosky skleneného kompozitu poškodeného delamináciou
Ing. Peter Vido, Ing. Jozefína Panáčková, doc. Ing. Jan Krmela, PhD., Ing. Rudolf Valášek **130**
Vyšetrovanie mechanických vlastností kompozitného systému kord–elastomér pre potreby výpočtového modelovania plášťov pneumatík

výpočetní metody

doc. Mgr. Ivan Kopal, Ph.D., doc. RNDr. Ladislav Matejíčka, CSc. **134**
Hľadanie inflexných bodov funkcie zadanej prostredníctvom experimentálnych dát

hutnictví ve světě **138**

„Články v tomto vydání jsou vytištěny ve stavu dodání od autorů a redakce neprováděla jazykovou úpravu.“

Inzerenti a objednatelé reklamy:

● Fakulta priemyselných technológií v Púchove, TUAD v Trenčíne

Foreword to the special edition of „Metallurgical Journal“

Dear colleagues and members of academic and scientific community,

It is my pleasure to introduce a new special edition of “Metallurgical Journal” (2013, Vol. LXVI, No. 7) to the interested professional audience. All the papers introduced in this journal give evidence about current outcomes of scientific research and development based on hard work and new investigation approaches of the scientific staff as well as doctoral undergraduates at Faculty of Industrial Technologies in Púchov, TnUAD.

The given presented papers can become the contribution material for the wide range of contemporary intensively discussed research and scientific topics relating to materials engineering and materials science including specific experimental approaches of materials research, chemistry, computational modelling and design with the reference to the various types of metallic as well as non-metallic materials which have been the subject of continual investigations in the sphere of materials engineering.

Presenting their results, all the authors believe that the introduced papers will be the contribution for the enhancement of the mutual cooperation between the scientist and researchers in order to implement the new obtained results into the industrial practice. Furthermore, this special edition with all the investigations can also be the inspiration and stimulus for the readers to cooperate and participate in research with our faculty.

Best regards,

prof. Ing. Ján Vavro, PhD.
Dean of Faculty of Industrial Technologies in Púchov, TnUAD

Hutnické listy č.7/2013, roč. LXVI
ISSN 0018-8069

neželezné kovy a slitiny

Study of Aluminium Alloys by Electronic Speckle Pattern Interferometry ESPI

Štúdium zliatin hliníka použitím elektronickej speckle interferometrie ESPI

Ing. Dana Bakošová, PhD.[1]

[1] University of Alexander Dubček in Trenčín, Faculty of Industrial Technologies, I. Krasku 491/30, 020 01 Púchov, Slovak Republic

In solving problems of elasticity and strength, current optical methods for deformation measurement are gaining more and more applications. The advantage of such methods is the measurement in a non-destructive way without assembly of measuring elements onto the critical areas of structures. One of these contactless measuring methods is electro-optical method ESPI that is based on the discovery of so-called speckle patterns. In this study, experimental investigation of vibration behaviour of square aluminium alloys plates by electronic speckle pattern interferometry (ESPI) is employed. Resonant frequencies and corresponding mode shape are obtained experimentally using the introduced method. The numerical calculations by the finite element method (Cosmos) are performed and the results are compared to the experimental measurements.

Keywords: *ESPI, aluminium alloy, FEM, resonant frequency, time coherency*

Pri riešení úloh výskumu mechanických deformácii povrchov, tepelných deformácii povrchov, vibrácií, malých posuvov objektov a to s presnosťou až na zlomok vlnovej dĺžky použitého laserového žiarenia, získavajú v súčasnosti čoraz väčšie uplatnenie optické metódy. Výhodou takýchto metód je meranie nedeštruktívnym spôsobom bez nutnosti aplikácie meracích prvkov na kritické miesta konštrukcií. Jednou z bezkontaktných metód merania je elektronická speckle-interferometria (ESPI). Elektrónová speckle pattern interferometria (ESPI) využíva vlastnosti laserových škvŕn (specklov) a digitálne spracovanie obrazu. Speckle štruktúra je obraz s nepravidelným rozložením intenzity, ktorý vzniká pri odraze koherentného svetla od opticky drsných povrchov alebo pri prechode cez prostredie s nepravidelnými zmenami indexu lomu. Pomocou ESPI so softvérovým vybavením aparatúry sa získajú obrazy deformácie meraného telesa v reálnom čase. Touto metódou sa môže merať ako statické zaťaženie, tak aj dynamické zaťaženie, ktorým je napríklad meranie vibrácií telesa - opäť v reálnom čase. Interferogram nám môže teda poskytovať dôležité informácie o vibračných módoch (vidoch), ale i o štruktúrnych defektoch v materiáli alebo o rezonančných frekvenciách. Základ metódy ESPI súvisí s vzájomnou interferenciou dvoch svetelných polí (lúčov). Jedno vlnové pole pochádza od odrazeného objektu (objektová vlna), druhé vlnové pole, ktoré je potrebné na vytvorenie interferencie sa nazýva referenčné pole alebo referenčná vlna. Obidve polia musia byť časovo koherentné, preto pochádzajú z toho istého zdroja koherentného svetla - z laseru. Práca sa zaoberá vyšetrovaním správania štvorcových dosiek vyrobených z vybraných hliníkových zliatin použitím ESPI. V experimentálnej časti sú stanovené rezonančné frekvencie spolu s príslušným vlastným tvarom kmitania dosky. Nameraná výsledky sú porovnané s hodnotami MKP pomocou programu Cosmos.

Kľúčové slová: *ESPI, hliníková zliatina, FEM, rezonančná frekvencia, časová koherencia*

Electronic Speckle Pattern Interferometry (ESPI) is an optical technique which enables interferometric measurements of surface displacements on almost any surface and material.

The non-contact and full-field measurement allows the calculation of the three dimensional distribution of the displacement and strain/stress of the object under test as a response to a mechanical or thermal loading. ESPI has been applied successfully in many fields including

automotive, aerospace, electronics and materials research and moreover, it can be also used for the study of material properties, fracture mechanics, fatigue testing, NDT and dynamic behaviour of a variety of components.

The Properties of Aluminum

Lightness: On a volume basis, aluminum is only about one-third the weight of steel. Significant weight savings can be gained in almost every type of mechanical application.

Durability: Aluminum has high resistance to atmospheric corrosion because it is able to form an impervious oxide skin on exposed surfaces immediately after exposure and therefore it can be used even in marine environment. According to the mentioned fact hereinbefore, it does not require the painting for protection.

Conductivity: The specific electrical conductivity of aluminum makes it indispensable for electronics and electrics. Aluminum cables carry twice as much current as copper of the same weight. High thermal conductivity makes it very suitable for heating and cooling applications.

Workability: Aluminum can be formed by all of the common metal-working techniques – it is workable more easily than most of any other metals with comparable properties. In the case of this metal, it is quite easy to use casting or die-casting methods to change it into precise and complex shapes. It can be forged, rolled to a superfine foil, and extruded into intricate sections as well as pressed into the required shapes. Its Superplastic alloys can be worked almost like vacuum-formed plastics. Aluminum is also one of the easiest and fastest materials to be machined.

Versatility: Aluminum alloys can be stiff or supple and it has to be pointed out that it is very strong and it has high corrosion-resistance. By alloying and heat treatment, it is easy to process this metal to meet a wide range of needs.

Attractiveness: Aluminium is a "clean" material. It looks good without further finishing and on the other side, it belongs to metals which are integral part of a wide range of applied coatings, from paints to coloured anodising.

Recyclability: Aluminum is reprocessed easily using 5 % of the energy needed for primary smelting: almost one third of all the aluminum used today is produced from scraps occurring either from production processes or from recycled products.

Method

The most widely used experimental setup to study vibration by ESPI is the time-averaged method. The schematic setup of ESPI optical system, as shown in figure 1, is employed to perform the out-of-plane vibration measurement of the resonant frequencies and mode shapes for composites plates. The He-Ne laser with wavelength λ = 632.8 nm is divided into two parts, the reference and object beams.

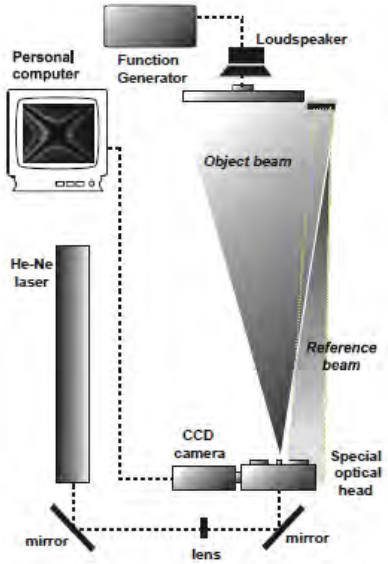

Fig. 1 Schematic diagram of ESPI setup for out-of-plane measurements
Obr. 1 Schematický nákres ESPI metódy

The object beam passes into the specimen and then reflects to the CCD camera. The reference beam is directed to the CCD camera via the mirror and reference plate. The CCD camera converts the intensity distribution of the interference pattern of the object into a corresponding video signal. The signal is electronically processed and finally converted into an image in the video monitor. The experimental procedure of the ESPI technique is performed in the following steps mentioned hereinafter. First, a reference image is taken after the specimen vibrates, then the second image is taken, and the reference image is subtracted by the image processing system. If the vibrating frequency is not the resonant frequency, only randomly distributed speckles will be displayed and fringe patterns will not be shown. However, if the vibrating frequency is in the neighborhood of the resonant frequency, stationary distinct fringe patterns will be observed. Then, the function generator will be turned carefully and slowly and subsequently, the number of fringes will be increased and the fringe pattern will become clearer as the resonant frequency is approached. The resonant frequencies and corresponding mode shapes can be determined at the same time using the ESPI optical system [1,2].

The Electronic Speckle Pattern Interferometry is used in various areas or applications. The following list shows a few examples:

- material testing – mechanical and thermo-mechanical behaviour (metal, ceramic, plastic, reinforced material, composite material),
- component testing (automotive, aerospace, medical, electronical…),
- defect recognition,
- failure analysis.

Hutnické listy č.7/2013, roč. LXVI
ISSN 0018-8069

Experimental part

The aluminum alloys Al99 and AlMg3 are the object of observation. It is connected with investigation of the resonant frequencies obtained in an experimental way by ESPI and their comparison to the numerical frequencies - Cosmos (fig. 2-11).

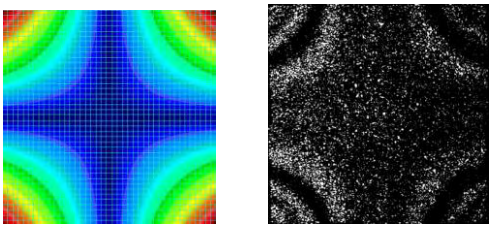

Fig. 2 Comparison of natural shapes of eigenfrequencies obtained by (mode shape 1,1) numerical calculation FEM (Cosmos) and ESPI - alloy Al99

Obr. 2 Porovnanie vlastných tvarov kmitania dosky (mód 1,1) MKP (Cosmos) a ESPI - zliatina Al99

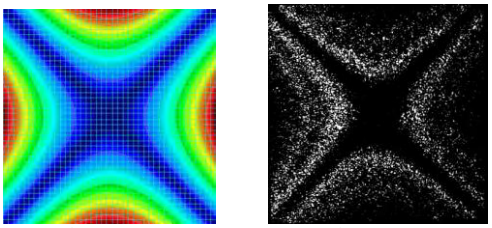

Fig. 3 Comparison of natural shapes of eigenfrequencies obtained by (mode shape X) numerical calculation FEM (Cosmos) and ESPI - alloy Al99

Obr. 3 Porovnanie vlastných tvarov kmitania dosky (mód X) MKP (Cosmos) a ESPI - zliatina Al99

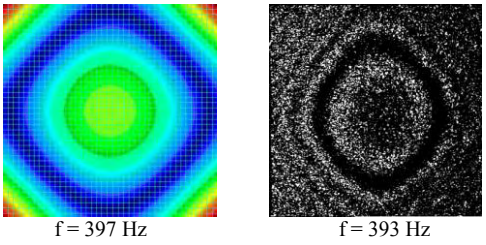

Fig. 4 Comparison of natural shapes of eigenfrequencies obtained by (mode shape O) numerical calculation FEM (Cosmos) and ESPI - alloy Al99

Obr. 4 Porovnanie vlastných tvarov kmitania dosky (mód O) MKP (Cosmos) a ESPI - zliatina Al99

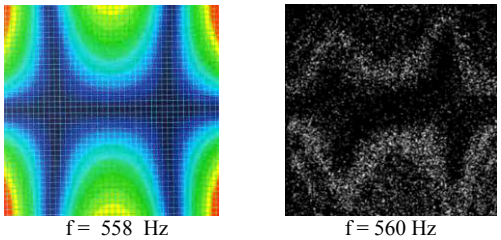

Fig. 5 Comparison of natural shapes of eigenfrequencies obtained by (mode shape 2,1) numerical calculation FEM (Cosmos) and ESPI - alloy Al99

Obr. 5 Porovnanie vlastných tvarov kmitania dosky (mód 2,1) MKP (Cosmos) a ESPI - zliatina Al99

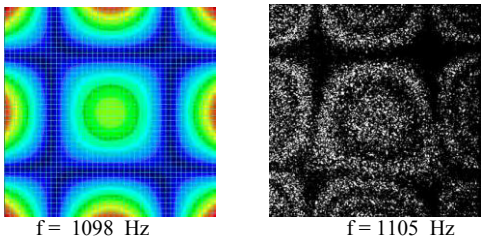

Fig. 6 Comparison of natural shapes of eigenfrequencies obtained by (mode shape 2,2) numerical calculation FEM (Cosmos) and ESPI - alloy Al99

Obr. 6 Porovnanie vlastných tvarov kmitania dosky (mód 2,2) MKP (Cosmos) a ESPI - zliatina Al99

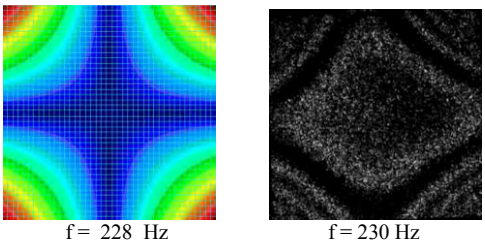

Fig. 7 Comparison of natural shapes of eigenfrequencies obtained by (mode shape 1,1) numerical calculation FEM (Cosmos) and ESPI - alloy AlMg3

Obr. 7 Porovnanie vlastných tvarov kmitania dosky (mód 1,1) MKP (Cosmos) a ESPI - zliatina AlMg3

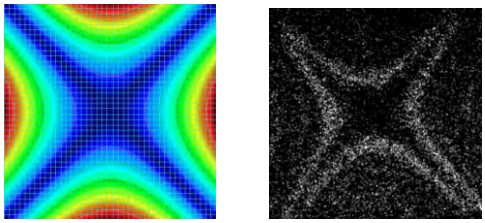

Fig. 8 Comparison of natural shapes of eigenfrequencies obtained by (mode shape X) numerical calculation FEM (Cosmos) and ESPI - alloy AlMg3

Obr. 8 Porovnanie vlastných tvarov kmitania dosky (mód X) MKP (Cosmos) a ESPI - zliatina AlMg3

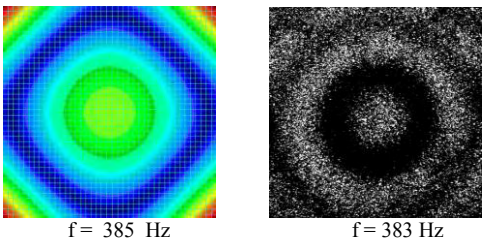

Fig. 9 Comparison of natural shapes of eigenfrequencies obtained by (mode shape O) numerical calculation FEM (Cosmos) and ESPI - alloy AlMg3

Obr. 9 Porovnanie vlastných tvarov kmitania dosky (mód O) MKP (Cosmos) a ESPI - zliatina AlMg3

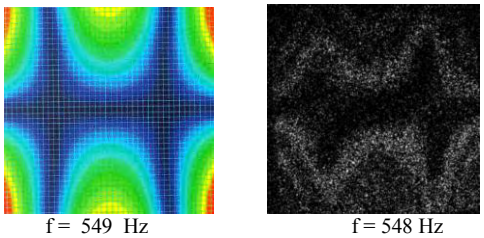

f = 549 Hz f = 548 Hz

Fig. 10 Comparison of natural shapes of eigenfrequencies obtained by (mode shape 2,1) numerical calculation FEM (Cosmos) and ESPI - alloy AlMg3

Obr. 10 Porovnanie vlastných tvarov kmitania dosky (mód 2,1) MKP (Cosmos) a ESPI - zliatina AlMg3

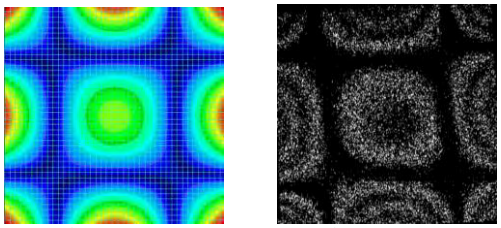

f = 1090 Hz f = 1085 Hz

Fig. 11 Comparison of natural shapes of eigenfrequencies obtained by (mode shape 2,2) numerical calculation FEM (Cosmos) and ESPI - alloy AlMg3

Obr. 11 Porovnanie vlastných tvarov kmitania dosky (mód 2,2) MKP (Cosmos) a ESPI - zliatina AlMg3

Conclusions

In relation to modes, the natural or own shapes of eigenfrequencies for selected modes obtained from ESPI measurements are identical with the own or natural shapes which were obtained on the basis of finite element method (FEM) by help of program system Cosmos. In both cases of investigation, almost all of measured modes were identified successfully and they were easily assigned to those which were obtained and displayed in a computational way. Obtained values of natural frequencies or eigenfrequencies and their own shapes can be utilized as the input data for optimizing procedure which will be useful and good choice for seeking material parameters, such as Young modulus E and Poisson ratio μ.

Literature

[1] RUSNÁKOVÁ, S., SLABEYCIUS, J., KOŠTIAL P., KOPAL, I., MOKRYŠOVÁ, M. Contact less measurement of material parameters by ESPI. In: Third youth Symposium on Experimental Solid Mechanics : Extended summaries. Bologna : University of Bologna, 2004, p. 31-32. ISBN 80-901080-8-8-44406

[2] RUSNÁKOVÁ, S., KOŠTIAL, P., KOPAL, I., MOKRYŠOVÁ, M., SLABEYCIUS, J., RUSNÁK, V. ESPI - the tool for identity dynamic stiffness parameters of various composite materials, In: 4th Youth symposium on Experimental solid mechanics : Danubia Adria symposium. Bologna : University of Bologna, 2005. p. 115-116.ISBN 88-901080-2-9-44406

Hutnické listy č.7/2013, roč. LXVI
ISSN 0018-8069

Analysis of Slag in the Production of Zinc Oxide

Analýza trosky pri výrobe oxidu zinočnatého

Ing. Natália Luptáková, PhD.[1], prof. Ing. Františka Pešlová, PhD.[1], Mgr. Evgenyi Anisimov, PhD.[2]

[1]University of Alexander Dubček in Trenčín, Faculty of Industrial Technologies, I. Krasku 1809/34, 020 01 Púchov, Slovak Republic
[2]Czech Technical University in Prague, Department of Materials Engineering, Karlovo nam. 13, 121 32 Prague 2, Czech Republic

The given paper is closely connected with determination of character and morphology of the waste material generated in the production of zinc oxide. Zinc oxide can be produced by variety of ways, but the most common method of production which is used in Slovakia is indirect, i.e. pyrolytic combustion of zinc and zinc alloys. This method is also called "French method" of manufacturing ZnO. But this mentioned method of preparation leads to the creation of the enormous amount of waste including chemical complexes of elements Fe, Zn and Al. Hazardous situations relating to occurrence of these elements are hidden in their ability to create ternary eutectic formations and in terms of mechanical properties, they have ability to create quite fragile structure which is unsuitable in the French process. The presence of the atmospheric oxygen as well as high temperature and pressure cause adhesion of these ternary eutectic formations to furnace. Stuck slag has the influence on rapid degradation of the linings and moreover it also decreases the production quality of ZnO. Analysis results introduced in this paper are significant information for minimizing of waste material as well as easier removing of stuck slag.

Keywords: *zinc, zinc oxide, slag, analysis of zinc slag*

Práca sa zaoberá charakterom a morfológiou odpadového materiálu, ktorý vzniká pri výrobe oxidu zinočnatého. Oxid zinočnatý sa môže vyrábať rôznymi spôsobmi, ale najčastejší spôsob výroby používaný na Slovensku je priamy, t.j. pyrolitické spaľovanie zinku a zliatin zinku. Táto metóda sa tiež nazýva „Francúzsky spôsob“ výroby ZnO. Oxid zinočnatý sa vyrába v taviacich peciach, ktorých súčasťou je aj výmurovka vytvorená zo žiaruvzdorných keramických materiálov. Pary zinku pri teplote vyššej ako 906 °C reagujú so vzdušným kyslíkom, vzniká oxid zinočnatý sprevádzaný luminiscenciou. Povrch steny výmurovky je porézny a zinkové pary sa snažia preniknúť cez tento materiál. Rýchlosť difúzie rôznych prvkov značne ovplyvňuje vysoká teplota v peci, ktorej výsledkom je vznik trosky na stenách výmuroviek. Vysoká teplota povrchu žiaruvzdorných materiálov a jej dobrá zmáčavosť zvyšuje množstvo tvorby nanášanej trosky. V tomto prípade vznikajú odpady, ktoré predstavujú značne množstvo prvotného materiálu. Jedná sa najmä o chemické komplexy prvkov železa, zinku a hliníka. Nebezpečenstvom výskytu týchto prvkov je ich schopnosť vytvárať potrojné eutektika, ktoré z hľadiska mechanických vlastností sú nevyhovujúce, lebo majú veľmi krehkú štruktúru a ovplyvňujú ďalší metalurgický proces v peci. Pokiaľ sa bude v danom priestore vyskytovať vzdušný kyslík, dochádza pri vysokých teplotách a podtlaku k adhéznemu priľnutiu týchto zlúčenín na výmurovky pecných agregátov. Vzhľadom k tomu, že vymurovky sú zvyčajne tvorené z keramických materiálov, dochádza k ich interakcii a vzniku následných nežiadúcich fáz. Takéto chemické reakcie sú príčinou znehodnotenia nie len vymurovky, ale aj samotnej vsádzky. Troska zvyčajne superponuje degradáciu vymuroviek, čím zhoršuje kvalitu a výťažnosť oxidu zinočnatého. Výskyt enormného množstva zinkovej trosky a jej penetrácia do stien žiaruvzdorných keramických materiálov predstavuje závažný problém pre popredných výrobcov ZnO na celom svete. Výsledky získaných analýz, budú slúžiť k návrhu minimalizácie nežiaduceho odpadu a eliminácii podmienok, ktoré umožňujú vznik takého produktu.

Kľúčové slová: *zinok, oxid zinočnatý, troska, analýzy zinkovej trosky*

Zinc oxide is used as a semi-product for production in many fields of production. The most important industries are the rubber, pharmaceutical and glass industries, manufacture of paints etc. Nowadays, production of ZnO by French process includes the biggest share of production in industrial society. Indirect production of ZnO starts by melting of zinc and following oxidation with oxygen from the air and it was developed by Le Clair in France in the years from 1840 to 1850 [1]. The raw material of this production method is the production of metallic zinc and its alloys. Zinc and its alloys are combusted in the muffle or rotary furnaces.

French process is considered to be the fastest and most productive method for industrial production of ZnO [2], but according to the practical experience, this type of production ZnO is not optimum for utilization of the product in all technological applications. The quality of ZnO depends on the starting (raw) materials. During processing of the waste zinc (approx. purity of Zn is

90 wt. %) from galvanic process containing other elements, such as Pb, Fe and Al, there is the occurrence of slag (waste material) which negatively affects the total production process of ZnO and final product.

The work is focused on the enormous amount of slag material. It is closely connected with the previous work [3, 4] in which the primary material has been studied. Detailed investigation of waste material will help in predicting the behaviour of the material in the metallurgical process. This knowledge can be used as prevention of slag occurrence or it can even help us to find a way for easier removal from the furnace aggregates.

Zinc oxide

From the chemical point of view, zinc oxide is white inorganic compound (fig. 1) and consists of Zn^{2+} cation and O^{-2} anion [5]. Layers occupied by zinc atoms alternate with layers occupied by the oxygen atoms. Compound ZnO has anisotropic character [6].

Pure ZnO crystallizes in the hexagonal (wurzite) crystal structure [5] with a lattice parameters a = 3.25 Ĺ and c = 5.12 Ĺ [6]. Character of crystal shape is dependent not only on the crystal lattice, but it also depends on the method of production ZnO associating with the primary crystallization. High attention is paid to research in the modern development of ZnO.

The production of ZnO is based on high speed of zinc vapour at speeds 0.1 Mach (30 $m.s^{-1}$) or higher [7] and temperature is in the range from 1,300 °C to 1,400 °C. Sublimation temperature of ZnO is 1,725 °C [6].
The production process is performed according to chemical reactions [7]:

$$Zn_{(l)} \rightarrow Zn_{(g)} \quad (1)$$

$$Zn_{(g)} + ″ O_{2\,(g)} \rightarrow ZnO_{(s)} \quad (2)$$

Fig. 1 Zinc Oxide powder
Obr. 1 Práškový oxid zinočnatý

Zinc slags

Slag is a secondary product of thermic combustion processes. The metallurgical slag is generated in the processing of molten metals in the liquid state. Components of raw material (especially compounds based on iron and aluminum), products generated at metallurgical reactions in the melt, removed particles of ceramic linings etc. float to the surface of the metal bath to form more or less continuous layer on the surface of the melt with furnace linings.

However, in metallurgy, slag has also many other important functions. The processing of liquid metals is complex thermodynamic process that occurs in the system the melt – the slag – the atmosphere. The key of usage is hidden in an appropriate melting temperature, chemical activity, the ability to absorb negative substances from the melt and slag fluidity as well as density must be in line with given conditions etc. The general production costs depend on the optimum selection of the slagging process.

Therefore, parameters of slag are monitored and controlled carefully. The most observed (studied) variables, parameters are e.g. chemical composition of individual elements, and the character of the raw material used, the primary composition of the resulting slag, the ability to create chemical compounds. These results can be obtained from the analysis of crystal system and they must be taken in account.

Analysis of zinc slags

Samples of the waste material (slag) which were prepared by French process have been chosen in the order to investigate and study the morphology of slag. The primary materials were zinc alloy (approx. 90 wt. % Zn). Selection of slag samples represents the given process of production and primary material. The chosen samples were from sediment samples and crystallized minerals and their composition stood for the primary element of the production process.

The first taken sample was from the places where three contiguous layers marked 1_A, 1_B and 1_C were accumulated in solidification. Each one layer has its specific chemical composition. The atomic absorption spectroscopy (Varian AA 240, SlovZink, a.s. Koseca) for selected substances shows that the highest share is created by matrix on the basis of the zinc (tab. 1) where the occurrence of Zn amount is over of 90 wt. %, except of samples No. 1_C, which contains 30.44 wt. % of accumulated lead at the expense of zinc.

Tab. 1 Results of chemical analyzes of samples No.1_A, 1_B, 1_C and sample No. 2
Tab. 1 Výsledky chemickej analýzy vzoriek č. 1_A, 1_B, 1_C a vzorky č. 2

Elements	1_A (wt.%)	1_B (wt.%)	1_C (wt.%)	2 (wt.%)
Zn	96.39	93.11	65.90	94.75
Pb	1.40	2.2	30.44	1.4
Cu	1.80	0.00082	2.1	0.014
Cd	0.00003	2.1	0.0001	0.00086
Fe	0.04	0.0043	0.52	0.055
Al	0.26	0.6	0.65	0.38

Sample No. 2 was taken from the top dross and it contained only minor amounts of Pb and other elements,

Hutnické listy č.7/2013, roč. LXVI
ISSN 0018-8069

while the largest proportion is formed by elementary of zinc.

From the chemical analyzes, it is clear that high weight percentage of Zn content remains in the waste materials and it does not pass into the final product – ZnO and it is connected with the enormous losses of pure zinc.

Investigation of the phases (JOEL SEM, JSM 7600F, CVUT in Prague) in the slag samples revealed that resulting mosaic phase (see the site bordered by red color - fig. 2) do not differ from the chemical composition of phases which are in the primary (raw) materials i.e. metal zinc. (These structures are published in [3]). Then, it follows that even at high temperature (about 1,400 °C), there is not change of the structure of the base material, which is preserved in slag during the metallurgical process.

High content of zinc as well as other elements, such as Fe and Cr was found out by the EDS analysis (JOEL SEM, JSM 7600F, CVUT in Prague). Globular phase is introduced in fig. 2 (see the site bordered by blue color) contained oxides of Al, Cr and carbides of Si but the main matrix consisted of Fe. Given results of chemical analysis (JOEL SEM, JSM 7600F, CVUT in Prague) are in accordance with AAS analysis.

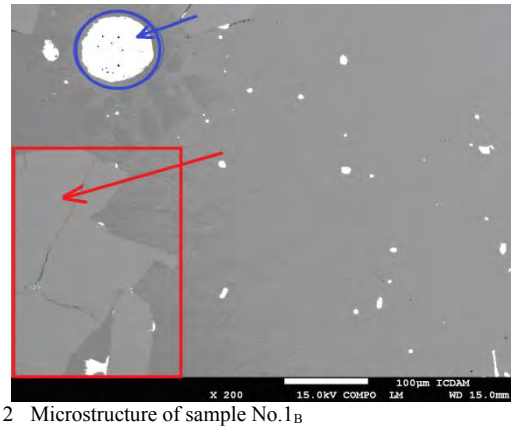

Fig. 2 Microstructure of sample No.1_B
Obr. 2 Mikroštruktúra vzorky č. 1_B

The analyzed sample (sample No. 3) was removed as a re-combused material. That sample could not be prepared by conventional methods of chemical analysis of slag - the evaporation of H_2SO_4 (1:3) but it was only dissolved in HCl (1:1) and heated to the boiling point of solution. After dissolution and following chemical analysis (Varian AA 240, SlovZink, Koseca), differences were found in the results of the analysis (Pb = 10.49 wt. %, Cu = 6.43 wt. %, Fe = 5.6 wt. %, Ni = 11.0 wt. % and Zn was undetectable). These differences could be caused by insufficient dissolving of the sample in boiling acid.

X-ray diffraction (Brűcker 8, KalfaCo, Co-lamp, SAV, Bratislava) for the samples showed that the sample contained about 50 wt. % $AlFe_3$ and other compounds (or minerals), such as Pb, ZnO (Zinc), Al_2O_3, Pb_3O_4, PbO_2 (Platnerite) and SiO_2 (Cristobalite). Analysis of results is shown in table 2. Setting the measurement - time to step determines the difference in cps (counts per second).

It is clear that some substances including Al_2O_3 (melting point 2040 °C, boiling point: 2977 °C), SiO_2 (melting point: 1,713 °C), Pb (melting point: 327.5 °C, boiling point: 1750 °C), Pb_3O_4 (melting point: 500 °C, boiling point: 800 °C), Zincite (ZnO) (melting point: 2690 °C, sublimation point: 1800 °C) and others elements or components remain in the slag because their boiling point is higher than the temperature of the production process of ZnO (about 1400 °C).

Tab. 2 X-ray diffraction results of the Sample No.3
Tab. 2 Výsledky röntgenovej difrakcie skúmanej vzorky č.3

Substances	Content of substances (wt. %)
$AlFe_3$	53.05
Pb	21.86
Pb_3O_4	8.16
ZnO	6.07
SiO_2	4.46
PbO_2	3.34
Al_2O_3	2.45

In the production of ZnO, re-crystallization of occurring elements is performed. Photo documentation of crystals (scanned on Stereomicroskop, Nikon SMZ 1500, CVUT in Prague) is shown in fig. 3.

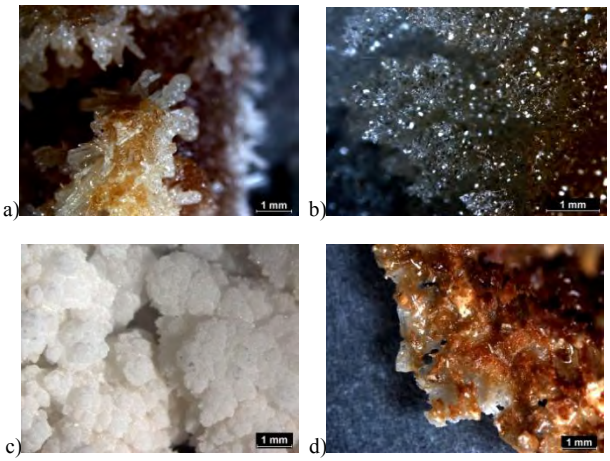

Fig. 3 Re-crystallized phases in the process of production ZnO
Obr. 3 Vykryštalizované fázy pri procese výroby ZnO

From the chemical analysis (Varian AA 240, SlovZink, Koseca), the composition of the crystal was obtained - the matrix is formed by the majority of Zn (99.88 wt. %) and other elements, such as Pb (0.0028 wt. %), Fe (0.0013 wt. %), and one thousandth of wt. % relating to Cu, Mn, Ni and Cd and it will subsequently affect their following growth.

Conclusions

The following hypothetical conclusions can be introduced on the basis of the study of samples of slag:

- Slag samples contained a enormous amount of ZnO which does not pass into the final product, but remains stuck as the slag on the lining of furnaces – more zinc, more losses in relation to final product.
- High temperature and low pressure are connected wirh the re-crystallization of some compounds, such as *Zincit* (ZnO), *Plattnerite* (PbO_2), *Cristobalite* (SiO_2), *Magnetite* (Fe_3O_4) and others compounds or minerals.
- If there is the presence of the lead and the time is long enough for its sedimentation, the higher presence of pure lead in the lower layer is much more probable.
- Slag contains the residues of iron and aluminum which have a higher melting point and boiling point. Iron and aluminum are evaporated at a temperature from 2520 °C to 2862 °C while zinc has boiling point 907 °C. It means that the resulting eutectics on the basis of Fe-Zn-Al and Zn-Al can have boiling point over 1000 °C and it is connected with increase in fuel consumption.
- The analysis of samples of slag should not be performed by method - *wet of chemical way* for AAS because of insufficient dissolution of the waste material either in HNO_3 or by evaporation of H_2SO_4. Suitable analysis is the X-ray diffraction using Co lamp. Using X-ray diffraction in crystals can be understood as the non-destructive method for determination of the internal structure of crystals and their qualitative and quantitative analyses can be done using obtained diffraction pattern.
- Investigation phases which occur in the slag sample revealed that the resulting phase is not different from the phases that are in the raw material and it means that at high temperature (about 1,400 °C), there is not any change of the structure of the raw material which remains in the process as slag.
- The resulting final product - zinc oxide in an imperfect production process of ZnO can contain Fe_2O_3 and Al_2O_3 and it causes that ZnO can be yellow-brown colour.
- In this case, the coke can be used to reduce the boiling point in the furnace and it means merging the French process with the American process.
- As a solution, it is recommended to find a suitable method of cleaning of the furnace after three days of continuous operation as well as pure zinc (marked SHG or HG) has to be used to furnace instead of hard Zn (less than 95 wt. % Zn) because this zinc contains such negative substances as iron, lead and aluminum and other elements.

Acknowledgement
This work has been supported by TAČR No. TA02011121.

Literature

[1] AUER, G., GRIEBLER, W.D., JAHN, B. *Industrial Inorganic Pigments.* 3rd ed., Wiley-VCH Verlag GmbH & Co. KGaA, Weinheim, 2005

[2] MAHMUND, S, et al. Nanostructure of ZnO fabricated via French process and its correlation to electrical properties of semiconducting varistors. *Synth. React. Inorg., Met.-Org., Nano-Met. Chem.*, 2006, 36, p. 155–159

[3] LUPTÁKOVÁ, N., BENÁK, M., HAJ-DUCHOVÁ, Ľ., PEŠLOVÁ, F. Micro-structure Analysis of Zinc and Zinc Alloys. In: Machine Modeling and Simulations. 16th International Slovak-Polish Conference – Trenčín: TnUAD. p. 373-378. ISBN 978-80-8075-494-5

[4] LUPTÁKOVÁ, N., KEBÍSKOVÁ, J., ANISIMOV, E., BENÁK, M., PEŠLOVÁ, F. Impact raw material for production zinc oxide in retort furnaces. In: METAL 2012, Conference proceedings. 21st International Conference on Metallurgy and Materials. – Ostrava: TANGER Ltd., Ostrava, 2012. p. 154. ISBN 978-80-87294-29-1

[5] ÖZGÜR, Ü., MORKOC, H. Optical Properties of ZnO and Related Alloys. Department of Electrical Engineering and Physics Department, Virginia Common-wealth University, Richmond, p. 23284-3072

[6] RIEDEL, R., CHEN, I. W. *Zinc Oxide*. Ceramics Science and Technology: Properties, Volume 2, Germany, 2010, p. 15-18. ISBN: 978-3-527-31156-9

[7] KOUDELKA L., HORÁK, J., JARIABKA, P. Morfology of polycrystalline ZnO and its physical properties. *Journal of Materials Science*, 1994, vol. 29, no. 6, p. 1497-1500.

Hutnické listy č.7/2013, roč. LXVI
ISSN 0018-8069

materiálové inženýrství

Hydrogen Embrittlement of High Strength Steels

Vodíkové skrehnutie vysokopevných ocelí

doc. RNDr. Ján Bezecný, CSc.[1], **Ing. Andrej Dubec**[1], **Ing. Róbert Vavrík**[1]

[1]University of Alexander Dubček in Trenčín, Faculty of Industrial Technologies, I. Krasku 491/30, 020 01 Púchov, Slovak Republic

The given paper is closely connected with the behaviour of the hydrogen after the diffusion process into the high strength steels. The given hydrogen can diffuse into the material in the different ways, namely it can diffuse from liquid as well as gas environment and by this way it can cause embrittlement of the steels. The combination of the several factors has the significant influence on the hydrogen embrittlement. In relation to the influencing factors, material strength, amount of diffused hydrogen and stress state represent these mentioned factors. Diffusion of the atomic hydrogen into the material can cause enormous decrease referring to the material ductility. Materials can be susceptible to cracks and formation of the brittle fractures during the loading under the yield strength – occurrence of the delayed fractures. Micro-morphology of the fracture surfaces is markedly influenced by mycrostructure and rate of deformation. The fracture surfaces contain intergranular facets with "crow legs" and microvoids representing the tunnels, the occurrence of which is connected with high pressure of the molecular hydrogen.

Keywords: *hydrogen, hydrogen embrittlement, high strength steel, delay fracture*

Vodík má vo všeobecnosti negatívny vplyv na materiálové vlastnosti a môže vyvolať aj ich značnú zmenu v podobe vodíkovej krehkosti. Významný vplyv na vodíkové skrehnutie má kombinácia faktorov ako sú pevnosť materiálu, množstvo nadifundovaného vodíka a napäťový stav, súvisiaci s mikroštruktúrou, geometriou súčiastky a pôsobiacim vonkajším napätím. Atomárny vodík má vďaka svojej malej veľkosti schopnosť rýchlo difundovať do materiálu a to už pri izbovej teplote. Vniknutie atomárneho vodíka do ocelí môže vyvolať značný pokles ťažnosti materiálu, náchylnosť k praskaniu a tvorbe krehkých lomov už pri namáhaní pod medzou sklzu. Tento jav je označovaný ako oneskorený, resp. zabrzdený lom. Vodík pri difundovaní do ocelí využíva, cesty najmenšieho odporu, ktorými sú poruchy kryštálovej mriežky a predovšetkým hranice zŕn, ktoré krehnú prednostne. Príspevok sa zaoberá vplyvom vodíka na morfológiu lomových plôch po jeho difúzii do vysokopevných ocelí. Vodík môže vnikať do materiálu z kvapalného prostredia, najčastejšie po povrchových úpravách ako sú galvanické pokovenie a morenie, alebo z plynného prostredia. Výraznú zmenu mechanických vlastností v materiáli vyvolávajú vnútorné napätia súvisiace s rekombináciou atomárneho vodíka na molekulárnu formu. So zvyšujúcou sa pevnosťou je zmena vlastností výraznejšia. Na detekciu navodíkovania ocelí sa využíva hodnotenie lomových plôch na REM a mechanické skúšky. Mikromorfológia lomových plôch je vo všeobecnosti predikovaná mikroštruktúrou a rýchlosťou deformácie. Mikromechanizmus šírenia sa trhliny je u navodíkovaných vysokopevných ocelí odlišný ako u navodíkovaných nízkopevných ocelí. U nízkopevných prevláda kvázištiepny mikromechanizmus, u vysokopevných interkryštalický mechanizmus šírenia trhliny. Z hľadiska mikromorfológie lomovej plochy môžeme na povrchu interkryštalických faziet pozorovať výskyt tzv. vlasových čiar (crow legs), a mikrodutiniek vo forme tunelov, vytvorených vysokým tlakom v oceli prítomného molekulárneho vodíka. Takýto charakter porušenia vysokopevných ocelí je podmienený dlhodobým pôsobením vonkajšieho zaťaženia.

Kľúčové slová: *vodík, vodíková krehkosť, vysokopevná oceľ, zabrzdený lom*

Diffusion of the hydrogen into the high strength steels is complicated process which depends on many specific factors and it represents the fundamental condition in relation to the hydrogen embrittlement [1]. The atomic form of hydrogen can be included into the reactive elements which makes efforts to find any reaction partner element. If the atomic form of hydrogen is connected with another atomic form of hydrogen, there is the formation of molecule H_2. Hydrogen is able to be in the weak bonds with the atoms of iron (Fe) on the surface of the component parts [2]. The occurrence of the crystalline lattice defects, i.e. traps, leads to

enormous influence on the diffusion rate and moreover, it has also influence on the final amount of the hydrogen diffused into the material. The high strength steels with the martensite structure exhibit higher number of the hydrogen traps than the steels without the martensite structure. The mentioned fact leads to the significant degree of the hydrogen diffusion in relation to the materials hereinbefore. From the aspect of the structure, the size of the austenite grain and degree of tempering after the hardening process are the important factors for hydrogen diffusion. Diffusion of the hydrogen into the material can be carried out from the liquid or gas environment [3].

Diffusion of hydrogen from liquid environment

In the liquid solutions, the process of diffusion is based on the electro-chemical reaction consisting of two stages. The first stage is connected with the occurrence of the adsorbed atoms on the surface of the steel (1).

$$H_3O^+ + e^- \rightarrow H_{ads} + H_2O \quad (1)$$

The adsorbed atoms of ions can arise on the basis of the reduction of water molecules if there is minimum concentration of hydrogen ions, for example in neutral and base environments.

$$H_2O + e^- \rightarrow H_{ads} + OH^- \quad (2)$$

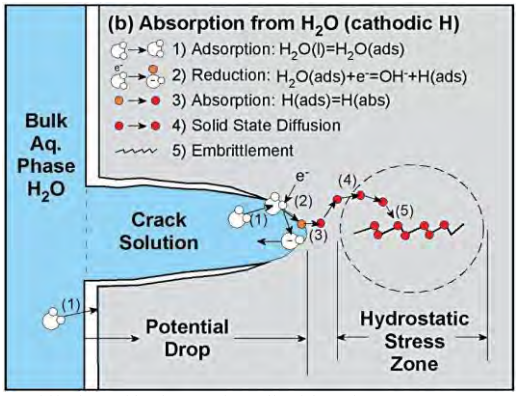

Fig. 1 Diffusion of hydrogen from liquid environment [5]
Obr. 1 Difúzia vodíka z kvapalného prostredia [5]

The second stage is connected with the occurence of hydrogen molecules on the basis of chemical recombination of atomic hydrogen (3).

$$H_{ads} + H_{ads} \rightarrow H_2 \quad (3)$$

The diffusion process into the high strength steels can be also influenced by the specific properties of the liquid environment with any impurities [3, 4].

Diffusion of hydrogen from gaseous environment

This process is commonly connected with the adsorption of the hydrogen molecules and it leads to the occurrence of the hydrogen atoms which are adsorbed on the surface and then, it is based on the subsequent absorption of hydrogen atoms into the metallic lattice [4]. Hydrogen is able to diffuse into the steel only if it is in its atomic form and the given process of diffusion is performed according to the chemical reactions (4), (5).

$$H_2 \rightarrow 2H_{ads} \quad (4)$$

$$2Fe + H_{ads} \rightarrow 2FeH_{ads} \quad (5)$$

where H_{ads} represents hydrogen atom which was adsorbed on the surface and FeH_{ads} represent the hydrogen which was diffused into the steel. The complete reaction without any intergrade of adsorption takes place according the reaction (6).

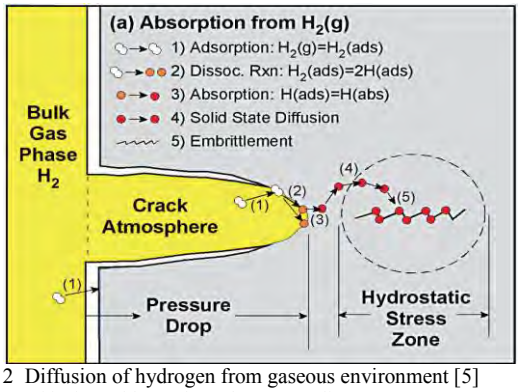

Fig. 2 Diffusion of hydrogen from gaseous environment [5]
Obr. 2 Difúzia vodíka z plynného prostredia [5]

$$2Fe + H_2 \rightarrow 2FeH_{ads} \quad (6)$$

The state of the steel surface, composition of the gas environment and the presence of the any additive agents has the significant influence on the hydrogen diffusion from the gas environment [3].

Morphology of fracture surface

The evaluation of the hydrogen embrittlement is most often performed by help of REM as well as mechanical tests. In relation to the high strength steels with the hydrogen content, the micro-morphology of the fracture surfaces has almost always intergranular (IG) character. The “crow legs” can be seen on the surface of the IG facets. These mentioned sites represent the areas of the local microplastic deformation at initiation of the delayed fracture shown in Fig. 4 [7].

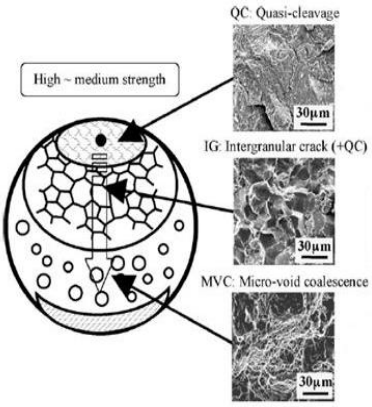

Fig. 3 Micro-morphology of fracture surface [6]
Obr. 3 Mikromorfológia lomovej plochy [6]

Hutnické listy č.7/2013, roč. LXVI
ISSN 0018-8069

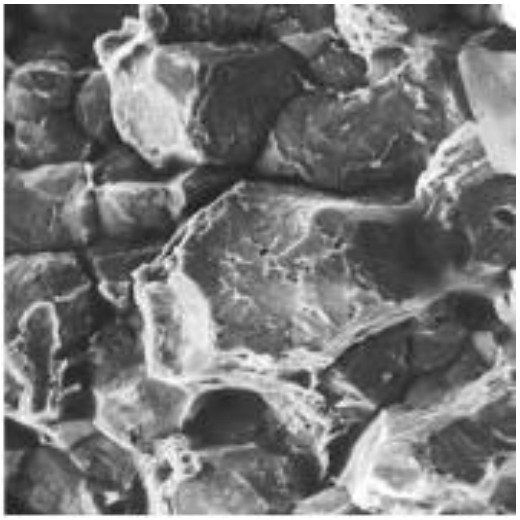

Fig. 4 Intergranular facets with crow legs [7]
Obr. 4 Interkryštalické fazety s vlasovými čiarami [7]

The occurrence of the microvoids (tunnels indented into the grain) is another specific feature in relation to the hydrogen embrittlement of the high strength steels and these microvoids are based on the action of high pressures of H_2 [7].

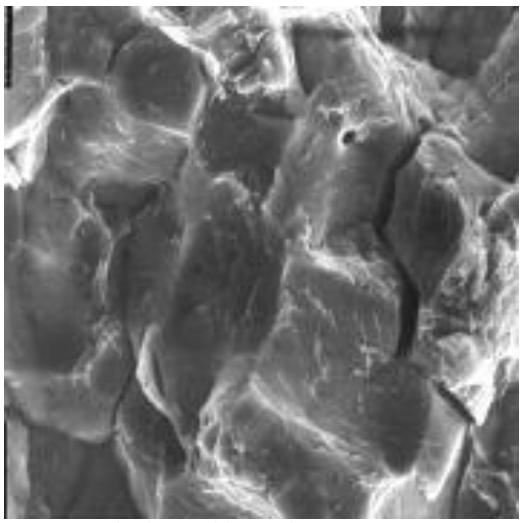

Fig. 5 Intergranular facets with tunnels [7]
Obr. 5 Interkryštalické fazety s tunelmi [7]

In relation to the high strength steels, there is the significant difference between the delayed fracture and laboratory fracture. The microrelief of the delayed fracture can be seen in the Fig. 3 and 4.

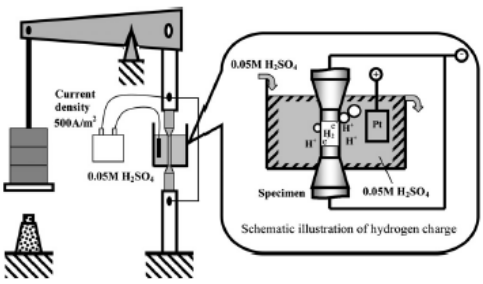

Fig. 6 Example of delayed fracture test [6]
Obr. 6 Príklad skúšky zabrzdeného lomu [6]

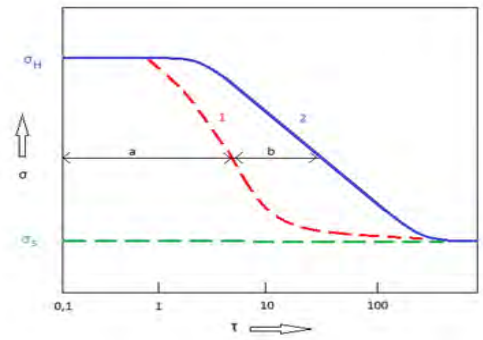

σ – strain, τ – time, σ_H – upper limit, σ_S – lower limit,
a – incubation time, b – time of crack propagation,
1 – time of crack initiation, 2 – time of final rupture

Fig. 7 Stages of delayed fracture
Obr. 7 Etapy zabrzdeného lomu

Discussion and conclusions

After diffusion into the steel, hydrogen in its atomic form can cause significant changes of mechanical properties and hydrogen embrittlement. Hydrogen diffusion into the steels can be carried out from the liquid as well as gas environment. The special method REM is used for detection of the hydrogen embrittlement or some suitable mechanical test can be used for investigation. The low strength steels were compared to the high strength steels with the high content of hydrogen and according to the comparison, there is the change of the quasi cleavage micromechanism of crack distribution into the intergranular mechanism and it is shown in the Fig. 3. The „crow legs“ and microvoids are the typical feature of the hidrogen embrittlement of high strength steels. The long-term outer loading is needed for occurence of the delayed hydrogen fractures.

Literature

[1] Entry of hydrogen into metals. [online], [cit. 2. 1. 2013]. Dostupné na: http://www.uni-saarland.de/fak8/wwm/research/phd_barnoush/hydrogen.pdf

[2] JANSEN, R., PREIKSCHAT, P. Hydrogen embrittlement. [online], [cit. 2. 1. 2013]. Dostupné na: http://www.surtec.com/en/knowledge/knowledge-repository/hydrogen-embrittlement-overview/

[3] SOJKA, J. Odolnost ocelí vůči vodíkové křehkosti. Ostrava: Vysoká škola báňská-Technická univerzita, 2007. s. 108. ISBN 978-80-248-1648-7

[4] SHREIR, L.L., JARMAN, R.A. et al. Corrosion (3rd Edition) Vol. 1-2. Elsevier, 1994. p. 3184. ISBN 978-0-7506-1077-3

[5] HERRING, D.H. Hydrogen embrittlement. *Wire Forming Technology International/Fall* 2010, vol. 13, no. 4, p. 64

[6] KOMATSUZAKY Y., HAENGSIK J., KUNIHIRO Y. Influence of yield strength levels on crack growth mode in delayed fracture of structural steels. *Engineering fracture mechanics*, 2008, vol. 75, no. 3-4, p. 551-559

[7] BEZECNÝ, J., ŠOPÍKOVÁ, Z. Control of Hydrogen Process of Screws after Surface Treatment. *Acta Metallurgica Slovaca Conference*, 2010, vol. 1, no. 2, p.94-98, ISSN 1335-1532

Degradation Processes of Materials Loaded by Thermal Shocks

Degradačné procesy materiálov zaťažených teplotnými šokmi

Ing. Adriána Pavúčková[1], **Ing. Michaela Fedorová**[1], **prof. Ing. Františka Pešlová, PhD.**[1]

[1]University of Alexander Dubček in Trenčín, Faculty of Industrial Technologies, I. Krasku 491/30, 020 01 Púchov, Slovak Republic

The given paper is closely connected with problems including the degradation of selected materials that have been exposed to thermal cyclic loading process. Steel Toolox 33 and Titanium steel represent the selected material samples which were loaded by thermal shocks and this investigation was done because of their usage as components in the glass industry where the individual component parts are expected to withstand high temperatures. The quality of material has the influence on total lifetime. If the materials are not suitable in the terms of structures, the correct conditions of heat treatment are not kept and it is connected with the occurrence of cracks and fractures. Inadequate thermal regimes (pre-heating) lead to the occurrence of the other stress states and these states increase the course of the degradation process decreasing lifetime of part. The facts mentioned hereinbefore are connected with the topic of this work which includes the study of the material response to the simulated thermal shocks influencing the material structure and they also lead to the degradation of the material.

Key words: *thermal shocks, degradation process, stress-strain states, cracks*

Práca sa zaoberá problematikou degradácie vybraných materiálov, ktoré boli vystavené cyklickému teplotnému zaťažovaniu. Vybrané materiály sú ocele, ktoré sa využívajú pre súčasti v sklárskom priemysle. V sklárskom priemysle sa hodnotené materiály Toolox 33 doporučujú ako náhrada za súčasne používané materiály Dominial ZF 2. Vzhľadom k tomu, že celková životnosť súčastí je ovplyvnená kvalitou materiálu, táto práca venovala pozornosť čistote štruktúry a všetkým heterogenitám, ktoré sa v daných štruktúrach nemajú vyskytovať. Pokiaľ sú materiály z pohľadu štruktúry nevyhovujúce, alebo sú zle tepelne spracované, dochádza k ich porušeniu. Sklárske materiály sú vystavené teplotnému zaťaženiu, ktoré nebýva rovnomerné a spôsobuje rôznu teplotnú napätosť na vonkajšom a vnútornom priemere. Z toho dôvodu je veľmi dôležitá teplotná rozťažnosť, ktorá sa najviac prejaví pri vysokých cyklických teplotách. Z pohľadu fraktografie boli tieto zmeny preukázané v lomových plochách a v charaktere porušovania. Je predpoklad, že teplotne zaťažený materiál sa v priebehu prevádzkovania materiálovo mení, čo sa prejavuje aj v krehkom transkryštalickom porušení. V prípade nedodržania teplotných režimov, čo sa týka predohrevov sú vnesené ďalšie napäťové stavy, ktoré degradačný proces superponujú, čím sa životnosť súčasti znižuje. Vonkajšie prostredie – uvoľnené prvky z plynových horákov spôsobujú agresivitu povrchu, čím prispievajú k rýchlejšej degradácii týchto materiálov. Práca sa venuje odozve materiálu na simulované teplotné šoky z pohľadu štruktúry, kde agresivita prostredia bola vylúčená. Pokiaľ by prebiehali simulované teplotné šoky vplyvom plynových horákov dochádzalo by k oxidácii povrchu, ktoré by skresľovali popis lomovej mechaniky, ktorá prebiehala vo vybraných materiáloch ocelí, porovnané s materiálom čistého titánu. Simulované experimenty sú potrebné aj pre vstupy do výpočtového modelovania napäťových stavov konštrukčných prvkov.

Kľúčové slová: *teplotné šoky, degradačný proces, deformačno-napäťové stavy, trhliny*

The ability of materials to withstand external loading in construction or in technical object is given by many factors. These factors are closely connected with the chemical composition of the materials [1]. These mentioned factors also include technological and construction parameters and the way of service. The loading beyond the critical limit causes the initiation of the degradation and the occurrence of the critical state of the rupture. The materials used for glass moulds are exposed to the various in-service factors. The types relating to the damage of the material are reflected in results involving character of fracture surfaces or behaviour of material after depletion of the plastic deformation (Fig. 1). In relation to the operating parts under the higher temperatures, there are the requirements to use the material which is resistant to the external loading and internal stresses. The cyclic heating also belongs to these critical states [2, 3].

The work is closely connected with the study of the degradation occurrence in relation to the selected materials that are under the influence of the simulated high-temperature shocks and these shocks are induced by the special testing device which is represented by the modified resistance spot welding device [4]. By help of this modified testing device, it is possible to create the thermal shocks in the materials and materials can be exposed to the short-time thermal shocks where the temperature is approximately 800-900^{o}C. The

Hutnické listy č.7/2013, roč. LXVI
ISSN 0018-8069

investigation and study of structural and mechanical changes of selected material during the whole test can be used for prediction of the initiation and development of the rupture.

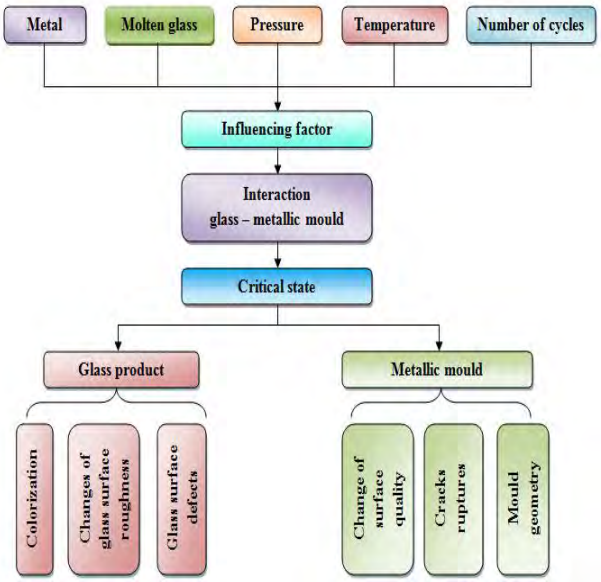

Fig. 1 Impact factors influencing the metallic mould degradation
Obr. 1 Faktory vplývajúce na degradáciu formy

Simulated tests

If the material is exposed to the sudden repeated changes of temperature, there is the occurrence of the fluctuating thermal stresses leading to the rupture, initiation which is similar to the thermal fatigue. This process is connected with occurrence of the cracks in the synergy with the influence of the stress-strain states. The mechanism relating to the crack distribution is comparable to the fatigue process. It is well-known [5], that many factors have the influence on the thermal fatigue (Fig. 2).

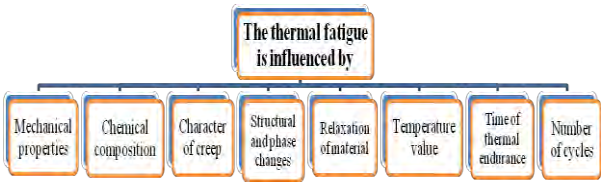

Fig. 2 Factors influencing the thermal fatigue
Obr. 2 Faktory ovplyvňujúce tepelnú únavu

Simulated thermal tests were performed for material Toolox 33 which is commonly used for parts under the thermal loading in the glass industry. As tested material, the pure titanium was also used for parts under the thermal loading. It is important to point out that the character of its structure is extremely sensitive to thermal changes [6].

Materials properties and chemical composition of the selected materials

Toolox 33 stands for hardened chrome-nickel steel. Its chemical composition is shown in Tab.1 and mechanical properties can be found in Tab. 2.

Tab. 1 Chemical composition of Toolox 33
Tab. 1 Chemické zloženie Toolox 33

Chemical composition								
[wt.%]							[ppm]	
C	Si	Mn	Cr	Ni	Mo	V	P	S
0.25	0.6	0.9	1.20	0.70	0.4	0.12 5	100	40

Tab. 2 Mechanical properties of Toolox 33
Tab. 2 Mechanické vlastnosti Toolox 33

Mechanical properties								
Tensile strength, Rm [MPa]		Yield stress, $R_p0.2$ [MPa]		Relative elongation, A5 [%]		Impact toughness, [J]	Hardness, [HBW]	Hardness, [HRC]
+20° C	+200° C	+20° C	+200° C	+20° C	+200° C			
1080	1010	955	860	16	12	60	31 0	29

Titanium is the material with perfect physical and mechanical properties (Tab. 3). It is resistant to corrosion and moreover, transformations of the microstructure are susceptible to temperature. The chemical composition of the commercial titanium is given in the Tab. 4.

Tab. 3 Chemical composition of Titanium
Tab. 3 Chemické zloženie titánu

Chemical composition [wt.%]			
O	Ca	Ti	Pt
18.94	0.57	80.46	0.02

Tab. 4 Mechanical properties of Titanium
Tab. 4 Mechanické vlastnosti titánu

Mechanical properties					
Tensile Strength Rm [MPa]	Yield strength [MPa]	Young´s modulus of elasticity [GPa]	Tensibility [%]	Hardness [HV]	Fracture toughness [MPa.m$^{1/2}$]
450 -650	270 -600	100 -105	5 - 25	155 - 165	55 - 60

Experiment

The prepared modified samples (Fig. 3) of investigated materials were exposed to the thermal shocks by help of the modified resistance spot welding device and the temperature relating to the thermal shocks was from 800 to 900°C. The number of the cycles for thermal shocks was influenced by the primary occurrence of the visible cracks. The cooling process of the sample was preformed continuously after the each fifth second when the sample was put into the water cooling medium. On the basis of the experimental results of three samples, it was possible to determine the number of cycles which can be withstood until rupture of the material. The sample of the Toolox 33 withstood 50 loading cycles until its rupture and in the case of the titanium sample, it was up to 700 cycles until rupture.

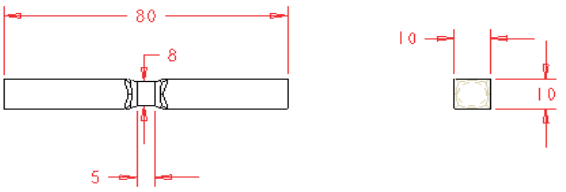

Fig. 3 Geometry and dimensions of the tested sample
Obr. 3 Geometria a rozmery skúšobnej vzorky

The initial materials (Fig. 4a, b) and materials exposed to the thermal shocks were processed in a metallographic way and subsequently, they were evaluated from the microstructural aspect.

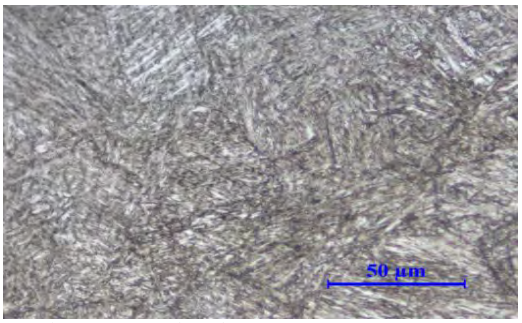

Fig. 4a Microstructure of Toolox 33
Obr. 4a Mikroštruktúra Toolox 33

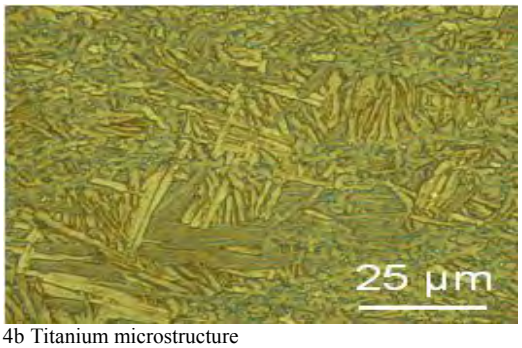

Fig. 4b Titanium microstructure
Obr. 4b Mikroštruktúra Titánu

Microstructural changes induced by thermal shocks

After the thermal shocks, the tested samples of titanium and Toolox 33 were cut and evaluated in the cross-sectional and longitudinal direction from the metallographic aspect. The purity of material was always analysed because it is very important for determination of the critical stress areas and it is also important for the character of the structural phases and changes in the microstructure.

The micropurity evaluation and character of Toolox 33 rupture

There was the occurrence carbonitrides in TOOLOX 33 and their morphology is shown in Fig. 5. These inclusions are hard, brittle and they are initiators of the rupture even at relatively small temperature or mechanical loading. It is very difficult to remove them by heat treatment.

Fig. 5 Areas with the occurrence of carbonitrides
Obr. 5 Lokality s výskytom karbonitridov

On the basis of the influence of the high thermal gradients and on the basis of oxides on the surface of the sample (cooling in the water leads to the generation of the corrosion products), there were enormous stress changes in the area under the surface and it was connected with the initiations of cracks which were subsequently distributed into the different sides (Fig. 6).

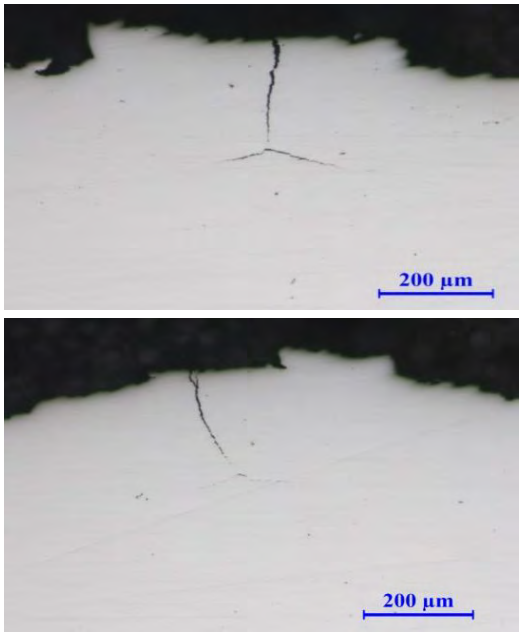

Fig. 6 The character of the cracks of Toolox 33
Obr. 6 Charakter trhlín v Tooloxe 33

The whole degradation process takes place very quickly because the microstructure of Toolox 33 consists of martensitic structure (Fig. 4a). Acicular martensitic structure affects the character and speed of the ruptures. Character of the rupture of TOOLOX 33 was also reflected in the change of rupture in relation to the resulting fracture surface. Tough character of the initial

Hutnické listy č.7/2013, roč. LXVI
ISSN 0018-8069

fracture area (Fig. 7a) was changed to brittle fracture (Fig. 7b) during thermal loading.

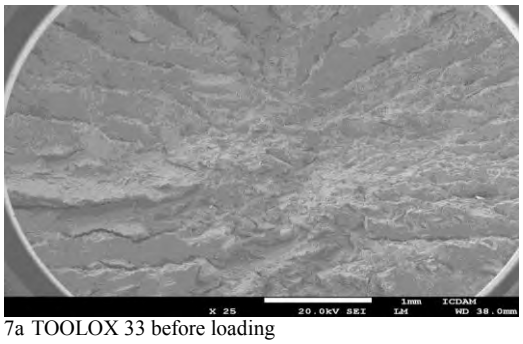

Fig. 7a TOOLOX 33 before loading
Obr. 7a Toolox 33 pred zaťažením

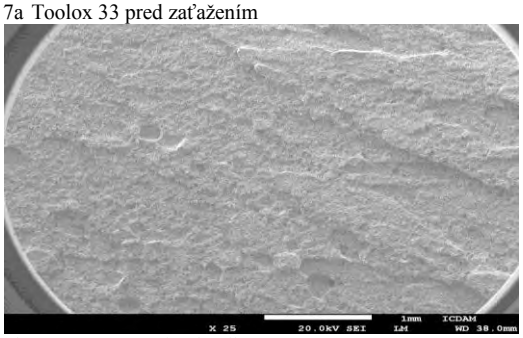

Fig. 7b TOOLOX 33 after loading
Obr. 7b Toolox 33 po zaťažení

The evaluation of Titanium after thermal shocks from microstructural aspect

After exposure to the thermal shocks, Titanium exhibited enormous surface change. There was the occurrence of the striations which became the initiation centers. This material withstood 300 cycles without any evidence about rupture. After the 400 cycles of loading, there was the occurrence of notches on the surface (Fig. 8) and these notches created the visual discontinuous lines and in the locations of the largest stress, the lines were the crack initiators.

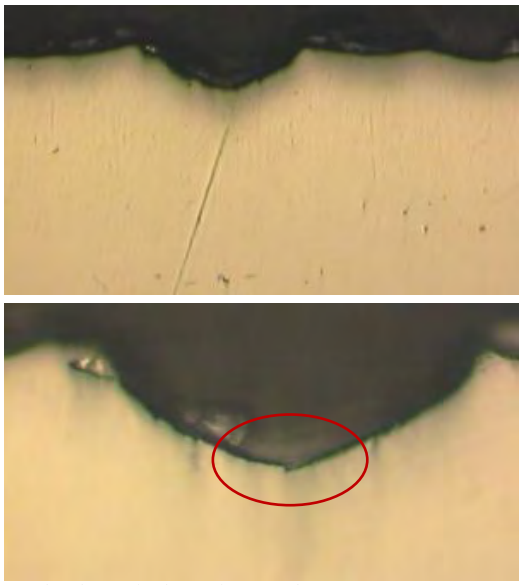

Fig. 8 The change in the surface roughness
Obr. 8 Zmena drsnosti povrchu

Little cracks can be caracterized as the decohesion of the grains acting on the surface and it can be seen in the area of titanium profile. The stress change in the area of fracture initiation has similar character as an initiation relating to the material fatigue. The "step by step" rupture can be seen in the investigated material and this type of rupture is caused by the change of thermal gradients. In the most cases, the little cracks were observed in the central part of the sample and these cracks were distributed to marginal areas of the sample. The cracks which are closely under the surface can be seen in the Fig. 9 and Fig. 10, 11.

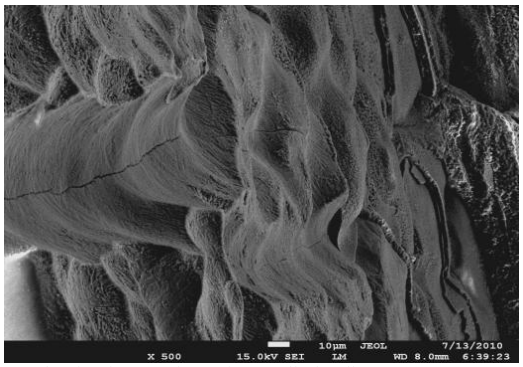

Fig. 9 The titanium surface after cyclic loading
Obr. 9 Povrch titánu po cyklovaní

In the course of the thermal cycling loading (cca 500 cycles), there was the accumulation of the short cracks (Fig. 10, 11). In relation to surface oxidic products, the given products created the brittle phases filling the occurred cracks and the given cracks were slowly distributed into the material [7].

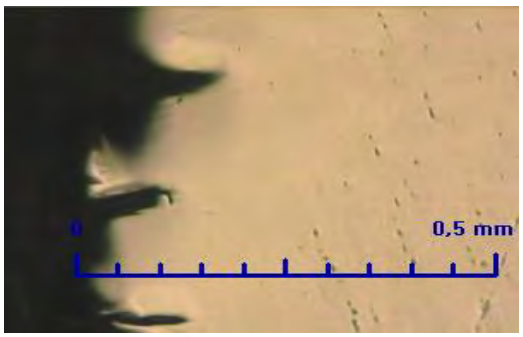

Fig. 10 Cracks at 500 cycles
Obr. 10 Trhliny pri 500 cykloch

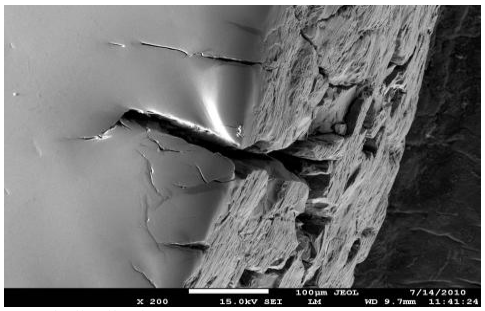

Fig. 11 Crack distribution
Obr. 11 Šírenie trhliny

The higher number of cycles could cause opening and closing of the crack as well as its subsequent distribution. After the 600 cycles of thermal loading, there was the uniform distribution of the cracks around the whole marginal area.

The thermal loading at 700 cycles led to the sample rupture which was around the whole marginal area and it had character of shallow cracks that were directed to the central area of the sample (Fig. 12). During the process of crack distribution, some of the cracks were joined in their marginal point and created boundaries for material fall-out. The crack details after the material fall-out can be seen in the Fig. 13.

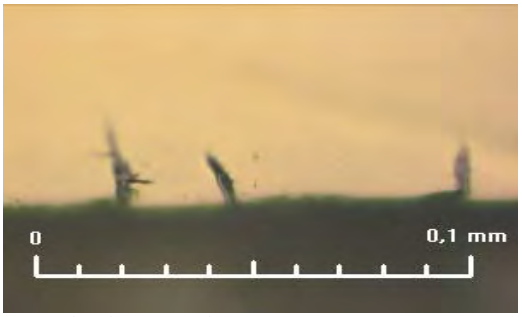

Fig. 12 Cracks after 700 cycles
Obr. 12 Trhliny po 700 cykloch

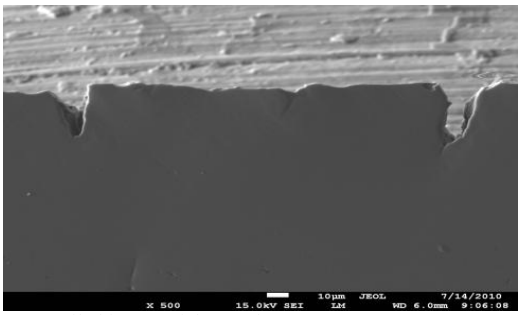

Fig. 13 Detailed image of the cracks
Obr. 13 Detail trhlín

In relation to the investigations, the assumption that the rupture mechanism should be different was confirmed because the selected materials (TOOLOX 33 and titanium) are different from the structural as well as chemical aspect.

Conclusions

According to the simulated test, it was possible to observe the initiation and behaviour of the cracks for selected materials. Samples of steel material (TOOLOX 33) have completely different fracture behaviour in comparison to the titanium material. Each one tested material had different behaviour under the critical loading conditions but it is clear that the heterogeneity of the structure could superpose a degradation process for each material. In relation to extremely loaded parts (thermal, mechanical, wear loading), material with high purity should be used or Toolox 33 could be coated by thin layer of Titanium which could eliminate or reduce the initiation of the rupture. Each one of the degradation processes is influenced by the internal stress-strain states and therefore it is necessary to reduce the residual stress from former processing technologies. On the basis of the simulated tests, we do not recommend material Toolox 33 without coating for glass parts which are exposed to thermal changes, corrosion wear, and mechanical loading.

Acknowledgements
We would like to give our thanks to Innovation Centre and diagnostics applications of materials at CTU in Prague - ICDAM (project OPPK CZ. 2 16/3 1. 00/21037).

Literature

[1] LUPTÁKOVÁ, N., KEBISKOVÁ, J., ANISIMOV, E., BENÁK, M., PEŠLOVÁ, F. Impact raw material for production zinc oxide in retort furnaces. *21st International Conference on Metallurgy and Materials,* Metal 2012, CD-ROM Article no. 234, Tanger Ostrava, 2012

[2] VAVRO, J., VAVRO, J., VAVROVÁ, A., KOVÁČIKOVÁ, P., VANC, R. Numeric Analysis of the Eigen frequencies of the Ductile Cast Iron with the Spheroidal Shape of Graphite and Grey Cast Iron with the Lamellar Shape of Graphite, *Hutnícke listy*, 2012, roč.LXV, č.7, p. 110 - 114, ISSN 0018-8069

[3] LUPTÁKOVÁ, N., HAJDUCHOVÁ, Ľ., PEŠLOVÁ, F. Microstructure analysis of zinc alloys, which have a minimum of 90 % Zn. *Hutnícke listy*, 2011, roč. XIV, č. 7. s. 119 - 121, ISSN 0018 – 8069

[4] KRÍDLA, M. Propose and experimentally verify a device for measuring cyclic thermal fatigue of metallic materials - *doctoral thesis*. FPT Púchov, 2010

[5] PUŠKÁR, A., KÁPOLKA, P. Terms creation of quarries and spread in construction materials. VA SNP Liptovský Mikuláš, 1994

[6] PAVÚČKOVÁ, A., FEDOROVÁ, M., JANEKOVÁ, M., KRÍDLA, M., PEŠLOVÁ, F. Degradation of the selected materials at thermal shocks. *Degradácia konštrukčných materiálov*, 2013, roč. XIII, s. 83 - 89, ISBN 978-80-554-0741-8

[7] KOŠTIALIKOVÁ, D., PEŠLOVÁ, F., HAJDUCHOVÁ, Ľ. The wear as the critical state and its influence on the reoperation of the implant. *Degradácia konštrukčných materiálov*, 2013, roč. XIII, s. 58 - 63, ISBN 978-80-554-0741-8

Fatigue of Construction Steel under the Cyclic Loading

Únava konštrukčnej ocele pri cyklickom zaťažení

Ing. Petra Kováčiková[1], **prof. Ing. Ján Vavro, PhD.**[1], **Ing. Rudolf Valášek**[1], **Ing. Ján Vavro jn., PhD.**[1]

[1]University of Alexander Dubček in Trenčín, Faculty of Industrial Technologies, I. Krasku 491/30, 020 01 Púchov, Slovak Republic

The given paper is closely connected with the whole complex of problems including identification of the fatigue characteristics for the construction or structural materials which are under the cyclic loading. Mechanical fatigue of the tested material is performed by help of device where the vibration stress occurs as the result of the rotation of the tested rod representing sample and moreover, the given rotating sample is loaded by bending. The accumulation of the damages as well as the change of service conditions can cause the damage of the service parts without any indications of the rupture. Therefore, the experiment is mainly focused on the effort to reduce the undesirable properties and to look for possible solutions relating to the prolongation of in-service time increasing the material resistance. The part of work is concerned with the experimental problems referring to the mechanical fatigue because there is the effort to determine material parameters, characteristics of the structural properties and investigation of the changes for material properties. The next one part is devoted to the creation of the computer models which can enable us to simulate various ways of loading process while the computer program system on the basis of finite element method (FEM) is used. This work is the combined experimental research including fatigue under the stress, computational analysis, evaluation and comparison of the obtained results because this approach can bring new important results for the future research and development relating to application of the investigated problem with the reference to mechanical fatigue and distribution of the fatigue cracks under the cyclic loading in the practical sphere.

Keywords: *fatigue, cyclic loading, Wöhler fatigue curve*

Príspevok sa zaoberá problematikou identifikácie únavových charakteristík konštrukčných materiálov pri cyklickom zaťažení. Mechanická únava materiálu sa skúša na zariadení, kde sa kmitavé napätie dosiahne rotáciou skúšobnej tyče, ktorá je zaťažená ohybom. Pri tejto skúške sa používajú skušobné vzorky s kruhovým prierezom austenitickej chrómniklovej ocele STN 17 240 a realizujú sa za normálnej teploty pri nami zvolenej frekvencii 15 Hz. Výsledkom skúšky na odstupňovaných hladinách zaťaženia je Wöhlerova krivka únavy a hodnota medze únavy. Kumulácia poškodenia a zmena prevádzkových podmienok môže poškodiť súčiastky, ktoré boli v prevádzke bez náznaku porušenia. Preto sa snažíme znižovať účinok týchto nežiaducich vlastností a hľadáme možnosti zvyšovania odolnosti materiálu na čo najdlhšiu prevádzkovú dobu. Časť práce sa zaoberá problematikou experimentov mechanickej únavy pre stanovenie materiálových parametrov, charakteristike štrukturálnych vlastností a sledovaniu zmien materiálových vlastností, pretože zmena týchto vlastností a parametrov ovplyvňuje celkové výsledné chovanie konštrukcií a ich súčastí. Výsledky z experimentov budú vstupnými parametrami na definovanie fyzikálnych a materiálových charakteristík pre druhú časť práce, ktorá sa bude zaoberať vytvorením výpočtových modelov, ktoré umožnia následujúce simulácie spôsobov zaťažovania, a to využitím výpočtového programového systému na báze metódy konečných prvkov (MKP). K zefektívneniu a urýchleniu práce pri modelovaní konštrukcie vzorky sa využíva CAD program. Táto práca predstavuje kombinovaný výskum experimentu v oblasti únavy namáhaním, výpočtovou analýzou, následné vyhodnotenie a komparáciu získaných výsledkov. To prinesie v praxi nové pohľady ale aj výsledky pre ďalší výskum a rozvoj aplikácie riešenej problematiky mechanickej únavy a šírenia únavových trhlín na základe cyklického zaťaženia.

Klúčové slová: *únava, cyklické zaťaženie, Wöhlerova krivka únavy*

The given paper is focused on the solution of the experimental problems in relation to the mechanical fatigue. The given research is performed for determination of the material parameters, characteristics of structural properties and observation of the changes with the reference to the material properties of the selected construction material. Experimental determination of the complete Wöhler curve and knowledge in all important material and geometric data of tested construction material is the fundamental condition for specification of the in-put parameters which are necessary for computer modelling process. The attention has to be paid to the total time during the creation of the computer model because it is closely connected with the acquisition of the quite fast response to the change of material, geometric and other

parametres. The change of material properties and parameters has influence on the total resultant behaviour of the final mechanical products and their parts [1- 4].

Characteristics of structural steel

According to the Slovak Technical Standards (STN), the austenitic chrome-nickel steel 17 240 was used for preparation of the tested samples. The chemical composition and mechanical properties of the material are introduced in the Tab. 1 and Tab. 2, respectively.

Tab. 1 Chemical composition of the material
Tab. 1 Chemické zloženie materiálu

	C	Mn	Si	P	S
Material 17 240	0.065	0.58	1.05	0.024	0.011
	Cr	**Ni**	**Mo**	**Cu**	**W**
	19.09	7.42	0.17	0.06	0.058

Tab. 2 Mechanical properties of the material
Tab. 2 Mechanické vlastnosti materiálu

Material 17 240	$R_{P0,2}$ [MPA]	R_M [MPA]	A [%]	Z [%]
	260	642	65.5	77.1

The microstructure of the chrome-nickel austenitic steel sample 17 240 is mainly composed of polyedric austenitic grains containing the high number of twins. The occurrence of delta-ferrite particles was observed in the surface layers and it can be seen in the Fig. 1.

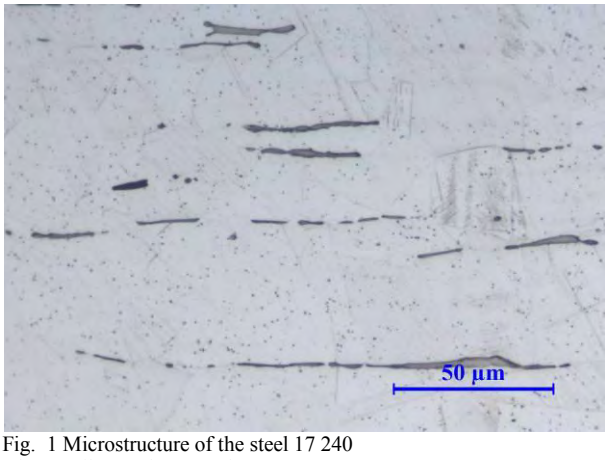

Fig. 1 Microstructure of the steel 17 240
Obr. 1 Mikroštruktúra ocele17 240

The investigation of the mechanical fatigue

The mechanical fatigue of material has been investigated by help of the special testing device where the vibration stress can be obtained by rotation of the tested rod which is loaded by help of bending. In relation to this testing procedure, only circular cross-section of the tested samples is acceptable. One stress cycle is performed during one revolution of the rod sample. The testing procedures were carried out at the standard room temperature and the selected frequency was 15 Hz. The whole testing process started by selection of the stress σ_1 for the first tested rod sample while the given stress was less by 10MPa than R_e for the given material. The distance of the ballast weight a was calculated for the specified diameter of the rod sample by help of the adequate relation (1) [2]

$$\sigma_{\max} = \frac{M_o}{W} = \frac{5F_z.a.l_o}{b.d^{š}}\left(MPa\right) \qquad (1)$$

where M_o [N.mm] – bend loading , F_z – gravitational force for ballast weight [N], a – distance of the ballast weight [mm], σ_{max} – stress intensity[MPa],, d – diameter of the sample [mm],, l_0 – distance between holding jaw and bearing[mm].

The graded stress was specified for each one sample at the same frequency after the breakage of the tested rod sample. The mentioned rule for the specific steps of the experimental procedure had to be performed until the creation of Wöhler fatigue curve. The cyclic loading process was carried out continuously from that moment when the rotation movement of the sample started to be fluent or steady. There was not any discontinuation of the testing process. The occurrence of the visible crack (Fig. 2) or fracture (Fig. 3) can be understood as the end of the testing process [3].

Fig. 2 The Sample after the testing process – fatigue fracture
Obr. 2 Vzorka po skončení skúšky – únavový lom

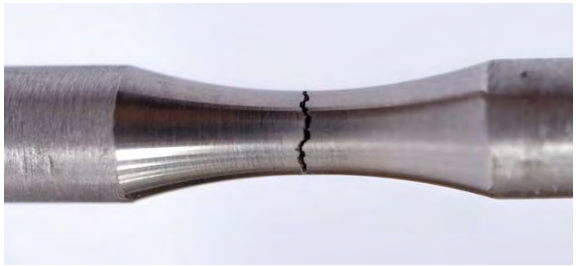

Fig. 3 The sample after the testing procedure – fatigue crack
Obr. 3 Vzorka po skončení skúšky – únavová trhlina

Results and discussion

In relation to the experimental procedure, the initial specified stress was less than the ultimate strength of the tested material and it means that the initial stress was 250 MPa. The specification or selection of the stress is closely connected with the occurrence of the crack or fracture. Testing the all of the samples, the stress was decreased gradually until the critical stress values were

Hutnické listy č.7/2013, roč. LXVI
ISSN 0018-8069

obtained because the acquisition of the critical stress values stand for the values when the tested rod sample is able to withstand the number of the vibrations because the number of vibrations is the fundamental unit for determination of the yield of fatigue. Based on the experimental accuracy, it was also necessary to perform the control test for at least one rod sample. The given control test can be carried out for the same stress or the stress can be less by 15 MPa. The value of the yield of fatigue as well as creation of Wöhler fatigue curve are the results of all these testing procedures while the same material is used for preparation of the samples which have the same proportions and moreover, the same graded loading is applied for the mentioned tested rod samples. The obtained results are shown in the tab. 3 and created Wöhler fatigue curve can be seen in the Fig. 4 [3].

Tab. 3 The results of the fatigue test
Tab. 3 Výsledky skúšky únavy

17 240	σ [MPa]	Number of cycles N
1	250	13 000
2	240	15 300
3	230	32 700
4	220	45 900
5	210	102 900
6	200	270 200
7	190	10 468 200
8	180	10 102 800

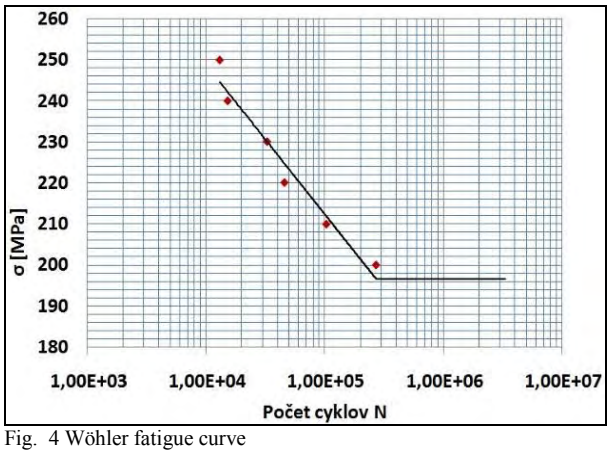

Fig. 4 Wöhler fatigue curve
Obr. 4 Wöhlerova krivka únavy

Conclusions

The given work is closely connected with the construction or structural material which was subjected to investigation in order to observe and specify its fatigue characteristics during its cyclic loading. From the aspect of the investigation, the determinations of the fatigue curve and computer analysis are the results of the uniaxial fatigue ways of the material loading. The measurement was performed by help of the special device where the sample is exposed to cyclic loading during the rotation movement. In relation to the experiment, there are the complex mechanical, physical and chemical phenomena in the sample during its loading and therefore, it is necessary to find the correct way which can help us to obtain the accurate and correct ways for control of measured experimental values. This experiment represents the combination in relation to the implementation and application of the modern computer modelling, the results of which can be compared to practical investigation of material fatigue which was caused by specific loading. The experimental part is going to be completed by creation of the computer model which enables us to create the computer simulations of the complex ways relating to loading process by using the program system on the basis of finite element method (FEM). To make the work more effective and faster during the modelling of the sample, the program CAD is going to be used. The program CAD can be applied for easy and fast creation of the geometry referring to the computer model. The given CAD program is connected with the selected finite element method (FEM) in ADINA program which is going to be used for all important calculations and simulation of the testing process. One of the important procedures of this investigation is focused on creation of the accurate sample geometry for determination of the in-put parameters from the experimental analysis and this is the way for the specification of the physical and material characteristics with the most confidential results [1].

Acknowledgements
This work has been supported by VEGA grant No.1/0530/11 and KEGA grant No. 007 TnUAD-4/2013.

Literature

[1] KOVACIKOVA, P., VAVRO, J., VAVRO, J. Jn., VALÁŠEK, R. *Identification of the fatigue characteristics of structural materials under cyclic loading.* In: XVIII. Slovak – Polish International Scientific Conference. Machine Modeling and Simulations, Žilinská Univerzita v Žiline, 2013. ISSN 1337-8996

[2] VELES, P. *Mechanické vlastnosti a skúšanie kovov.* Alfa, Bratislava, 408 strán, 1985, ISBN 63 – 559 – 85

[3] STN 420 363: *Skúšanie kovov, skúšky únavy kovov, metodika skúšania.* Vydané 1. 10. 1986

[4] KLESNIL, M., LUKÁŠ, P. *Únava kovových materiálov pri mechanickom namáhaní.* Academia, Praha, 1975

[5] TREBUŇA, F., ŠIMČÁK, F., HUŇADY, R. Kmitanie a modálna analýza mechanických sústav. 1. vyd. Košice, 2012, 236 s. ISBN 978-80-553-1206-4

[6] ŠIMČÁK, F., ŠTAMBORSKÁ, M., HUŇADY, R. Analýza plastickej deformácie materiálov využitím digitálnej obrazovej korelácie. *Chemické listy,* 2011, vol. 105, no. S, p. 564-567. ISSN 0009-2770

Use of Multi-disc Brakes in Terms of Materials

Použitie lamelových bŕzd z hľadiska materiálov

Ing. Lenka Hazuchová[1], **doc. Ing. Jan Krmela, Ph.D.**[1]

[1]University of Alexander Dubček in Trenčín, Faculty of Industrial Technologies, I. Krasku 491/30, 020 01 Púchov, Slovak Republic

This paper deals with types of discs used in the aircraft brakes in terms of materials. The current trend of military and civil aircraft development is the economic theory of "affordable aircraft". In relation to all the on-board systems, the major emphasis is hidden in high reliability, high efficiency, minimum weight, minimum installation space and also the minimum cost. Probable development is expected particularly in use of high efficient materials for the purpose of longer life and in reduction of costs. The given development is also expected in relation to the use of brake discs made of hybrid materials that can absorb much higher levels of energy and the use of electromagnetically controlled systems which eliminate the risk of ignition. Electrically controlled multi-disc brakes transmit the rated torque by discs friction. These discs are gripped and released by electromagnet. These brakes have very small size according to the size of transmitted torque. They are characterized by rapid increase of torque at the nominal value and the small residual torque when brakes are off. The brakes respond quickly to pulse and thereby increase the accuracy and efficiency of machinery without any transmission elements. To increase the braking force of the braking system is necessary to find a suitable material with better values than conventional materials used in multi-disc brakes. The used material has to comply with conditions of high brake efficiency at higher temperatures and also has to be strong enough to avoid cracking during operation. This is a composite material with ceramic matrix CMCs. This material was developed to overcome the brittleness of monolithic ceramics to ceramics used as construction material in rockets, jet engines, protective outer layer of the spacecraft, aircraft brakes, and so on.

Keywords: *aircraft, multi-disc brake, ceramic matrix composite*

Tento príspevok sa zaoberá druhmi lamiel používaných v leteckých brzdách z hľadiska materiálov. Súčasný trend vývoja ako vojenských, tak civilných lietadiel je daný ekonomickou teóriou „cenovo dostupných lietadiel". Zo všetkých palubných systémov sa najvyšší dôraz kladie na vysokú spoľahlivosť, vysokú účinnosť, minimálnu hmotnosť, minimálny priestor pre inštaláciu a tiež minimálne náklady. Pravdepodobný vývoj sa očakáva najmä v oblasti používania vysoko účinných materiálov za účelom vyššej životnosti a s cieľom znížiť náklady. Ďalej v oblasti používania brzdových lamiel z hybridných materiálov, ktoré sú schopné absorbovať oveľa vyššie hladiny energie a použitie elektromotorom ovládaných bŕzd, ktoré eliminujú riziko vznietenia. Elektricky radené lamelové brzdy prenášajú menovitý krútiaci moment trením lamiel, ktoré sú zvierané a uvoľňované pôsobením elektromagnetu. Tieto brzdy majú vzhľadom k veľkosti prenášaného krútiaceho momentu veľmi malé rozmery. Sú charakterizované rýchlym nárastom krútiaceho momentu na menovitú hodnotu a malým zvyškovým momentom pri vypnutí. Preto tieto brzdy rýchlo reagujú na impulz a tým zvyšujú presnosť a výkon strojov bez akýchkoľvek prevodových článkov. Tým znižujú rozmery a hmotnosť pohonných jednotiek. Kvôli zvýšeniu brzdiacej účinnosti brzdového systému je potrebné nájsť vhodný materiál s lepšími hodnotami, ako u bežných materiálov používaných pri výrobe lamelových bŕzd. Použitý materiál musí spĺňať podmienky vysokej brzdnej účinnosti aj pri vyšších teplotách a takisto musí byť dostatočne pevný, aby nepraskol počas prevádzky. Týmto materiálom je kompozit s keramickou matricou CMCs. Tento materiál bol vyvinutý na preklenutie krehkosti monolitných keramických materiálov s cieľom využiť keramiku ako konštrukčný materiál v rôznych prostrediach, ako sú rakety, prúdové motory, ochranné vonkajšie vrstvy vesmírnych lodí, brzdy lietadiel a pod.

Kľúčové slová: *lietadlo, lamelová brzda, kompozit s keramickou matricou*

Types of discs used in brakes are different. The reason is connected with the specification where in aircraft they will be used on the base of their chemical composition. Besides of braking effect, the important thing in multi-disc brake (Fig. 1) is friction and temperature. Heat dissipation during braking is influenced by discs splining. The shaping of cooling slots is dependent on the materials used for multi-disc brakes [1].

Disc materials

The development has led to the fact that the internal and external discs were coated with friction material (Fig. 2). Initially, sintered materials, organic paper and then carbon deposits were used. Requirements for the „wet" disc brakes are:

- high-dynamic friction coefficient,

Hutnické listy č.7/2013, roč. LXVI
ISSN 0018-8069

- constant friction through whole life, independent on load,
- low noise and vibration,
- high temperature resistance,
- long life with low wear,
- low rolling resistance,
- compatibility with various types of oil [2].

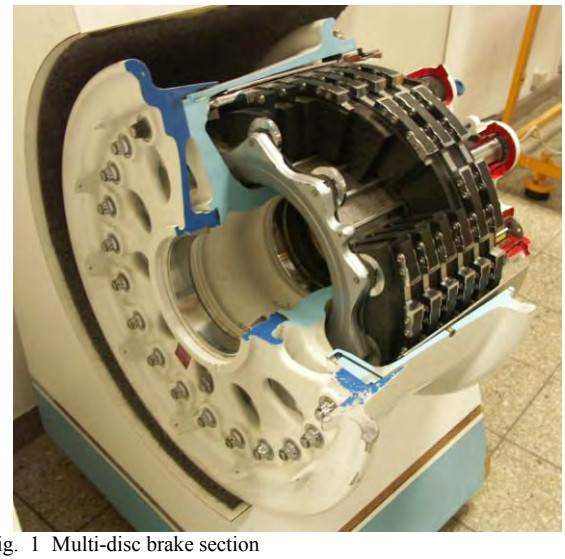

Fig. 1 Multi-disc brake section
Obr. 1 Rez lamelovou brzdou

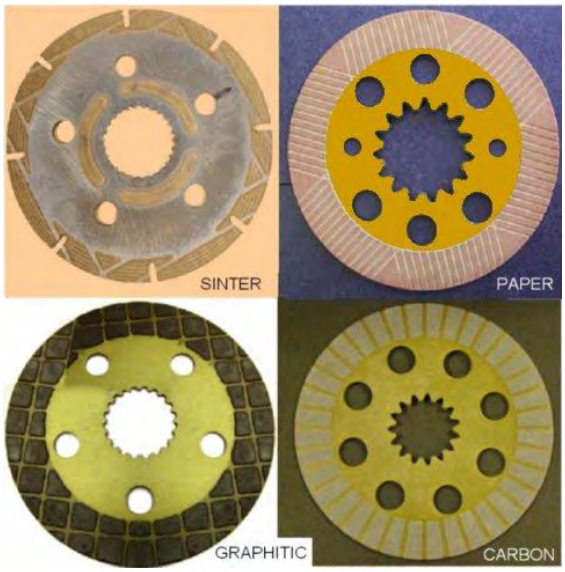

Fig. 2 Use of different friction materials in brakes [1]
Obr. 2 Použitie rôznych trecích materiálov v brzdách [1]

Ceramic matrix composites (CMCs)

Use of ceramic composites in engines will increase their operating temperature and decrease of cooling additions. The use of lightweight ceramic materials instead of heavy superalloys will mean saving gain weight. Although CMCs are promising structural materials, their use is still limited by the lack of suitable reinforcements, processing difficulties, durability and cost.

Ceramic matrix can solidify either continuous or discontinuous fibres, for example particles, whiskers or chopped fibres. Regarding the mechanical properties of whiskers, they are the most attractive way for reinforcement, but their use creates health risks. Continuous fibres are more efficient from a mechanical point of view, but they are more expensive and harder in relation to ceramic matrix in terms of design, processing and use.

CMCs can be classified according to chemical composition of the matrix and reinforcement:

Non-oxidic CMCs have been most studied. The most famous are carbon fibres and silicon carbide (SiC). Carbon fiber is also used for reinforcing composites with epoxy matrix. This is why they are the cheapest (except glass fibres). To avoid compatibility problems, especially at high temperatures, oxygen-free fibres are usually inserted into non-oxidic matrices. The first material was the combination of CMC matrix carbon/carbon fiber (C/C). This composite was originally designed for rocket engines and thermal protective shields for missiles. Later, there was the use of combination of C/SiC and SiC/SiC, which have been developed due to oxidation resistance increase.The used matrix of silicon nitride was also less stable at high temperatures than silicon carbide.

Oxide CMCs are usually the best solutions in terms of thermodynamics for long-term applications in oxidizing atmospheres. Oxide fibres, even if they are refractory, tend to grain growth at high temperatures, resulting in degradation of strength properties and presents results in a low creep resistance. In addition, they have a higher specific gravity than carbon fiber (4 g/cm^3 for Al_2O_3 and 2g/cm^3 for C, [3]).

The following CMCs properties were chosen for discs and they are shown in Table 1.

Tab. 1 CMCs composite properties [3]
Tab. 1 Vlastnosti kompozitu CMCs [3]

Mechanical properties	
Young's modulus of elasticity	90 – 100 GPa
Traction strength	14 – 23 MPa
Limit of stress	14 – 23 MPa
Elongation	0 %
Vickers hardness	67 – 74 HV
Fracture toughness	5.7 – 6.3 MPa·m$^{1/2}$
Physical properties	
Melting temperature	3200 – 3400 °C
Specific heat	754 – 758 J/kg·K
Dilatability coefficient	0.6 – 8.2·10^{-6}·K^{-1}
Heat conductivity	10 – 69 W/m·K
Max. operational temperature	2002 – 2102 °C
Electric resistance	1070 – 2690 μΩ·cm

CMCs may be produced from the gas or liquid phase. Each of these methods has advantages and disadvantages. The gas phase, at CVI process (Chemical Vapor Infiltration) the reinforcing particles typically fill matrix, which is precipitated from the gaseous precursor, e.g. hydrocarbon to carbon, etc. There are several versions of the CVI process. The most famous is the isothermal/isobaric CVI transmission, a relatively slow process in which mass transfer takes place by diffusion and is accompanied by the formation of pores and varying degrees of coating. This allows simultaneous application of more layers on larger quantity, possibly different shapes, is very flexible. For these reasons it is preferable in larger operations. It is suitable for the small components production [3].

Deposition technology from liquid phase is a filament coated by interphase and watered by liquid matrix precursor. The RMI process (Reacted Melt Infiltration) is a fiber impregnated by melt using capillary forces, which reacts with the solid phase and usually strengthens distributed fibres (SiC - Si in the matrix is prepared by infiltration of liquid silicon through reinforced carbon fiber) or by atmosphere (at Al_2O_3 - Al matrix is created by liquid metal infiltration and chemical reaction with an oxidising atmosphere). Among the other benefits, RMI process is very fast and can be used to produce coarse pieces. The materials produced this way have low porosity and high thermal conductivity [3]. Fig. 3 represents carbon brakes as sample.

Fig. 3 Carbon brakes from Messier-Bugatti-Dowty [1]
Obr. 3 Karbónové brzdy od firmy Messier-Bugatti-Dowty [1]

Conclusions

The increase of the braking force of UAV´s brakes and small disc size in the space of main landing gear were the subject of the investigation in order to find a suitable materials with better values than those which are commonly used and known for the multi-disc brakes production. The material used for the brake design has to require high braking efficiency conditons even at high temperatures. The material has to be strong enough to avoid cracking during the activity. The reason is connected with the loose of fitting plates in the brake. The selected material is the ceramic matrix composite (CMCs). This composite will be dealt in terms of computational modeling and material parameters for the purpose to meet all the demanding requirements relating to the aircraft industry.

Literature

[1] HAZUCHOVÁ, L. Návrh lamelovej brzdy dopravného prostriedku so zohľadnením na účinnosť, spoľahlivosť a údržbu. Diploma work. Trenčín, Slovak Republic : Trenčianska univerzita Alexandra Dubčeka v Trenčíne, Fakulta špeciálnej techniky. 2013. 62 p. (in Slovak)

[2] HAVELKA, V. Konstrukce a projektování letadel II. Skriptá. Praha, Czech Republic : ČVUT. 1986 (in Czech)

[3] NASLAIN, R. Ceramic matrix composites. Université Bordeaux 1, 33600 Pessac. France

Hutnické listy č.7/2013, roč. LXVI
ISSN 0018-8069

Biologically Important Materials with Cu^{2+} Ions and Heterocyclic Compounds and their Thermal Properties

Biologicky významné materiály s Cu^{2+} iónmi a heterocyklickými zlúčeninami a ich termické vlastnosti

Ing. Zuzana Harmatová[1], prof. Ing. Eugen Jóna, DrSc.[1], Ing. Jana Medvecká, PhD.[2]

[1]University of Alexander Dubček in Trenčín, Faculty of Industrial Technologies, I. Krasku 491/30, 020 01 Púchov, Slovak Republic
[2]Slovak University of Technology, Faculty of Chemical and Food Technology, Radlinského 9, SK- 812 37 Bratislava, Slovak Republic

The paper is closely connected with the investigation of the thermal behaviour relating to the materials with biologically important compounds including $Cu(2Xbz)_2(nia)_2(H_2O)_2$ and $Cu(2Xbz)_2(denia)_2(H_2O)_2$ (X=Cl,Br) where 2-ClBz and 2-Brbz are 2-chloro and 2-bromobenzoate anions and nia = nicotinamide or denia = N,N-dietylnicotynamide. Nicotinamide is a nitrogen-donor ligand that has been used for the treatment of various skin diseases (atopic eczema, psoriasis, skin cancer). In order to enhance understanding relating to drug-metal ion interactions, we have been studying the thermal and spectral properties of studied complexes. Thermal decomposition of all studied compounds is carried out on the basis of three steps. The first step of decomposition is always connected with release of water molecules in the case of all studied compounds. The final product of thermal decomposition is CuO. The thermal stability of the studied compounds can be ordered in this way: (I)<(II)<(IV)<(III).

Keywords: *N,N- dietylnicotynamide nicotinamide ,bromobenzoate anions*

Predkladaná práca sa zaoberá štúdiom termických vlastností materialov s biologicky významnými zlúčeninami: $Cu(2Xbz)_2(nia)_2(H_2O)_2$ a $Cu(2Xbz)_2(denia)_2(H_2O)_2$ (X=Cl,Br), kde 2-ClBz a 2-Brbz sú 2-chloro a 2-bromobenzoátové anióny, (nia) je nikotínamid a (denia) je N,N- dietylnikotínamid. Nikotínamid je dusíkatý ligand, ktorý sa používa pri liečbe rôznych kožných ochorení (atopický ekzém, svrab, rakovina kože). Za účelom lepšieho pochopenia interakcií kovových iónov s liečivami na báze dusikatých ligandov, sme študovali termálne a spektrálne vlastnosti pripravených komplexov. Termálne a spektrálne analýzy sú veľmi dôležité metódy pre charakterizáciu materiálov, pretože mnohí autori aplikovali tieto techniky pre rôzne materiálové charakterizácie. Dôvodom prípravy materiálov s biologicky významnými zložkami a štúdiom ich termického správania je objaviť funkciu stopových prvkov pre živý organizmus a úsilie pripraviť nové potenciálne liečivá s obsahom Cu^{2+}iónov (meďnaté ióny vykazujú protizápalové, antireumatickú a antibakteriálnú aktivitu). Heterocyklické zlúčeniny majú významnú úlohu s mnohých biologickými systémami najmä N - darca ligandných systémov jednotlivých súčastí niekoľkých vitamínov a liečiv. Informácie o vzťahu medzi štruktúrou a tepelným rozkladom komplexov a štúdium vplyvu príslušného kovu a ligandu na povahe procesu tepelného rozkladu sú veľmi významné. N - heterocyklicé zlúčeniny majú už samotné antibakteriálne, antireumatické, antidiabetické, protizápalové a ďalšie fyziologické účinky. Pri štúdiu termických vlastností týchto materiálov pomocou TG a DTG sa zistilo, že termický rozklad študovaných zlúčenín prebieha v troch stupňoch. Pri zahrievaní v prvom stupni unikajú molekuly vody. Konečným produktom termického rozkladu je CuO (oxid meďnatý). Termická stabilita skúmaných zlúčenín vzrastá v poradí: (I)<(II)<(IV)<(III).

Kľúčové slová: *N,N- dietylnikotínamid, nikotínamid, brombenzoátové anióny*

The investigation and acquisition of the information relating to relationship between the structure and thermolysis is very important from the aspect of materials with metal ions. This study is a continuation of previously reported studies [1,2] describing the thermal properties of metal complexes with heterocyclic ligands. Thermal and spectral analyses are very useful methods for materials characterisation. Therefore, many authors have applied these techniques for various materials characterization [3,4]. Heterocyclic compounds play a significant role in many biological systems, especially N - donor ligand systems being a component of several vitamin and drugs [5]. Nicotinamide is a nitrogen donor ligand that has been used for the treatment of various skin diseases (atopic enzema) psoriasis and shin cancer [6]. In order to enhance understanding of drug-metal ion interactions, we have been studying the thermal properties of Cu (II)

complexes with 2-chloro- and 2-bromobenzoic acid (2-ClbzH, 2-BrbzH), nicotinamide (nia) and N,N-dietylnicotinamide (denia). This paper describes the preparation of following complexes: $[Cu(2\text{-}Clbz)_2(nia)_2)(H_2O)_2]$ (I), $[Cu(2\text{-}Brbz)_2(nia)_2)(H_2O)_2]$ (II), $[Cu(2\text{-}Clbz)_2(denia)_2)(H_2O)_2]$ (III) and $[Cu(2\text{-}Brbz)_2(denia)_2)(H_2O)_2]$ (IV) and moreover, the thermal (TG, DTG) analysis of prepared complexes is also involved here in this paper.

Experimental

The compounds were prepared in this following way: Copper (II) acetate was solved in appropriate solvent and the stoichiometric amount of (nia) or (denia) was added under stirring. After few minutes of reaction of the mixture under stirring, the stoichiometric amount of appropriate acid (2-chloro- or 2-bromobenzoic acid) was added. The obtained products were filtrated off, washed with water and dried in air at ambient temperature.

Measurement

The contents of C, H and N were determined by elemental analysis. Thermal properties were studied with a Derivatograph OD 102 (MOM) Budapest in air atmosphere with a sample mass of 150 mg and from room temperature up to ~ 1500˚C. A heating rate was 10˚C min^{-1} and it was chosen for all measurements.

Results and discussion

The analytical data of the studied complexes, reported in Table 1, show a good agreement between the experimental and calculated data.

The thermal decomposition data of the compounds I-IV are shown in Table 2.

Tab. 1 Analytical data of studied compounds
Tab. 1 Analytické údaje študovaných zlúčenín

Complex		Theoretical %				Experimental %			
		C	H	N	Cu	C	H	N	Cu
$Cu\ (2\text{-}Clbz)_2\ (nia)_2\ (H_2O)_2$	(I)	42.68	3.69	8.55	9.70	47.70	3.67	8.53	9.69
$Cu(2\text{-}Brbz)_2(nia)_2\ (H_2O\ )_2$	(II)	41.18	3.25	7.53	8.54	42.24	3.23	7.61	8.51
$Cu(2\text{-}BClbz)_2(denia)_2\ (H_2O)_2$	(III)	52.95	5.20	7.26	8.11	53.23	5.26	7.30	8.28
$Cu\ (2\text{-}Brbz)_2(denia)\ (H_2O)_2$	(IV)	48.00	4.75	6.53	7.37	47.70	4.71	6.55	7.42

Tab. 2 Thermal decomposition data of the compounds I-IV
Tab. 2 Termické údaje zlúčenín I-IV

Complex	DTG		TG	
	T_{max} / °C	Temp. interval / °C	Δm(found/calc.) / %	Lost component
I	69	42 – 134	5.50/5.50	2 H_2O
	219	134 – 420	61.00/61.04	$(nia)_2$ + (2-Clbz)
	568	420 – 660	24.00/23.75	(2-Clbz)
II	80	46 – 141	5.00/4.84	2 H_2O
	219	141 – 422	59.50/59.71	$(nia)_2$ + (2-Brbz)
	618	422 – 729	26.50/26.89	(2-Brbz)
III	141	53 – 194	6.30/6.00	$2H_2O$
	351	194 – 482	62.6/62.7	$(denia)_2$+ (2-Clbz)
	664	482 – 798	54.5/54.8	(2-Clbz)
IV	138	52 – 216	4.2/4.1	H_2O
	341	216 – 488	41.8/41.8	$(denia)_2$ + (2-Brbz)
	682	488 – 775	46.7/46.5	(2-Brbz)

Hutnické listy č. 7/2013, roč. LXVI
ISSN 0018-8069

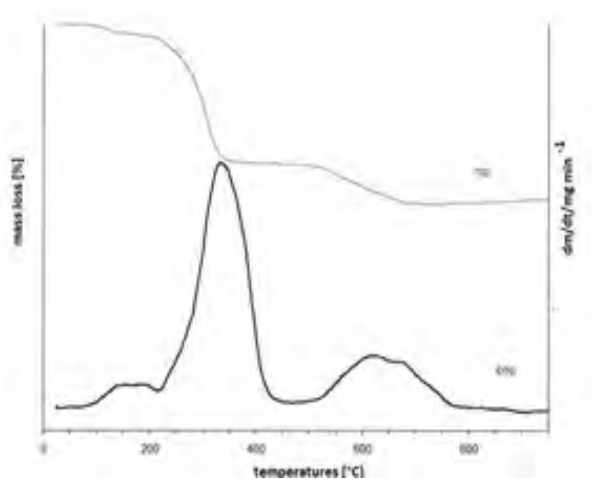

Fig. 1 TG and DTG curves of $Cu(2\text{-}Brbz)_2(denia)_2(H_2O)_2$
Obr. 1 TG a DTG kriviek $Cu(2\text{-}Brbz)_2(denia)_2(H_2O)_2$

Thermal decompositions of the studied compounds are multi-stage processes (Fig. 1 can be used as example). The subsegment detachment of the ligands was observed. The final solid product was always CuO. The DTG curves of the complexes (I) and (II) indicate (Table 2) that they are thermally stable up to ~ 42-46 ˚C. In relation to these temperatures, the successive decomposition to CuO begins. This is followed by three mass-loss steps. These steps were attributed to the formation of two intermediate products, such as $Cu(2\text{-}Xbz)_2(nia)_2$ and Cu(2-Xbz)(X = Cl or Br). All the process of the decomposition was connected with formation of final product CuO. The thermal decomposition scheme is as follows:

$$[Cu(2–Xbz)_2(nia)_2(H_2O)_2] \rightarrow Cu(2Xbz)_2(nia)_2 \quad (I)$$

$$Cu(2–Xbz)_2(nia)_2 \rightarrow Cu(2–Xbz) \quad (2)$$

$$Cu(2–Xbz) \rightarrow CuO \quad (3)$$

The obtained results correlate with the thermal decomposition of similar complexes with N,N – dietylnicotinamide (denia) (Table 2).

Conclusions

In relation to the all studied compounds, losses of decomposition products [$2H_2O$, 2 nia or 2 denia + Cu (2-Xbz) and Cu(2-Xbz)] occur (on the TG and DTG curves) in three steps. The first step of decomposition is always connected with release of water molecules in the case of all studied compounds. The thermal stability of the studied compounds can be ordered in this way: (I)<(II)<(IV)<(III).

Literature

[1] JÓNA, E., LAJDOVÁ, L., KVASNICOVÁ, L., LEDVAYOVÁ, S., PAJTÁŠOVÁ, M., ONDRUŠOVÁ, D., LIZÁK, P., MOJUMDAR, S.C. Thermal properties of solid complexes with biologicalls important heterogcilc ligands. Part III. *J. Termal. Anal Calorim.* 2011, 10, p. 817-821

[2] JÓNA, E., LAJDOVÁ, L., LODUHOVÁ, M., LEDVAYOVÁ, S., PAVLÍK, V., MONCOL, J., LIZÁK, P., MOJUMDAR, S.C. Thermal properties of solid complexes with biologicalls ipomrtant hererogalic ligands. Part IV. *J. Thermal. Anal. Calorim.* 2012, 108, p. 921-926

[3] PAJTÁŠOVÁ, M., ONDRUŠOVÁ, D., JÓNA, E., MOJUMDAR, S.C., LALIKOVÁ, S., BAZYLÁKOVÁ, T., GREGOR, M. Spectral and thermal characteristics of copper (II) carbozylates with fatty acid chains and their benzothiazole adducts. *J. Thermal. Anal. Calorim*. 2010, 10, p. 769-767

[4] MORICOVÁ, K., JÓNA, E., PLŠKO, A., MOJUMDAR, S.C. Thermal stability of $LiO.SiO_2.TiO_2$ gels evaluated by the induction period of crystallization. *J. Thermal. Anal. Calorim.*, 2010, 150, p. 817-820

[5] MOJUMDAR, S.C., MELNÍK, M., JÓNA, E. Thermal and IR properties of Mg(III) complexes with heterogclic ligands. *Thermochim. Acta*, 2000, 352-353, p. 127-132

[6] MAKARA, G.M., KESERN, G.M., KAJTÁR-PEREDY, M., ANDERSEN, W.K. Nuclear magnetic resonance and molecular modeling study on my co phenolic acid. *J. Med. Chem.,* 1996, 39 p. 1236-1242

Calculation of the Apparent Activation Energy of the Relaxation Transitions in Polymeric Materials

Výpočet aktivačnej energie relaxačných prechodov polymérnych materiálov

doc. Mgr. Ivan Kopal, Ph.D.[1]

[1]University of Alexander Dubček in Trenčín, Faculty of Industrial Technologies in Púchov, I. Krasku 491/30, 020 01 Púchov, Slovak Republic

The frequency multiplexing experiments carried out using dynamic mechanical analysis provide quantification of the apparent activation energy of the relaxation transitions in polymeric materials on the basis of application of Arrhenius equation. This approach is focused on an Arrhenius plot. Over a limited frequency range, this plot represents a straight line. There is the slope of the best-fit line of Arrhenius plot yields apparent activation energy. The program code is written in the software system Matlab® which is also introduced in this study. It provides an automatic quantification of the apparent activation energy of the relaxation transitions in polymeric materials from frequency multiplexing temperature scans of damping factor and dynamic loss modulus. This program code is extended with author's short notes and it is free for any non-commercial applications.

Keywords: *DMA, apparent activation energy, relaxation transitions, Arrhenius plot*

Dynamická mechanická analýza predstavuje jednu z najvhodnejších metód vyšetrovania relaxačných javov rôznych materiálov. Kľúčovým relaxačným procesom pre akýkoľvek materiál je pritom sklovitý prechod pri teplote T_g, ktorý je častokrát označovaný termínom α-prechod alebo α-relaxácia. Nakoľko oblasť sklovitého prechodu predstavuje pomerne široký interval teplôt bez diskontinuálnej zmeny T_g, za teplotu sklovitého prechodu sa obvykle považuje stred tohto intervalu. Amorfné polymérne materiály pod touto teplotou zvyčajne vykazujú jeden, prípadne viacero sub-T_g relaxácií, resp. sekundárnych relaxácií, ktoré sa označujú ako β, γ a δ prechody a objavujú sa v poradí klesajúcej teploty. Relaxačné prechody polymérov súvisia s rôznymi konformačnými zmenami makromolekulových reťazcov pri rozličných teplotách a môžu nastať až po prekonaní energetickej bariéry, brániacej ich príslušným pohybom, na čo je potrebné dosiahnutie aktivačnej energie. Hodnotu aktivačnej energie pre jednotlivé relaxačné prechody je možné kvantifikovať prostredníctvom dynamickej mechanickej analýzy polymérov realizovanej metódou multifrekvenčných skenov, pri ktorej je vzorka vyšetrovaného materiálu podrobená malému vonkajšiemu cyklickému namáhaniu sinusoidálneho typu s viacerými rôznymi frekvenciami aplikovanými simultánne. Závislosť stratového modulu alebo stratového faktora od teploty pri rôznych frekvenciách umožňuje zostrojiť Arrheniov graf v tvare závislosti logaritmu aplikovanej frekvencie od prevrátenej hodnoty teploty ich maxima. Ak bude mať táto závislosť lineárny charakter, potom smernica jej najlepšieho fitu lineárnou funkciou determinuje hodnotu aktivačnej energie relaxačného prechodu. V tejto práci je uvedený voľne šíriteľný Matlab® kód umožňujúci automatickú kvantifikáciu aktivačnej energie relaxačných prechodov polymérnych materiálov z multifrekvenčných teplotných skenov ich stratového faktora, ktorý je doplnený o stručné autorské komentáre a použiteľný aj pre dynamický stratový modul.

Kľúčové slová: *DMA, formálna aktivačná energia, relaxačné prechody, Arrheniov graf*

Dynamic mechanical analysis (DMA) represents one of the most appropriate methods to investigate relaxation events of various materials. A key relaxation process in any material is a glass transition at a temperature T_g, which is frequently referred to as an α-transition or as α-relaxation. The T_g point is defined as a temperature at which the amorphous materials experience a physical change from a hard and brittle condition to very flexible rubbery-like state. Because of the glass transition event covers a range of temperatures without discontinuity in measured T_g, T_g is generally taken as a mid-point of this range [1]. For amorphous polymers, besides the glass transition, one or more sub-T_g phenomenon can be also main chain or the large side movement and γ-transition relates to the movements occurring in the side chain of observed. They are referred to β, γ and δ transitions at temperatures T_β, T_γ and T_δ and appear in order of the descending temperature. These transition processes are result of local segmental motions occurring in glassy state. They are determined by different conformational changes in the polymer chains at different temperatures; they determine structure and affect all properties of polymeric materials. By local is meant that only a small group of atoms are involved in the sub-T_g processes the pure existence of which proves that material in glassy state is a dynamic one. The glass transition occurs when large segments of polymer chains start moving, β-transition is related to either localized movement in the polymers. The δ-transition is related to very small motions within polymer macromolecule [2]. Each

Hutnické listy č.7/2013, roč. LXVI
ISSN 0018-8069

transition event can occur after exceeding of energy barrier which inhibits a particular macromolecular polymeric chain movement. Focus of this study is activation energy E_a itself and it is required to exceed energy barrier. It is quantified and based on results from DMA analysis for chosen polymeric material.

Dynamic mechanical analysis

The DMA represents a technique set for registration of viscoelastic material response to an external cyclic mechanical sinusoidal load. Consecutive analysis of this response allows determination of storage modulus E', loss modulus E'', loss factor tan δ and other material characteristics as a function of temperature, frequency, time, stress, as well as atmosphere or as a combination of these parameters [3]. The results of DMA tests are typically provided as a plot of E', E'' and tan δ versus temperature, time or frequency of the mechanical load of material sample with defined geometrical shape. The storage modulus E' refers to the ability of a material to store the energy and it is related to the stiffness of the material. The dynamic loss modulus E'' represents the heat dissipated by the sample as a result of material's given molecular motions and this reflects the damping characteristics of the polymer. The loss factor tan δ is the ratio of E' and E'' which are components of complex modulus E^* representing the ratio of the dynamic stress to dynamic strain [4]. Functional dependencies of E', E'' and tan δ on temperature enable the identification of all above mentioned transition temperatures [5] as well as determination of several important polymeric material characteristics [6].

One of powerful means for analyzing polymers by DMA is through the use of frequency multiplexing experiments. In this approach, a sample is simultaneously subjected to a number of different frequencies (five or more) in order to clearly define the effects of frequency, or time on the mechanical responses exhibited by the polymer. From results of dynamic viscoelastic measurements via the frequency multiplexing mode of DMA, the apparent activation energy of various relaxation transitions can be investigated. In this study, we present a method of calculation of apparent activation energies of polymer´s transition events upon the DMA frequency multiplexing curves using Matlab® code listed below.

An example of typical DMA frequency multiplexing curves for five DMA frequencies is shown on Fig. 1.

The extracted sections of the functional dependency tan δ versus temperature for applied DMA frequencies 0.5, 1, 2, 5 and 10 Hz in the temperature ranges from – 100 °C to 80 °C and from 100 °C to 145 °C are presented in Fig. 2 and Fig. 3. This extraction allows us to study relaxation transitions areas occurring around maximum tan δ values with more details.

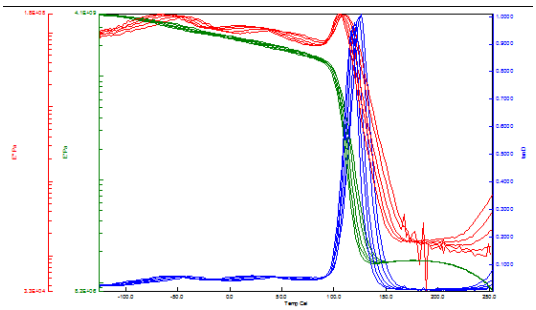

Fig. 1 Example of frequency multiplexing DMA curves
Obr. 1 Príklad typických multifrekvenčných DMA kriviek

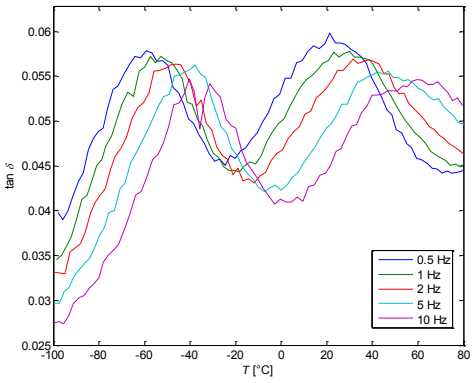

Fig. 2 The tan δ curves in the range from – 100 °C to 80 °C
Obr. 2 Krivky tan δ v intervale teplôt od – 100 °C to 80 °C

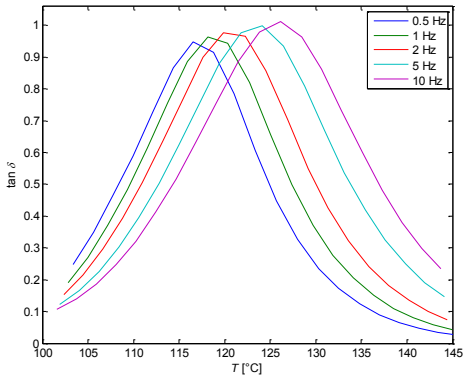

Fig. 3 The tan δ curves in the range from 100 °C to 145 °C
Obr. 3 Krivky tan δ v intervale teplôt od 100 °C to 145 °C

Calculation of apparent activation energies of relaxation events of polymers

The apparent activation energy E_a for glass transition of polymers is interpreted as a height of energy barrier that has to be overcome by the relative translational motion of chain segments for the transition to occur. The E_a may be based on many effects that produce cumulative results when material is stressed. It is very similar to the concept of activation energy but it relates to a probability of not exceeding some measurable attribute [7]. The shift in the tan δ peak temperature with respect to the applied DMA frequency increase can be used to assess the apparent activation energy E_a associated with the polymer. An Arrhenius plot can be produced in which the log f of the frequency f is plotted against the inverse of tan δ peak temperature $1/T$. Over a limited frequency range, the

response is linear and the slope of the best-fit line yields the apparent activation energy E_a [8]. The Arrhenius plot for the temperature interval from 100 °C to 145 °C is presented on Fig. 4. The quality of fitting process is documented on Fig. 5 in the form of future observation results prediction with a 95 % confidence bounds level. Finding the best fit, ln f values at 1 Hz and 2 Hz fr[illegible]

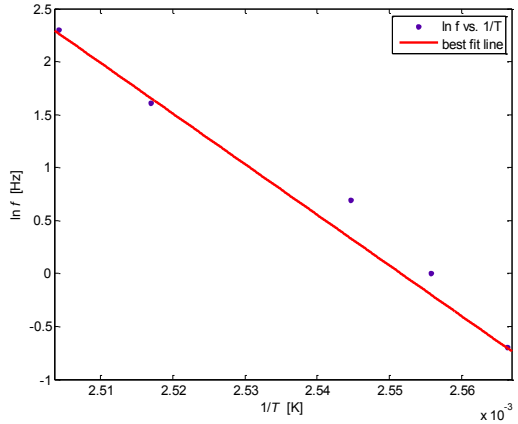

Fig. 4 The Arrhenius plot for the range from 100 °C to 145 °C

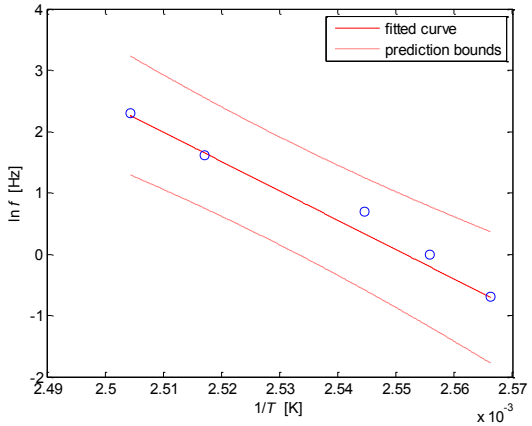

Fig. 5 The prediction of future results with 95 % confidence bonds level

Obr. 5 Predikcia budúcich výsledkov s 95 %-ným intervalom spoľahlivosti

Matlab® code

Following computer program for calculation of the apparent activation energy was created in MATLAB® environment and it is considered to be a freeware code for non-commercial use. It is assumed that result of the DMA frequency multiplexing analysis is stored in the variable data (i, j) where all odd columns j contain temperatures and even columns contain corresponding tan δ values for individual frequencies. The code can be used for loss modulus analysis as well. The glass transition value of E_a is located in a range from 170 to 840 kJ/mol, whereas sub-T_g relaxations have apparent activation energy in the range from 40 kJ/mol to 80 kJ/mol [9].

```
% apparent activation energy computation

Ts = 100;                   % starting temperature
Te = 145;                   % final temperature
f = [0.5 1 2 5 10];         % vector of frequncies
a = [ 2 3]                  % exclude frequency
i = 1;                      % counter setting
for j = 1 : 2 : size(data,2)
    % temperature matrix for individual frequencies
    T(:,i) = data(:,j);
    Tan(:,i) = data(:,j+1);
    i = i + 1;              % counter setting
end
for i = 1 : length(f)
    % inicial temperature index
    s = find(T(:,i) >= Ts,1,'first');
    % terminal temperature index
    e = find(T(:,i) <= Te,1,'last');
    % selected temperature range
    selT = T(s:e,:);
    % corrensponding tan Delta range
    selTan = Tan(s:e,:);
end

% maximum tan Delta from selection
i = max(max(selTan));
% tan Delta(T) thermal dependecy representation
figure, plot(selT,selTan)
axis([Ts Te 0 i+0.05*i])    % axis border set
xlabel('\itT \rm[°C]')      % axis x title
ylabel('tan \it\delta')     % axis y title
legend('show')              % legend display

% maximum tan Delta values and their indexes
[maxTan,indTan] = max(selTan);
% corresponding temperature for tan Delta maximum
for i = 1 : length(f)
   TmaxTan(i) = selT(indTan(i),i);
end
% natural logarithm of frequency
F = log(f);
% inverse absolute temperature
K = 1./(273.15 + TmaxTan);

% create a new figure
figure
% createFit function calling
[cf_,gof] = createFit(K,F,a);

% activation energy calculation
Ea = - cf_(1)*8.314472/1000

% createFit Function

function [cf_,gof] = createFit(K,F,a);

% Set up figure to receive datasets and fits
f_ = clf;
figure(f_);
set(f_,'Units','Pixels','Position',[474 58 824 592]);
legh_ = []; legt_ = {};     % handles and text for legend
xlim_ = [Inf -Inf];         % limits of x axis
```

```
ax_ = axes;
set(ax_,'Units','normalized','OuterPosition',[0 0 1 1]);
set(ax_,'Box','on');
axes(ax_); hold on;
 % Plot data originally in dataset "F vs. K"
K = K(:);
F = F(:);
h_ = line(K,F,'Parent',ax_,'Color',[0.333333 0
0.666667],...
   'LineStyle','none', 'LineWidth',1,...
   'Marker','.', 'MarkerSize',12);
xlim_(1) = min(xlim_(1),min(K));
xlim_(2) = max(xlim_(2),max(K));
legh_(end+1) = h_;
legt_{end+1} = 'F vs. K';

% Nudge axis limits beyond data limits
if all(isfinite(xlim_))
    xlim_ = xlim_ + [-1 1] * 0.01 * diff(xlim_);
    set(ax_,'XLim',xlim_)
else
    set(ax_, 'XLim',[0.0025036892693109576,
    0.0025668549839077703]);
end

% Apply exclusion rule "excF"
if length(K)~=5
   error('Exclusion rule ''%s'' is incompatible with
''%s''.','excF','K');
end
ex_ = false(length(K),1);
ex_(a) = 1;
ok_ = isfinite(K) & isfinite(F);
if ~all( ok_ )
    warning( 'GenerateMFile:IgnoringNansAndInfs', ...
    'Ignoring NaNs and Infs in data' );
end
ft_ = fittype('poly1');

% Fit this model using new data
if sum(~ex_(ok_))<2          % too many points excluded
   error('Not enough data left to fit ''%s'' after applying
exclusion rule ''%s''.','fit 1','excF')
else
   % cf_ = fit(K(ok_),F(ok_),ft_,'Exclude',ex_(ok_));
   [cf_,gof] = fit(K(ok_),F(ok_),ft_,'Exclude',ex_(ok_));
end
% Or use coefficients from the original fit:
if 0
   cv_ = { -44037.454547060683,
112.52896728006966};
   cf_ = cfit(ft_,cv_{:});
end

 % Plot this fit
h_ = plot(cf_,'fit',0.95);
legend off;  % turn off legend from plot method call
set(h_(1),'Color',[1 0 0],...
   'LineStyle','-', 'LineWidth',2,...
   'Marker','none', 'MarkerSize',6);
legh_(end+1) = h_(1);
legt_{end+1} = 'fit 1';

% Done plotting data and fits
hold off;
leginfo_ = {'Orientation', 'vertical', 'Location',
'NorthEast'};

% create legend
h_ = legend(ax_,legh_,legt_,leginfo_{:});
set(h_,'Interpreter','none');
xlabel(ax_,'');      % remove x label
ylabel(ax_,'');      % remove y label
xlabel('1/\itT  \rm[K]')
ylabel('ln \itf  \rm[Hz]')
h_ = figure, plot(cf_,'predobs',0.95);
hold on, plot(K,F,'o')
xlabel('1/\itT  \rm[K]')
ylabel('ln \itf  \rm[Hz]')
```

Conclusions

In this study, there is the freeware Matlab® code which allows the automatic calculation of apparent activation energy of relaxation transitions in polymeric materials by means of DMA frequency multiplexing tan δ as well as storage modulus temperature curves.

Literature

[1] MENARD, K. *Dynamic Mechanical Analysis: A Practical Introduction*. 2nd ed., CRC Press, 1999, ISBN-10 1420053124, p. 438

[2] DROBNY, J.G. *Handbook of Thermoplastic Elastomers: 9 - Thermoplastic Polyurethane Elastomers.* Elsevier, 2009, ISBN 978-0-8155-1549-4, p. 215-234

[3] LIPTÁKOVÁ, et al. *Polymérne konštrukčné materiály.* Žilinská univerzita, Slovakia, 2012, ISBN 978-80-554-0505-6, p. 189

[4] KREVELEN, V., NIJENHUIS, A. *Properties of Polymers.* Elsevier Science, 2009, ISBN 9780080548197, p. 1032

[5] PASTOREK, M., KRMELA, J., KOVÁČ, K. *Určenie modulu pružnosti osobných plášťov pneumatík.* In: TechMat´12. Pardubice: Univerzita Pardubice, 2012, ISBN 978-80-7395-537-3. p. 83-89

[6] UHERKOVÁ, S., SLALKOVÁ, P., JÓNA, E., KOVÁČ, K., PAVLÍK, V. *Preparation of PVA/SO Blends and Study of their thermo.mechanical Properties.* In: Polyméry 2012. Bratislava: SAV, 2012, ISBN 978-80-970923-0, p. 54-55

[7] MANZUR, A., HERNANDEZ-SANCHEZ, F. *Activation Energy for the Glass Transition of a Confined Elastomer in HDPE/PP Blends*. In: Journal of Macromolecular Sciencew, Part B: Physics, 2006, vol. 45, ISSN 0022-2348, p. 139–152

[8] ALVEZ, N.M, et al. *Molecular mobility in a thermoset as seen by TSR and DMA near Tg*. In: Mat Res Innovat, Springer, 2001, No. 4, ISSN 1433-075X, p. 170-178

[9] NOBUAKI O. *Activation Energy Analysis by Dynamic Viscoelastic Measurements*. In: DMS, 2012, no. 7, p. 1-3

Detection of Primary and Secondary Relaxation Transitions in Hardened Polyurethane by Two Different Methods

Zisťovanie primárnych a sekundárnych relaxačných prechodov tvrdeného polyuretánu pomocou dvoch rôznych metód

Ing. Karol Kováč[1], **doc. Mgr. Ivan Kopal, PhD.**[1]

[1]University of Alexander Dubček in Trenčín, Faculty of Industrial Technologies, I. Krasku 491/30, 020 01 Púchov, Slovak Republic

This article deals with the detection of primary and secondary relaxation transitions in hardened polyurethane which was used as a matrix in a nanocomposite filled by single walled carbon nanotubes. We used the pulse transient method for measurement of the thermophysical parameters (thermal diffusivity, thermal conductivity and specific heat capacity) in temperature range from 348.15 K to 448.15 K and in relation to the given measurement procedure, Transient Tester 1.02. was used as the special device to obtain all the important data for the evaluation and analysis of the measurement. The measuring of viscoelastic properties was closely connected with utilization of the dynamic mechanical analysis in temperature range from 150 K to 520 K using the device Perkin Elmer DMA Diamond while the liquid nitrogen was used for cooling the samples. Both used methods confirmed the secondary relaxation β transition. By using dynamic mechanical analysis, the primary relaxation transition, glass transition and the secondary relaxation transition, γ transition were detected.

Keywords: *Dynamic Mechanical Analysis, relaxation transitions, polyurethane, Pulse Transient Method*

Tento článok je zameraný na zistenie primárnych a sekundárnych relaxačných prechodov v tvrdenom polyuretáne, ktorý je použitý ako matrica v nanokompozite plnenom jednostennými uhlíkovými nanorúrkami. Tento materiál bol vyrobený v Trnave zmiešaním dvoch chemicky rozdielnych zložiek: polyolu a izokyanátu. Následne bol vytvrdený použitím vysokého tlaku, aby dosiahol tlakový modul pružnosti a koeficient stlačiteľnosti v rozsahu 20 - 60 MPa. Na prvé meranie bola použitá pulzná prechodová metódu na určenie troch základných termofyzikálnych parametrov (tepelnej vodivosti, teplotnej vodivosti a hmotnostnej tepelnej kapacity). Tieto merania boli vykonané na zariadení 1.02 Transient Tester v teplotnom rozsahu od 248,15 K do 348,15 K pri teplotnom kroku 10 K. Jedno meranie trvalo 7 minút a dve hodiny sa vzorka teplotne stabilizovala. Každé meranie bolo opakované šesťkrát, pričom vypočítaná relatívna odchýlka merania bola pri každej teplote menšia ako 1 %. Druhá použitá metóda bola dynamická mechanická analýza vykonaná na zariadení Perkin Elmer DMA Diamond, na ktorom boli namerané viskoelastické parametre (elastický modul, stratový modul a stratový faktor). Merania na DMA boli vykonané v teplotnom rozsahu od 150 K do 520 K pri aplikovanej frekvencií 1 Hz. Vzhľadom ku vysokej spotrebe kvapalného dusíka pri takýchto nízkych teplotách bolo vykonané len jedno meranie. Analyzovaním teplotnej závislosti hmotnostnej tepelnej kapacity sme zistili, že táto závislosť má dvoj lineárny charakter, pričom teplota pri ktorej dochádza k zlomu linearity je 288,15 K. Táto závislosť má stúpajúci charakter, pričom analytické riešenie tejto závislosti potvrdilo výraznú zmenu stúpania za uvedenou teplotou. Pomocou dynamicko mechanickej analýzy bol identifikovaný sekundárny β prechod pri teplote 290 K a sekundárny γ prechod pri teplote 215 K z teplotnej závislosti stratového modulu. Teplotná závislosť elastického modulu preukázala sklený prechod pri teplote 380 K.

Kľúčové slová: *dynamická mechanická analýza, relaxačné prechody, polyuretán, pulzná prechodová metóda*

Polyurethanes represent one of the most versatile plastic materials. The nature of chemistry allows polyurethanes to be adapted to solve many challenging problems, to be molded into unusual shapes and to enhance industrial and consumer products by adding comfort, warmth and convenience to our lives. Polyurethanes are formed by reaction of a polyol with a diisocyanate in the presence of suitable catalysts and additives. Because a variety of diisocyanates and a wide range of polyols can be used to produce polyurethanes, a broad spectrum of various materials can be produced to meet the needs of specific applications. You need not to look for polyurethane because you can find it almost everywhere. Polyurethanes can be found in mattresses and couches, insulations, liquid coatings, paints, tough elastomers such as roller blade wheels, soft flexible foam toys, some elastic fibers and many other places and applications [1].

Polymers, nanocomposites, concretes, glasses, steels, ceramics are representatives of the materials which can be characterized by applications as materials in markedly nonequilibrium states. In the study of polymers and their applications, it is very important to understand the

Hutnické listy č.7/2013, roč. LXVI
ISSN 0018-8069

concept of the primary and secondary relaxation transitions. For these materials, the study of relaxation transitions is important for detection:

a) at which temperature material changes its physical properties,
b) at which temperature material losses its mechanical properties and
c) at which temperature material degrades [2,3].

Material

In this work, we study the hardened polyurethane, which will be used as a matrix in nanocomposite filled by the single walled carbon nanotubes. Our polyurethane was synthesized from PX 522/HT POLYOL and PX 521-522 HT ISO ISOCYANATE. The mixing was carried out in a vacuum chamber for degassing of a polymerization mixture. Subsequent curing process was carried out for 4 hours at 80 °C and for 16 hours at 100 °C. Each sample was pressed by the displacement speed of 2 mm /min to a force of 100 kN. Pressure modulus and the coefficient of compressibility were in the 20-60 MPa range of tension..

Pulse transient method

The pulse transient method can be used for determination of three basic thermophysical parameters – thermal conductivity, thermal diffusivity and specific heat capacity from only one measurement. The basic principle of this method is to supply the heat pulse through the planar heat source to the specimen, which had its temperature stabilized before the measurement. Using a thermocouple, that is located on the opposite side of the sample as a heat source, we can record the dynamic thermal response. In the Fig. 1, the principle of the pulse transient method is shown [4].

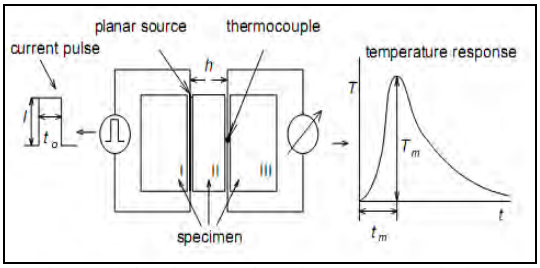

Fig. 1 The principle scheme of the pulse transient method [3]
Obr. 1 Principiálna schéma pulznej prechodovej metódy [3]

Our specimen set had three pieces of cylindrical shape, because we needed to simulate an unbounded specimen which was placed in the isothermal vacuum chamber. The nickel folium 20 μm thick heat source with radius of 0.015 m was placed between the first and the second part and it had the same radius as the specimen. The live connection of a 30 nm thick differentially connected Chromel-Alumel thermocouple was placed between the second and the third part of the specimen set. The second connection of the thermocouple was placed on heat exchanger. The constant temperature was kept there by help of thermostat and it was measured by using 100 Ω platinum resistance. Heating up of the sample was provided by a current pulse for the duration of 13 s at the driving voltage of 1.4 V and a supply electric current was 1 A. The temperature response of specimen was measured during 420 s. The time of temperature stabilization of specimen at each temperature was 120 minutes.

DMA - dynamic mechanical analysis

The Dynamic mechanical analysis is one of the most sensitive methods which can be used for characterization and interpretation of mechanical behavior of material. The principle of this method is based on monitoring viscoelastic response of material, which is loaded by small oscillation strain [5]. DMA distributes the viscoelastic response of material in relation to two components of dynamic modulus:

- real component which represents elastic modulus *E*',
- imaginary component which represents loss modulus *E*''.

We used dynamical mechanical analysis for detection of primary as well as secondary relaxation transitions in polymeric structures and this analysis was also used for the characterization of the viscoelastic behavior in long range temperature interval from 150 K to 520 K at a constant heating rate of 3 K per minute. DMA was performed by help of Perkin Elmer Diamond DMA with tension clamp mode at frequency 1 Hz. We can make measurements from temperature 120 K by using liquid nitrogen. All specimens had the same rectangular shape (30 mm x 6 mm x 1,5 mm).

Results and discussion

In the Fig. 2, we can see the temperature dependency of elastic modulus and loss modulus which are presented in logarithmic scale. We can also see the temperature dependency of the loss factor which is presented according to the secondary scale. From the first view, the primary relaxation transition – glass transition can be seen at temperature approximately 380 K. This relaxation transition is caused by the tearing of hydrogen bridges or by the weakening of interactions – Van der Waals forces.

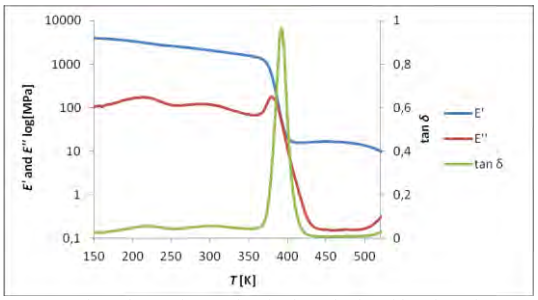

Fig. 2 Complete dynamic mechanical analysis of hardened polyurethane at frequency 1 Hz
Obr. 2 Kompletná dynamická mechanická analýza tvrdeného polyuretánu pri frekvencii 1 Hz

In the Fig. 3, we present the temperature dependency of loss modulus *E*". We detected the local maximum at temperature about 380 K which represents the glass transition. We detected two other maximums which represent secondary transitions. Loss modulus shows the local maximum at temperature about 290 K and it corresponds to the secondary relaxation transition β. This transition is a result of movement of side chains and neighboring atoms of the main chain of the tested polyurethane. The loss modulus has also a third local maximum which represents the secondary transition γ at temperature 215 K. This transition may be caused by movement of soft and hard segments, of which our hardened polyurethane is composed, because it contains isocyanate and alcohol groups.

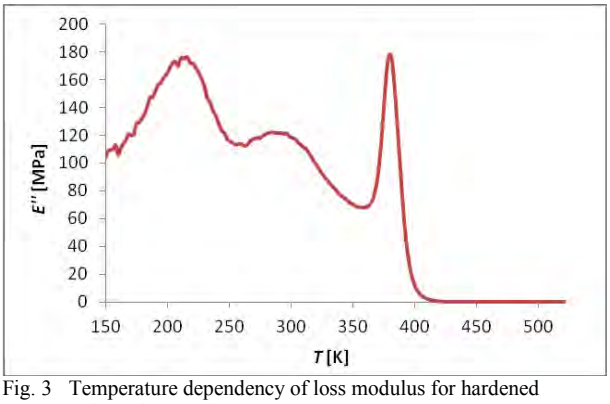

Fig. 3 Temperature dependency of loss modulus for hardened polyurethane at frequency 1 Hz
Obr. 3 Teplotná závislosť stratového modulu pre tvrdený polyuretán pri frekvencii 1 Hz

In the Fig. 4, we can see the temperature dependency of specific heat capacity in a wide temperature range from 248.15 K to 341.5 K. From the first view we can say that specific heat capacity has a significantly increasing character in the dependency on temperature. It is seems as a two linear dependency. From this dependency, we detected the secondary β transition approximately at temperature 288.15 K.

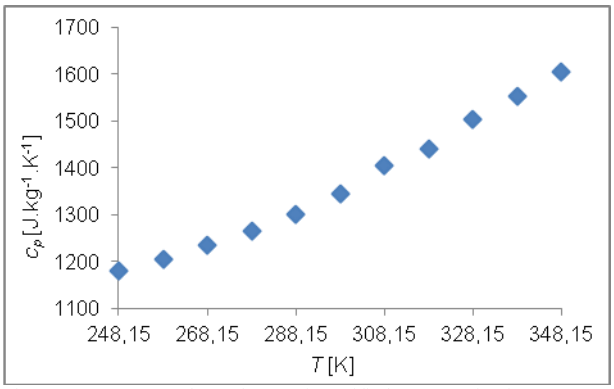

Fig. 4 Temperature dependency of specific heat capacity for hardened polyurethane
Obr. 4 Teplotná závislosť špecifickej tepelnej kapacity pre tvrdený polyuretán

From temperature 288.15 K, the increase of specific heat has a steeper character and it we can see in the Fig. 5. We made a linear regression with analytical equations for two parts of this functional dependency. From these two equations, which describe the linear dependencies, the coefficients 3.0136 and 5.1112 are very important. These coefficients represent the level of increase of the determined analytical curves.

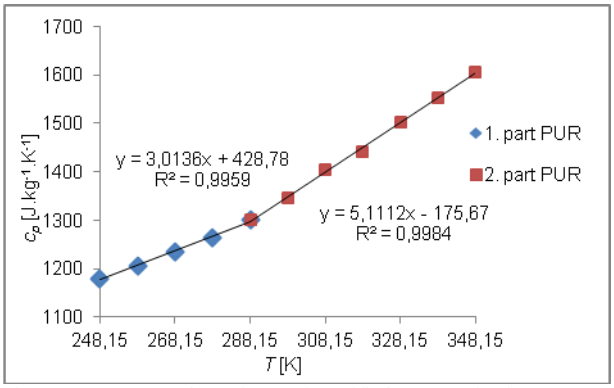

Fig. 5 Temperature dependency of specific heat capacity for hardened polyurethane and its analytical solution
Obr. 5 Teplotná závislosť špecifickej tepelnej kapacity pre tvrdený polyuretán a jej analytické riešenie

Conclusions

We detected the primary relaxation transition - glass transition at temperature 380 K, secondary relaxation transition β at temperature 290 K and secondary relaxation γ at temperature 215 K by using dynamic mechanical analysis.

Using the pulse transient method, we confirmed secondary relaxation transition β by analysis of the temperature dependency of specific heat capacity at temperature 288.15 K.

Literature

[1] DROBNY, J.G. *Handbook of Thermoplastic Elastomers: 9 - Thermoplastic Polyurethane Elastomers.* Elsevier, ISBN 978-0-8155-1549-4, 2007, p. 215-234

[2] STRUIK, L.C.E. *Volume relaxation and secondary transitions in amorphous polymers*. Polymer. 1987, vol. 28, issue 11, 1987, p. 1869-1875

[3] CHEN, S., WANG, Q., WANG, T. *Damping, thermal, and mechanical properties of carbon nanotubes modified castor oil-based polyurethane/epoxy interpenetrating polymer network composites.* Materials and Design. 2012, vol. 38, p. 47-52

[4] BOHÁČ, V., DIEŠKA, P., KUBIČÁR, Ľ. *The Heat Loss Effect at the Measurements by Transient Pulse Method.* Measurement Science Review. ISSN 1335-8871, 2007, vol. 7, no. 2, p. 24-27

[5] MENARD, K. *Dynamic Mechanical Analysis: A Practical Introduction.* Baca Raton, CRC Press, ISBN-10-1420053124, 2007

Hutnické listy č.7/2013, roč. LXVI
ISSN 0018-8069

Dynamical Mechanical Properties of NR/Polysaccharide Blends

Dynamicko mechanické vlastnosti zmesí NR/polysacharid

doc. Ing. Petra Skalková, PhD.[1], **Ing. Róbert Janík, PhD.**[1], **Ing. Monika Štrbáková**[1]

[1]Faculty of Industrial Technologies, University of Alexander Dubček in Trenčín, I. Krasku 491/30, 020 01 Púchov, Slovak Republic

In the last years, polymer blends have attracted the attention of researchers of polymeric materials due to the possibility of tailoring their properties by blending two or more polymers. Also, it is a fact that polymer blends have been extensively used in a large number of applications, because a certain polymeric blend may offer properties that allow its application where the individual constituting polymers would not be applied. A wide variety of procedures for analyzing elastomeric vulcanizate are available but most of them are time-intensive because of the inextractible nature of the cross-linked system. Dynamic mechanical analysis (DMA) is found to be very sensitive for characterization of glass-transition temperature, visco-elastic properties and, in particular, the adhesion between the elastomer blend and coating.

Keywords: *polymer blends, dynamic mechanical properties, polysaccharide, tensides*

Použitie kaučukov nachádza uplatnenie pri výrobe pneumatík, technickej gumy, oplášťovanie káblov, pogumovanie textilu, pri výrobe obuvi a pod. K tomu, aby sa dosiahli spracovateľské a aplikačné vlastnosti, je nutné z kaučukov a rôznych chemických prísad, pripraviť kaučukovú zmes. Chemické prísady do zmesí sú ropného pôvodu a teda majú negatívny vplyv na životné prostredie. V poslednom období sa tejto problematike venuje väčšia pozornosť, tým že sa skúšajú nahradiť biopolymérmi, ktoré majú pozitívny vplyv na životné prostredie a sú biologicky odbúrateľné. K uvedeným biopolymérom patria polysacharidy, najmä škrob, celulóza, lignín a ich deriváty. Polysacharidy sú obnoviteľné suroviny, ktoré sú rastlinného pôvodu. Vzájomnú nemiešateľnosť spôsobuje odlišná štruktúra syntetických a prírodných polymérov. Tento negatívny fakt je možné odstrániť pridaním tretej zložky s vhodnými vlastnosťami akými sú napr. tenzidy a kompatibilizátory. Práca sa zaoberá prípravou a štúdiom zmesí prírodného kaučuku (NR) a galaktomanánu Locust Bean Gum (LBG) s DS 0,28 v troch množstvách (0; 27,6; 55 dsk) za a bez prítomnosti tenzidu, dodecyl sulfát sodný (SDS). Množstvo tenzidu SDS v zmesi bolo 0 a 3 dsk. Sledoval sa vplyv biopolyméru LBG a tenzidu SDS na dynamicko mechanické vlastnosti, jako je elastický modul (G´), viskózny modul (G´´) a tlmiaci faktor (tgδ) elastomérnych zmesí prostredníctvom metódy DMA. Najvyššie hodnoty elastického a viskózneho modulu dosahovali plnené zmesi NR/27,6 dsk LBG/3 dsk SDS), NR/55 dsk LBG/3 dsk SDS a zmes NR/55 dsk LBG/0 dsk SDS). Prítomnosť tenzidu mala pozitívny vplyv na elastický modul G´ zmesí prírodného kaučuku plneného polysacharidom LBG. Najnižšie hodnoty elastického a viskózneho modulu mala neplnená zmes (NR/0 dsk LBG/0 dsk SDS). Množstvo plniva ovplyvňuje teplotu skelného prechodu NR/LBG/SDS zmesí. Najnižšiu hodnotu tg δ dosahovala zmes NR/27,6 dsk LBG/0 dsk DSS a zmes NR/55 dsk LBG/0 dsk DSS).

Kľúčové slová: *polymérne zmesi, dynamickomechanické vlastnosti, polysacharid, tenzidy*

Polymer blends are being used extensively in numerous applications; this statement is also true with rubber blends, especially in tyre manufacture. Apart from blends of common rubbers, specialty rubber is also being utilized, depending on service demands and components of the tyre [1-3]. Natural rubber (NR) is known to exhibit numerous outstanding properties such as good oil resistance, low gas permeability, improved wet grip and rolling resistance, coupled with high strength; having properties resembling those of synthetic rubbers. Natural rubber coming from latex is mostly polymerized isoprene with a small percentage of impurities in it. This limits the range of properties available to it, although addition of sulphur and vulcanization are used to improve the properties. Synthetic rubber is any type of artificially made polymer material which acts as an elastomer. Synthetic rubber serves as a substitute for natural rubber in many cases, especially when improved material properties are needed. A wide variety of particulate fillers are used in the rubber industry for various purposes, of which the most important are reinforcement, reduction in material costs and improvements in processing [4, 5]. Reinforcement is primarily the enhancement of strength and strengthrelated properties, abrasion resistance, hardness and modulus [6, 7].

Experiment

Materials

Natural rubber SMR 20 (NR) was purchased from Kuala Lumphur Malaizia. Sodium dodecyl sulfate (SDS) was

supplied from Aldrich. Galactomannan - Locust Bean Gum (LBG) with DS = 0.28 was supplied from Aldrich.

Preparation of NR/LBG blends

Polysaccharide LBG was melt-blended with NR in Brabender Plasti – Corder PLE 331. Mixing was performed at 80 and 90 °C and 50 rpm. The contents of LBG were 0; 27.6; 55 parts per hundred rubber (phr), respectively. SDS was used at two different amounts, namely 0 and 3 phr. Blends were vulcanized with the following formula: stearic acide, ZnO, Flavex, N-tert-Butyl-2-benzothiazolesulfenamide and sulphur. The temperature of vulcanization was 150 °C.

Dynamic mechanical analysis

Dynamic mechanical analysis (DMA) was carried out for the rubber samples in DMA Perkin Elmer, operating in the tension mode from -90 to 100 °C at frequency of 60 Hz and amplitude 20 μm with a programmed heating rate of 30 °C.min^{-1}.

Results and discussion

The sulphur molecules facilitate the breaking of the double bonds of the NR backbone by entering in between the chains of natural rubber and make new bonds with each other. The entering of sulphur molecule in between the chains of NR makes more room to accommodate LBG in between the layers of NR. Since the sulphur molecules make new bonds with NR by breaking up double bond of the NR backbone.

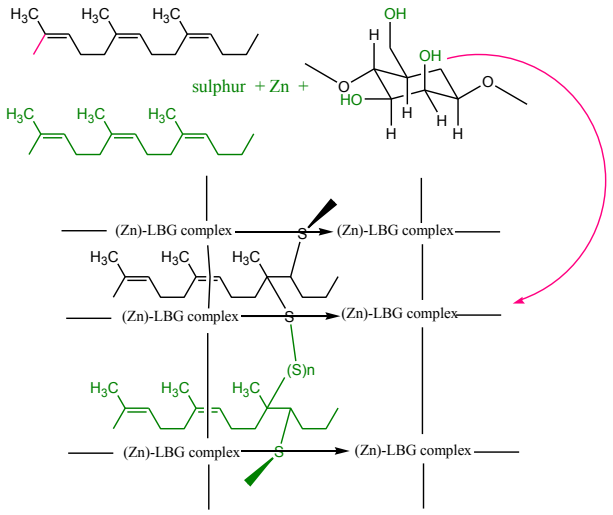

Fig. 1 Proposed mechanism for interaction of the cross linked NR/LGB blend
Obr. 1 Navrhnutý mechanizmus reakcie sieťovania NR/LBG zmesi

The filler (LBG) and the crosslinking agents enter in between the molecular chains of NR and make new bonds with each other. The breaking of the double bond in the natural rubber backbone makes two active sites and a crosslinking network between sulfur and natural rubber. In addition to that crosslinking network, LBG molecules can make a complex with zinc metal. Accelerator and crosslinking agent, like zinc oxide (ZnO) were used in the blend preparation stage to generate active sites in the NR backbone for the crosslinking of the matrix. These accelerator not only make active sites in the NR backbone by breaking the C=C double bond but also have a major role in the deprotonation of the galactomannan Locust Bean Gum and make them participate in the crosslinking network. The results suggest that zinc ion forms loose complexes with the C2 or C3hydroxyl groups of mannose. The incorporation of fillers makes interruption in the alignment process of chains [8]. When filler loading is increased, more weak interfacial regions between filler surface and rubber matrix are formed. The resultant Zn-LBG complex diminishes the crystalline nature of the blend. A reaction mechanism is suggested and is shown in Fig. 1.

Dynamic mechanical analysis (DMA) was carried out for elastomeric blends of NR with various amounts of filler and surfactant. Fig. 2, 3 and 4 show the representative plot of the effect of temperature on storage (G´), loss (G´´) moduli, and damping factor (tg δ). In Fig. 2, the characteristic sigmoidal variation of storage modulus with temperature is observed for all samples. It passes from the glassy to the rubbery state through different regions with the decrease in the stiffness of the samples [9]. Highest values of storage modulus G´ has NR/27.6phr LBG/3phr SDS blend, below Tg (-46 °C). The lowest values of G´ has NR/0phr LBG/0phr SDS blend. Presence of surfactant SDS had positive effect on storage modulus of NR blends filled with galactomannan LBG. For all blens, storage modulus G´ sharp to drops up until -50 °C.

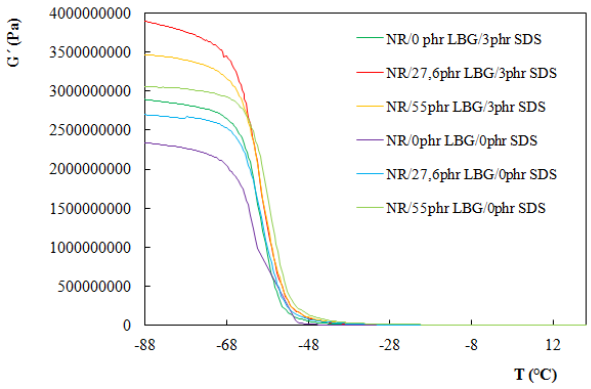

Fig. 2 Effect of temperature on storage modulus G´for elastomeric blends with different amount of LBG and SDS
Obr. 2 Vplyv teploty na elastický modul G´pre elastomérne zmesi s rôznym obsahom LBG a tenzidu SDS

The loss modulus G´´ and damping sharply increase, attaining a maxima and then dropping off with the rise in temperature, can seen on Fig. 3. Blends of NR/27.6phr LBG/3phr SDS and NR/55phr LBG/3phr SDS achieved the maximum of loss modulus G´´ at -58 °C. For NR/55phr LBG/0phr SDS this maximum of G´´ is shifted to higher values (-56 °C). The lowest value of G´´ had unfilled blend NR/0phr LBG/0phr SDS, whereby maximum of G´´ was achieved at -60,5 °C.

Hutnické listy č.7/2013, roč. LXVI
ISSN 0018-8069

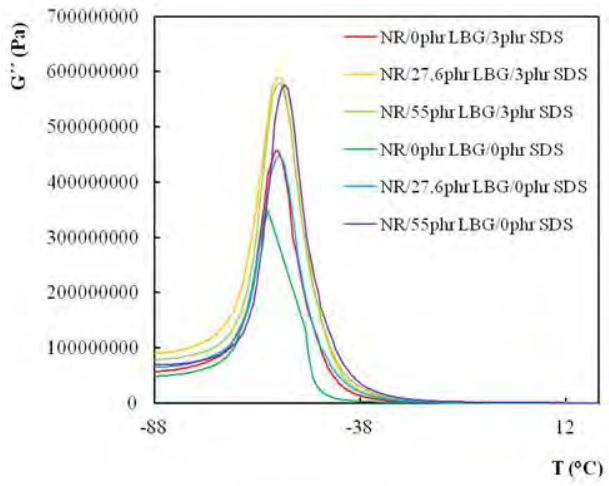

Fig. 3 Effect of temperature on loss modulus G´´for elastomeric blends with different amount of LBG and SDS
Obr. 3 Vplyv teploty na viskózny modul G´´pre elastomérne zmesi s rôznym obsahom LBG a tenzidu SDS

Fig. 4 shows the presentative plot of temperature dependence of tg δ for the elastomeric blends. One distinct transition relaxation peak for NR system is seen here. The loss modulus G´´ follows a trend similar to tg δ.

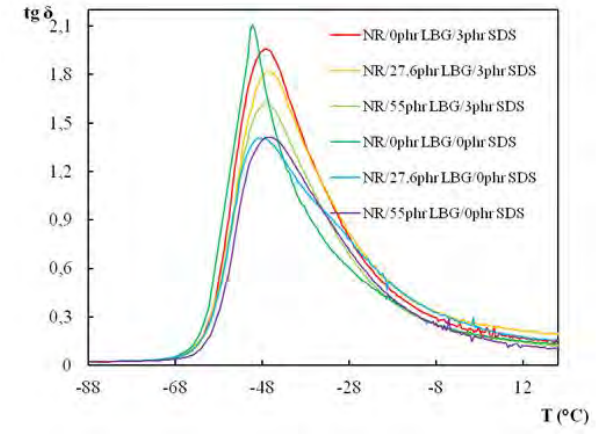

Fig. 4 Effect of temperature on damping factor tg δ for elastomeric blends with different amount of LBG and SDS
Obr. 4 Vplyv teploty na tlmiaci faktor pre elastomérne zmesi s rôznym obsahom LBG a tenzidu SDS

Tab. 1 Dynamic mechanical properties of elastomeric blends
Tab. 1 Dynamicko mechanické vlastnosti elastomérnych zmesí

	NR/0phr LGB/3phr SDS	NR/27.6phr LGB/3phr SDS	NR/55phr LGB/3phr SDS	NR/0phr LGB/0phr SDS	NR/27.6phr LGB/0phr SDS	NR/55phr LGB/0phr SDS
T_g (°C)	-47	-46	-47	-50	-49	-46
tg δ_{max}	1.96	1.82	1.62	2.12	1.40	1.42

Specific details relating to the tg δ peak temperatures and peak values for all the blends are collated in Tab. 1. TheTg value has been selected from the peak position of tan δ as a function of temperature.

Amount of filler affects glass transition temperature of NR/LBG/SDS blends. Maximum of tg δ was achieved for unfilled blends NR/0phr LBG/0phr SDS. The lowest value of tg δ was achieved for blends NR/27,6phr LBG/0phr SDS and NR/55phr LBG/0phr SDS.

Conclusions

The DMA results of NR/LBG/SDS blends clearly reveal one transition in the tg δ curve. The modulus values are different though the blends are more or less similar in composition. Size of peak at T_g characterizes reinforcement effect of filler. Dynamic mechanical analysis offers a rapid, potent and precise approach to identify and assess complicated elastomer compositions.

Literature

[1] TURI, E.A. Thermal Characterization of Polymeric Materials, 2nd edn., Academic Press, New York, 1997

[2] ZHANG, W., ZHANG, X., LIANG, M., LU, C. Mechanochemical preparation of surface acetylated cellulose powder to enhance mechanical properties of cellulose filler reinforced NR vulcanizates. *Composites Science and Technology* 68(12), 2008, p. 2479-2484

[3] LIONETTO, F., MAFFEZZOLI, A. Relaxations during the postcure of unsaturated polyester networks by ultrasonic wave propagation, dynamic mechanical analysis and dielectric analysis, *Journal Polymer Science B: Polymer Physics* 43, 2005, p. 596–602

[4] ANGELLIER, H., MOLINA-BOISSEAU, S., DUFRESNE, A. Mechanical properties of waxy maize starch nanocrystal reinforced natural rubber, *Macromolecules* 38(22), 2005, p. 9161-9170

[5] SUPHADON, N., THOMAS, A.G., BUSFIELD, J.J.C. The viscoelastic behavior of rubber under a complex loading. II. The effect large strains and the incorporation of carbon black, *Journal of Applied Polymer Science,* 117, 2010, p. 1290–1297

[6] ASIFULAH, K., MOHTASHIM, H.S., TAE-SUN, CH. Correlating dynamical mechanical properties with temperature and clay composition of polymer-clay nanocomposites, *Computational Materials Science* 45, 2009, p. 257-265

[7] HUSSAIN, A.I., ABDEL, K., IBRAHIM, A. Effect of Modified Linen Fibre Waste on Physic-mechanical Properties of Polar and Non-polar Rubber, *Journal of Natural Science*, 8(8), 2010 p. 82-89

[8] JACOB, M., THOMAS, S., VARUGHESE, K.T. Mechanical Properties of Sisal/oil Palm Hybrid Fiber Reinforced Natural Rubber Composites, *Journal of Composites Science Technology* 64, 2004, p. 955-965

[9] PAUL, D.R., BUCKNALL, C.B. *Polymer Blends, Vol. 1*, New York: Wiley Interscience, 1-14, 2000

Study of Curing Characteristics of Rubber Compounds Containing Fillers on the Basis of Natural and Synthetic Zeolite

Štúdium vulkanizačných charakteristík kaučukových zmesí s obsahom plnív na báze prírodného a syntetického zeolitu

Ing. Lenka Špániková[1], prof. Ing. Darina Ondrušová, PhD.[1], Ing. Slavomíra Domčeková[1], Ing. Katarína Holcová[1], Ing. Michaela Ďurčeková[1]

[1]University of Alexander Dubček in Trenčín, Faculty of Industrial Technologies in Púchov, I. Krasku 491/30, 020 01 Púchov, Slovak Republic

Rubbers became the essential utility material in our everyday lives. To achieve the desired properties of rubbers, fillers are added. Fillers have a crucial role in providing durability and reducing the price of final product. Two main groups of filler are known: black (carbon black) and non-black (light, mineral fillers). In present, the special attention is paid to the non-black fillers by many researchers. The aim of this study was to investigate the effect of the fillers – modified forms of zeolite, on rheology and curing characteristics of rubber compounds. The zeolites form a group of aluminosilicates with three-dimensional structure allowing their modification. The natural (clinoptilolite) and synthetic (Y) zeolite was modified by NH_4Cl, $CoCl_2$ solutions and by saturation with vapors of organic dithiophosphate accelerator. All prepared fillers were applied into rubber compounds. The obtained values of vulcanization characteristics of rubber compounds containing prepared fillers were compared with the values of reference rubber compound containing the commercial filler – carbon black.

Keywords: *zeolite, modification, filler, rubber compound, vulcanization characteristics*

Vďaka svojim unikátnym vlastnostiam sú gumárenské výrobky veľmi dôležitými materiálmi používanými v rôznych oblastiach priemyslu. Na dosiahnutie požadovaných vlastností sa do gumárenských zmesí pridávajú plnivá, ktoré sú dôležitou skupinou gumárenských surovín. Podľa základnej definície je plnivo pevná látka, ktorá sa používa na modifikáciu vlastností materiálu, v ktorom je dispergovaná. Už od počiatku gumárenskej výroby malo plnivo rozhodujúcu úlohu najmä v zabezpečení potrebnej životnosti výrobku, ako aj v jeho zlacňovaní. Plnivá bežne používané v zmesiach možno rozdeliť do 2 hlavných skupín. Prvou skupinou sú čierne plnivá (sadze), druhou skupinou sú plnivá svetlé - minerálne plnivá, medzi ktoré zaraďujeme aj hlinitokremičitany, najmä íly a zeolity. Minerálne plnivá sú známe zlepšením tvrdosti a pevnosti gumy. Zeolity sú kryštalické hlinitokremičitany prírodného alebo syntetického pôvodu. Vo svojej mikropórovitej štruktúre obsahujú slaboviazané a ľahko vymeniteľné katióny (napr. Na^+, K^+). Vyznačujú sa výbornými sorpčnými vlastnosťami, vratnou hydratáciou a dehydratáciou, vysokou selektivitou. Tieto vlastnosti ich predurčujú na rôznorodé využitie. Zároveň vysoká sorpčná schopnosť a iónovýmenné vlastnosti umožňujú širokú škálu modifikácií prírodných ako aj syntetických zeolitov. V súčasnosti je výskum mnohých vedcov zameraný na využitie zeolitov ako plniva v gumárenských zmesiach. Prezentovaná práca je zameraná na prípravu modifikovaných foriem prírodného zeolitu (klinoptilolitu) a syntetického zeolitu (Y) a ich aplikáciu do modelových gumárenských zmesí vo funkcii plniva. Zeolity boli modifikované roztokmi NH_4Cl, $CoCl_2$ a sýtením výparmi organického ditiofostátového urýchľovača. Modifikované plnivá boli použité na prípravu modelových gumárenských zmesí. U pripravených gumárenských zmesí bol hodnotený vplyv pripravených plnív na reologické vlastnosti a vulkanizačné charakteristiky.

Kľúčové slová: *zeolit, modifikácia, plnivo, gumárenská zmes, vulkanizačné charakteristiky*

One of the most important components of rubber compounds are fillers. In rubber compounds, they are added in order to adjust processing properties, to reduce price as well as modify mechanical properties, such as strength, hardness, tensile elongation, resistance to abrasion and aging [1]. Two main groups of filler are known: black (carbon black) and non-black (light, mineral fillers). Carbon black, the most important filler in rubber industry, is well-known for its carcinogenicity and negative effect on living environment and health of human being. For all that, its usage is not consistent with an increasing effort of people to protect living environment. On the basis of the mentioned facts, application of easily available, especially natural materials (such as aluminosilicates) is investigated by many researchers.

Zeolites are natural or synthetic aluminosilicate materials and the capability to exchange cations is one of their most useful properties and moreover, this property determines their usage in various fields. Zeolites consist of aluminum and siliceous tetrahedrons which are bound in definite way forming a crystal structure with vacancies, channels and pores (fig. 1).

Hutnické listy č.7/2013, roč. LXVI
ISSN 0018-8069

The electronegative charge of the alumino-silicate framework is compensated by alkaline or alkaline earth metal cations. On the basis of the size, charge or synthesis conditions, cations can occupy various geometric sites. They could be fully or partially substituted by other alkaline, alkaline earth or transitional metal cations without destruction of the crystal framework [2-4].

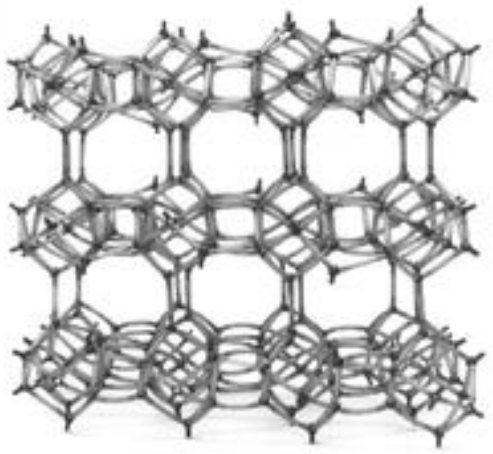

Fig. 1 Channels and pores in structure of zeolite [5]
Obr. 1 Kanáliky a póry v štruktúre zeolitu [5]

Clinoptilolite is one of the zeolite species and it can be found in abundance in many deposits around the world. It belongs to the heulandite group [6].

Synthetic Y type zeolite has a pore size 0.9 nm. Its chemical composition in dehydrated state is given by the formula $Na_2O.Al_2O_3.4{,}5SiO_2$. It is widely used as molecular sieve for special separation processes.

Experimental

In this work, natural zeolite (clinoptilolite) and synthetic zeolite (Y) were used as fillers. Natural and synthetic zeolite was processed by crushing and sieving of particles where the largest size of the sieved particles was 0.045 mm. Natural zeolite was firstly modified with NH_4Cl solution leading to preparation of NH4 form of clinoptilolite. Co-clinoptilolite and Co-Y-zeolite was prepared by ion-exchange process between NH_4-clinoptilolite (resp. Y-zeolite) and $CoCl_2$ solution. Unmodified and modified natural and synthetic zeolite was processed for 1hour lasting heating at 200 °C in dryer and then heated zeolites were exposed to vapor saturation of dithiophosphate accelerator and these types of filler was prepared:

- synthetic zeolite (SZ)
- Co^{2+} synthetic zeolite (SZ_{Co})
- natural zeolite (NZ)
- Co^{2+} natural zeolite (NZ_{Co})

Prepared fillers were added into eight rubber compounds in amount of 10 and 20 phr. One reference rubber compound (R) with carbon black as filler was prepared as comparative compound. All mixtures were prepared by two-step mixing in laboratory blender called Plastograph-Brabender [7]. In the first step, natural rubber together with activator of vulcanization (ZnO), stearic acid and mentioned fillers were mixing for 12 minutes. After 24 hours, base compounds were mixed with dithiophosphate accelerator and sulphur for 6 minutes. Both steps of mixing were carried out at 90 °C and rate of rotation blades was 50 rpm.

Prepared compounds were left for 24 hours at laboratory temperature and then rheological properties and curing characteristics (M_L, M_H, t_{s2}, t_{90}, R_v) were found out by vulcameter Monsanto 100 at the temperature 150 °C during 60 min [8]. Obtained values of vulcanization characteristics of rubber compounds containing prepared fillers were compared with the values of reference rubber compound.

Results and discussion

Measured and calculated results from determination of rheology and vulcanization behavior of prepared rubber compounds are summarized in Tab. 1 and shown in figures 2-4.

Tab. 1 Vulcanization and processing characteristics of the rubber compounds
Tab. 1 Vulkanizačné a spracovateľské vlastnosti gumárenských zmesí

	M_L (Nm)	M_H (Nm)	Ts_2 (min)	T_{90} (min)	R_v (min^{-1})
R	8.20	27.30	3.27	19.61	6.12
SZ10	8.80	18.10	2.64	21.18	5.39
SZ20	8.40	15.20	3.51	43.77	2.48
SZ_{Co}10	9.70	23.00	2.30	8.99	14.95
SZ_{Co}20	9.80	22.20	2.23	8.88	15.04
NZ10	6.40	18.80	3.20	23.08	5.03
NZ20	6.30	18.10	3.05	21.86	5.32
NZ_{Co}10	6.40	21.00	2.59	19.25	6.00
NZ_{Co}20	6.40	21.70	2.45	15.01	7.96

All compounds filled with SZ and SZ_{Co} have higher values of minimum torque moment M_L (fig. 2) but compounds filled with NZ and NZ_{Co} have lower values of M_L in comparison with reference compound (R). It can indicate lower viscosity of compounds with fillers on the basis of natural zeolite.

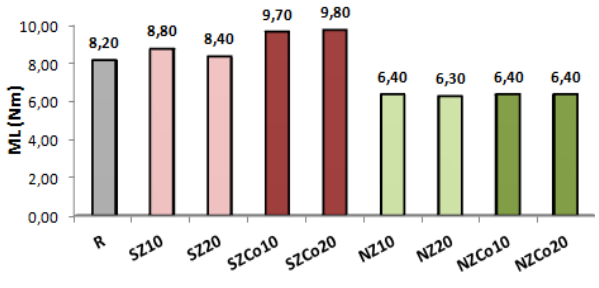

Fig. 2 Minimum torque moment M_L of rubber compounds
Obr. 2 Minimálny krútiaci moment gumárenských zmesí

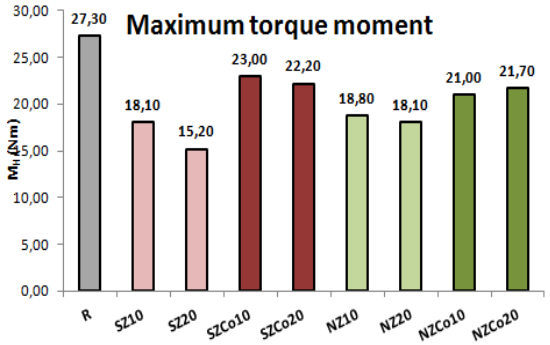

Fig. 3 Maximum torque moment M_H of rubber compounds
Obr. 3 Maximálny krútiaci moment gumárenských zmesí

The maximum torque moment M_H (fig. 3) decreases with increasing content of prepared fillers in rubber compounds. It indicates lower stiffness of mentioned rubber compounds. Lower values of M_H can indicate lower viscosity and lower crosslink density of compounds filled with zeolite fillers.

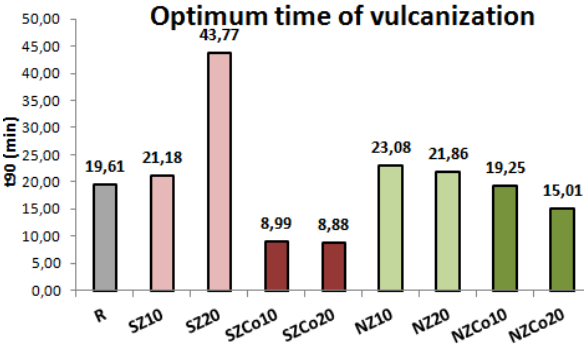

Fig. 4 Optimum time of vulcanization t_{90} for rubber compounds
Obr. 4 Optimálna doba vulkanizácie t_{90} gumárenských zmesí

Based on the results of optimum vulcanization time t_{90} for rubber compounds (fig. 4), it can be considered that there is the protraction of optimum curing time (in comparison to standard compound (R) filled with carbon black) after application of fillers (SZ_{10}, SZ_{20}, NZ_{10}, NZ_{20}) which were modified only by saturation with vapors of dithiophosphate accelerator. Opposite effect, shortening of optimum curing time, can be observed in case of application of fillers (SZ_{Co10}, SZ_{Co20}, NZ_{Co10}, NZ_{Co20}) which were firstly modified with cobalt (II) cations and subsequently by saturation with vapors of dithiophosphate accelerator. On the basis of the above, it can be concluded that previous modification of zeolite by cobalt (II) cations makes bonding of dithiophosphate accelerator more effective.

Conclusions

In relation to this investigation, there were 4 types of fillers prepared and then the effect of these fillers on the curing characteristics was observed for the rubber compounds. The best results were observed in the case of compounds with the fillers which were modified by cobalt II cations and by saturation of dithiophosphate accelerator vapors. The influence of the prepared fillers SZ_{Co} and NZ_{Co} in the rubber compounds was evident in relation to the optimum curing time which was shorten by 50 % in comparison to the reference compound. Lower values of the curing time are positive factor from the aspect of the effective production process.

Acknowledgement
This work has been supported by VEGA No.1/0530/11 and KEGA No.007 TnuAD – 4/2013

Literature

[1] VAVRO, J., HAJSKÁ, H., VAVRO, J. jr., VAVROVÁ, A.: The experimental and theoretical Analysis of Separations Extension in personal Tyres. *Metalurgija,* 2010, Vol. 49, No.2, p. 583-586, ISSN 0543-5846

[2] MATIK, M., VÁCLAVÍKOVÁ, M., HREDZÁK, S., LOVÁS, M., JAKABSKÝ, Š. Možnosti modifikácie zeolitu oxidmi železa a jeho využitia pri odstraňovaní Pb(II) z vodných roztokov, *Acta Montanistica Slovaca,* 2004, 9, p. 418-422

[3] FAGHIHIAN, H., BOWMAN, R.S. Adsorption of chromate by clinoptilolite exchanged with various metal cations, *Water Research,* 2005, 39, p. 1099-1104

[4] IVANOVA, E., KOUMANOVA, B. Adsorption of sulfur dioxide on natural clinoptilolite chemically modified with salt solutions, *Journal of Hazardous Materials,* 2009, 167, p. 306-312

[5] SMART, L., MOORE, E. Solid state chemistry: an introduction, 3rd edition, CRC Press, 2005. 407 p. ISBN 0-7487-7516-1

[6] INGLEZAKIS, V.J. The concept of "capacity" in zeolite ion-exchange systems, *Journal of Colloid and Interface Science* 281, 2005, p. 68-79

[7] STN 62 1425: Príprava gumárenských zmesí

[8] STN 62 1416: Gumárenské zmesi. Stanovanie vulkanizačných charakteristík na vulkametri

Hutnické listy č.7/2013, roč. LXVI
ISSN 0018-8069

Evaluation of Experimental Results for Selected Rubber Compounds before and after Aging Degradation

Vyhodnocovanie experimentálnych výsledkov vybraných materiálových charakteristík gumárenských zmesí pred a po zostarnutiu

Ing. Monika Struharňanská[1], doc. Ing. Jan Krmela, Ph.D.[1], Ing. Peter Vido[1]

[1]University of Alexander Dubček in Trenčín, Faculty of Industrial Technologies, I. Krasku 491/30, 020 01 Púchov, Slovak Republic

The paper is focused on the investigation of the tire rubber compounds and influence of degradation on their mechanical properties. The aging of rubber compounds may occur in their own production, but it can be also connected with the technological process in the production. One of the ways how to simulate the selected degradation processes of rubber compounds is the use of software systems based on the finite element method as computer numerical methods. The selected degradation process of alluvial mixtures is evaluated by computational modeling in combination with experimental investigations. A new alluvial mixture in comparison to degraded one is evaluated in the paper. The tensile strength obtained from static tensile tests in uniaxial tension is evaluated and compared. The Mooney-Rivlin parameters are set on the basis of dependencies mentioned hereinbefore. Using simulations, we can find the potential modifications in technological processes and production of the tire in order to minimize the aging degradation.

Keywords: *tire, rubber compounds, degradation, experiment, cyclic loading*

Príspevok je orientovaný na problematiku gumárenských zmesí plášťov pneumatík. V plášťoch pneumatík sú gumárenské zmesi v interakcii s výstužnými materiálmi. Ku starnutiu gumárenských zmesí môže dochádzať pri ich vlastnej výrobe, ale aj v technologickom procese vo výrobe. Na degradáciu gumárenskej zmesi má vplyv mnoho faktorov. Pre vyhodnotenie je preto potrebné poznať chemické zloženie gumárenskej zmesi, ako aj ich mechanické vlastnosti. Jednou z možností, ako simulovať vybrané degradačné procesy gumárenských zmesí a ich vplyv na mechanické charakteristiky vyrobených elastomérov, je využitie programových systémov na báze metódy konečných prvkov ako počítačovej numerickej metódy. Skúšobné vzorky boli vyrobené z gumárenských zmesí zamiešaných pred 2 a viac rokmi. Výrazným faktorom, ovplyvňujúcim degradáciu, je vplyv vzdušného ozónu. Bude hodnotený vybraný degradačný proces nánosových zmesí výpočtovým modelovaním v kombinácii s experimentmi. S týmto úzko súvisí návrh verifikačných kritérií, na základe ktorých je možné výsledky z výpočtov dobre objektívne posúdiť s výsledkami z experimentov. V príspevku je hodnotená nánosová zmes nová v porovnaní s degradovanou. Vyhodnotené sú formou porovnania závislosti ťahovej sily na predĺžení, získaných zo statických skúšok v ťahu. Na základe týchto závislostí sú stanovené Mooney-Rivlinové parametre. V príspevku bola stanovená metodika pre cyklické zaťaženie pre elastoméry vyskytujúce sa v plášťoch pneumatík. Meranie závislostí bude ďalej prebiehať pre všetky jednotlivé zmesi, ako pre nové vzorky, tak aj pre vzorky po starnutí. Simuláciami môžeme nájsť potenciály v technológii procesov a produkcii plášťov pneumatiky, aby tieto typické degradačné starnutie bolo minimalizované. Na základe výsledkov možno zlepšiť výrobu nánosových zmesí plášťov pneumatík resp. navrhnúť opatrenia vedúce k zníženiu vplyvu starnutia na materiálové charakteristiky aj chemickým zložením gumárenských zmesí.

Kľúčové slová: *pneumatika, gumárenská zmes, degradácia, experiment, cyklické zaťažení*

Research is focused on tire rubber compounds in the interaction with reinforcing materials. Due to effect of various factors, the degradation of mixtures may occur. One of the ways how to reduce or minimize the degradation effect is connected with the simulation of the degradation processes of rubber compounds using the software systems based on finite elements (FEM). By these simulations, we try to find the potential solution in relation to the degradation processes occurring during the process of tire manufacture.

Composite materials in tire casings

In the terms of material, the tire can be defined as very complex polycomponent material with specific properties. It is necessary to take into account these characteristics in relation to the computational models in the form of adequate material models that would best describe each part of composite casing. In relation to the tire composite casings, they are the composites with reinforcing fibers and polymer matrix called steel cord

buffer, overlay buffer and carcass plies. The contact between the vehicle and the road is provided through the tire, and its role is to transfer forces. Basic material – the matrix is a binder and the second component has a firming effect. The different parts of the tire are shown in Fig.1.

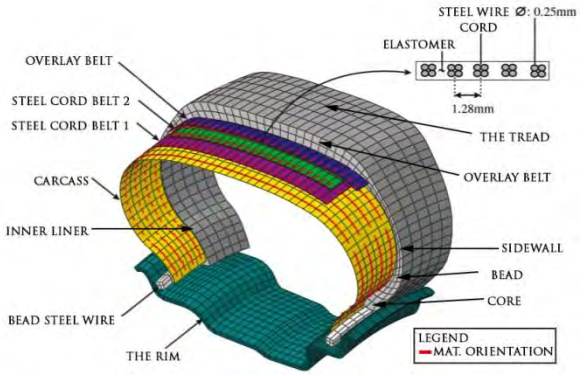

Fig. 1 Specific parts of tire casing
Obr. 1 Špecifické časti plášťa pneumatiky

It is important to define composite materials to specify and utilize the individual material parameters, and then we can create the computational model of the tire based on the given individual parametres. Composites with reinforcing fibers and composites with polymeric matrix are suitable to solve a given problem, because they are strong and tough fibers implemented into softer plastic matrix and by this way, the enhancement of the material mechanical properties can be gained. The given mechanical properties involve strength, toughness, fatigue resistance and tenacity of the composite. Elastomer degradation is caused by the influence of atmospheric oxygen and it is called oxidative aging. At normal temperatures and operating conditions for automobile tires, this aging can be observed after the long time. On average, it can be recognized after 4–8 years of tire service. Degradation of the rubber mixture is influenced by many factors and for good evaluation, it is necessary to know the chemical composition of the rubber compounds, as well as their mechanical properties. After receiving the necessary information about rubber mixtures, it is possible to carry out simulations of selected forms of degradation processes with the help of software systems based on FEM [1].

Procedure for solving the problem

The rubber compounds have been provided from the production line of the tire casing and they were subsequently homogenized by help of the laboratory double cylinder at a temperature of 65–70 °C. Samples were left for at least 24 hours at room temperature. We continued with determination of vulcanization characteristics using the rheometer Monsanto 100 at 150 °C and vulcanization curve was recorded for 60 minutes. Prepared rubber mixtures were left to vulcanize by help of hydraulic press at 150 °C while the pressure was 20 MPa and it lasted 30 min. After leaving them for at least 16 hours, the samples in form of double-sided blades with size A1 in accordance with ISO 37 [5] were subsequently cut [2].

Tension tests

Tested samples in the form of double-sided blade were pulled in uniaxial tension using the universal test machine Hounsfield H20K-W. During the test, the movement speed of jaws was 25 mm / minute and temperature was 23 ± 2 °C. The values of strength and elongation to the break are necessary for the following evaluation of the required characteristics. In Fig. 2, there is the tested sample with a detail of fracture surface after tensile test which belongs to the destructive tests of materials.

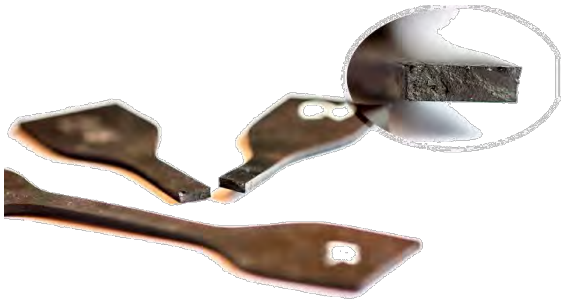

Fig. 2 The test specimen with detail of the fracture surface after the tensile test
Obr. 2 Skúšobná vzorka s detailom lomovej plochy po skúške v ťahu

Hardness tests

The hardness was determined by indentation of the indentor which is part of durometer IRHD (Fig. 3). The indented depth of testing indentor pressed into the material was measured according to ISO 48 [6]. Hardness value is inversely proportional to the depth of penetration of the tip, representing indentor, into the material and depends on the elastic modulus and viscoelastic properties of the material. Hardness was measured at 23±2 °C and five tested samples were used and the thickness of each one was 6 mm thickness [2].

Fig. 3 Hardness measurement using durometer IRHD
Obr. 3 Meranie tvrdosti tvrdomerom IRHD

Elastomeric compounds before and after aging

The tested samples were made of rubber compounds which were blended two or more years ago. A significant factor affecting the degradation is the

Hutnické listy č.7/2013, roč. LXVI
ISSN 0018-8069

impact of air ozone which acts on the mixture. Fig. 4 shows the evaluated dependency of force on the elongation of alluvial mixtures assigned as B09, B10 and B13.

For sample B10, it can be concluded that the elongation to break of sample after degradation was approx. 90 mm and force 46 N shows that the curve of dependency of force on elongation is similar to curve for a new sample. For higher values of elongation to break, the course of dependency is different in comparison to the other samples [3].

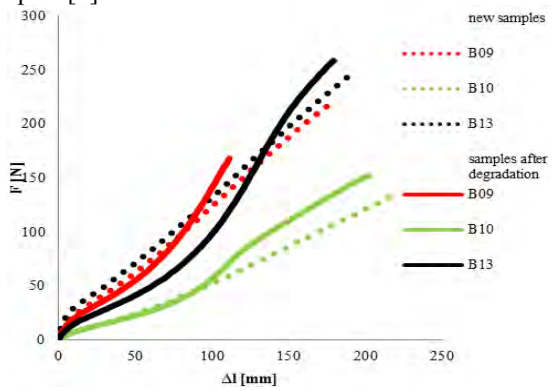

Fig. 4 Dependency of force on the elongation from the static tensile test in uniaxial tension for new samples and samples after aging
Obr. 4 Závislosti sily od predĺženia zo statickej skúšky v ťahu v jednoosej napätosti pre nové vzorky a vzorky po starnutí

The dependence of tension on the elongation of new samples as well as samples after aging were also measured and evaluated. In Fig. 5, there are shown and the samples B09 and B10 where the evaluation is based on mutual comparison of parametres within the each one sample while the given parametres stands for sample when it was new and when it was after aging. A significant difference in dependence between new samples and samples after degradation is noticeable. In the case of sample B10, the results for a new sample and results for the same sample after aging are similar due to the elongation of 115 % (equal to the tension approximately 3 MPa). We can conclude that the change is caused by the impact of air ozone acting on the given samples during the period of three years [3, 4].

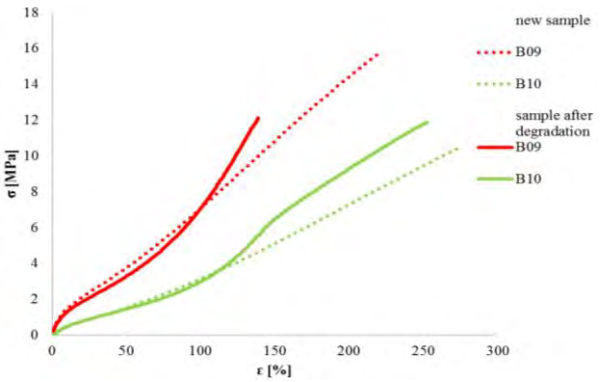

Fig. 5 Dependence of tension from the elongation of samples B09 and B10, new samples and the samples after aging
Obr. 5 Závislosť napätia od pomerného predĺženia vzoriek B09 a B10, novej vzorky a po starnutí

Cyclic loading of the sample by tensile test

Another experiment was focused on cyclic loading of mixture marked as B08 as the new sample and the sample 44 after aging. Samples in the form of double-sided blades were tested in uniaxial tension by test machine Hounsfield H20K-W. The sample was placed in the clamps of device (Fig. 6), where for first tension, the initial value was 80 mm and the speed of movement of jaws was 50 mm / minute. Subsequently, the initial length of measurement at each cycle was varied within ± 0.25 mm due to the impossibility to stop the machine prcisely at the desired length.

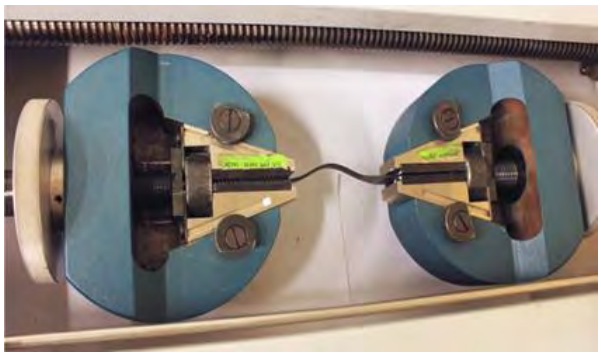

Fig. 6 Test specimen in clamps of testing machine
Obr. 6 Vzorka upevnená v čeľustiach skúšobného zariadenia

In relation to the elongation, the sample was tested for 10 % (8 mm), 15 % (12 mm) and 20% (16 mm) with the reference to the initial values and five measurements were performed for each cycle. Each cycle consisted of loading and releasing. After clamping in jaws and after requested elongation in a given measured cycle, the sample is manually stopped for about 30 seconds to print the outputs of measured values from the testing machine in the form of diagrams. The distance between the clamps was measured by sliding caliper gauge and this length became the input starting point for the next cycle. The sample was clamped in clamps during the whole measurement throughout the all cycles.

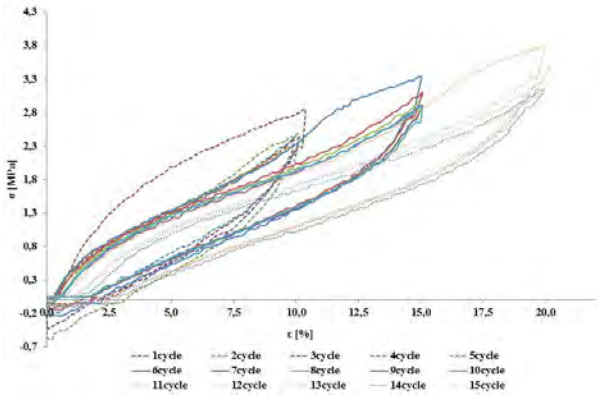

Fig. 7 Dependency of stress from elongation of the sample B08 in cyclic loading
Obr. 7 Závislosti napätia od pomerného predĺženia vzorky B08 pri cyklickom zaťažení

Evaluation of cyclic loading for samples marked as B08 and 44

From dependence of the force from elongation for samples B08 and 44, the dependence of tension from elongation during cyclic loading was evaluated. Individual dependencies are shown in Figures 7 and 8.

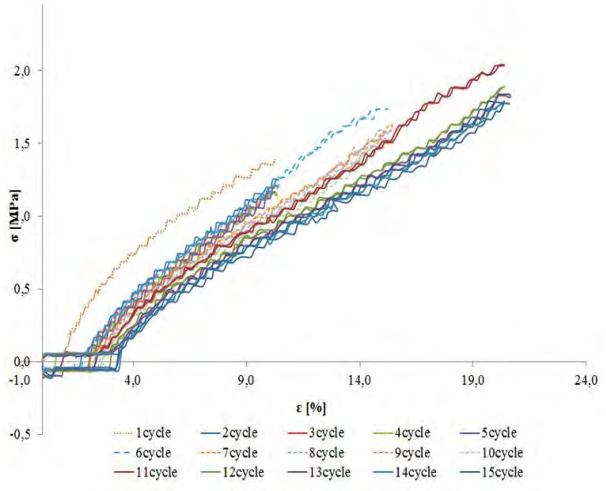

Fig. 8 Dependencies of tension from elongation for samples 44 in cyclic loading
Obr. 8 Závislosti napätia od pomerného predĺženia vzorky 44 pri cyklickom zaťažení

Conclusions

Based on performed experiments it can be concluded that aging has a significant impact on the course of stress-deformation characteristics from the tensile tests. The methodology for cyclic loading of elastomers occurring in the casings of tires was determined. Measurement of the dependencies will continue for each individual mixture relating to the new samples as well as the samples after aging. The results will also be used for calculations of Mooney-Rivlin parameters which will be the input data for calculations in software systems based on the finite element method (ANSYS, MARC). Wrong evaluation of the investigated material and other characteristics can significantly affect their resulting values used for the calculations in FEM. These results are part of the research performed during the dissertation work of the author of the article and it is focused on „Verification of experimental results of the selected material characteristics of rubber compounds." On the basis of the results, the production of alluvial mixtures for tire casings can be improved and it is also possible to propose measures leading to the reduction of the impact of aging on the material characteristics by changes of chemical composition of rubber compounds.

Literature

[1] DRDÁKOVÁ, J., STRUHARŇANSKÁ, M., KRMELA, J. *Selected physical – mechanical properties of specific composite materials with elastomer*. In ARSA 2012, Slovak Republik, 2012, ISBN 978–80–554–0606–0, p. 1785–1788

[2] DRDÁKOVÁ, J., STRUHARŇANSKÁ, M., KRMELA, J. *Vybrané fyzikálno – mechanické vlastnosti špecifických kompozitných materiálov s elastomérmi*. In Semdok 2013, Slovak Republik, 2013, ISBN 978–80–554–0629–9, p. 104-107

[3] KRMELA J., DRDÁKOVÁ, J., KOVÁČ I., VIDO P., PASTOREK M., STRUHARŇANSKÁ M. *Determination of Mooney–Rivlin Parameters of Rubber Used for Rubberizing of Steel cords as an Input for FEA Models of Tire*, Hutnícke listy, Czech Republic: 2012, 65, (7), ISSN 0018-8069, p. 104-106

[4] VIDO P., PASTOREK M., DRDÁKOVÁ, J., STRUHARŇANSKÁ, M, KRMELA, J. *Stanovenie materiálových charakteristík pre verifikáciu výpočtových modelov plášťou pneumatík.* QUAERE 2013, International Scientific Conference, Czech Republic, 2013, ISBN 978-80-905243-7-8, p. 2611-2616

[5] Standard ISO 37(orig. STN 62 1436), *Guma. Stanovenie ťahových vlastností*, edition 1982-03- 29

[6] Standard ISO 48(orig. STN 62 1433), *Guma. Stanovenie tvrdosti v medzinárodných jednotkách (tvrdosť od 30 do 85 IRHD)*, edition 1981-04- 14

Novel Fillers for Natural Rubber Blends: Organically Modified Montmorillonite and Starch

Nové plnivá gumárenských zmesí: organicky modifikovaný montmorilonit a škrob

Ing. Vladimíra Krmelová, PhD.[1], **Ing. Ladislav Janek, PhD.**[1], **doc. Ing. Iva Sroková, PhD.**[1], **RNDr. Vlasta Sasinková**[2], **Mgr. Agáta Laurenčíková, PhD.**[3]

[1]University of Alexander Dubček in Trenčín, Faculty of Industrial Technologies, I. Krasku 491/30, 020 01 Púchov, Slovak Republic
[2]Slovak Academy of Sciences, Institute of Chemistry, 845 38 Bratislava, Slovak Republic
[3]Slovak Academy of Sciences, Institute of Electrical Engineering, 841 04 Bratislava, Slovak Republic

The presented work deals with the chemical modification of natural biopolymer- potato starch and sodium salt of montmorillonite (Na^+MMT) layered clay for their utilization as fillers to natural rubber for tire tread blends. For hydrophobization of hydrophilic starch the esterification method was used. In the first step the starch xanthate was prepared. In the second step the starch xanthate was modified by two alkylammonium salts: dioctadecyl dimethyl ammonium chloride ($C_{38}H_{80}NCl$) and octadecyl trimethyl ammonium bromide ($C_{21}H_{46}NBr$). Two organically modified MMT were prepared from Na^+MMT layered clay by ion exchange capacity method using different alkylammonium salts as modifier. The structural properties of prepared derivatives were characterized by FT-IR spectroscopy. Organically modified MMT derivatives were characterized by X-ray powder diffraction, too.

Keywords: *fillers, montmorillonite, starch, FT-IR spectroscopy*

Príspevok sa zaoberá chemickou modifikáciou prírodného biopolyméru – zemiakového škrobu a vrstveného ílu Na^+MMT a ich charakterizáciou s cieľom ich následného využitia vo funkcii plnív behúňových zmesí v gumárenskom priemysle na báze prírodného kaučuku. U škrobu sa zvolil postup hydrofobizácie so sulfidom uhličitým (CS_2), kde sa v 1. kroku pripravil medziprodukt xantogenát škrobu s priemernou veľkosťou jeho čiastočiek ~ 200 nm. Xantogenát škrobu sa následne modifikoval v 2. kroku dvomi alkylmóniovými soľami N,N – dimetyl- N,N – dioktadecylamonium chloridom ($C_{38}H_{80}NCl$) a N – oktadecyl- N,N,N – trimetylamonium bromidom ($C_{21}H_{46}NBr$) iónovo-výmennou reakciou za vzniku modifikovaných derivátov škrobu s označením C21XŠ a C38KŠ. Z vrstveného ílu sodnej soli montmorilonitu (Na^+MMT) sa pripravili tiež dva organicky modifikované MMT iónovo výmennou reakciou s alkylamóniovými soľami s označením C21MMT a C38MMT. Pripravené deriváty xantogenátu škrobu a MMT sa charakterizovali FT-IR spektroskopiou, C21MMT a C38MMT aj rontgenovou difrakcnou analyzou (RTG). FT-IR spektrá C21XŠ a C38XŠ vykazovali pás pri ~ 663 cm^{-1} odpovedajúci C-S väzbe, pomerne vysoké pásy pri 2916 cm^{-1} a 2950 cm^{-1}, ktoré prislúchajú symetrickým a asymetrickým vibráciam metylénových skupín dlhého alkylu amóniovej soli. Taktiež obsahovali pás pri ~ 1489 cm^{-1} a 1468 cm^{-1} prislúchajúci kvarternemu dusíku R_3N^+H. Spektrá modifikovaných C21MMT a C38MMT na rozdiel od Na^+MMT obsahovali nový pás pri ~ 1483 cm^{-1} a 1468 cm^{-1} prislúchajúci deformačným vibráciam δ kvarterného dusíka R_3N^+H. Interkalačné procesy molekúl $C_{38}H_{80}NCl$ a $C_{21}H_{46}NBr$ do medzivrstvových priestorov sodného MMT sa potvrdili IČ spektroskopiou ako i RTG. Difrakčné parametre C21MMT a C38MMT boli merané v rozsahu 3 do 30°. Zo získaných hodnôt medzivrstvovej vzdialenosti d(001) možno posúdiť úspešnú interkaláciu organických katiónov do medzivrstvového priestoru Na^+MMT čo je nutná podmienka pre úspešnú interkaláciu kaučukových reťazcov do medzivrstvia.

Kľúčové slová: *plnivá, montmorilonit, škrob, FT-IR spektroskopia*

Nowadays, applications of bio – and renewable resources as feedstock for the chemical industry have a great importance. Biopolymers made of renewable sources offer a sustainable alternative to petroleum-based polymers. The disadvantage of these biopolymers is their hydrophilic character. Utilization of montmorillonite (MMT) and biopolymers in natural rubber and styrene-butadiene was tested and studied in [1, 2]. The disadvantage of these layered clays is hidden in their hydrophilic character which causes more difficult disperse to the hydrophobic rubber matrix. For the application of starch and MMT as fillers or additives to hydrophobic polymers, their hydrophobic modification is necessary. The presented work deals with the chemical modification of natural biopolymer – potato starch and sodium salt of montmorillonite (Na^+MMT) layered clay with different alkylammonium salts for their utilization as fillers to natural rubber for tire tread blends. The structural properties of prepared derivatives of starch and organically modified MMT were characterized by Fourier-transform infrared (FT-IR) spectroscopy.

Organically modified MMT derivatives were characterized by X-ray powder diffraction, too.

Experiment

Materials and methods

Potato Starch (22 % amylose, 78 % amylopektin, 12 % moisture content) was used from Spolana a. s. (Neratovice, Czech Republic). Na^+MMT with ion exchange capacity 100 meq/100g was used from Süd Chemie (Germany). Dioctadecyl dimethyl ammonium chloride ($C_{38}H_{80}NCl$) and octadecyl trimethyl ammonium bromide ($C_{21}H_{46}NBr$) were from Sigma – Aldrich Chemie (Steinheim, Germany).

Fourier-transform infrared (FT-IR) spectra were obtained by help of the Nicolet 6700 spectrometer with an ATR extension piece (Smart orbit diamond) with using 128 scans at a resolution of 4 cm^{-1} at the Institute of Chemistry, SAS (Bratislava, Slovak Republic).

X-ray measurements were performed using a Philips diffractometer 1050, using Cu Kα radiation, 12kW, in the range of 3–30° (2θ), step 0,05° at the Institute of Electrical Engineering, SAS (Bratislava, Slovak Republic).

Preparation of alkylammonium salts of starch xanthate (C21XS and C38XS): C21XS and C38XS were prepared in two steps of modification. In the first step, the starch xanthate (XS) was prepared by hydrophobization of hydrophilic starch with CS_2 in an analogical way as in [3]. In the second step, the starch xanthate was modified by ion exchange capacity method with two alkylammonium salts $C_{38}H_{80}NCl$ and $C_{21}H_{46}NBr$ [3].

10 g of starch was blended with 300 ml of distilled water to form a paste. Then, 6.5 ml of sodium hydroxide (5 mol/l) was added into the paste and the mixture was kept under stirring for 30 min. After that, 1.5 ml CS2 was added into the mixture under strong stirring for 1 h. Next, $C_{38}H_{80}NCl$ (14.56 g) or $C_{21}H_{46}NBr$ (13.85 g) was added into the mixture and the mixture was kept under stirring for 4 h. Subsequently, the mixture was washes and finally dried at 40 °C to obtain modified starch xanthate (C21XS and C38XS).

Preparation of organically modified MMT: organically modified MMT were prepared from Na^+MMT layered clay by ion exchange capacity method with 100 meq/100 g using $C_{38}H_{80}NCl$ and $C_{21}H_{46}NBr$ as modifier in an analogical way as in [4].

20 g of the Na^+MMT was dispersed in 500 ml of distilled water/ethanol (1:1) under stirring for 1 h at room temperature. Than equivalent amount of $C_{38}H_{80}NCl$ (11.73 g) or $C_{21}H_{46}NBr$ (7.85 g) was added into the mixture and stirred for 24 h. The modified MMT was separated by filtration and washes with mixture of water and ethanol (1:1). Finally, it was dried at 40 °C to obtain modified MMT (C21MMT and C38MMT).

Results and discussion

The natural biopolymer – potato starch and sodium salt of montmorillonite (Na^+MMT) layered clay were modified with alkylammonium salts ($C_{38}H_{80}NCl$ and $C_{21}H_{46}NBr$) for their utilization as fillers to natural rubber for tire tread blends. Preparation of alkylammonium salts of starch xanthate (Table 1) and organically modified MMT is described in experimental part.

Tab. 1 Reaction condition of starch xanthate modification with alkylammonium salts ($C_{21}H_{46}NBr$ and $C_{38}H_{80}NCl$) at 20 °C
Tab. 1 Reakčné podmienky modifikácie xantogenát škrobu s alkyl amóniovými soľami pri teplote 20 °C

Sample	Molar mass XS:salt	Time (hour)	Reaction time (h)	Yield (g/g)[a]
C21XS	1 : 1	H_2O	24	2.22
C38XS	1 : 1	H_2O	24	2.16

[a]Expressed as g of the recovered derivative per g XS

For the characterization of novel fillers (C21XS, C38XS, C21MMT and C38MMT), FT-IR spectroscopy was used. FT-IR spectra of starch xanthate compared to C21XS and C38XS are shown in Fig. 1 and Na^+MMT and its modified forms C21MMT and C38MMT are shown in Fig. 2. The main absorption band in FT-IR spectra of montmorilonites (Fig. 2) was located near 1100 cm^{-1} and it belongs to the Si-O stretching vibrations. The position of the hydroxyl stretching band at 3615 cm^{-1} in IR spectra of MMT is typical for Al-rich octahedral layer minerals. Modified MMT (Fig. 2) and XS (Fig. 1) show characteristic bands at ~ 2918 cm^{-1} and ~ 2948 cm^{-1} attributed to asymmetric and symmetric stretching methylene groups from alkylamonium salts. They also show new bands at ~ 1489 cm^{-1} a 1468 cm^{-1} attributed to quaternary nitrogen R_3N^+H. The spectra of C21XS and C38XS shows band at ~ 663 cm^{-1} attributed to C-S bond.

The obtained XRD spectra of Na^+MMT and organically modified MMT (C21MMT and C38MMT) are shown in Fig. 3 and they were analyzed for the calculation of the corresponding values of the basal montmorilonites spacing. Sample of Na^+MMT shows symmetric diffraction d(001) = 1.25 nm as the value of the distances which is typical for pure layered sodium montmorillonite. The largest distance between layer d(001) was observed for C38MMT and it was 1.98 nm. For C21MMT, it was 1.85. The d(001) values prove successful intercalation of the organic cations into the interlayer space of Na^+MMT because it is necessary for successful intercalation of rubber chains.

Hutnické listy č.7/2013, roč. LXVI
ISSN 0018-8069

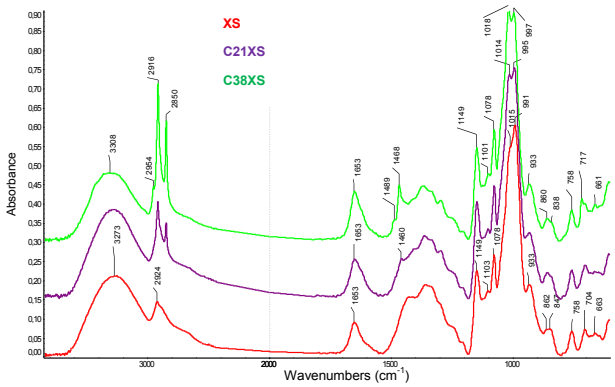

Fig. 1 FT-IR spectra of starch xanthate compared to C21XS and C38XS
Obr. 1 FT-IR spektrá XŠ v porovnaní s C21XŠ a C38XŠ

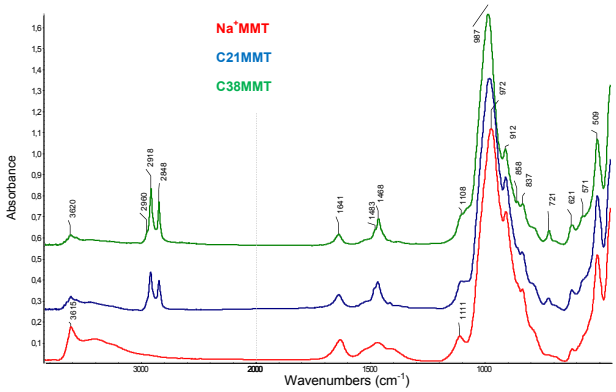

Fig. 2 FT-IR spectra of Na^+MMT and its modified forms C21MMT and C38MMT
Obr. 2 FT-IR spektrá Na^+MMT a jeho modifikovanej formy C21MMT a C38MMT

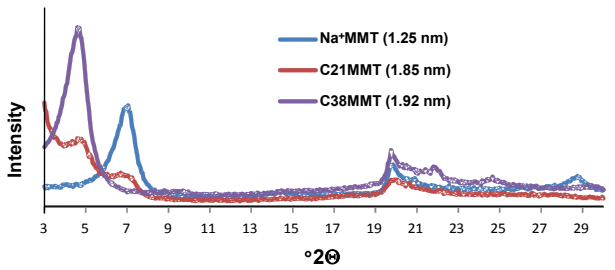

Fig. 3 XRD spectrum of Na^+MMT and organically modified MMT (C21MMT and C38MMT)
Obr. 3 Porovnanie Rtg. difrakčného záznamu organomodifikovaných montmorillonitov a Na^+MMT

Conclusions

Organically modified montmorillonite (C21MMT and C38MMT) and alkylammonium salts of starch xanthate (C21XS and C38XS) were prepared and their structural properties were characterized. Modification of starch xanthate was confirmed by FT-IR spectroscopy. Modification of Na^+MMT was confirmed by FT-IR spectroscopy method and X-ray powder diffraction. Prepared derivatives can be used as fillers to natural rubber for tire tread blends.

Acknowledgement
This work was financially supported by the Slovak Grant Agency VEGA, projects No. 2/0062/09.

Literature

[1] ZHENG, G., GUOJUN, S., WEISHENG, L., PEIYAO, L., LI, G., HAMHUA, L., XION, H. Preparation and properties of styrene butadiene rubber/natural rubber/organo-bentonite nanocomposites prepared from latex dispersion. *Applied Clay Science*, 2009, Vol. 46, p.241-244

[2] ALEXY, P., FERANC, J., KRAMÁROVÁ, Z., HAJŠOVÁ, M., ĎURAČKA M., MOŠKOVÁ, D., CHODÁK, I., ILISCH, S. Application of lignins in rubber compounds. *KGK Kautschuk Gummi Kunststoffe*, 2008, Vol. 61(1-2), p. 26-32

[3] WANG, ZF., PENG, Z., LI, DS., LIN, H., ZHANG, KX., SHE, XD., FU, X. The impact of esterification on the properties of starch/natural rubber composite. *Composites Science and Technology*, 2009, Vol. 69, p. 1797-1803

[4] BHARDWAJ, D., SHARMA, M., SHARMA, P., TOMAR, R. Synthesis and surfactant modification of clinoptilolite and montmorillonite for the removal of nitrate and preparation of slow release nitrogen fertilizer. *Journal of Hazardous Materials*, 2012, Vol. 227-228, p. 292-300

Influence of Cu^{2+} Kaolin Filler on Thermal and Structural Characteristics of Rubberizing Components

Vplyv plniva Cu^{2+} kaolínu na termické a štruktúrne charakteristiky gumárenských zložiek

prof. RNDr. Mariana Pajtášová, PhD.[1], **Ing. Andrea Feriancová, PhD.**[1], **Ing. Zuzana Jankurová, PhD.**[1], **Ing. Katarína Holcová**[1], **Ing. Janka Paliesková**[1]

[1]University of Alexander Dubček in Trenčín, Faculty of Industrial Technologies, I. Krasku 491/30, 020 01 Púchov, Slovak Republic

Inorganic (mineral) fillers based on kaolin are important ingredients which affect the characteristics of polymer mixtures and their products. In the introduced study, natural kaolin has been modified by treatment of copper acetate. The next step was connected with the study of interactions between vulcanizing ingredients, such as stearic acid (SA), benzothiazole and modified Cu^{2+}kaolin filler by thermal analysis (DTA,TG) and infrared spectroscopy (IR). By treatment of copper acetate at the presence of NaOH on kaolin, monohydrate copperhydroxyacetate complex was formed. Heating Cu^{2+}kaolin with stearic acid led to creation of copper stearate and it was confirmed by IR spectra corresponding to stretching vibrations of the carboxyl group COO^-. Present copper complex has impact on the mutual interaction between the modified Cu^{2+}kaolin and benzothiazole. Results from DTA, TG and IR spectroscopy confirmed these mentioned conclusions.

Key words: *kaolin, vulcanizanizing ingredients, IR spestroscopy, thermal analysis.*

Kaolín je významná prírodná surovina, ktorá sa používa v gumárenskej praxi ako plnivo. Plnivá v polymérnych zmesiach znižujú spotrebu kaučuku a cielene ovplyvňujú vlastnosti gumárenských výrobkov. Modifikáciou kaolínu organickými alebo anorganickými molekulami je možné získať nanoplnivá s požadovanými vlastnosťami. V práci je študovaný vplyv modifikovaného Cu^{2+} kaolínu na interakcie s gumárenskými zložkami: kyselinou stearovou vo funkcii aktivátora a s benztiazolom vo funkcii urýchľovača. Pri modifikácii kaolínu roztokom octanu meďnatého v prítomnosti NaOH vznikla nová meďnatá zlúčenina. Metódou IČ spektroskopie - z rozdielu hodnôt asymetrických a symetrických valenčných vibrácii karboxylovej skupiny [$\Delta = \nu_{as}(COO^-) - \nu_s(COO^-)$], $\Delta = 130\ cm^{-1}$, sa potvrdil vznik monohydrátu acetáto-trihydroxodimeďnatého komplexu. Tento záver potvrdzuje aj termická analýza, kde je na DTA krivke pozorovaný intenzívny exotermický pík pri 272 °C, ktorý zodpovedá rozkladu meďnatej soli. Meďnatá forma kaolínu bola použitá na štúdium interakcii z gumárenskými zložkami. Pri zahriatí modifikovanej formy Cu^{2+} kaolínu s kyselinou stearovou vznikol stearan meďnatý, ktorého teplote topenia zodpovedá endotermický pík 109 °C zaznamenaný na DTA krivke CuKA+SA pri termickej analýze. Na IČ spektre sú pozorované absorbčné pásy zodpovedajúce valenčným asymetrickým a symetrickým vibráciám karboxylátového aniónu COO^-. Prítomný meďnatý komplex ovplyvnil vzájomné interakcie medzi modifikovaným CuKA a benztiazolom. Na DTA krivke CuKA+Bt je pozorovaný exotermický pík pri 335 °C, ktorý prisudzujeme termickému rozkladu benztiazolu, ktorý sa fyzikálne naviazal na povrchu modifikovaného kaolínu. V IČ spektrách CuKA sa v prítomnosti benztiazolu pozorovali pásy valenčnej C-H vibrácie aromatického kruhu, valenčné vibrácie benzénového jadra C=C a pásy valenčnej vibrácie funkčných skupín C=N a N=C-S.

Kľúčové slová: *kaolín, gumárenské zložky, IČ spektroskopia, termická analýza.*

Kaolin is a hydrated aluminum silicate from a group of natural kaolinite – serpentine clays which have at least one dimension in range of 1-100 nm. Due to the low price (lower than that of silica) and the choice of reinforcement (soft or hard kaolin), it is the most widely used as light-colored filler. Nowadays, it is one of the most important kaolin mineral fillers for rubber mixtures. In recent years, there has been an increasing interest in utilizing kaolin for its capacity to adsorb inorganic and also organic molecules. It showed that kaolinite could be used as a substitute for activated carbon as an adsorbent due to its availability and low price as well as its good sorption properties [1].

The layered structure of kaolinite consists of silica tetrahedral (SiO_4) units stacked together with gibbside octahedral (AlO_6) units. The layers are held together by hydrogen bonds between the oxygens in one of the alumina octahedral bonds between the oxygens in one layer and the hydroxyl groups in the next layer [2-3]. The hydrogen bonding between the adjacent layers prevents expansion (swelling) of kaolin beyond its basal spacing of 0.72 nm. The unit cell of kaolinite has

Hutnické listy č.7/2013, roč. LXVI
ISSN 0018-8069

a neutral charge. Kaolinite has a relative low cation-exchange capacity (CEC) 3-15 meq/100 g of clay and small surface area, which is not more than 20 m^2/g [4].

Basal spacing of clays can be expanded by incorporating (intercalation) of organic/inorganic compounds. Intercalation is a reversible process and may involve exchange of cations from interlayer, adsorbtion of polar molecules through ion-dipole interactions, hydrogen bonding, and protonation [2]. The conditions employed in the preparation of these materials depend on the inorganic matrix. Advances in the preparation of hybrid organic-inorganic materials by intercalation of organic molecules into kaolin represented the possibility for developing new and interesting materials [3, 5].

The rubber industries contribute significantly to the nation's economy. The additives that form vulcanizing system include: curing agents, accelerators, activators, retarders and inhibitors. Stearic acid (SA) acts as activator of the accelerator and sulfur element to promote construction of sulfur crosslinking to the unsaturated part of long rubber chains under the vulcanization conditions as temperature, pressure, time. Benzothiazole (Bt) plays a role as activator of sulfur vulcanization [6].

In the given study, natural kaolin from Kaznejov has been modified with treatment of copper acetate. The second step dealt with study of interactions between vulcanizing ingredients: stearic acid (SA), benzothiazole and modified Cu^{2+}kaolin (CuKA) filler. Clay characteristics and the effects of the treatments were examined by techniques of infrared spectroscopy (FTIR) and by thermogravimetry/differential thermal analysis (DTA/TG).

Experiment

Kaolin sample used in this investigation was from a natural deposit Kaznejov. Its chemical composition was 44.9 % SiO_2, 47.49 % Al_2O_3, 3.34 % K_2O, 1.45 % Fe_2O_3, 1.61 % TiO_2 and LOI (lost of ignition) 9.24 %. Chemicals for chemical treatment such as copper acetate ($Cu(CH_3COO)\cdot H_2O$), sodium hydroxide (NaOH) and stearic acid (SA) were purchased from local supplier (Centralchem, Ltd.) and benzothiazole Bt was purchased from merk, Ltd. and used without further purification.

Modified Cu^{2+}kaolin and the effects of the treatments with rubber chemicals were investigated by thermal analysis (TG/DTA) and infrared spectroscopy (FTIR).

The thermogravimetry TG and DTA was carried out by help of Derivatograph MOM Hungary from room temperature up to 800 °C in an air atmosphere at a heating rate of 10 °C.min^{-1}. Infrared absorption spectra were recorded by a FTIR Spectrometer Tensor 27 in the 4000-400 cm^{-1} wavelength range with the resolution of 4 cm^{-1}. The KBr pressed disk technique was used.

At first, the modification with copper acetate, there was prepared a sample: 10.0 g of kaolin natural sample was dispersed in 100 ml (0.2 M) $Cu(CH_3COO)\cdot H_2O$. The mixture was mixed for 30 min. and then NaOH was added to the dispersion. The mixture was mixed for 6 hours. Excess salts were removed by washing three times with deionized water and suspension was centrifuged (4000 rpm, for 40 min). The resulting sample were designated CuKA. This precursor was mixed with rubber chemicals (SA and Bt) in the ratio of 1:1 by mass in porcelain mortar. We prepared systems of two components with kaolin. The second step was connected with heating samples containing SA and Bt at cure temperature 140 °C. The interactions between CuKA and rubber chemicals were investigated by thermal analysis and infrared spectroscopy.

Results and discussion

Thermoanalytic curves of CuKA are shown on Fig. 1. An intense exothermic effect (mass lost ~ 3 wt. %) is observed at ~272 °C and is attributed to the decomposition of copper salts. It can be assumed that through modification of kaolin, with copper acetate in the presence of NaOH, Cu^{2+} hydroxy acetate was created and it was ligated into the structure of kaolin [7]. At higher temperature, the effect characteristic of dehydroxylation of kaolin was observed [8]. The dehydroxylation temperature of kaolin increased from 565 °C to 583 °C.

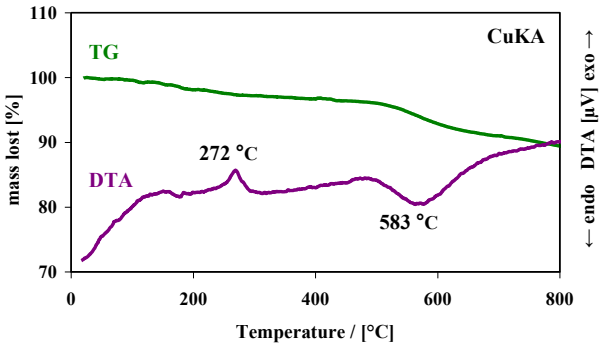

Fig. 1 DTA/TG curves of Cu^{2+}kaolin CuKA
Obr. 1 DTA/TG záznam Cu^{2+} kaolínu CuKA

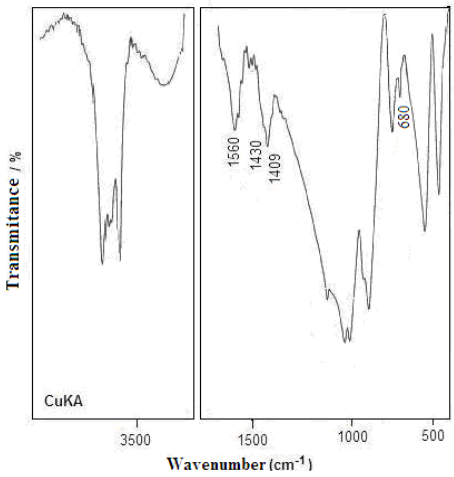

Fig. 2 IR spectrum of CuKA in the range 4000-500 cm^{-1}
Obr. 2 IČ spektrum CuKA v rozsahu 4000-500 cm^{-1}

The infrared spectrum of CuKA is given on Fig. 2. New absorption bands at 1560 and 1430, 1409 cm^{-1} are related to the asymmetric and symmetric stretching vibrations of carboxylate group $\nu_{asym}COO^-$ and $\nu_{sym}COO^-$. From the value $\Delta = \nu_{asym}(COO^-) - \nu_{sym}(COO^-)$, $\Delta = 130\ cm^{-1}$, it is possible to confirm formation of monohydrate copper(II)hydroxyacetate complex $[Cu_2(OH)_3COO]\cdot H_2O$. A valence vibration of Cu-O-H at 680 cm^{-1} is observed too, and on the base of this fact, carboxylate anions can be coordinated at copper atoms through oxygen atom [9].

On the basis of the DTA curve of CuKA+SA in Fig. 3, two small endothermic effects at 78 °C and 109 °C are observed. The first one corresponds to the melting point of stearic acid; the second one indicates that after heating process, Cu2+kaolin with stearic acid copper stearate has been formed. According to literature data, melting point of copper stearate is about ~ 106-119 °C [10].

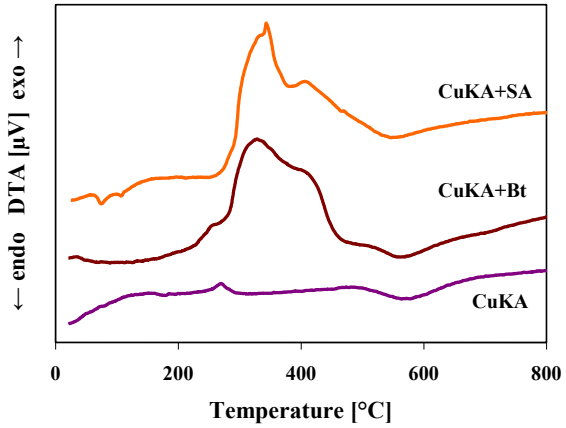

Fig. 3 DTA/TG curves of samples CuKA, CuKA+Bt, CuKA+SA
Obr. 3 DTA/TG záznam vzoriek CuKA, CuKA+Bt, CuKA+SA

The most intense change on the DTA curve of CuKA+Bt (Fig. 3) shows a broad exothermic peak with a maximum at 335 °C. We assume that given exotherm is related to the thermal decomposition of benzothiazole, which was physically bound to the surface of the modified kaolin [11]. Transition metal cations (Cu^{2+}) are characterized by relatively strong coordination properties and allowed creating complex with Bt compound whose thermal degradation is shifted to higher values than the thermal decomposition of pure benzothiazole (267 °C).

The infrared spectrum of CuKA+SA is given in Fig. 4. Vibration bands at ~ 1705-1707 cm^{-1} and ~ 1472-1413 cm^{-1} are atributed to the asymmetric and symmetric stretching vibration of the carboxylate group ν_{asym} (COO) and ν_{sym} (COO) in free stearic acid. New absorption bands at 1586 cm^{-1} and 1470-1444 cm^{-1} corresponding to the symmetric and asymmetric stretching vibration of carboxylate group ν_{asym} (COO^-) and ν_{sym} (COO^-) are observed. Heating Cu^{2+}kaolin with stearic acid copper stearate was formed and it is connected with IR spectra corresponding to stretching vibrations of the carboxyl group COO^- [12].

In IR spectrum of CuKA+Bt (Fig. 5) new bands at ~ 3060 and 3050 cm^{-1} corresponding to the stretching vibration of CH aromatic ring of benzothiazole were observed. Skeletal vibration corresponding to the stretching vibration of the benzene ring C = C occurs at ~ 1553-1581 cm^{-1}. The IR spectra also revealed belts stretching vibration of C = N and N = C-S group at ~ 1454-1452 cm^{-1} and at ~ 1420-1426 cm^{-1} [13]. These new bands confirmed that when modified form of Cu^{2+}kaolin with benzothiazole was heated, there was complex compound created. Benzothiazole with different transition metal ions forms complex compounds, and it is the most frequently coordinated through the atom of nitrogen or sulfur, respectively [14].

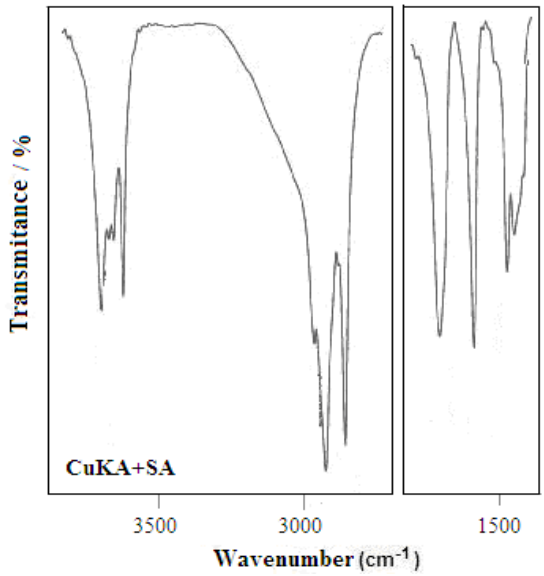

Fig. 4 IR spectrum of CuKA+SA
Obr. 4 IČ spectrum CuKA+SA

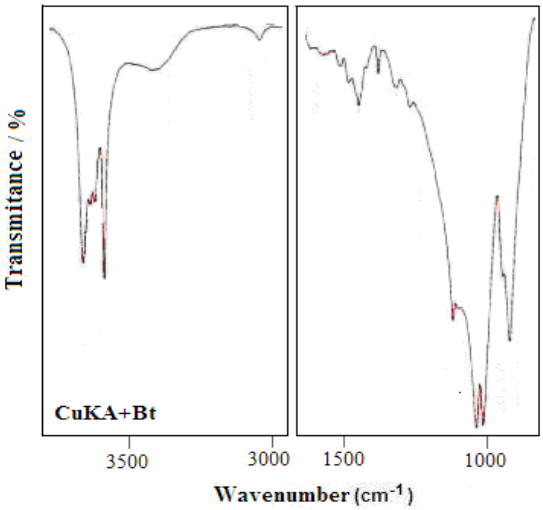

Fig. 5 IR spectrum of CuKA+Bt
Obr. 5 IČ spektrum CuKA+Bt

Conclusions

The presented article was focused on examining the interactions between modified inorganic fillers on the basis of Cu^{2+}kaolin and curing components stearic acid and benzothiazole without the use of a polymeric matrix. At first, there was the modification of Cu^{2+}kaolin prepared by treatment with copper acetate in the presence of NaOH. By method of thermal analysis and IR spectroskopy, the formation of monohydrate copperhydroxyacetate complex was confirmed. Heating Cu^{2+}kaolin with stearic acid, copper stearate was created and it is connected with IR spectra corresponding to stretching vibrations of the carboxyl group COO^-. Present copper complex has impact on the mutual interaction between the modified CuKA and benzothiazole. In IR spectra of CuKA systems with benzothiazole, the stretching vibrations of C-H groups of aromatic ring and stretching vibrations of benzene ring C=C stretching vibration bands C=N and N=C-S were observed. Modification of filler by Cu^{2+} cations promote mutual interacting of kaolin with accelerator on the base of thiazole and with activator - stearic acid. The presented results provide new information about the use of modified clay products in the function of fillers and it which can be verified by preparation of model rubber mixtures.

Acknowledgement
The authors wish to thank the Slovak Grant Agency VEGA: 1/0530/11 and KEGA: 007TnUAD-4/2013 for financial support.

Literature

[1] BHATTACHARYYA, K.G., GUPTA, S.S. Adsorption of a few heavy metals on natural and modified kaolinite and montmorillonite: A review. *Advanced Colloid and Interface Science,* 2008, 140, p. 114-131

[2] MELO, J., COSTA, T.C., MEDEIROS, A.M., PASKOCIMAS, C.A. Effects of thermal and chemical treatments on physical properties of kaolinite. *Ceramics International,* 2010, 36, p. 33-38

[3] AVILA, R.A., FARIA, E.H., CIUFFI, K.J., NASSAR, E.J. New synthesis strategies for effective functionalization of kaolin and saponite with lily lating agents. *Journal of Colloid and Interface Science,* 2010, 341, p. 186-193

[4] BHATTACHARYYA, K.G., GUPTA, S.S. Calcined tetrabutylammonium kaolinite and montmorillonite and adsorption of Fe(II), Co(II), Ni(II) from solution. *Applied Clay Science,* 2009, 46, p. 216-221

[5] JIANG, M., JIN, X., LU, X., CHEN, Z. Adsorption of Pb(II), Cd(II), Ni(II) and Cu(II) onto natural kaolinite clay. *Desalination,* 2010, *252*, p. 33-39

[6] MALÁČ, J. *Gumárenská technologie*. učební texty. Univerzita Tomáše Bati ve Zlíně, Zlín, 2005

[7] PAJTÁŠOVÁ, M., FERIANCOVÁ, A., PALIESKOVÁ, J., JÓNA, E. Thermal and XRD analysis of intercalation process of kaolin with DMSO and Cu^{II} ions. *Hutnícke listy,* 2012, LXV (7), s. 49-52

[8] PTÁČEK, P., KUBÁTOVÁ, D., HAVLICA, J., BRANŠTETR, J., ŠOUKAL, F., OPRAVIL, T. Isothermal kinetic analysis of the thermal decomposition of kaolinite. *Thermochimica Acta,* 2010, 501, p. 24-29

[9] DANILO, C., PEREIRA, DE FARIA D.L., CONSTANTINO, R.L. Cu^{II} hydroxy salts: characterization of layered compounds by vibrational spectroscopy. *J. Braz. Chem. Soc*., 2006, 17 (8), p. 1651-1657

[10] NUHA, A., AGUS, A., ABDUL RAZAK, R., LEE, T.S. 11th International Annual Symposium on Sustainability Science and Management, 2012, p. 944-949

[11] MANOHAR, D.M., KRISHNAN, K.A., ANIRUDHAN, T.S. Removal of mercury (II) from aqueous solutions and chlor-alkali industry wastewater using 2-mercaptobenzimidazole clay. *Water reaserch*, 2001, 36, p. 1609-1619

[12] MAHDI, H.A., KADHUM, M.Y., ANATIEL, A.H. Studies on the thermal stabilization for Polyvinyl chloride by some metal stearates. *J.Thi-Qar Sci*., 2011, 2 (4), p. 1991-2009

[13] PAJTÁŠOVÁ, M., ĽALÍKOVÁ, S., ONDRUŠOVÁ, D., FERIANCOVÁ, A., JANKUROVÁ, Z., CHOCHULOVÁ, A. Sorption of benzothiazole and 2-methylbenzothiazole on Ca- and Co-monoionic forms of montmorillonite. *Hutnícke listy,* 2011, 64 (7), p. 145 – 147

[14] PAJTÁŠOVÁ, M., ONDRUŠOVÁ, D., JÓNA, E., MOJUMDAR, S.C., ĽALÍKOVÁ, S., BAZYLÁKOVÁ, T., GREGOR, M. Spectral and thermal characteristic of copper (II) carboxylates with fatty acid chains and their benzothiazole aducts. *J Therm. Anal. Calorim*, 2010, 100, p. 769-777

Degradation of Properties of Rubber Mixtures in Biofuels

Degradácia vlastností gumárenských zmesí v biopalivách

Ing. Michal Dubovský[1], doc. Ing. Milan Olšovský, PhD.[1], doc. Ing. Pavel Švanda, PhD.[2]

[1]University of Alexander Dubček in Trenčín, Faculty of Industrial Technologies, Department of materials engineering and environment, I. Krasku 491/30, 020 01 Púchov, Slovak Republic
[2]University of Pardubice, Jan Perner Transport Faculty, Department of mechanics, materials and machine parts, Czech Republic

In the past two centuries, humankind has consumed about 90 % of non-renewable fossil fuels for energy purposes and transport. At current consumption of fuels, oil resources will be depleted approximately in 50 years. Today, it is necessary to find new raw materials to satisfy of energy needs of humankind in the future [6]. Development of renewable energy sources, such as bioethanol and biodiesel has a big influence on sources of energy in the future to reduce the dependence on oil as well as to reduce the impact on the environment strengthening of economies in rural locations. In aero turbo engines (ATCE), rubbers on the basis of NBR are used and they are characteristic for excellent physical and mechanical properties. The impact of biofuels mixtures and aviation fuel JET A1 on the rubber blends was evaluated in this paper. The results presented in our paper showed that the maximum content of bio-fuel in aviation fuel JET A1 can be only up to 20 wt. %.

Keywords: *biofuel, rubber seal, resistance, physical-mechanical properties*

Rast populácie a rastúci dopyt po energiách v sektore dopravy spôsobuje rýchle vyčerpávanie fosílnych palív. Používanie bionafty môže významne znížiť našu závislosť na fosílnych palivách a tak pomôcť znížiť znečistenie životného prostredia. Avšak, existujú obavy o kompatibilite používaných tesniacich materiálov v bionafte. Pre analýzu správania sa polymérnych materiálov, ktoré sú vystavené pôsobeniu zmesi biopalív, sa používajú dlhodobé ponorné testy. Výsledky degradácie polymérov sú stanovené zo štrukturálnych zmien, napučiavania, zmeny hmotnosti, tvrdosti, zmena objemu a rozmerov a zmeny mechanických vlastností ako sú tvrdosť, pevnosť v ťahu a ťažnosť. Všetky tieto zmeny ukazujú, že absorpcia paliva a extrakcia rozpustných zložiek, ako sú zmäkčovadlá a iné prísady, sa líšia podľa typu použitej gumárenskej zmesi. Pri prechode na biopalivá treba zvážiť aj také aspekty, ako budú jednotlivé súčasti motorov reagovať na zmenu pohonného agregátu. Bionafta „MERO" druhej generácie je stále jediným alternatívnym palivom, ktoré sa používa v spaľovacích motoroch. Je možné ho aj kombinovať napr. s PVC a tým dosiahnuť ešte lepšie funkčné a úžitkové vlastnosti, ako napr. vyššia odolnosť voči ozónu alebo napučaniu. Biopalivá sú ekologickejšie a sú považované za obnoviteľný druh energie, nakoľko k produkcii tohto typu sa používa rastlina s názvom jatropha. V tomto príspevku sa hodnotí zmeny mechanických vlastností ako aj zmeny povrchovej morfológie gumárenských zmesí pomocou rastrovacej elektrónovej mikroskopie (REM). Ako biopalivo bola použitá bionafta z repkového oleja a bioetanol. Gumárenské zmesi boli vystavené pôsobeniu rôznej koncentrácií biopalív v leteckom petroleji JET A1 pri rôznych teplotách. Z nameraných výsledkov je evidentné, že zmes biopalív a leteckého petroleja JET A1 spôsobuje zníženie mechanických vlastností gumárenských zmesí.

Kľúčové slová: *biopalivo, gumové tesnenie, odolnosť, fyzikálno-mechanické vlastnosti*

Biodiesel, which is a relatively clean-burning, renewable fuel produced from new and used animal and vegetable oil, could be used to replace at least a portion of the diesel fuel consumed worldwide. The performance of biodiesel in cold conditions is markedly worse than that performance of petroleum diesel. At low temperatures, biodiesel forms wax crystals, which can clog fuel lines and filters in a vehicle fuel system [7].

The presented work [8] was focused on the comparison of degradation of physical properties for five types of polymers (EPDM, NBR, CR, SR and PTFE) with palm biodiesel by static immersion tests in B0 (diesel), B10 (10 % biodiesel in diesel), B20, B50 and B100 (100 % biodiesel). Tensile strength and hardness were greatly reduced in the case of EPDM and CR but for Q, PTFE and NBR, the changes were not so significant. Authors of the mentioned paper concluded that the overall sequence of compatible elastomers in palm biodiesel is to be: PTFE > SR > NBR > EPDM > CR. In the most of mentioned investigations, the description of the static immersion test is based on the diffusion of liquid in stress-free rubber, but only few investigations involve the swelling of polymer in the presence of stresses. Most of them deal with the interaction between diffusion of liquid and large deformation without any explicit relation to cyclic and fatigue response of rubber. Authors [9] designed a compression device to evaluate the durability of industrial rubber components exposed to aggressive environment, e.g. oil in biofuel system

Hutnické listy č.7/2013, roč. LXVI
ISSN 0018-8069

during their service. The apparatus is comprised of four rectangular stainless steel plates with spacer bars in between and thus the pre-compression can be introduced for the rubber specimens while they are immersed into diesel. They found that swelling in rubbers increases with the increase of palm biodiesel content and decreases with the increase of pre-compressive strain. It was also observed that the presence of biodiesel significantly reduces the mechanical strength of the rubber.

Results and discussion

In our paper, there is the investigation of the change of mechanical properties of rubber blends and the change of surface morphology using scanning electron microscopy (SEM). Rubber blends were exposed to higher and lower temperature (+100 °C and -17 °C) as well as laboratory temperature (23 ± 2 °C). Samples became brittle at 100 °C temperature, therefore it was not possible to perform tensile test for them. Fuel composition and conditions of measurement are shown in table 1. These parameters were measured for rubber mixtures: tensile strength and elongation (ISO 37) and surface morphology degradation using scanning electron microscopy (SEM). We have made two parallel measurements for each one condition.

Tab. 1 Test conditions
Tab. 1 Podmienky experimentu

Sample	The test conditions (content of biofuel, temperature)
0	Standard – without fuel action; Laboratory temperature
1	5 % FAME; laboratory temperature
2	10 % FAME; laboratory temperature
3	15 % FAME; laboratory temperature
4	5 % FAME; -17 °C
5	10 % FAME; -17 °C
6	15 % FAME; -17 °C
7	5 % bioethanol; laboratory temp.
8	10 % bioethanol; laboratory temp.
9	15 % bioethanol; laboratory temp.
10	5 % bioethanol; -17 °C
11	10 % bioethanol; -17 °C
12	15 % bioethanol; -17 °C
13	5 % FAME; 100 °C
14	10 % FAME; 100 °C
15	15 % FAME; 100 °C

Mechanical properties of rubber mixtures

In table 3, there is the presentation of the physical and mechanical properties of the rubber blends which are exposed to mixtures FAME and aviation fuel JET A1. Reduction of tensile properties is caused by absorption of more amount of liquid into rubber as well as extraction of soluble constituents of the rubber mixtures. In comparison to the conventional diesel fuels, esters are characterized by increased polarity and this polarity also has influence on the degradation of rubber blends. Samples 4 - 6 showed even higher values than the standard and it can be attributed to low temperatures that slow the process of swelling.

Tab. 2 Mechanical properties of the samples after 3000 h influence of biofuel
Tab. 2 Mechanické vlastnosti vzoriek po 3000 h pôsobenia bionafty

Sample	Tensile strength [MPa]	Elongation [%]	Density [g.cm^{-3}]
0	17.9	123	1.344
1	14.3	111	1.319
2	15.5	128	1.316
3	16.7	134	1.307
4	16.7	131	1.343
5	19.1	128	1.368
6	19.0	141	1.352

Tab. 3 Mechanical properties of the samples after 3000 h influence of bioethanol
Tab. 3 Mechanické vlastnosti vzoriek po 3000 h pôsobenia bioetanolu

Sample	Tensile strength [MPa]	Elongation [%]	Density [g.cm^{-3}]
0	17.9	123	1.344
7	18.5	121	1.316
8	16.7	127	1.329
9	15.9	121	1.346
10	18.4	125	1.352
11	18.0	121	1.369
12	17.5	128	1.353

The table 3 shows only the tensile properties of rubber blends which are exposed the effect of bio-fuel mixture (bioethanol and aviation fuel JET A1) at room temperature and temperature -17 °C. Strengths of blends at low temperatures are significantly higher than the standard and this is linked to washing out of non-rubber additives of the rubber mixtures and increasing of filler content in the samples and in relation to the density of mixtures, it remained practically constant.

The surface morphology change of rubber compounds using scanning electron microscope (SEM)

SEM photographs of rubber blends used in our test are shown in the figure 1 – 10. Surfaces of rubber blends were investigated at magnification 1000x. It can be seen that the degradation of sample surfaces was not observed and it corresponds to the previous studies where the authors present that optimum addition of bio-fuel into aviation fuel is up to 30 wt. % [10 - 13]. In table 1 are the surfaces morphology change of selection samples. The fuel affect on rubber gasket 3000 h.

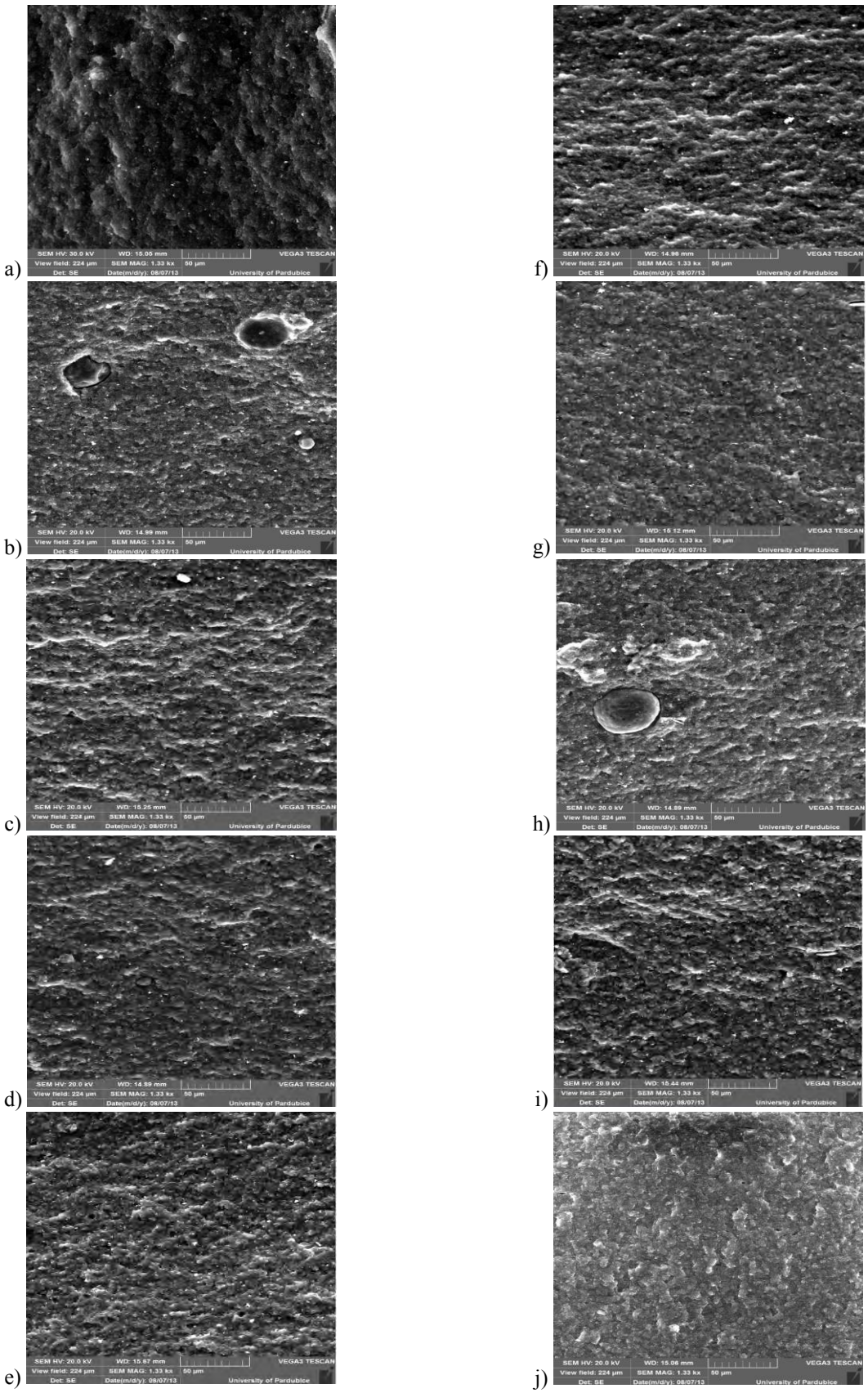

Fig. 1 The surface morphology of selected samples exposed to 3000 h of fuel: a) sample 0, b) sample 1, c) sample 2, d) sample 3, e) sample 6, f) sample 7, g) sample 8, h) sample 9, i) sample 12, j) sample 15; (1000x magnification)

Obr. 1 Morfológia povrchu vybraných vzoriek po 3000 h pôsobenia paliva: a) vzorka 0, b) vzorka 1, c) vzorka 2, d) vzorka 3, e) vzorka 6, f) vzorka 7, g) vzorka 8, h) vzorka 9, i) vzorka 12, j) vzorka 15; (zväčšenie 1000x)

Conclusions

Degradation of rubber materials in bio-fuels mixtures was investigated by static immersion test. The following points had been concluded on the basis of this study:

- upon exposure to rapeseed biodiesel at different temperatures, the degradation of physical and mechanical properties of rubber mixtures was observed;
- rubber mixtures exposed to the influence of mixture bioethanol and aviation fuel JET A1 at low temperatures showed higher values than standard and it is caused with washing out non-rubber additives of the rubber mixture as well as increasing the filler content in the samples;
- surface of samples exposed to bio-fuels was investigated by scanning electron microscopy (SEM). The degradation of surface morphology was not observed.

Literature

[1] ALVES, M.S., MELO, S.V., MEDEIROS, S.J. Palm and Soybean Biodiesel compatibility with fuel system elastomers. Tribology International, 2013, Vol. 65, p. 74–80, ISSN 0301-679X

[2] HOCKO, M. Možnosti využitia netradičných palív pre pohon leteckých turbokompresorových motorov. In: 6. Medzinárodná konferencia Nové trendy v rozvoji letectva, sekcia 1. letecké strojárstvo a environmentalistika, VLA Košice 9 – 10 September. p. 21–25

[3] HOCKO, M. Použitie zmesi biopaliva „MERO“ s leteckým petrolejom pre pohon leteckých turbokompresorových motorov. In: Zborník abstraktov zo 7. Medzinárodnej vedeckej konferencie „Nové trendy rozvoja letectva“, 6 – 8 September. 2006, LF TUKE

[4] HOCKO, M., BAJUSZ, P. Possibilities of using the unconventional fuels to drive aeronauctical turboject engines, Košice Letecká fakulta TUKE, Acta Avionica ročník VIII; 2006. p. 12, 5

[5] CHRÁSTOVÁ, V., BORSIG, E. Makromolekulová chémia. STU Bratislava; 1996

[6] CVENGROŠ, T., CVENGROŠ ,M. Motorové biopalivá – ich súčasný stav a perspektívy. Agrobioenergia – časopis Združenia pre poľnohospodársku biomasu, 2008, roč. 3, č. 4, s. 5–8, ISSN 1336-9660

[7] ZULETA, C.E. et al. The Oxidative Stability of Biodiesel and its Impact on the Deterioration of Metallic and Polymeric Materials: a Review. Journal of the Brazilian Chemical Society, 2012, Vol. 23, No. 12, p. 2159–2175, ISSN 0103-5053

[8] HASEEB, A.S.M.A. et al. Degradation of physical properties of different elastomers upon exposure to palm biodiesel. Energy, 2011, Vol. 36, Issue 3, p. 1814–1819, ISSN 0360-5442

[9] CHAI, B.A. et al. Development of a compression test device for investigating interaction between diffusion of biodiesel and large deformation in rubber. Polymer Testing, 2011, Vol. 30, Issue 8, p. 867–875, ISSN 0142-9418

[10] LAZAR, T. Inovatívne výstupy z transformovaaného experimentálneho pracoviska s malým prúdovým motorom. Košice: Elfa; 2011. p. 348

[11] OLŠOVSKÝ, M. a kol. Vplyv obsahu biozložiek v zmesi biopaliva MERO a leteckého petroleja na vlastnosti gumových tesnení palivových sústav leteckých motorov. In: Zborník z 8. medzinárodnej vedeckej konferencie Nové trendy rozvoja letectva. Košice; 11. – 12. 9. 2008

[12] KRAJČI, J. Vplyv prídavku biopaliva na gumové tesnenia leteckých motorov (diplomová práca). Púchov: FPT TnUAD; 2009, 59 s.

[13] DUBOVSKÝ, M. Vplyv prevádzkových podmienok na gumové tesnenia palivových sústav s biopalivom (diplomová práca). Púchov: FPT TnUAD; 2012, 66 s.

Výstavba peletizačního závodu v USA

AK Steel to start construction of pellet plant. Metallurgical Plant and Technology 2013, č. 4, s. 8

Americké společnosti AK Steel a Magnetation Inc. založily společný podnik Magnetation JV, který financuje výstavbu závodu na výrobu vysoce jakostních pelet v Reynolds ve státě Indiana. Pelety budou odebírat vysoké pece firmy AK Steel ve státech Ohio a Kentucky. Nový závod bude pokrývat asi 50 % spotřeby pelet. Tím společnost AK Steel rozšíří svui vertikální integraci a získá kontrolu nad cenovou strukturou výchozích surovin a zvýší svou soběstačnost.

Výstavba plánovaná na 18 měsíců již probíhá a počítá se se zahájením výroby ve 4. kvartále 2014. Po záběhovém provozu by měl závod vyrábět 3 mil. t pelet ročně.

L J

Influence Structures of Knitted Fabrics on the Air Permeability

Vplyv štruktúry pletenín na priepustnosť vzduchu

doc. Ing. Pavol Lizák, PhD.[1]

1University of Alexander Dubček in Trenčín, Faculty of Industrial Technologies, I. Krasku 491/30, 020 01 Púchov, Slovak Republic

This article deals with the influence of air permeability on the Structures of knitted fabrics. Our researched material is the knitted fabrics made with polypropylene fibre. The comfort is defined as "the absence of displeasure or discomfort" or "a neutral state compared to the more active state of pleasure". Clothing comfort includes three main considerations: psychological, sensorial and thermo-physiological comfort. The thermo-physiological comfort, entails both thermoregulation and moisture management. It is known that fiber type, yarn properties, fabric structure, finishing treatments and clothing conditions are the main factors affecting thermo-physiological comfort. In this paper, the influence of structural properties and characteristics of the fiber on the air (thermo-physiological comfort), of single jersey knitted fabrics was investigated.

Keywords*: single jersey, thermo-physiological comfort, air permeability, analysis*

V práci sa zaoberáme problematikou vplyvu priepustnosti vzduchu na štruktúre pletenín, ktorá je ovplyvňovaná okrem hustoty pletenín aj jej pórovitosťou. Skúmaným materiálom v našej práci boli pleteniny vyrobené z polypropylenových vlákien a ich zmesí s bavlnou, vlnou a elastanom. Hlavným cieľom tejto práce bolo vykonať analýzu porozity zvoleného textilného súboru pletených výrobkov vyrobených z POP vlákien vyrobených v Chemosvite Fibrocheme a následne teoreticky analyzovať vzťah porozity materiálu voči prestupu vzduchu.

Pre daný experiment boli zvolené záťažné pleteniny z POP a zmesových vlákien využívaných na výrobu tepelne odolných športových odevov. Pretože štruktúra pleteniny je pomerne nestabilná a variabilná, teoretické modely nie sú vždy schopné tento fakt dostatočne zohľadniť a správne vyhodnotiť.

Porozita textílií predstavuje kľúčový parameter pri hodnotení priedušnosti materiálu. Priepustnosť vzduchu patrí k dôležitým faktorom ovplyvňujúcim komfort daného textilného výrobku, a preto je pomerne podstatné vykonávať skúšky priepustnosti vzduchu. Avšak priepustnosť vzduchu je vlastne funkciou porozity materiálu, preto údaj o porozite predstavuje cennú informáciu.

V súčasnosti existuje niekoľko metód ako porozitu materiálu stanoviť. Jednu z používaných metód na zisťovanie tohoto parametru predstavuje obrazová analýza NIS Element.

Táto práca pojednáva o využití obrazovej analýzy na účely hodnotenia textílií v oblasti textilnej metrológii, resp. na ich vnútornú analýzu a vyhodnotenie fyziologických vlastností textílií, konkrétne prestup vzduchu. Ide o analýzu štruktúry textílií, charakteristiky variability v 3D textilnej architektúre a o rôzne výskumy distribúcie a transportu vzduchu v textilných vrstvách.

Kľúčové slová*: single jersey, termo-fyziologický komfort, priepustnosť vzduchu, analýza*

The term comfort is defined as "the absence of displeasure or discomfort" or "a neutral state compared to the more active state of pleasure". Clothing comfort includes three main considerations: psychological, sensorial and thermo-physiological comfort. The thermo-physiological comfort, the subject of this research, entails both thermoregulation and moisture management. It is known that fiber type, yarn properties, fabric structure, finishing treatments and clothing conditions are the main factors affecting thermo-physiological comfort [1].

Anand S. [2] proved that fabric thickness, enclosed still air and external air movement are the major factors that affect the heat transfer through fabric. Greyson and Havenith, mentioned that heat and water vapor resistance increases with the increment of material thickness and air entrapped.

Hes et. al [3] developed a new functional knitted fabric possessing double layers by using different yarn components (like polypropylene and cotton) in order to maximize the transport moisture.

This paper discusses the use of image analysis for the evaluation of fabrics in the textile metrology, respectively their internal analysis and evaluation of the physiological properties of textiles. Whether it's analysis of the structure of textiles, characteristics variability in 3D textile architecture, or the various researches distribution and transport of air in textile layers

Hutnické listy č.7/2013, roč. LXVI
ISSN 0018-8069

approach is advanced and accurate method of assessment.

The main objective of this work is to analyse the porosity of the selected file knitted textile products made from fibers produced POPs in Chemosvit Fibrochem and then theoretically analysed the relationship 3D porosity of the material parameter versus resistance of the material to transfer air. For this experiment were selected weft knit of POP and blended fibers using for producing heat-resistant sportswear. Because the structure of knitting is quite unstable and variable, theoretical models are not always able to adequately take into account this fact and properly evaluated.

In this paper, the influence of structural characteristics and raw material content of single jersey knitted fabrics on the air (thermo-physiological comfort), was investigated.

Experimental

Materials

Single jersey structures were knitted using 3x 100 % POP, POP/2% elastan, 50/50%, POP/mikr, 50/50% POP/cotton, 50/50% POP/wool and 100 % POP double. Knitting process of the single jersey knitted fabrics was performed on flat knitting machine (Fig. 1).

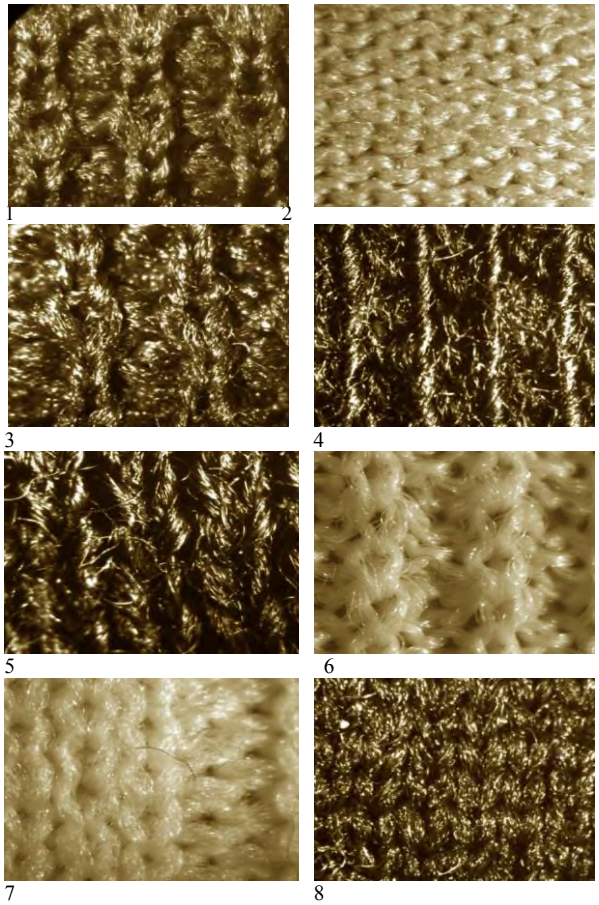

Fig. 1 Knitted fabrics structure with 8 different raw materials contents
Obr. 1 Štruktúra pletenín s 8 rôznými materiálovými zloženiami

Experimental work is focused on getting the most perfect image selected weft knitted by image analysis, namely the evaluation of porosity and its relationship with breathable material. Since this is a method for determining the physiological properties of textiles, it was necessary to address a number of important tasks:

- measurement of porosity by image analysis
- calculate the porosity traditional way
- analysis of the relationship of porosity and permeability of air

Methods and instruments

Structural properties of knitted fabrics

Structural properties of knitted fabric (course density H_r, cm^{-1}; andwale density, H_s, cm^{-1}), fabric thickness h (mm) mass per unit area ρ_s (g/m^2) are determined according to standard methods. Porosity P is calculated according to the equations (1):

$$P = \left(1 - \frac{\rho_s}{\rho_v * h}\right) * 100 \quad (1)$$

The symbols represent the following variables: ρ_s - mass per unit area (g/m^2), ρ_v - mass density (kg/m^3), h - fabric thickness (mm).

Air permeability

Air permeability fabric is defined as the amount of air that passes through material per unit time at a specified pressure. Air permeability is an important factor affecting the physiological comfort, it is involved in the transport of moisture away from the body to the environment. Air permeability fabric is mainly influenced by the characteristics of the pores in the fabric. It is thus clear that the pore size and its distribution are a function of geometry fabrics. Average yarns, finishes and density of rows and columns, length of ears are the main factors affecting the porosity of the fabric. Porosity is then linked to the very important properties such as air permeability, water, colouring, and other properties.

Permeability and porosity are very closely linked. Created a theoretical model to predict values for permeability fabric from which it results that the pore size and permeability tight linear relationship exists. Investigation of the air permeability was performed according to the standard EN ISO 9237:1999.

An FF-12 Metrimpex instrument was used with difference in contact pressure of 50 Pascal area of the sample 20 cm^2.

Results and discussion

Structural characteristics

In table 1 and 2 are density and the structural characteristics of knitted fabrics with different raw material content

Tab. 1 Density of the knitted fabrics with different raw material content
Tab. 1 Hustota pletenín s rôzným materiálovým zložením

No.	Knitted fabrics	H_r (cm^{-1})	H_s (cm^{-1})	H_c (cm^{-2})
1	100% POP (green)	7	18.5	129.5
2	POP/2% elastan	21.5	14.5	311.7
3	POP/mikr 50/50	15.5	6	93
4	POP/ba 50/50	8	9	72
5	vl/POP 50/50	11	8	88
6	100% POP (white)	12	6	72
7	100% POP (white r)	12.5	8	100
8	100% POP (double)	16.5	12	198

Tab. 2 Structural characteristics of the knitted fabrics with different raw material content
Tab. 2 Štrukturálne charakteristiky pletenín s rozným materiálovým zložením

No.	Knitted fabrics	h (mm)	ρ_s (g/m^2)	ρ_v (kg/m^3)	P (%)
1	100% POP (green)	0.64	154	980	75.4
2	POP/2% elastan	0.53	107	970	79.2
3	POP/mikr 50/50	0.72	98	80	86.1
4	POP/ba 50/50	1.28	179	1255	88.8
5	vl/POP 50/50	1.14	156	1150	88.1
6	100% POP (white)	0.64	116	980	81.5
7	100% POP (white r)	0.53	96	980	81.5
8	100% POP (double)	0.70	133	980	80.6

As the density (H_c) increases and the mass per unit area (ρ_s) also increase, but not the thickness (h) as a result of the different raw material content of the fabrics (Fig. 2).

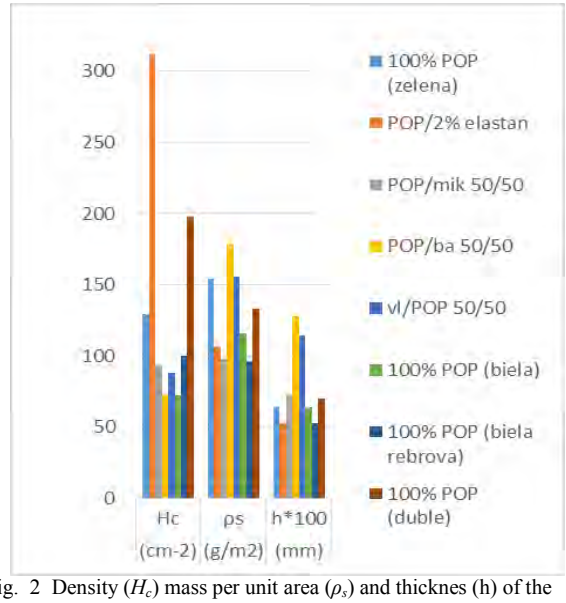

Fig. 2 Density (H_c) mass per unit area (ρ_s) and thicknes (h) of the knitted fabrics with different raw material content
Obr. 2 Hustota (H_c) plošná hmotnosť (ρ_s) a hrúbka (h) pletenín s rozným materiálovým zložením

Air permeability

In table 3 air permeability values are given (Fig. 3).

Tab. 3 Air permeability of the knitted fabrics with different raw material content
Tab. 3 Priepustnosť vzduchu pletenín s rozným materiálovým zložením

No.	Knitted fabrics	Air permeability Q (dm^3/h)	Coefficient of variation CV (%)
1	100% POP (green)	4435	7.79
2	POP/2% elastan	3982.5	5.41
3	POP/mikr 50/50	6855	2.43
4	POP/ba 50/50	3067	10.02
5	vl/POP 50/50	4930	3.61
6	100% POP (white)	6235	4.75
7	100% POP (white r)	5430	6.24
8	100% POP (double)	5275	4.26

Hutnické listy č.7/2013, roč. LXVI
ISSN 0018-8069

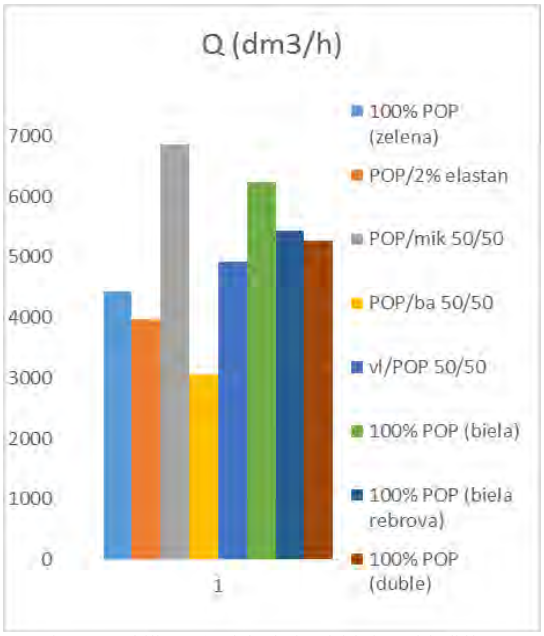

Fig. 3 Air permeability (Q) of the knitted fabrics with different raw material content
Obr. 3 Priepustnosť vzduchu (Q) pletenín s rozným materiálovým zložením

Air permeability have the increase, i.e. their value decreases as the mass per unit area. More dominant influence of the structural characteristics on the air compared to raw material content is noticeable.

Conclusions

The results indicate that the structural characteristics of the knitted fabric have dominant influence on thermo-physiological comfort, as opposed from the raw material content. On the Fig. 4 we can see influence porosity on the transfer of air.

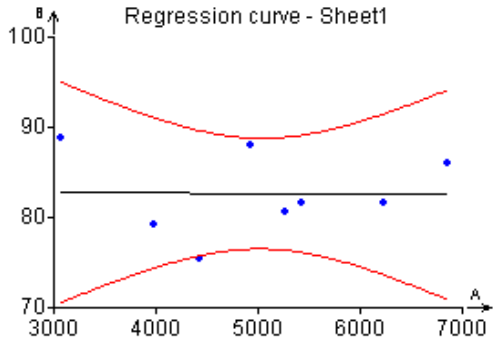

Fig. 4 Influence porosity on the transfer of air
Obr. 4 Vplyv porosity na prestup tepla

The density and mass per unit area of the knitted fabrics determine the air and water vapour permeability and thermal characteristics. The final assessment of the thermo-physiological comfort depends on the wearing conditions. According to this, a single jersey made of 50/50% POP-cotton will provide the best comfort when being worn on lower temperatures, while a single jersey of 100% POP on higher temperatures. The single jersey made of 50/50% POP-wool did not show the highest thermal resistance as expected because of its raw material content, which is a result of the structural characteristics i.e. lower density of the fabric.

Acknowledgements
This work was supported by project of Slovak Grant Agency (KEGA: 002 TnUAD 4/2011).

Literature

[1] OGLAKCIOGLU N., MARMARALI A. Thermal comfort properties of some knitted structures. *Fibres &Textiles in Eastern Europe*, 2007, vol. 15, p. 64-65
[2] ANAND S. Sportswear Fabrics. *Knitting International*, 2003, p. 23-25
[3] HES L., GERALDES M.J., ARAÚJO M. How to Improve the Thermal Comfort with High Performance PP Fibres. In 2nd AUTEX Conference Proceeding, Bruges, Belgium, 2002, p. 428-430

Carboxymethylcellulose Cinnamates – Preparation and Characterization

Cinamáty karboxymetylcelulózy – príprava a charakterizácia

Ing. Vladimíra Krmelová, PhD.[1], doc. Ing. Iva Sroková, PhD.[1], Dr inż. Iwona Stachurek[2], RNDr. Vlasta Sasinková[3]

[1]University of Alexander Dubček in Trenčín, Faculty of Industrial Technologies, I. Krasku 491/30, 020 01 Púchov, Slovak Republic
[2]Higher School of Labour Safety Management, 40-007, Katowice, Poland
[3]Slovak Academy of Sciences, Institute of Chemistry, 845 38 Bratislava, Slovak Republic

The novel polymeric surfactants were prepared from carboxymethylcellulose (CMC, DS=1) by the esterification reaction with cinnamic acid (CA). The hydrophobization was performed in reaction medium H_2O/N,N dimethylformamide with N,N' – carbonyldiimidazole or N,N' - dicyclohexylcarbodiimide as activators of carboxylic acid group and 4 – dimethylaminopyridine as catalyst at various reaction conditions using conventional heating source at assistance of microwave radiation. The structural features of the obtained water-soluble CMC derivatives were characterized by Fourier transform infrared spectroscopy (FT-IR) and UV spectroscopy. The results indicate that application of microwave heating allowed shortening the reaction time down to several minutes in comparison to esterification reaction lasting up to 24 h at conventional heating.

Keywords: *carboxymethylcellulose, polymeric surfactants, cinnamic acid, microwave irradiation, FT-IR spectroscopy*

Príspevok sa zaoberá prípravou nových derivátov karboxymetylcelulózy (CMC) – cinamátov karboxymetylcelulózy (CA-CMC) a ich charakterizáciou. Cinamáty karboxymetylcelulózy sa pripravili chemickou modifikáciou CMC kyselinou škoricovou (CA) v reakčnom prostredí H_2O/DMF za aktivácie CA dicyklohexylkarbodiimidom (DCCI) alebo karbonyldiimidazolom (CDI), za katalýzy 4 – dimetylaminopyridinom (4-DMAp) za rôznych reakčných podmienok účinkom konvenčného ohrevu ako i mikrovlnného žiarenia. Aktivátor kyselín DCCI alebo CDI sa použil analogicky ako v práci Wondraczka pri príprave fotoaktívnych dextránov. CA-CMC deriváty sa charakterizovali fourierovou transformačnou infračervenou spektroskopiou (FT-IR) a UV spektroskopiou. Pripravili sa vodorozpustné deriváty CMC s nízkym stupňom substitúcie, čo potvrdili FT-IR a UV spektrá. Reflexné spektrá CA-CMC derivátov a východiskovej CMC sa merali metódou ATR. V FT-IR ATR spektrách sa sledoval najmä pás pri vlnočte 1707 cm^{-1}, ktorý je nižší v porovnaní s esterovými skupinami (1730 cm^{-1}), čo súvisí s konjugáciou násobnej väzby a aromatického jadra zvyšku kyseliny škoricovej. UV spektrá vybraných cinamátov CMC vykazujú široký absorpčný pás v oblasti vlnových dĺžok od 230-350 nm s absorbčným maximom pri vlnovej dĺžke ~ λ = 280 nm, ktorý zodpovedá π-π konjugácii C=C väzby s aromatickým jadrom cinamátovej skupiny a je porovnateľný s hodnotami uvedenými v literatúre pre iné cinnamáty. Použitie mikrovlnného žiarenia pri chemickej modifikácií CMC umožnilo skrátiť reakčný čas prípravy esterov CA-CMC z hodín na 1 až 2 minúty. Pokračovaním práce bude štúdium povrchovo-aktívnych a antioxidačných vlastností pripravených CA-CMC derivátov.*

Kľúčové slová: *karboxymetylcelulóza, polymérne surfaktanty, kyselina škoricová, mikrovlnné žiarenie, FT-IR spektroskopia*

During the last years, a fast growing interest for biopolymeric surfactants from plant resources has been noticed, because they are environmentally friendly, biocompatible and can be potential substitutes of synthetic oil-derived products. Moreover, they have potential use in various industrial applications such as food, environmental protection, pharmaceutical, textile and other sectors [1]. This has led to increasing research activities in the field of amphiphilic polysaccharide derivatives. Recently, there has been a considerable number of studies reported on polymeric surfactants prepared by partial hydrophobization of commercial or non-commercial polysaccharides such as hydroxyethyl cellulose (HEC) [2], carboxymethylstarch (CMS) [3]. As a further polysaccharide, a commercially available anionic cellulose derivative carboxymethylcellulose (CMC) was used for targeted hydrophobic modification in order to prepare ionic polymeric surfactants. From the various reaction used for modification of CMC, esterification reaction under conventional heating have been most investigated in our papers [4, 5]. Nowadays, attention has been paid to application of the new heating system - microwave radiation, which replaces the classical one in many diverse areas of chemistry, including chemical modifications of carbohydrates [6]. There are few reports concerning the application of microwave heating in chemical modification of polysaccharides, such as cellulose [7], hydroxyethylcellulose [8], carboxymethyl-starch [9], chitosan [10] and whereby some of the reactions were

Hutnické listy č.7/2013, roč. LXVI
ISSN 0018-8069

performed under solvent-free conditions. In comparison to the conventional heating technique, the application of microwave heating extensively shorted the reaction time of syntheses. Prolongation of microwave exposure during succinylation of cassava starch in water led to increase in reaction efficiency and thus to higher degree of substitution [11]. But Satge C. [7] reported that increasing in radiation time of cellulose esterification beyond one minute was connected with cellulose degradation. Similarly, the extension of microwave radiation time from 1 to 3 and 5 min of transesterification reaction between rapeseed oil triacyl glycerides (RO) and carboxymethylcellulose induced de-esterification reaction.

In the previous reports [5, 12] we reported partially hydrophobization of CMC by the transesterification using RO, fatty acid methyl esters of rapeseed oil and microwave radiation with controlled power as heating source. In this study the partial hydrophobization of CMC by esterification with cinnamic acid using conventional and microwave heating source was investigated.

Experiment

Materials and methods

CMC (Na^+ salt; DS_{CM} = 1; Mw = 741 kDa, Walsrode, Germany) was gift from Prof. Thomas Heinze (Center of Excellence of Polysaccharide Research, Friedrich Schiller University of Jena, Germany). The cinnamic acid (CA), carbonyldiimidazole (CDI), dicyclohexyl-carbodiimid (DCCI) and 4 – dimethylaminopyridine (4-DMAp) were commercial products from Sigma-Aldrich Chemie (Steinheim, Germany). N,N-Dimethylformamide (DMF) and acetone were from Lachema (Brno, Czech Republic). All chemicals were used without further purification. The reactions were carried out in the dark to avoid photoreaction as described by Wondraczek [13].

Fourier-transform infrared (FT-IR) spectra were obtained by the Nicolet 6700 spectrometer with an ATR extension piece (Smart orbit diamond) using 128 scans at a resolution of 4 cm^{-1} at the Institute of Chemistry, SAS (Bratislava, Slovak Republic). The spectra were baseline corrected and normalized to the intensity of the absorption band at 1155 cm^{-1}.

UV spectra of CMC derivatives dissolved in water (1 mg/1 ml) were obtained by help of the SpectroFlex 6600 (WTW Weilheim, Germany).

Synthesis of CA-hydrophobized CMC derivatives (CA-CMC):

(a) Conventional heating esterification – CMC (0.5 g) was dissolved in 25 ml distilled water under stirring at room temperature for 1 h. Subsequently, CA (0.25-1.5 g) in 15 ml DMF and appropriate amounts of DCCI (molar ratio CA : DCCI, 1:1) was added to the CMC solution. The reaction mixture with addition of 4-DMAp (0.05 g) as catalyst agent was stirred at laboratory temperature (or 70-80 °C) for 1-24 h. Subsequently, the product was poured into 4-6 volumes of acetone and the precipitated derivative was separated by filtration, subsequently washed with acetone, and extracted in a Soxhlet apparatus with acetone for 20 h to remove the unreacted acylation agent and degradation products.

(b) Microwave-assisted esterification – CMC (0.5 g) was dissolved in 25 ml distilled water under stirring at room temperature for 1 h. Subsequently, CA (0.25-1.5 g) in 15 ml DMF and appropriate amounts of CDI (for mass ratio 1:2, 0.84 g) in 10 ml DMF was added to the CMC solution. The reaction mixture with addition of 4-DMAp (0.05 g) as catalyst, was allowed to proceed for 1 and 2 min (with 5 min of stirring between each minute of irradiation) of microwave irradiation in modified domestic microwave oven Sencor SMW 2220 (2.45 GHz) at microwave power 280 W. The recovery and purification of the CMC derivative was carried out as described in method (a). The reaction temperature was measured after reaction.

Results and discussion

The carboxymethylcellulose functionalization was performed through esterification with cinnamic acid activated by CDI or DCCI in H_2O/DMF media with addition of 4-DMAp as catalyst. Various reaction conditions and using of both conventional and microwave heating were served to prepare water-soluble CMC derivatives.

The reaction conditions and characteristics of the derivatives prepared by conventional heating are summarized in Table 1 and derivatives prepared by microwave irradiation at controlled power 280 W are summarized in Table 2. The yields ranging between 0.32 and 0.45 g per 0.5 g CMC, except derivative CA-CMC IV, indicate losses of the derivatives during their separation from the reaction medium.

Tab. 1 Effect of reaction conditions on the yield and FT-IR characteristics of CA-CMC derivatives prepared under conventional heating.
Tab. 1 Vplyv reakčných podmienok na výťažky a spektrálne charakteristiky CA-CMC derivátov pripravených účinkom klasického ohrevu.

CA-CMC sample	CMC:CA (mass ratio)	Time (hour)	Temp. (°C)	Yield[a] (g/g)	EE[b] (A_{2918}/ A_{1155})
I	2 : 1	24	Lab.	0.32	0.126
II	1 : 1	24	Lab.	0.39	0.507
III	1 : 2	1	70	0.45	0.622
IV	1 : 3	1	80	0.58	0.125

[a] Expressed as g of the recovered derivative per 0.5 g CMC (on dry mass basis), [b] Extent of esterification expressed as the intensity of the $\nu_{as}CH_2$ absorption band.

Tab. 2 Effect of reaction conditions on the yield and FT-IR characteristics of CA-CMC derivatives prepared at controlled microwave power 280 W.
Tab. 2 Vplyv reakčných podmienok na výťažky a spektrálne charakteristiky CA-CMC derivátov pripravených účinkom mikrovlnného ohrevu.

CA-CMC sample	CMC:CA (mass ratio)	Time (min)	Temp. (°C)	Yield[a] (g/g)	EE[b] (A_{2918}/ A_{1155})
V	2 : 1	1	72	0.42	0.047
VI	2 : 1	2	70	0.45	0.128
VII	1 : 2	2	75	0.43	-
VIII	1 : 3	2	75	0.42	0.111

[a] Expressed as g of the recovered derivative per 0.5 g CMC (on dry mass basis), [b] Extent of esterification expressed as the intensity of the $\nu_{as}CH_2$ absorption band, - not determined

Because the elemental analysis of the derivatives (not shown) gave insignificant differences from the data obtained with the starting CMC, the FT-IR ATR spectra were used to estimate the extent of esterification. As illustrated in Fig. 1, the spectral patterns of the derivatives were similar to those of the starting polysaccharide. They showed typical absorptions of the cellulose backbone (ν_{OH} 3259 cm^{-1}, C-O stretching and ring vibration at 1200 – 895 cm^{-1}) and strong asymmetric stretching [$\nu_{as}(COO^-)$] vibration of the carboxylate anions at 1585 cm^{-1} and symmetric stretching [$\nu_s(COO^-)$] vibration at ~ 1412 cm^{-1}. In the spectra of CA-CMC derivatives IV and VIII obtained at a much higher CMC/CA mass ratio (1:3) using both heating sources, signal at 1707 cm^{-1} indicated the presence ν(C=O)stretching of the ester groups. The shift from a more typical absorbance band at 1730 cm^{-1} is attributed to the double bond conjugated with the aromatic ring structure, what is in accordance with literature [14].

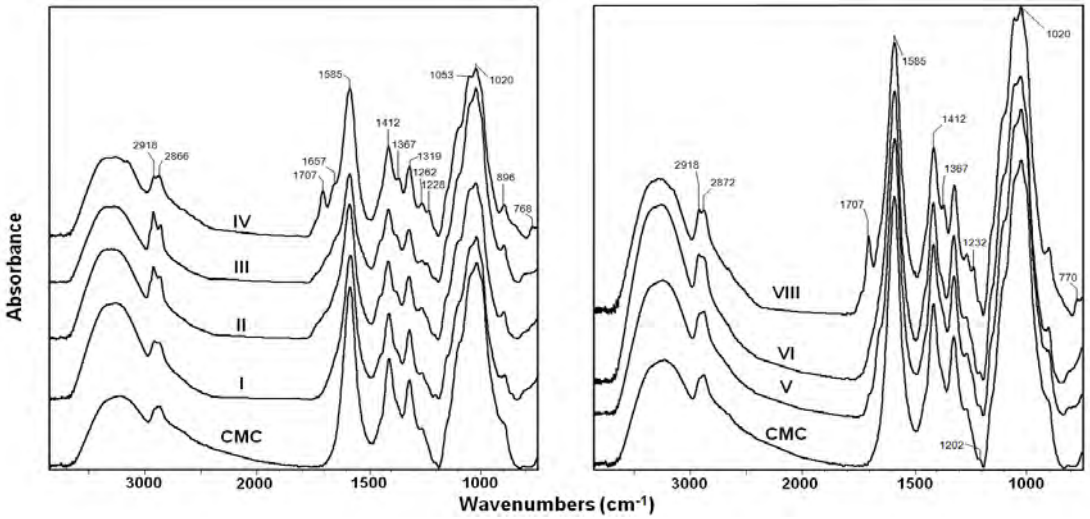

Fig. 1 FT-IR spectra of selected CA-CMC derivatives prepared under conventional heating (CA-CMC I-IV) and under microwave irradiation (CA-CMC V-VIII).
Obr. 1 FT-IR spektrá vybraných CA-CMC derivátov pripravených účinkom konvenčného ohrevu (CA-CMC I-IV) a mikrovlnného žiarenia (CA-CMC V-VIII).

The spectra showed also increased intensities of the absorption band at ~ 2918 cm^{-1} and 2866 cm^{-1}, respectively and it is attributed to the $\nu_{as}(CH_2)$ and $\nu_s(CH_2)$ vibrations of the introduced substituents. Whereas only derivatives IV and VIII displayed absorption band at 1707 cm^{-1} in the FT-IR spectra, we used to express the extent of esterification (EE) absorbance ratio the $\nu_{as}(CH_2)$ vibration and the skeletal ν(C-O-C) vibration at 1155 cm^{-1} typical of cellulose, i.e. A_{2918}/A_{1155}, too. The results are summarized in Tables 1 and 2. As shown in Table 1, the EE values of derivatives prepared using conventional heating, except of CA-CMC IV, were low and slightly increased with increasing mass ratio CMC to CA. EE values of derivatives prepared using microwave irradiation except of CA-CMC VIII increased with prolongation of microwave exposure (Table 2). However in our previous paper, prolongations of microwave exposure led to decreasing of EE [12].

For further characterization and confirmation of CMC functionalization by cinnamic acid the UV spectroscopy was used. The UV spectra of CA-CMC derivatives and unmodified CMC are shown in Fig. 2. The spectra of the CMC esters exhibit the same absorbance characteristic as the cinnamic acid (not shown). An intense absorbance at ~ 280 nm is characteristic of the vinylene C=C absorbance of the cinnamate group [15]. However the unmodified CMC does not show any distinct absorbance in the UV region.

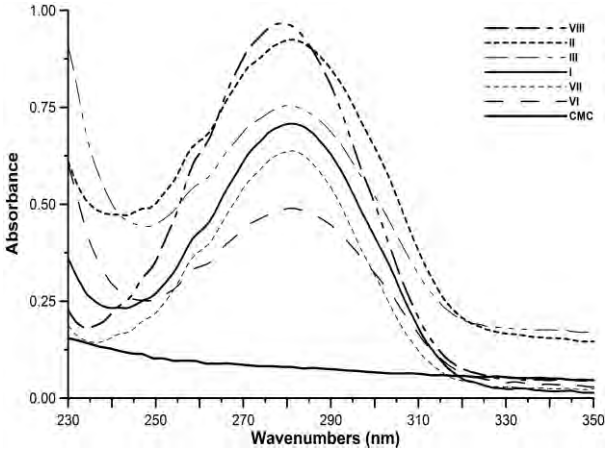

Fig. 2 UV spectra of selected CA-CMC derivatives compared to an unmodified carboxymethylcellulose.
Obr. 2 UV spektrá vybraných CA-CMC derivátov v porovnaní s nemodifikovanou karboxymetylcelulózou.

Conclusions

It was shown that water-soluble CA-CMC derivatives can be prepared under mild reaction conditions using both conventional and microwave heating. Microwave irradiation permits to shorten the esterification time from 24 h at conventional heating to several minutes. The achieved degree of esterification of prepared CA-CMC derivatives was very low. The determination of surface-active and antioxidative properties of derivatives will be subject of future investigations.

Acknowledgement
This work was financially supported by the Slovak Grant Agency VEGA, projects No. 2/0062/09.

Literature

[1] TADROS, T.F. Applied Surfactants: Principles and Applications. Wiley-VCH, Weinheim, 2005, p. 634

[2] SROKOVÁ, I., MINÍKOVÁ, S., EBRINGEROVÁ, A., SASINKOVÁ, V., HEINZE, T. Novel O-(hydroxyethyl)cellulose-based biosurfactants. *Tenside Surfactant Detergents*, 2003, Vol. 40, p. 73-76

[3] ŽOLDÁKOVÁ, A., SROKOVÁ, I., SASINKOVÁ, V., HIRSCH, J., EBRINGEROVÁ, A. Biosurafactants based on partially esterified O-(carboxymethyl)starch. *Chemical Papers*, 2005, Vol. 59, p. 362-367

[4] TOMANOVÁ, V., SROKOVÁ, I., SASINKOVÁ, V. Synthesis and Surface-Active Properties of Carboxymethylcellulose Esters Obtained by Microwave Assisted Transesterification of Vinyl Laurate. *Journal of Life Science*, 2012, Vol. 5(1), p. 74-80

[5] TOMANOVÁ, V., PIELICHOWSKI, K., SROKOVÁ, I., ŽOLDÁKOVÁ, A., SASINKOVÁ, V., EBRINGEROVÁ, A. Microwave-assisted synthesis of carboxymethylcellulose-based polymeric surfactants. *Polymer Bulletin*, 2008, Vol. 60, p. 15-25

[6] CORSARO, A., CHIACCHIO, U., PISTARA, V., ROMEO, G. Microwave-assisted chemistry of carbohydrates. *Current Organic Chemistry*, 2004, Vol. 8, p. 511-538

[7] SATGÉ, C., VERNEUIL, B., BRANLAND, P, GRANET, R., KRAUSZ, P., ROZIER, J., PETIT, C. Rapid homogenous esterification of cellulose induced by microwave irradiation. *Carbohydrate Polymers*, 2002, Vol. 49, p. 373-376

[8] MINÍKOVÁ, S., SROKOVÁ, I., SASINKOVÁ, V., MALOVIKOVÁ, A., EBRINGEROVÁ, A. Hydrophobic Modification of O-(2-hydroxyethyl)cellulose by microwave-assisted transesterification. *Tenside Surfactant Detergents*, 2009, Vol. 46, p.163-168

[9] ČÍŽOVÁ, A, SROKOVÁ, I., SASINKOVÁ, V. MALOVIKOVÁ, A., EBRINGEROVÁ, A. Carboxymethyl Starch Octenylsuccinate: Microwave- and Ultrasound-assisted Synthesis and Properties. *Starch/Stärch*, 2008, Vol. 60, p. 389-397

[10] KUMAR, ASK., KALIDHASAN, S., RAJESH, V., RAJESH, N. Microwave assisted preparation and characterization of biopolymer-clay composite material and its application for chromium detoxification from industrial effluent. *Advanced Materials Letters*, 2011, Vol. 2(6), p. 383-391

[11] JYOTHI, AN., RAJASEKHARAN KN., MOORTHY SN, SREEKUMAR, J. Microwave-assisted synthesis and characterization of succinate derivatives of cassava (Manihot esculenta Crantz)starch. *Starch/Stärke*, 2005, Vol. 57, p. 556-563

[12] TOMANOVÁ, V., SROKOVÁ, I., EBRINGEROVÁ, A., SASINKOVÁ, V. Surface-Active and Associative Properties of Lonic Polymeric Surfactants Based on Carboxymethylcellulose. *Polymer Engineering Science*, 2011, Vol. 51(8), p. 1476-1483

[13] WONDRACZEK, H., HEINZE, T. Efficient Synthesis and Characterization of New Photoactive Dextran Esters Showing Nanosphere Formation. *Macromolecular Bioscience*, 2008, Vol. 8, p. 606-614

[14] HOLSER, RA., MITCHELL, H., O'KURU, H., HIMMELSBACH, VW. Preparation and Characterization of 4-Methoxy Cinnamoyl Glycerol. *Journal of the American Oil Chemist's Society*, 2008, Vol. 85, p. 347-351

[15] GUPTA, P., TRENOR, SR., LONG, TE., Wilkes GL. In Situ Photo-Cross-Linking of Cinnamate Functionalized Poly(methylmethacrylate-co-2-hydroxyethyl acrylate) Fibers during Electrospinning. *Macromolecules*, 2004, Vol. 37, p. 9211-9218

Modified 4-O-glucuronoxylan: Preparation and Surface-active Properties

Modifikovaný 4-O-glukuronoxylán: príprava a povrchovo-aktívne vlastnosti

Ing. Vladimíra Krmelová, PhD.[1], **Ing. Alena Bielaková**[2]

[1]University of Alexander Dubček in Trenčín, Faculty of Industrial Technologies, I. Krasku 491/30, 020 01 Púchov, Slovak Republic
[2]Jonson Controls, 038 41 Martin, Slovak Republic

In this paper, a method of preparation of biopolymers from 4-O-glucuronoxylan (XY) under microwave radiation is presented. Partial hydrophobization of 4-O-glucuronoxylan was performed by transesterification reaction between vinyl laurate (VILA) and XY in different reaction media at various reaction conditions using microwave radiation with controlled power as heating source. The obtained VILA-XY esters were characterized by fourier-transform infrared (FT-IR) spectroscopy and their solution behaviour was investigated by surface activity measurement. In spite of moderate surface tension-lowering effects, the water-soluble derivatives with low degree of esterification showed excellent emulsifying activity for 'oil in water' type emulsions and it indicates their potential to broaden the field of various applications.

Keywords: *4-O-glucuronoxylan, biopolymers, microwave radiation, FT-IR spectroscopy*

Príspevok sa zaoberá prípravou biopolymérov z 4-O-glukuronoxylánu účinkom mikrovlnného žiarenia, ich charakterizáciou a štúdiom povrchovo-aktívnych vlastností. Parciálna hydrofobizácia 4-O-glukuronoxylánu (XY) sa uskutočnila transesterifikáciou vinyl laurátu (VILA) a XY v prostredí DMF, za katalýzy K_2CO_3, pri teplote 120 – 130 °C a hmotnostnom pomere XY:VILA od 1:1 až 1:5. Modifikácie sa uskutočnili v mikrovlnnom zariadení MILESTONE s regulovateľným výkonom a teplotou v dvoch stupňoch. V prvom stupni boli nastavené parametre reakcie a to výkon (200–300 W) a teplota, ktorá v priebehu 5 min narastala z laboratórnej teploty na teplotu reakčnú (120–130 °C). V druhom stupni reakcia pokračovala pri zvolenej reakčnej teplote a reakčnom čase 2–5 min. Pripravené vodorozpustné VILA-XY deriváty sa charakterizovali fourierovou – transformačnou infračervenou spektroskopiou (FT-IR), ktorá potvrdila prípravu derivátov VILA-XY s nízkym stupňom substitúcie. FT-IR spektrá VILA-XY derivátov a východiskového XY sa merali v tuhej fáze v KBr tabletách. V FT-IR spektrách sa sledoval najmä pás pri vlnočte 1740 cm^{-1}, prislúchajúci valenčným vibráciám ν(CO) esterových skupín. Na základe nameraných FT-IR spektier možno usúdiť, že so zvyšujúcim sa hmotnostným pomerom XY:VILA, a použitím katalyzátora sa zvyšuje intenzita pásu prislúchajúceho CO vibráciám. U všetkých pripravených derivátov sa testovali povrchovo-aktívne vlastnosti a to emulgačná účinnosť, povrchové napätie (γ_{min}) a kritická micelárna koncentrácia (cmc). Deriváty znižovali povrchové napätie iba mierne ~ 59,54 mN/m. Avšak povrchová aktivita derivátov bola zvýšená v roztokoch solí (0,5M roztoku NaCl). Prítomnosť 0,5 M NaCl mala za následok väčšie zníženie povrchového napätia vody (až na 50.6 mN/m). Kritická micelárna koncentrácia sa taktiež s prídavkom soli posúvala k nižším hodnotám (do 0,5 g/L). Napriek tomu, že sa deriváty vyznačovali miernym znižovaním povrchového napätia, vyznačovali sa vynikajúcimi emulgačnými účinnosťami porovnateľnými s komerčným emulgátorom Tweenom 20.

Kľúčové slová: *4-O-glucuronoxylan, biopolyméry, mikrovlnné žiarenie, FT-IR spektroskopia*

Low molecular weight natural materials are as attendant solids in the wood mass of e.g. cellulose, lignin and other materials. These materials include hemicelluloses, water–soluble xylans and 4-O-methyl-glucuronoxylans from beech wood and from the other natural materials. During the last years, considerable interest has been directed to amphipilic polymers because of the variety of their possible pharmaceutical, biotechnological and industrial applications [1]. They can be prepared by partial hydrophobization of commercial and non-commercial polysaccharides [2, 3]. 4-O-glucuronoxylan is a polysaccharide raw material which can give product after controlled chemical modification of hydroxyl groups of variety of novel functional properties, e.g. biosurfactants, thermostable polymers, etc. Extraction of xylans, their chemical modification and the applicability was described by Ebringerová [4]. A further review summarizes the chemical modification of xylan by Heinze et al. [5]. In the latest publication, the potential of xylan as biomaterial resource was described by Ebringerová [6]. Many esters of xylan were prepared by classical esterification methods of polysaccharides in homogeneous and heterogeneous conditions.

Recently, there has been a growing interest in the use of microwave heating in organic synthesis, eliminating the use of solvents and catalysts and also dramatically reducing the amount of wastes and volatile organic compounds. Every kind of reaction performed with a classical heating system (oil bath, heating mantle) can be performed with microwave radiation, with the presence of a component that is able to absorb

microwaves. There are few reports concerning the application of microwave heating in the esterification of cellulose and cellulose derivatives [7, 8], some of them have been performed under solvent-free conditions.

In continuation of our research on functionalization of xylan-type polysaccharides by partial hydrophobization, this paper is focused on the microwave assisted synthesis of water-soluble amphiphilic 4-O-glucurono-xylans derivatives using the vinyl laurate (VILA) as esterifying agents.

Experiment

Materials and methods

4-O-glucuronoxylan X-86 D (XY) was a waste product (water soluble polysaccharide) of the isolation of xylans from beech wood meal. It contains 12.4 % of 4-O-methyl-D-glucuronic acid, corresponding to the xylose/uronic acid molar ratio of 12:1, representing a degree of substitution of the xylan chain DS=0.10, and an average number molecular mass was 32 500 (Institute of Chemistry, SAS, Bratislava, Slovakia).

Vinyl laurate (VILA) was purchased from Fluka Chemika, Sigma Aldrich Chemie (Steinheim, Germany). N,N-Dimethylformamide (DMF) and potassium carbonate (K_2CO_3) were commercial products from Sigma-Aldrich Chemical Co. (Schnelldorf, Germany). Tween 20 (oxyethylated sorbitol monolaurate) was from Aldrich Chemical Co. (Steinheim, Germany).

Fourier-transform infrared (FT-IR) spectra were obtained by help of NICOLET Magna 750 spectrometer with DTGS detector and OMNIC 3.2 software using 128 scans at a resolution of 4 cm^{-1}. The samples (2.0 mg) were pressed into pellets of KBr (200 mg) in Institute of Chemistry, SAS (Bratislava, Slovak Republic).

Synthesis of 4-O-glucuronoxylan (XY) with VILA under microwave radiation: XY (0.5 g) was added into 25 mL DMF and stirred at room temperature for 2 h. Subsequently, VILA (0.5–2.5 g) was added to the XY suspension. The reaction mixture, with and without addition of K_2CO_3 (0.07 g in 5 mL water) as catalyst, was under permanent stirring exposed to microwave heating in two stages, using the microwave reactor 'Milestone' (maximum 1000 W power) equipped with a magnetic stirrer (Sorisole, Italy). In the first stage lasting 5 min, the power was increased from 0-300 (500, 600) W and the temperature increased from room to reaction temperatures (90–115 °C). In the second stage (300 W power), the reaction continued at the selected reaction temperature and measuring process of the reaction time started. After reaction, the product was poured into 4-6 volumes of methanol and the precipitated derivative was separated by filtration, thoroughly washed with methanol, and extracted in a Soxhlet apparatus with methanol for 8 h to remove the unreacted acylation agent and degradation products.

Surface-active properties of XY derivatives

Emulsifying efficiency
The emulsifying efficiency was tested for emulsion of the 'oil in water' (O/W) type. The emulsion was prepared by mixing 9 mL water containing 0.05 g of the tested derivative and 1 mL of paraffinic oil dyed with SUDAN IV using the laboratory mixer (Heidolph DIAX 600) at 20 500 rpm for 1 min. The stability of the emulsion was estimated at three time intervals after the emulsions had been prepared, i.e. 5 min (h_1), 1 h (h_2) and 24 h (h_3), and expressed in terms of the height (mm) of the oil and cream layers were formed on the surface of the emulsion.

Surface tension
The surface tension of polysaccharide solution in water or 0.5 M aqueous NaCl in the concentration range 0.0391–2.5 $g \cdot L^{-1}$ was determined at 25 ºC using the Du Nouy ring apparatus. Surface tension data were plotted against the logarithm of polysaccharide concentration in order to obtain the critical micelle concentration (*cmc*) and the corresponding surface tension (γ_{min}), as it was described in previous papers [8].

Results and discussion

The partial hydrophobization of 4-O-glucuronoxylan was performed by transesterification of VILA under microwave radiation with controlled power in DMF. A series of water-soluble derivatives was synthesized by varying the XY/VILA mass ratio, reaction time and temperature and power profiles of the microwave reactor as listed in Table 1. The aim was to prepare the water-soluble xylan ester derivatives but it can be expected only for derivatives of low hydrophobization degree. The XY/VILA mass ratios varied from 1:1 to 1:5. As can be seen, the yields varied mainly around 0.63–0.46 g derivative per 0.5 of starting XY and in some experiments the yields were noticeably lower indicating material loss during the recovery procedures of the derivative. The products were characterized by FT-IR spectroscopy, measured in relation to KBr pellets. The FT-IR spectra of the derivatives also show a pattern of absorption bands similar to that of the starting glucuronoxylan. The FT-IR spectra (Fig. 1) provided a qualitative proof of the introduced ester function, which gave the characteristic ν(C=O) absorption band at 1740±4 cm^{-1}. However, at very low esterification extent, the ester group vibration appeared as a shoulder and the same 4-O-glucuronoxylan esters (derivates I, II) don't show characteristic vibrations for C=O bands. The FT-IR spectrum of derivatives (IV-VI) prepared under similar conditions but with K_2CO_3 as a catalyst show very intensive peak of characteristic ν(C=O) absorption band at 1740 cm^{-1}. The FT-IR spectra show, next to the ester vibration, absorption bands of the $\nu_{as}(COO^-)$ and $\nu_s(COO^-)$ vibrations at 1605±2 cm^{-1} and 1417±2 cm^{-1}, respectively. The implementation of lauroyl groups is further supported by the increase of the bands at 2926±2 cm^{-1} and 2856±2 cm^{-1} which are attributed to

Hutnické listy č.7/2013, roč. LXVI
ISSN 0018-8069

$\nu_{as}(CH_2)$ and $\nu_s(CH_2)$ vibrations, respectively in relation to the methylenic chain. The surface-active properties of the xylan derivatives were characterized by surface tension (γ_{min}), critical micelle concentration (*cmc*) and emulsifying efficiency. As shown in Table 2, the esterified derivatives did not have suppressing effect on the surface tension of water. The γ_{min} values decreased the surface tension of water in the range from 64.87 mN/m to 54.2 mN/m and the *cmc* ranged between 2.45 g/L and 0.15 g/L. Similar effects were reported for other biopolymeric surfactants [9] as well as for derivatives prepared from water-insoluble glucuronoxylan from beech sulfite pulp [10]. However, the surface activity of all VILA-XY derivatives was strengthened when it was measured in 0.5 M of aqueous NaCl.

Tab. 1 Reaction conditions and yields of VILA-XY derivatives prepared in the DMF medium at controlled microwave power
Tab. 1 Reakčné podmienky a výťažky VILA-XY derivátov pripravených v prostredí DMF účinkom mikrovlnného žiarenia

VILA-XY sample	XY:VILA (mass ratio)	Time[a] (min)	Temp. (°C)	Power (W)	Yield[b] (g/g)
I	1 : 1	2	120	300	0.40
II	1 : 3	2	120	300	0.55
III	1 : 3	5	120	300	0.46
IV[d]	1 : 3	5	130	200	0.45
V[c,d]	1 : 3	5	130	200	0.46
VI[c,d]	1 : 5	5	130	200	0.63

[a] Measurement after the 1st stage of microwave heating;
[b] Expressed as g of the recovered derivative per 0.5 g XY (on dry mass basis);
[c] The 1st stage lasted only 3 min; [d] K_2CO_3 was used as a catalyst.

Tab. 2 Surface-active properties of selected hydrophobized VILA-XY derivatives and unmodified XY
Tab. 2 Povrchovo-aktívne vlastnosti vybraných derivátov VILA-XY a nemodifikovaného xylánu

VILA-XY sample	Oil/cream layer[a] (mm/mm)			γ_{min} (mN/m)		*cmc* (g/L)	
	h_1	h_2	h_3	water	NaCl	water	NaCl
I	0/0	0/16	0/14	62.3	-	no have	-
II	0/1	0/11	0/11	60.3	-	no have	-
III	0/0	0/18	0/16	59.54	56.32	1.95	1.05
IV	0/6	0/13	0/12	64.87	62.16	2.45	2.20
V	0/2	0/10	0/14	54.20	50.03	0.15	0.05
VI	0/0	0/13	0/14	61.16	51.80	0.35	0.31
XY	0/0	0/12	0.5/9	60.5	-	no have	-
Tween 20	0/0	0/0	0/8	-	-	-	-

[a] Height of the oil and cream layers formed on the surface of the emulsion after 5 min (h_1), 1 h (h_2) and 24 h (h_3);
- Not determined.

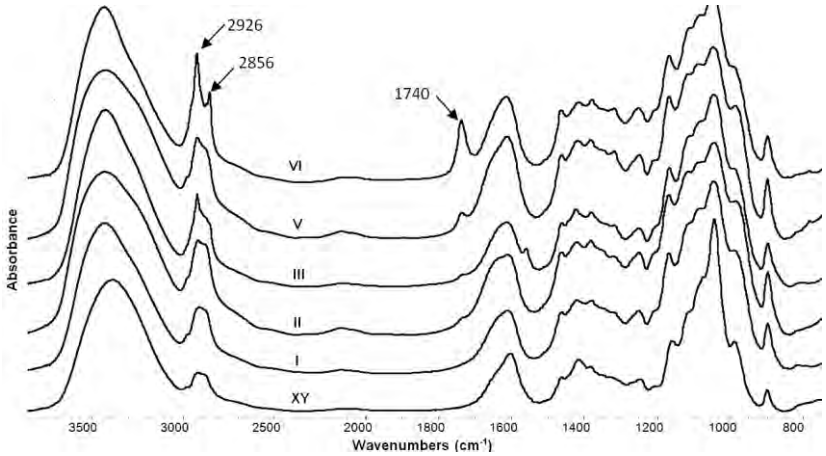

Fig. 1 FT-IR spectra of XY and selected VILA-XY derivatives prepared by transesterification of VILA in the DMF medium
Obr. 1 FT-IR spektrá XY a vybraných VILA-XY derivátov pripravených transesterifikáciou VILA v prostredí DMF

In spite of the aqueous solution of some of the derivatives, considerable emulsifying ability was displayed. Most of the tested derivatives gave emulsions of the oil/water type with excellent emulsifying

Hutnické listy č.7/2013, roč. LXVI
ISSN 0018-8069

efficiency comparable to that of the commercial emulsifier Tween 20.

Conclusions

Water-soluble VILA-XY derivatives with low extent of esterification and acceptable surface-active properties can be prepared using the microwave radiation which substantially reduces the reaction time down to several min and in some cases, lower reaction temperatures can be used, when it is compared to the conditions of transesterification methods performed under classical heating [11]. Although the hydrophobized XY derivatives did not have pronounced lowering effect on the surface tension of water, they exhibited excellent emulsifying properties which were comparable or even better than that of the control – the synthetic emulsifier Tween 20.

The prepared amphiphilic XY derivatives are potential polymeric biosurfactants, which are exploitable in various technical, pharmaceutical, biotechnological and industrial applications. Due to the relatively low amount of introduced ester functions (the low degree of esterification), the biodegradability of the XY should not be changed. The presented microwave-assisted transesterification method might substitute the toxic, hazardous and time-consuming classical esterification processes for preparing polysaccharide-based surfactants.

Acknowledgement
This work was financially supported by the Slovak Grant Agency VEGA, projects No. 2/0062/09.

Literature

[1] TANAKA, R., MEADOWS, J., PHILLIPS, G.O., WILLIAMS, P.A. Viscometric and spectroscopic studies on the solution behaviour of hydrophobically modified cellulosic polymers. *Carbohydrate Polymers*, 1990, Vol. 12, p. 443-459

[2] BATAILLE, I., HUGUET, J., MULLER, G., MOCANU, G., CARPOV, A. Associative behaviour of hydrophobically modified carboxymethylpullulan derivatives. *International Journal of Biological Macromolecules* 1997, Vol. 20, p. 179-191

[3] ŽOLDÁKOVÁ, A., SROKOVÁ, I., SASINKOVÁ, V., HIRSCH, J., EBRINGEROVÁ, A. Biosurafactants based on partially esterified O-(carboxymethyl)starch. *Chemical Papers*, 2005, Vol. 59, p. 362-367

[4] EBRINGEROVÁ, A. Hemicelluloses as biopolymeric raw materials. *Das Papier,* 1992, Vol. 46, p. 726-733

[5] HEINZE, T., KOSCHELLA, A., EBRINGEROVÁ, A. In: Hemicellulose: Science and Technology Washington: American Chemical Society, ACS symposium Series, 2004, Vol. 864, p. 312-325

[6] EBRINGEROVÁ, A. The potential of xylan as biomaterial resources. In: Habibi Y and Lucia LA (ed) *Polysaccharide Building Blocks: A Sustainable Approach to the Development of Renewable Biomaterials*, John Wiley & Sons, Inc., Hoboken New Jersey, 2012, p. 331-366

[7] SATGÉ, C., VERNEUIL, B., BRANLAND, P, GRANET, R., KRAUSZ, P., ROZIER, J., PETIT, C. Rapid homogenous esterification of cellulose induced by microwave irradiation. *Carbohydrate Polymers*, 2002, Vol. 49, p. 373-376

[8] MINÍKOVÁ, S., SROKOVÁ, I., SASINKOVÁ, V., MALOVIKOVÁ, A., EBRINGEROVÁ, A. Hydrophobic Modification of O-(2-hydroxyethyl)cellulose by microwave-assisted transesterification. *Tenside Surfactant Detergents*, 2009, Vol. 46, p.163-168

[9] TOMANOVÁ, V., PIELICHOWSKI, K., SROKOVÁ, I., ŽOLDÁKOVÁ, A., SASINKOVÁ, V., EBRINGEROVÁ, A. Microwave-assisted synthesis of carboxymethylcellulose-based polymeric surfactants. *Polymer Bulletin*, 2008, Vol. 60, p. 15-25

[10] GRONDALL, M., TELEMAN, A., GATENHOLM, P. Effect of Acetylation on the material properties of glucuronoxylan from aspen wood. *Carbohydrate Polymers*, 2003, Vol. 52, p. 359-366

[11] ALBURTO, J., ALRIC, L., BORREDON, E. Organic solvent – free transesterification of various starches with lauric acid methyl ester and triacyl glycerides. *Starch / Stärke*, 2005, Vol. 57, p. 145-152

koroze, povrchová úprava

New Potential Adhesive Agents for Deposition Rubber Mixtures

Nové potenciálne adhézne činidlá gumárenských nánosových zmesí

Ing. Marián Božek[1], **doc. Ing. Milan Olšovský, PhD.**[1]

[1]University of Alexander Dubček in Trenčín, Faculty of Industrial Technologies, I. Krasku 491/30, 020 01 Púchov, Slovak Republic

The paper presents the problems of adhesion between rubber mixtures and steel cords. The object of the investigation was to find out how to change the properties of a basic mixture after incorporation of different adhesion agents which were based on cobalt. Cobalt agents were not used in the mixture as the complex form but they were applied as the form of organic compounds. Therefore, we expected, it could be more easily dispersible in rubber mixture. Adhesive agents are dosed according to two procedures. The investigation was focused on two different series of samples: the first one series of samples containing a constant amount of adhesive agents and the second series with a constant amount of cobalt in the mixture. We compared the adhesion, physical and mechanical properties, vulcanization characteristics and crosslink density of these mixtures. On the basis of the measurements and tests, we developed conclusions and proposals relating to the research and development for the application in the future investigations.

Keywords: *adhesion, rubber, steel cord, mechanical properties*

Príspevok sa zaoberá problematikou adhézie gumárenských zmesí na pomosadzený oceľový kord. Neustále vzrastajúce nároky na výrobky zvyšujú aj nároky na pevnosť adhézneho spoja. Pri vystužených gumárenských výrobkoch je mimoriadne dôležitá adhézia medzi kaučukovou matricou a výstužnými materiálmi. Všeobecne adhézia oceľových materiálov ku gume je zlá, preto je neustále snaha hľadať mechanizmy a spôsoby ako ju zlepšiť. V našej práci sme vybrali celkom 6 nových látok, ktoré by mohli byť použité ako náhrada v súčasnosti používaných adhéznych činidiel. Sú to látky, ktoré počas vulkanizácie spolu s vulkanizačným systémom vytvoria rad zlúčenín, ktoré zlepšia adhéziu gumy (kaučuku) k povrchu oceľového materiálu. Povrch oceľového materiálu však musí byť povrchovo upravený. Objektom skúmania v práci bolo zistiť, ako sa zmenia vlastnosti základnej nánosovej zmesi po pridaní rôznych adhéznych činidiel na báze kobaltu. Sú to látky, ktoré počas vulkanizácie spolu s vulkanizačným systémom vytvoria rad zlúčenín, ktoré zlepšia adhéziu gumy (kaučuku) k povrchu oceľového materiálu. Kobaltnaté činidlá sme do zmesi nezapracovali vo forme komplexu, ale vo forme organických zlúčenín, čo je prijateľnejšie hlavne z environmentálneho hľadiska. Očakávali sme, že môžu byť ľahšie dispergovateľné do kaučukovej zmesi. Adhézne činidlá sme dávkovali podľa 2 postupov. Prvá séria vzoriek obsahovala konštantné množstvo adhézneho činidla, druhá séria konštantné množstvo kobaltu v zmesi. S vybranými zlúčeninami vo funkcii adhéznych činidiel sme pripravili štandardné gumárenské zmesi, ktoré sa používajú pri výrobe nánosových zmesí na pätku autoplášťov. Porovnávali sme adhéziu, mechanické vlastnosti, vulkanizačné charakteristiky a sieťovú hustotu zmesí. Ďalším dôležitým aspektom je v súčasnosti už vo všetkých priemyselných výrobách aj environmentálne hľadisko a znižovanie množstva surovín a materiálov potrebných na výrobu výrobku.

Kľúčové slová: *adhézia, guma, oceľový kord, mechanické vlastnosti*

For rubber products, such as tyres and conveyor belts, it is extremely important to pay attention to adhesion between the rubber matrix and the reinforcing materials. High demands in relation to products lead to increase adhesive bond strength. To ensure sufficient strength and stiffness of rubber products, the steel reinforcement materials are mainly used [1, 2].

Hutnické listy č.7/2013, roč. LXVI
ISSN 0018-8069

Generally, adhesion between steel materials and rubber mixtures is bad, so we have to find mechanisms and ways to improve it. In relation to the rubber mixtures, the one of the possible solutions is connected with the addition of constituents which are also called adhesive agents. These are substances that together with vulcanization system create compounds during vulcanization and by this way, they can improve adhesion of rubber to the surface of the steel material. The surface of steel material has to be modified with brass, zinc and bronze [3, 4].

Another important aspect has been already introduced by all industrial production and this aspect includes environmental perspective and quantity reduction of materials needed for manufacture of the product. Therefore, nowadays, there is still the effort to find the way for the achievement of the mentioned objectives. The facts and objectives introduced in the previous text can be also applied for adhesive agents [5].

In our work, six new substances were chosen and they were used as substitute agents instead of commonly used adhesion agents. The new chosen adhesion agents were based on cobalt and they are not in the form of a complex compounds. Our samples have an active substance which is bound in organic matter and moreover, they are acceptable from an environmental point of view. Their structure is very similar to the structure of used rubber mixtures. So they could be better dispersible in rubber mixtures [6, 7].

We prepared the rubber mixtures with selected adhesion agents to be used as the standard rubber mixtures which are commonly used as deposition mixtures in the manufacture and subsequently, processing system, physical, mechanical and adhesion tests of prepared mixtures were done. Finally, all the samples were compared to the standard.

Results and discussion

To determine the adhesion, 14 rubber mixtures (samples) were prepared while the preparation of all these tested samples was resulting from the standard deposition mixture (characterization of samples is in Tab. 1). In the mixtures, only the content and type of the adhesive agent was changed. Other components of rubber mixtures were identical in all cases. The first series of samples (1 - 6) contained a constant amount of adhesion agents (10.27 phr. in the mixture). Second series of samples (7 - 12) contained a constant amount of cobalt in the mixture (0.6 g Co).

Tab. 1 Characterization of adhesive system in samples
Tab. 1 Charakteristika adhézneho systému vo vzorkách

Sample	Characterization	Content of adhesive agent
1	cobalt borate	constant content of adhesive agent
2	cobalt stearate	
3	cobalt oleate	
4	soap mixture 1	
5	soap mixture 2	
6	zinc soap	
7	cobalt borate	constant content of cobalt
8	cobalt stearate	
9	cobalt oleate	
10	soap mixture 1	
11	soap mixture 2	
12	zinc soap	
13	commercial product - MANOBOND C620	
14	standard	

soap mixture 1 = acids of rapsol oil : stearic acid = 7 : 3, content of cobalt = 8.60 %

soap mixture 2 = acids of rapsol oil : stearic acid = 1 : 1, content of cobalt = 7.70 %

MANOBOND C680 = adhesive promotor; producer: OMK UK LIMITED, contents of cobalt = 22.50 %; density = 1.4 $g.cm^{-3}$

Determination of adhesion

The principle of the measurement was to determine the adhesion of the standard rubber mixtures used in the manufacture of bead wires where adhesive agents based on cobalt were modified. Mixtures were prepared in the form of foil pulled out from the laboratory calender. The foil was directly moulded to be used as steel cord.

After comparison to the standard mixture, the increase of adhesion was observed for all samples. The significant increase was observed in the case of zinc soap and soap mixture 2 but values of the commercial product (Manobond C680) were not overcome by any of our samples.

Subsequently, the adhesion test was performed for samples with a constant amount of cobalt in the mixture. In figure 2, it is shown that some samples showed an increase of adhesion (cobalt stearate, mixed soap 2). However, the decrease was also observed for some samples (cobalt borate, mixed soap 1, zinc soap). Therefore, we can assume that the increased amount of adhesive agents can also act as a plasticizer and it leads to reduction of adhesion.

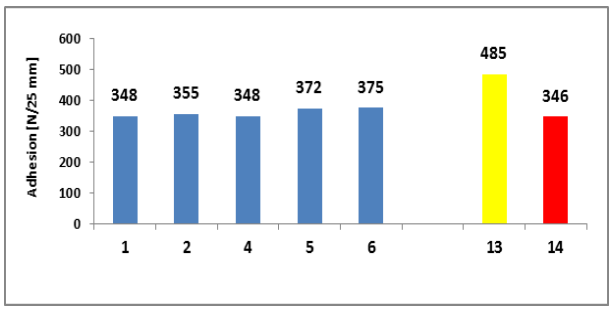

Fig. 1 Adhesion of samples with constant content of adhesive agents in mixture
Obr. 1 Adhézia vzoriek s konštantným obsahom adhéznych aditív v zmesi

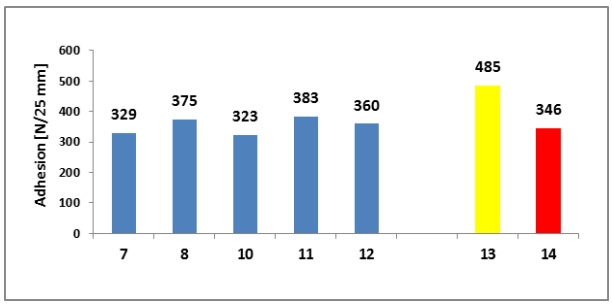

Fig. 2 Adhesion of samples with constant content of cobalt in mixture
Obr. 2 Adhézia vzoriek s konštantným obsahom kobaltu v zmesi

Determination of tensile properties and hardness

Tensile properties include a number of parameters in relation to stress/strain. In the case of the tensile strength, it is important to pay attention to strain resulting from stress, elongation at break and shear stress. For the test, the blades were prepared while the working part was 6 mm in diameter and the thickness was from 2 to 2.5 mm. The tested samples were left at for 24 h at room temperature. Tests were carried out at the feed speed of jaw 50 mm.min^{-1} under room temperature.

Tab. 2 Mechanical properties of vulcanizates
Tab. 2 Mechanické vlastnosti vulkanizátov

Sample	Tensile strength (MPa)	Elongation (%)	Hardness (IRHD)
1	9.95	232	82.9
2	12.76	448	84.8
3	8.75	156	85.7
4	11.29	241	86.2
5	11.34	252	86.7
6	12.72	543	81.8
7	11.31	315	81.4
8	9.29	363	87.2
9	7.67	127	87.6
10	8.39	329	84.2
11	6.18	188	88.9
12	12.06	646	81.5
14	14.68	296	76.1

There was not any sample which would have overcome the tensile strength of the standard mixture. The closest values were observed in the case of sample 2 (cobalt stearate) as well as samples 6 and 12 (zinc soaps). On the other hand, the elongation significantly increased for these samples (including sample 8) and it led to the excellent flexibility of the blends. The feature of good flexibility was also observed for samples 7 and 10.

The hardness increase was found out for all the tested samples. Soap mixture 2 (samples 5 and 11) showed the highest increase and it was similar to the sample 8 and sample 9. This means that all the mentioned mixtures were much more resistant to impact and it is very important aspect in the case of tyre bead.

Determination of crosslink density

The cubes with dimensions 5 × 5 × 2 mm were cut out from all of the prepared mixtures. Then, the given cubes were immersed into the solution of xylene with Dusantox IPPD because of measurement of swelling degree in different time intervals.

The fig. 3 shows that samples 1, 4 and 5 are the closest to the values of the crosslink density of the standard mixture. None of the samples overcame the given value. This means that all samples with a constant amount of the added adhesion agents reduced quantitative measure vulcanization of rubber mixtures and the number of chemical cross-links between polymer chains is smaller. We can see some changes when there is the constant amount of cobalt in the mixture. Sample 10 (mixed soap 1) shows a significant increase of the number of incurred crosslinks. It means that rapeseed oil acids in this mixture helped to increase the crosslink density. On the other side, the other samples except of sample 7 (cobalt borate) reached unsatisfying values. The constant amount of cobalt in the mixture results in the reduction in the speed and efficiency of vulcanization and it has a direct impact on the results of the crosslink density of these mixtures.

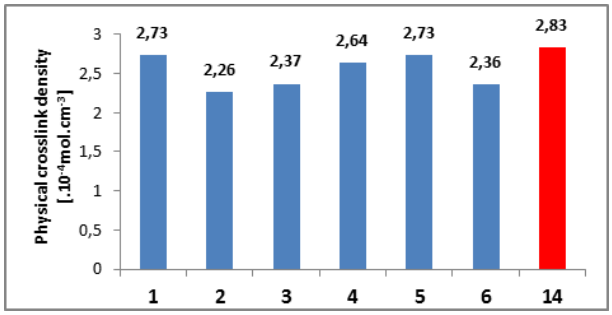

Fig. 3 Crosslink density of vulcanizates with constant content of adhesive agents in mixture
Obr. 3 Fyzikálna sieťová hustota vulkanizátov s konštantným obsahom adhéznych činidiel v zmesi

Hutnické listy č.7/2013, roč. LXVI
ISSN 0018-8069

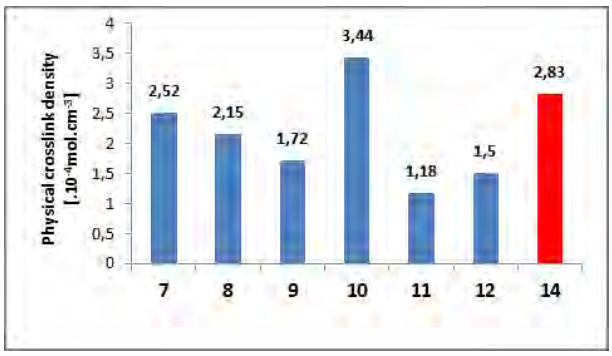

Fig. 4 Crosslink density of vulcanizates with constant content of cobalt in mixture

Obr. 4 Fyzikálna sieťová hustota vulkanizátov s konštantným obsahom kobaltu v zmesi

Conclusions

Adhesion values of tested mixtures are higher than the adhesion values of standard mixture. On the other hand, the values of tested samples did not reach the values which are utilized and specified for the samples with a commercial type of adhesive agent (Manobond C680) which is the commonly used adhesion agent in practice. This may be caused by higher content of cobalt in Manobond C680 (22.5 %). The same amount of active substance in the mixture (22.5 %) leads to the usage of the higher amount of the adhesive agent but it has negative impact on mechanical properties including tensile strength.

In relation to vulcanization characteristics, we can conclude that all of our samples of adhesion agents prolong the optimum vulcanization time but there is the reduction of the vulcanization start.

According to the obtained values, it can be concluded that lower values of the rate coefficients of vulcanization lead to slower vulcanization and the course of vulcanization curves is less "sharp" than in the case of the standard but all the samples show a steady shape of vulcanization curves.

All vulcanizates exhibit higher hardness values IRHD and higher values of elongation. Elongation parameter of mixtures is very important feature because it can improve "leaks" of mixture into the steel wire. Higher values of hardness can have negative influence on this effect. Tensile strength of all vulcanizates is lower in comparison to standard mixture.

After correct modification of dosage in relation to tested adhesion agents, it is possible to substitute the commonly used adhesion agents based on cobalt-bound complex. Our samples can be also preferable from an environmental point of view and moreover, their chemical structures are converging to used rubber mixtures. This can also result in time savings in relation to incorporation of agents to the rubber mixtures in the future.

Literature

[1] POISSON, C., HERVAIS, V. *Adhesion properties improve using binder /EVA blend.* In: Journal of Applied Polymer Science. ISSN 0021-8995, 2006, vol. 122, no. 101, p. 118-127.

[2] QIN, R. Y.: Adhesion at partially restructured polymer surfaces. In: Schreiber Colloids and Surfaces. ISSN 0927-7757, 1999, č. 156, p. 85-93.

[3] VICKERMAN, J.C., BRIGGS, D.: *Surface analysis by mass spectrometry.* In: Publications and Surface Spectra Limited. ISSN 1520-5835, 2001, č 28, pp. 202-284.

[4] HOUFEK, J. a kol.: *Roztok pro úpravu kovů před vulkanizací gumy*. CZ patent 2004-1230, 2004.

[5] DATTA, J. et al.: S*teel cord adhesion promoting accelerators*. Akzo Nobel N.V. Intellectual Property Dept. Arnhem (NL), WO patent: WO/2003/070820, 2002.

[6] PUCHKOV, A. F., TURENKI, S. V.: *Blocked Diisocyanate as a Promoter of Rubber Adhesion to Brass-Plated Metal Cord*. Volgograd: Volgograd State Technical University, 2005, ISSN 1070-4272.

[7] ZIEGLER, E.: *Investigation of the influence of stearic acid on rubber–brass adhesion*. In: Fall 180th Technical Meeting of the Rubber Division of the American Chemical Society, Inc. Cleveland, Ohio, October 11-13, 2011, ISSN 1547-1977.

The Modified Clay Materials and their Influence on the Properties of Polymeric Materials

Modifikované ílové materiály a ich vplyv na vlastnosti polymérnych materiálov

prof. RNDr. Mariana Pajtášová, PhD.[1], Ing. Zuzana Jankurová, PhD.[1], Ing. Andrea Feriancová, PhD.[1], Ing. Janka Paliesková[1], Ing. Katarína Holcová[1]

[1]University of Alexander Dubček in Trenčín, Faculty of Industrial Technologies, I. Krasku 491/30, 020 01 Púchov, Slovak Republic

The given paper deals with the preparation of modified clay materials and their subsequent applications to polymeric materials. We studied parameter changes of vulcanization characteristics (minimum torque M_L, maximum torque M_H, processing safety of compound t_s, optimum time of vulcanization $t_{c(90)}$, rate coefficient of vulcanization R_v) for unvulcanized model rubber compounds, physical-mechanical properties (tensile strength, tensibility, hardness) of resultant vulcanizates. The mentioned results were compared to values of standard model compound without addition of prepared modified filler. Prepared modified clay materials in the function of filler as well as in the function of accelerating agents of sulfur vulcanization could be used due to their of the eco-friendly influence on the environmental sphere and moreover, they can improve production efficiency of rubber compounds.

Keywords: *polymeric materials, vulcanization characteristics, physical and mechanical properties, modified clay materials*

V práci sa zaoberáme prípravou modifikovaných ílových materiálov pripravených z dioktaédrického smektitu štruktúrneho typu 2:1 (montmorillonit) s interkaláciou organických molekúl urýchľovačov sírnej vulkanizácie na báze tiofosfátov a ditiofosfátov a zároveň ich aplikáciou do modelových gumárenských zmesí vo funkcií plnív. Na prípravu modifikovaných ílových materiálov sa vybrali dva typy urýchľovačov sírnej vulkanizácie na báze tiofosfátov a ditiofosfátov, konkrétne sa vybrali rýchle urýchľovače sírnej vulkanizácie, a to kvapalný urýchľovač na báze ditiofosfátu zinočnatého (V) a kvapalný urýchľovač na báze polysulfidových tiofosfátov (R). Modifikované ílové materiály boli pridávané do modelových gumárenských zmesí vo forme čiastočnej náhrady štandardne používaného plniva – sadzí typu N660. Priebeh sírnej vulkanizácie modelových gumárenských zmesí sa hodnotil na základe vybraných parametrov vulkanizačných charakteristík v porovnaní so štandardnou zmesou. Z reometrických záznamov vulkanizačných kriviek modelových gumárenských zmesí sa určili základné parametre vulkanizačného procesu, konkrétne minimálny krútiaci moment M_L, maximálny krútiaci moment M_H, spracovateľská bezpečnosť zmesi t_s, optimálny čas vulkanizácie $t_{c(90)}$, koeficient rýchlosti vulkanizácie R_v. U modelových vulkanizátov s obsahom modifikovaných ílových materiálov sa testovali a hodnotili vybrané fyzikálno-mechanické vlastnosti (pevnosť, ťažnosť, tvrdosť), poskytujúce informáciu o správaní sa výsledných vulkanizátov v stave statického namáhania. Z nameraných hodnôt vulkanizačných charakteristík a fyzikálno-mechanických vlastností študovaných polymérnych materiálov vyplýva, že je možná čiastočná náhrada štandardne používaného plniva, novými modifikovanými ílovými materiálmi s interkaláciou tiofosfátových alebo ditofosfátových zlúčenín, ktoré plnia funkciu plniva a zároveň môžu prispievať k urýchleniu procesu vulkanizácie.

Kľúčové slová: *polymérne materiály, vulkanizačné charakteristiky, fyzikálne a mechanické vlastnosti, modifikované ílové materiály*

In recent years, polymeric materials have taken important place and growth in industrial production in terms of their applications and have become an indispensable part of everyday life. They are used almost in all industrial branches where they represent one of the important articles in relation to production and consumption of various types of engineering materials [1, 2, 6]. In the production of polymers, the development is focused on improvement of the production processes which can lead to production of the polymeric materials with improved properties. Worldwide and rapid development and industrial growth of polymeric materials has been closely connected with the development and research of polymers in the self-governing regions and there are the investigations including the mutual combination of different polymers or they are combined with any other non-polymeric materials creating polymeric composite materials [3, 4]. In the material research of the polymeric

materials, the current trend includes research of polymers in combination with clay minerals. The economic as well as environmental aspects are the reasons for the mentioned investigation of clay minerals with polymers. Compared to conventional types of filler, small amount of clay mineral can have beneficial effect on modification of the physical and chemical properties relating to polymeric materials. The influence of filler on polymeric materials depends on its physical properties, such as particle size, surface reactivity, surface area, electrical charge of the particle and chemical properties, such as reactivity with accelerators and pH [5].

Experiment

The natural bentonit was used as initial material for the preparation of Co-form of montmorillonite and this initial material was extracted from the locality with the name Stará Kremnička - Jelšový Potok. The chemical composition of bentonite was: SiO_2 59 %, Al_2O_3 20 %, Fe_2O_3 2 %, FeO 0.3 %, TiO_2 0.2 %, CaO 2.2 %, MgO 4 %, K_2O 0.7 %, Na_2O 0.4 % and the content of montmorillonite was 80 %. The predominant form of natural bentonit is the sodium-calcium form but calcium represents the predominant constituent. Therefore, the bentonite has to be processed using the subsequent saturation by calcium chloride solution while its concentration is 0.1 mol.dm^{-3} and this process of saturation leads to preparation of montmorillonite Ca-form. The excess salt was eluted with distilled water until the reaction with silver nitrate solution was negative for chloride anions. The cobalt form was prepared from calcium form under the same conditions mentioned hereinbefore. The modified clay materials were prepared by the sorption of selected accelerators of sulphur vulcanization while the accelerators were based on thiophosphate polysulfide (R) and zinc dithiophosphate (V). The selected accelerators were intercalated from the gas phase to the interlayer of montmorillonite. Prepared modified clay materials were added into the compound replacing the conventional filler in an amount of 1 phr. We evaluated the impact of the prepared fillers on properties of the resultant compounds and vulcanizates. We studied parameter changes of vulcanization characteristics for unvulcanized model rubber compounds and physical-mechanical properties of resultant vulcanizates. The results were compared with values of standard model compound without addition of prepared modified filler. The model rubber compounds were prepared by two-step mixing in laboratory mixer of type Brabender with volume of chamber 70 cm^3 and 50 revolutions per minute and the procedure was done according to STN. The first mixing step was performed at 100 °C where the additives (natural Rubber SMR20, ZnO, stearic acid, carbon black, modified clay materials – CoMMT (1), CoMMT+V (2), CoMMT+R (3), plasticizer) were added to the model rubber compound during 12 minutes. The second mixing step was performed at 90 °C and it included addition of the vulcanization system (sulfur, Sulfenax CBS) during 6 minutes. The mixed model rubber compounds were homogenized during the first and the second steps in laboratory double-rolled device.

Results and discussion

Effect of modified clay materials on the course of sulfur vulcanization of model rubber compounds was evaluated on the basis of vulcanization characteristics. Based on the evaluated rheometric results of vulcanization curves, the values of vulcanization characteristics are presented in Tab. 1 and their graphical presentation is shown in Fig. 1 and 2.

Tab. 1 Vulcanization characteristics of model rubber compounds
Tab. 1 Vulkanizačné charakteristiky modelových gumárenských zmesí

compounds	S	1	2	3
M_L [N.m]	7.9	7.5	7.3	6.7
M_H [N.m]	43.6	41.4	40.6	43.8
t_s [min]	5.16	5.7	5.42	4.81
$t_{c(90)}$ [min]	9.46	10.2	9.63	9.1
R_v [min^{-1}]	23.26	22.22	23.75	23.31

The resultant values of the maximum torque M_H (Fig. 1) for model rubber compounds 1 and 2 are lower in comparison to standard compound. The decrease of values leads to lower stiffness as well as the lower viscosity of the prepared model compounds at the end of vulcanization. Model rubber compound 3 has similar or comparable values to standard (S) and it means good compatibility with the rubber matrix of modified filler.

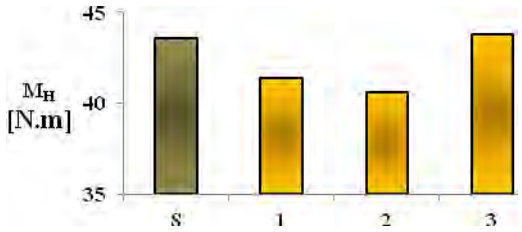

Fig. 1 Maximum torque of model rubber compounds
Obr. 1 Maximálny krútiaci moment modelových gumárenských zmesí

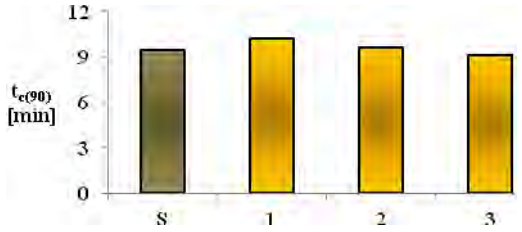

Fig. 2 Optimum time of vulcanization for model rubber compounds
Obr. 2 Optimálna doba vulkanizácie modelových gumárenských zmesí

Compared to standard model compound, the value of optimum time $t_{c(90)}$ (Fig. 2) for rubber compound 3 is

Hutnické listy č.7/2013, roč. LXVI
ISSN 0018-8069

lower. The decrease of optimum time contributed to accelerating the process of vulcanization while the decrease of the optimum time was gained by the presence of modified clay filler which contained accelerators of sulphur vulcanization and these accelerators were intercalated to the interlayer of clay material.

The results of the evaluation of selected physical and mechanical properties of resultant model vulcanizates are presented in Tab. 2 and their graphical presentations are shown in Figs. 3, 4 and 5.

Tab. 2 Physical-mechanical properties of resultant model vulcanizates
Tab. 2 Fyzikálno-mechanické vlastnosti výsledných modelových vulkanizátov

vulcanizates	S	1	2	3
Tensile strength [MPa]	23.7	24.7	23.9	21.5
Tensibility [%]	329	365	366	315
Hardness [IRHD]	64	62	62	64

On the basis of the results of the tensile strength (Fig. 3), it can be seen that the model vulcanizates 1 and 2 reached comparable or even higher values in comparison to the standard model vulcanizate. The slight decrease of tensile strength has been detected in the case of the model vulcanizate 3 and it can be connected with a weaker interaction and bond between the filler and rubber matrix.

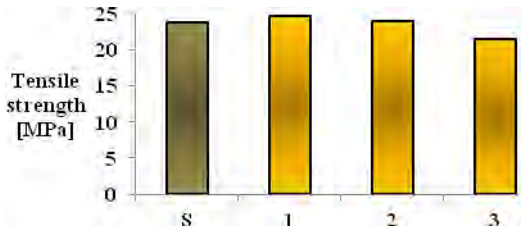

Fig. 3 Tensile strength of resultant model vulcanizates
Obr. 3 Pevnosť v ťahu výsledných modelových vulkanizátov

In relation to the model vulcanizates 1 and 2, the measured values of tensibility (Fig. 4) are higher in comparison to the standard model vulcanizate and it can be especially an advantage for elastic applications.

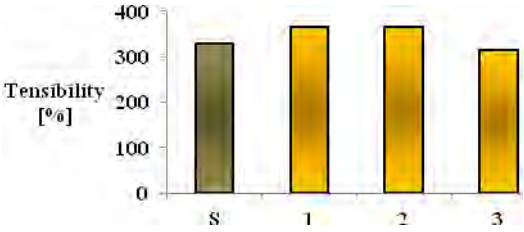

Fig. 4 Tensibility of resultant model vulcanizates
Obr. 4 Ťažnosť výsledných modelových vulkanizátov

The lower values of hardness (Fig. 5) for resultant model vulcanizates 1 and 2 indicated good incorporation of the filler into the mixture and good compatibility with the rubber matrix.

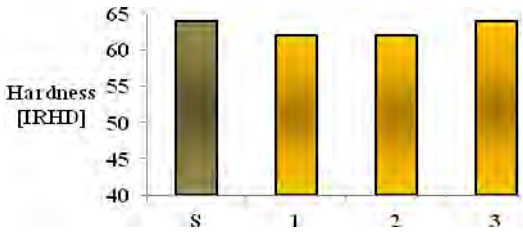

Fig. 5 Hardness of resultant model vulcanizates
Obr. 5 Tvrdosť výsledných modelových vulkanizátov

Conclusions

The main aim of the paper was to prepare modified clay materials and to study their influence on the properties of polymeric materials.

According to the obtained results of vulcanization characteristics and physical and mechanical properties of studied polymeric materials, we can conclude that conventional filler can be replaced partially by modified clay materials.

Acknowledgements
The authors are grateful to the Slovak Grant Agency VEGA 1/0530/11, 1/0185/12 and KEGA 007TnUAD-4/2013 for financial support.

Literature

[1] KYSELÁ, G., HUDEC, I., ALEXY, P. Výroba a spracovanie kaučukov a gumy. Bratislava: STU, 2010. 296 s. ISBN 978-80-227-3324-3

[2] DULEBOVÁ, Ľ., SOBOTOVÁ, L., BADIDA, M. Influence of environment on selected properties of plastics used in automotive industry. In: Strojárstvo EXTRA, 2011, p. 2-5

[3] ALEXY, P. Technológia spracovania polymérov. STU, Bratislava, 2011, ISBN 978-80-227-3430-7

[4] LIPTAKOVÁ, T., ALEXY, P., GONDÁR, E., KHUNOVÁ, V. Polymérne konštrukčné materiály. Žilina: Žilinská univerzita, 2012. 189 s. ISBN 978-80-554-0505-6

[5] PALATY, S., JOSEPH R. Synergism of Xanthate/ Dithiocarbamate Accelerator in Carbon. *Iranian Polymer Journal,* 2004, vol. 13(2), p. 85-91

[6] VAVRO, J., HAJSKÁ, H., VAVRO, J.jr., KOVÁČIKOVÁ, P. Analysis of the Defects in Tyres for freight Vehicles at the dynamic Loading, Machine Modelling and Simulations. Poznaň : Politechnika Pozňanska, 2012. 193–200. ISBN 978-83-923315-2-0

Review: prof. Ing. Darina Ondrušová, PhD.
prof. Ing. Tatiana Liptáková, PhD.

Hutnické listy č.7/2013, roč. LXVI
ISSN 0018-8069

Cyclic Oxidation Resistance of SiAl Diffusive Protective Coatings Deposited by CVD Process on Ni-Superalloys

Odolnosť difúznych ochranných SiAl povlakov deponovaných CVD procesom na Ni-superzliatinách

doc. Ing. Marta Kianicová, PhD.[1], **Ing. Jaroslav Trník**[1], **Ing. Ján Kafrík**[1], **Ing. Ondřej Dvořáček**[2]

[1]University of Alexander Dubček in Trenčín, Faculty of Industrial Technologies, I. Krasku 491/30, 020 01 Púchov, Slovak Republic
[2]PBS Velká Bíteš, a.s., Vlkovská 279, 595 12 Velká Bíteš, Czech Republic

The main aim of the given experimental work is closely connected with the resistance testing of SiAl diffusive protective coatings. The investigation of the resistance against cyclic oxidation atmosphere was the main purpose in this paper. This kind of the protective coating was deposited by CVD method on nickel superalloys Inconel 713LC and MAR-M247. The experimental part includes long-time cyclic oxidation test, where tested samples casted from mentioned superalloys were placed into the special inductive furnace. Tested samples were left in the furnace for 23h in relation to the each one testing cycle. There was only air atmosphere in the furnace with temperature 1100 °C. The tested samples were put out of furnace after each second cycle and then, they were weighed to investigate mass changes of samples. After 24 cycles, the oxidation resistance of both superalloys with SiAl coating was very good and there were not any noticeable damages from the macroscopic aspect. In the case of pure superalloy MAR-M247 (superalloy without coating), the fast declination of oxidation resistance was observed. The significant damages were not determined in relation to the resistance of Inconel 713LC without coating.

Keywords: *SiAl coating, superalloy, oxidation resistance*

Hlavným cieľom experimentálnej práce bolo zistiť odolnosť SiAl difúznych ochranných povlakov voči cyklickej oxidačnej atmosfére. Experimentálna práca prebehla v kooperácií so spoločnosťou PBS Velká Bíteš, a.s., ktorá zabezpečila vzorky niklových zliatin pre povlakovanie a testovanie oxidačnej odolnosti. Tento druh ochranných povlakov bol na vzorky niklových superzliatin Inconel 713LC a MAR-M247 deponovaný CVD technológiou, pomocou metódy "Pack cementation", pri ktorej je povlakovaná vzorka umiestnená priamo do práškovej zmesy. V experimentálnej časti práce sa popisuje dlhodobý cyklický oxidačný test, kde vzorky odliate zo spomínaných zliatin sa umiestnili do indukčnej pece. Testované vzorky zotrvali v peci 23 hodín, čo predstavuje jeden skúšobný cyklus. Teplota v testovacej peci bola 1100 °C. Každý druhý cyklus sa vzorky vybrali z pece a zvážili, aby sa zistili hmotnostné zmeny vzoriek po cykloch. Výsledky ukázali, že oxidačná odolnosť oboch zliatín s ochranným SiAl povlakom bola veľmi dobrá, po 24 cykloch bez badateľných poškodení. Vrstva ochranných oxidov je stabilná a dostatočne adherentná, neodlupuje sa a stale plní funkciu bariéry medzi ochranným povlakom a vonkajším oxidačným prostredím. Takéto oxidy bránia budúcej oxidácií povrchov vzoriek. Predpokladá sa, že životnosť MAR-M247 s ochranným povlakom bude minimálne ešte ďalších 24 cyklov, kým nastane odlupovanie ochranných oxidov a úbytok hmotnosti vzoriek. Z hľadiska mechanického zaťaženia má ale SiAl povlak nevýhodu, vykazuje krehké správanie a môže dôjsť k vzniku trhlín. V prípade čistej zliatiny MAR-M247 oxidačná odolnosť klesala veľmi rýchlo. Už po druhom oxidačnom cycle bol hmotnostný úbytok vzoriek výrazne nižší ako pôvodná hmotnosť vzoriek s povlakom. To znamená, že oxidy vytvorené na vzorke bez povlaku nie sú dostatočne stabilné, odlupujú sa, čím opakovane vystavujú povrch zliatiny oxidačnej atmosfére. Inconel 713LC bez ochranného povlaku odolával cyklickej oxidácií bez významných poškodení.

Kľúčové slová: *SiAl povlak, superzliatina, oxidačná odolnosť*

The aero engines and their parts operate in very aggressive environments where high temperatures, increasing temperature gradients, thermo-mechanical stresses and a presence of oxidizing and corrosive atmospheres can be found. The most loaded parts of aircraft engines are turbine blades. They are mainly casted from nickel-base superalloys which are able withstand only average condition referring to corrosion and oxidation. Therefore is necessary to use protective coatings from the aspect of lifetime increasing and failure prediction [1].

There are two types of protective coating from the point of view of corrosion and oxidation resistance. Diffusive protective coatings and overlay multilayer coatings. Considering the blades, diffusive aluminide coatings are thin physical barriers between base material (substrate) and the external environment. Diffusive aluminide coating consists of intermetallic compound β-NiAl

which is formed on the basis of the substrate influence but it is important to point out that Ni superalloys has to be used as the substrate. General composition of overlay coatings is MCrAlX, where M represents Ni, Co, Fe or combination of these elements. X involves such elements as Y, Si, Ta, Hf, etc. Another class of protective coatings includes TBC - Thermal barrier coatings and they are composed of ceramics [2].

During service, the most common degradation of the protective coatings is connected with degradation modes, such as the high-temperature oxidation, hot corrosion, damage by thermal and thermo-mechanical fatigue, mechanical damage by erosion and creep degradation during overheating.

In the case of high-temperature oxidation, alloying elements in material react with oxygen from atmosphere and some or all metallic elements are transformed to their oxides. Oxide layer is created on the material surfaces and its thickness increases with increasing temperature. Oxide layer is useful for most of metals only if this layer is stable and adherent and forms thermally growth oxides or TGO. This TGO layer formed on top of coating is diffusive barrier against next oxidation. Only Al_2O_3, Cr_2O_3 and SiO_2 are understood as protective oxides. If there is lack of the given protective oxides, there is rapid oxidation of the material surface and it causes weight loss as well AS material thickness. [3]

Experimental

The cyclic oxidation resistance of SiAl diffusive protective coating deposited on nickel superalloys was investigated in the experimental part. Technology of deposition is called chemical vapor deposition (CVD), especially "pack cementation" method of this deposition technology was used. Inconel 713LC and MAR-M247 with SiAl protective coating were exposed to oxidation atmosphere in furnace. Subsequently, oxidation test of pure superalloys without SiAl coating was carried out in order to do mutual comparison. Chemical composition of Inconel 713LC is showed in Tab. 1.

Tab. 1 Chemical composition of Inconel 713Lc
Tab. 1 Chemické zloženie superzliatiny Inconel 713LC

Wt.%	Cr	Al	Mo	Nb	Ti	Zr
Inconel 713LC	11.85	5.8	4.54	2.27	0.72	0.11
	Mo	**C**	**B**	**P**	**S**	**Ni**
	4.54	0.04	0.015	0.006	0.004	Bal.

Second superalloy MAR-M247 consists of elements given in Tab. 2.

Tab. 2 Chemical composition of MAR-M247
Tab. 2 Chemické zloženie superzliatiny MAR-M247

Wt.%	Cr	Al	Mo	W	Ti	Ta
MAR M-247	8.4	5.5	0.7	10.0	1.0	3.0
	Hf	**C**	**Co**	**B**	**Zr**	**Ni**
	1.5	0.15	10.0	0.015	0.05	Bal.

Microstructure of Inconel 713LC as well as MAR-M247 includes the γ matrix strengthen by γ´ phase with the shape of cuboidal Ni_3 (Al,Ti) as coherent precipitates and complex carbides [4]. The tested samples with cylindrical shape were casted from mentioned superalloys and dimensions of samples were about (14 x 5) mm. Disc samples in ceramic bowl were placed into induction furnace with temperature 1100 °C. After 23 h, the tested samples were put out from furnace and they were immediately exposed to the cooling process in the air at room temperature for 1h and then the mass changes were measured. This mentioned description represents one oxidation cycle. Mass changes of samples were written down after the each 2nd cycle and the photos were done. After the 10th cycle, the period of measurement was changed from 2 to 5 cycles because mass as well as surface changes were negligible. Initial state of samples before the cyclic oxidation test is shown in Fig. 1 where the 1st row represents the samples of *IN* 713LC without coating and the 2nd one represents the samples of the same material with coating.

Fig. 1 Samples of Inconel713LC before test
Obr. 1 Vzorky Inconel 713LC pred testom

The samples casted from MAR-M247 are shown in Fig. 2 and this photo was taken before the test procedure. The 1st row represents the samples of MAR-M247 without coating and the 2nd one represents the samples of the same material with coating.

Fig. 2 Samples of MAR-M247 before test
Obr. 2 Vzorky MAR-M247 pred testom

In the Tab. 3, there are the mutual comparisons of the samples of IN713LC where one series of samples are with coating and another series represent the samples without coating.

Hutnické listy č.7/2013, roč. LXVI
ISSN 0018-8069

Tab. 3 Mutual comparison of IN713LC with and without coating after test.
Tab. 3 Vzájomné porovnanie vzoriek IN713LC bez povlaku a s povlakom po teste

	IN 713LC		IN 713LC + SiAl
2. cycle		2. cycle	
4. cycle		4. cycle	
6. cycle		6. cycle	
8. cycle		8. cycle	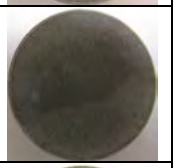
10. cycle		10. cycle	
15. cycle		15. cycle	
20. cycle		20. cycle	

Tab. 4 Mutual comparison of MAR-M247 with and without coating after test.
Tab. 4 Vzájomné porovnanie vzoriek MAR-M247 bez povlaku a s povlakom po teste

	MAR-M247		MAR-M247 + SiAl
2. cycle		2. cycle	
4. cycle		4. cycle	
6. cycle	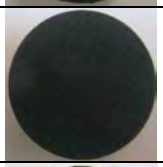	6. cycle	
8. cycle	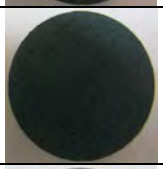	8. cycle	
10. cycle		10. cycle	
15. cycle		15. cycle	
20. cycle		20. cycle	

After the 10th cycle, the samples of M247 without coating exhibited the values under the m_0 and they had to be were excluded from test because they were expected to be absolutely damaged.

Conclusions

Casted samples from nickel superalloys Inconel 713LC and MAR-M247 were coated by protective SiAl coating using CVD process. SiAl coating was deposited on cylindrical samples in coating furnace by "pack cementation" method. Both types of superalloys were exposed for 23 h. to oxidation atmosphere at 1 110° C. During heating time, samples masses were increased, because of occurrence of the protective oxides on the samples surface. Each 2nd cycle was connected with the record of the weight of samples to find out mass changes and progress of cyclic oxidation.

- The resulting graph of the sample masses showed that the samples of IN 713LC without protective coating were exposed to 24 cycles up to now and after observation by visual control, there was not any noticeable damage. Behaviour of samples is surprised and other course is subject of next research.
- After the 24 cycles, the sample surfaces of IN 713LC with the SiAl coating are without any significant ruptures. The thin oxidation scale is stable and it ensures the protective function. Mass of samples has rapid increasing tendency and it has been still under the investigation process.

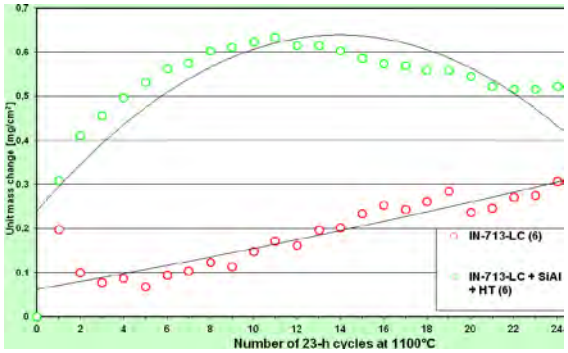

Fig. 3 Resulting graph of mass ganges of IN 713LC with and without SiAl coating

Obr. 3 Výsledný graf hmotnostných zmien IN 713LC s povlakom a bez povlaku

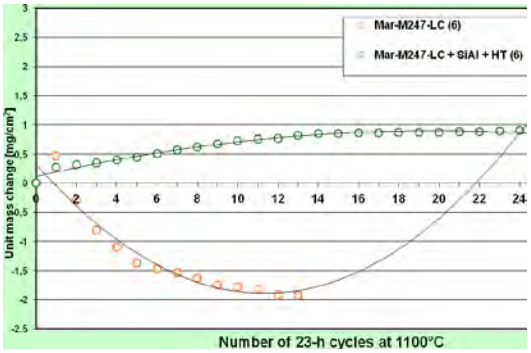

Fig. 4 Resulting graph of mass ganges of MAR-M247 with and without SiAl coating

Obr. 4 Výsledný graf hmotnostných zmien MAR-M247 s povlakom a bez povlaku

- MAR-M247 without the protective coating withstood only 2 cycles in the oxidation atmosphere. After the 2nd oxidation cycle, the mass was changed and fell down rapidly in comparison to the initial mass – m_0.
- MAR-M247 with SiAl coating showed very good cyclic oxidation resistance and nowadays, we are not able to specify the given cycle of the coating damage or rupture as well as its lifetime. On the other side, the SiAl seems to be the most suitable coating because it exhibits the best results after exposure to the aggressive environment bud there is one disadvantage in relation to the mechanical loading because the given coating becomes brittle.

Literature

[1] POKLUDA, J., KIANICOVÁ, M. Gas Turbines. Damage and Performance Assessment of Protective Coatings on Turbine Blades. Ed. Gurrappa Injeti. Sciyo. India 2010

[2] BOSE, S. *High temperature Coatings*. Elsevier Science & Technology Books, 2007.232 p. ISBN 0750682523

ASM Handbook: Failure Analysis and Prevention, 2002. Vol. 11, ISBN: 0- 87170-704-7

[3] SAVOLAINEN, K. Materials selection for high temperatureapplications, 2005. 105 p. ISBN 951-22-7892-8, Helsinky 2005

[4] KIANICOVÁ, M., SLÁMEČKA, K., POKLUDA, J. Damage of diffusion coatings on turbine blades. In Metal 2011: 20 mez. metal. konference: 18. – 20. 5. 2011. Brno, Hotel Voroněž, Česká republika. Brno: TANGER: Květen, 2011, s. 840 – 847. ISBN 978-80-87294-24-6

Zpracování hutních plynů na bioetanol

Siemens and LanzTech partner to transform steelmill offgases into bioethanol. Iron & Steel Technology, August 2013, s. 11-12

Firmy Siemens Metals Technologies a LanzTech podepsaly desetiletou smlouvu na vývoj a prodej ekologického zařízení pro hutě. V rámci této spolupráce se dále rozpracovává fermentace plynů s obsahem uhlíku, vznikajících v hutích, na bioetanol a další plyny s cílem komerčního využití.
Vysokopecní plyn, koksárenský plyn, konvertorový plyn a případně další plyny vznikající v hutích obsahují velké množství CO a CO_2. Na celosvětové produkci CO_2 se tyto plyny podílejí 6,7 %. Při výrobě 1 t oceli vzniká 1,8 t CO_2.

Patentovaný postup biologické fermentace těchto plynů, původně vyvinutý firmou LanzTech, umožňuje výrobu bioetanolu, kyseliny octové, acetonu, isopropanolu, n-butanolu nebo 2,3-butanediolu. Globální odbyt na etanol se odhaduje na 80 mil. t, a to převážně jako biopalivo. Na rozdíl od bioetanolu vyráběného ze zemědělských produktů, neprobíhá výroba z hutních plynů na úkor výroby potravin. Množství vznikajícího CO_2 je o 50 až 70 % nižší než u paliv vyrobených z ropy.

Firma LanzaTech již má od r. 2008 zkušební zařízení v Auckland na Novém Zélandu, které zpracovává plyny z hutí. V roce 2012 byla v Baosteel a v Shougang v Číně uvedena do provozu zařízení na přeměnu plynů na etanol s roční výrobností 300 t. Na základě těchto zkušeností firmy Siemens a LanzaTech spouštějí několik komerčních projektů v různých částech světa.

L J

Hutnické listy č.7/2013, roč. LXVI
ISSN 0018-8069

Study of Hot Corrosion Resistance of Ni-superalloys with Diffusion Coatings

Štúdium koróznej odolnosti Ni-superzliatin s difúznymi povlakmi za vysokých teplôt

doc. Ing. Marta Kianicová, PhD.[1], **Ing. Ján Kafrík**[1], **Ing. Jaroslav Trník**[1], **Ing. Ondřej Dvořáček**[2]

[1]University of Alexander Dubček in Trenčín, Faculty of Industrial Technologies, I. Krasku 491/30, 020 01 Púchov, Slovak Republic
[2]PBS Velká Bíteš, a.s., Vlkovská 279, 595 12 Velká Bíteš, Czech Republic

Hot corrosion resistance of nickel base superalloys with diffusion coatings is analyzed in the paper. Diffusion coatings created protective, heat – activated layer which separated superalloy from aggressive environment. Two types of superalloys were used in experiment: IN 713 LC and MAR M 247. Both superalloys have polycrystalline microstructure and they are prepared by vacuum castings. First type - Al coating was applied with the help of method "out – of – pack" which provide good control during coating process. Second type - Si Al coating was applied by method "pack – cementation". Hot corrosion stands for accelerated oxidation at elevated temperature inducted by a thin film of fused salt deposit. Corrosive environment was created by tablets Na_2SO_4 at 900 °C. Cross-sections of samples were analyzed with the help of SEM with EDS microanalysis.

Keywords: *superalloys, diffusion coatings, hot corrosion*

Článok sa zaoberá vysokoteplotnou koróznou odolnosťou niklových superzliatin s difúznymi povlakmi. Difúzne povlaky tvoria ochrannú tepelne aktivovanú vrstvu, ktorá oddeľuje superzliatinu od agresívneho prostredia. Pri teste boli požité dva druhy niklových superzliatin: IN 713 LC a MAR M 247. Obe superzliatiny majú polykryštalickú mikroštruktúru a používajú sa pri metóde vákuového odlievania. Prvý typ - Al povlak bol aplikovaný pomocou metódy "out – of – pack". Pri tejto metóde nie je vzorka v kontakte s práškovou zmesou a proces sa uskutočňuje v retortových alebo vákuových peciach. V priebehu depozície je privádzaný do pece nosný plyn, ktorý umožňuje transport plynov vytvárajúcich povlak ku vzorke. Hlavné výhody tohto procesu sú: povlakovaný materiál nie je v kontakte s práškovou zmesou, čo zvyšuje kvalitu povrchu vzniknutého povlaku a taktiež zvyšuje kontrolu nad procesom. Druhý typ - SiAl povlak bol deponovaný pomocou metódy "pack – cementation". Korozívne prostredie bolo vytvorené pomocou tabliet Na_2SO_4 (0.3 g) pri teplote 900 °C. Makro a mikroštruktúrne analýzy z povrchov a rezov jednotlivých vzoriek boli hodnotené na SEM Hitachi a pomocou EDS mikroanalýzy. Makroskopická analýza všetkých vzoriek ukázala, že vzorky bez povlaku vykazujú najväčšie korózne napadnutie. Pričom najhoršiu odolnosť voči vysokoteplotnej korózii mala vzorka MARu M 247 bez povlaku. Makroskopické porovnanie vzoriek s Al povlakmi ukázalo lepšiu odolnosť voči vysokoteplotnej korózii u superzliatiny MAR M 247.Vzorky s SiAl povlakom mali podľa očakávaní najlepšiu odolnosť voči vysokoteplotnej korózii avšak v ich neprospech napovedá fakt, že kremík v povlaku spôsobuje zvýšenie krehkosti povlaku, čím sa znižuje schopnosť povlaku odolávať nárazom pevných častíc. Tento experiment bol uskutočnený v spolupráci s firmou PBS Velká Bíteš a. s., Velká Bíteš, Česká Republika a Sliezskou Politechnikou v Katowiciach, Poľsko.

Kľúčové slová: *superzliatiny, difúzne povlaky, vysokoteplotná korózia*

The main types of protective coatings used for gas turbine components can be classified as follows: diffusion aluminide coatings overlay coatings and thermal barrier coatings. Diffusion aluminide coatings are based on the intermetallic compound β-NiAl that is formed under the influence of the substrate. Upon oxidation exposure, a tenacious aluminium oxide film is formed on the surface of the aluminide and serves as the primary barrier against further reaction with environmental constituents [1, 2, 3]. For some gas turbine applications, the lifetime of a stressed part can be limited by its hot-corrosion resistance rather than by its stress- rupture strength. Hot corrosion involves attack by molten salt and it is commonly sodium and potassium sulphate that enter the turbine hot section as contaminants from the air and fuel and can result in rapid loss of material [4, 5].

Experiment

Composition of samples

Two types of Ni – superalloys were used for hot corrosion test: IN 713 LC and MAR M 247. Samples from these superalloys were made by vacuum casting. Each superalloy was tested without, with diffusion Al – coating and with SiAl – coating.

Al – coating was applied by the "out – of – pack" method. Thickness of coating was in the range (50 ± 5) µm.

SiAl – coating was created by "pack – cementation" method. Thickness of coating was in the range (90 ± 5) µm.

Philosophy of test

Coated and uncoated samples with tablets sodium sulphate were placed into the furnance and heated to 900 °C. Each type of sample has 8 pieces (numbers). These pieces were sequentially taken from furnance in graduated time intervals and it allowed to analyze the time course of hot corrosion behaviour. Time range of test was 80 hours. After the test, the samples were cut (Fig. 1, 2) and electron microanalysis was performed for cross-sections. In this paper, samples without coating and with Al as well as SiAl – diffusion coating are mutually compared after 63 hours in furnance. Time-consuming test did not allow the analyses of the other samples. These will be the subject of the future analyses.

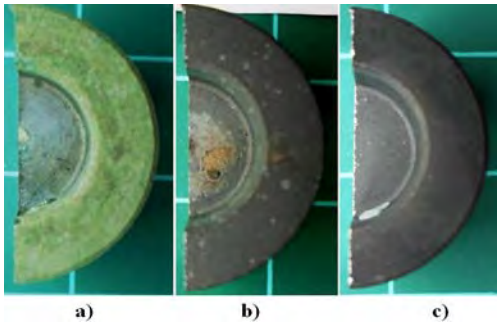

Fig. 1 IN 713 LC + 0.3 g Na_2SO_4 after 63 hours at 900°C
a) without coating, b) with Al – coating c) with SiAl – coating
Obr. 1 IN 713 LC + 0.3 g Na_2SO_4 po 63 hodinách pri 900°C
a) bez povlaku, b) s Al – povlakom c) s SiAl – povlakom

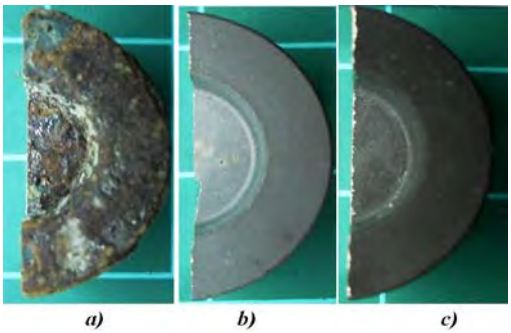

Fig. 2 MAR – M 247 + 0.3 g Na_2SO_4 after 63 hours at 900°C
a) without coating, b) with Al – coating c) with SiAl - coating
Obr. 2 MAR – M 247 + 0.3 g Na_2SO_4 po 63 hodinách pri 900°C
a) bez povlaku, b) s Al – povlakom c) s SiAl – povlakom

Analyses of samples

Cross-sections of samples were analyzed by the help of scanning electron microscope with EDS detector which was used for plane analysis (Fig. 3, 4). Results are summarized in Tab. 1 and 2.

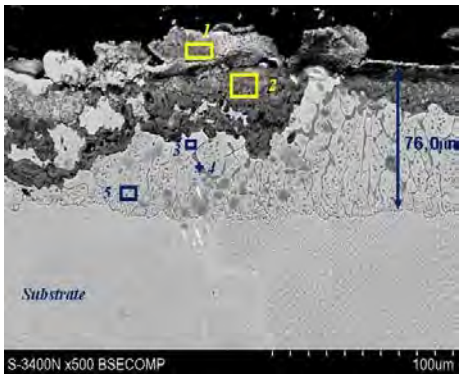

Fig. 3a) IN 713 LC + 0.3 g Na_2SO_4 after 63 hours at 900°C without coating
Obr. 3a) IN 713 LC + 0.3 g Na_2SO_4 po 63 hodinách pri 900°C bez povlaku

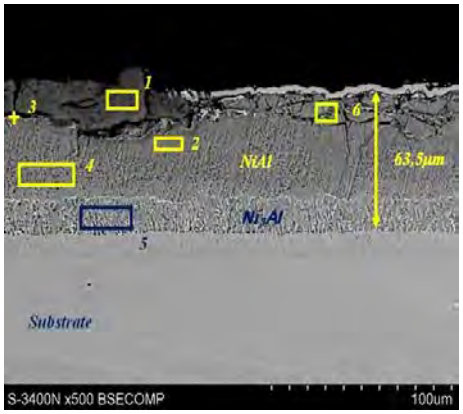

Fig. 3b) IN 713 LC + 0.3 g Na_2SO_4 after 63 hours at 900°C with Al – coating
Obr. 3b) IN 713 LC + 0.3 g Na_2SO_4 po 63 hodinách pri 900°C s Al – povlakom

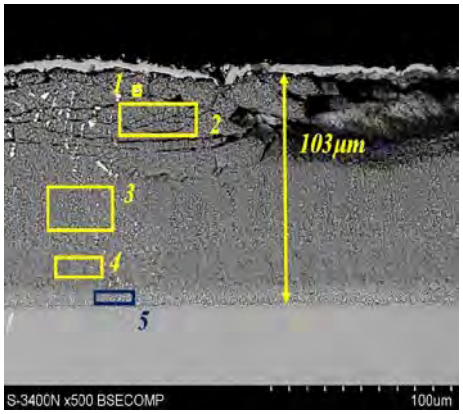

Fig. 3c) IN 713 LC + 0.3 g Na_2SO_4 after 63 hours at 900°C with SiAl – coating
Obr. 3c) IN 713 LC + 0.3 g Na_2SO_4 po 63 hodinách pri 900°C s SiAl – povlakom

Hutnické listy č.7/2013, roč. LXVI
ISSN 0018-8069

Tab. 1 At. % of elements in areas indicated in fig. 3
Tab. 1 At. % prvkov v plochách podľa obr. 3

Type of samples	at. %	Na-K	Al-K	Si-K	S-K	Cr-K	Ni-K
IN 713 LC without coating	1	-	10.9	0.5	-	0.9	77.2
	2	2.2	14.1	0.4	0.9	21.8	47.5
	3	-	5.1	-	0.7	1.1	88.7
	4	-	0.4	-	51.4	32.8	14.2
	5	-	6.8	-	10.7	5.8	72.8
IN 713 LC + Al coating	1	-	12.2	2.7	-	8.5	50.8
	2	-	45.0	-	-	2.5	52.5
	3	-	6.5	-	-	1.2	75.9
	4	-	45.6	-	-	1.5	52.9
	5	-	25.3	-	-	23.9	45.7
	6	-	48.5	-	-	1.9	49.6
IN 713 LC + SiAl coating	1	-	21.0	8.1	-	10.3	33.5
	2	-	43.6	3.8	-	9.2	39.8
	3	-	46.9	0.3	-	8.0	41.6
	4	-	44.8	-	-	3.1	51.1
	5	-	22.5	-	-	23.4	42.5

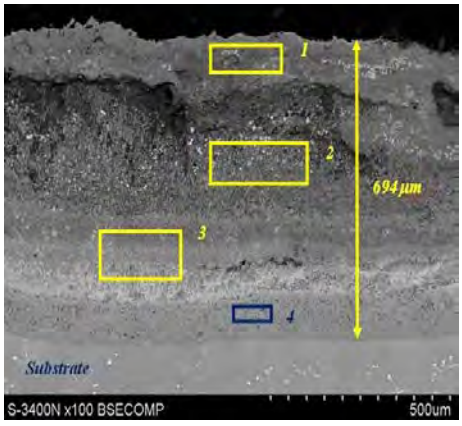

Fig. 4a) MAR – M 247 + 0.3 g Na_2SO_4 after 63 hours at 900°C without coating
Obr. 4a) MAR – M 247 + 0.3 g Na_2SO_4 po 63 hodinách pri 900°C bez povlaku

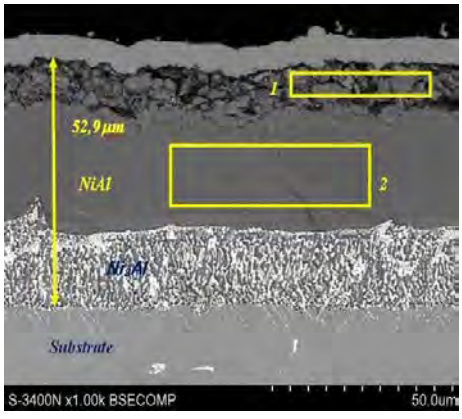

Fig. 4b)MAR – M 247 + 0.3 g Na_2SO_4 after 63 hours at 900°C with Al – coating
Obr. 4b) MAR – M 247 + 0.3 g Na_2SO_4 po 63 hodinách pri 900°C s Al – povlakom

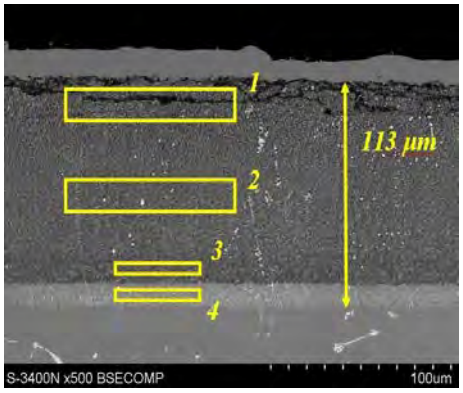

Fig. 4c) MAR – M 247 + 0.3 g Na_2SO_4 after 63 hours at 900°C with SiAl – coating
Obr. 4c)MAR – M 247 + 0.3 g Na_2SO_4 po 63 hodinách pri 900°C s SiAl – povlakom

Tab. 2 At. % of elements in areas indicated in fig. 4
Tab. 2 At. % prvkov v plochách podľa obr. 4

Type of samples	at. %	Na-K	Al-K	Si-K	S-K	Cr-K	Ni-K
MAR-M 247 without coating	1	1.5	17.7	3.1	6.6	25.3	27.4
	2	4.9	21.1	-	6.0	12.6	42.2
	3	-	10.6	-	2.1	18.2	48.5
	4	-	9.4	-	4.0	1.4	73.7
MAR-M 247+ Al coating	1	-	46.1	0.5	-	2.6	46.3
	2	-	45.9	-	-	3.0	45.5
MAR-M 247 + SiAl coating	1	-	47.2	2.8	-	7.0	34.5
	2	-	42.0	3.1	-	7.1	38.4
	3	-	44.4	-	-	3.0	43.9
	4	-	23.1	4.3	-	19.4	32.7

Discussion and conclusions

Macroscopic analysis shows that, the samples without coating exhibit greater corrosion attack than the samples with coatings. Sample of MAR M 247 without coating was the most attacked by corrosion process and the subsequent measurement of thicknesses relating to corroded material confirmed results of the macroscopic analysis (Fig.1, 2). Fig. 5 shows graphic thickness comparison of corroded material for the samples without coating.

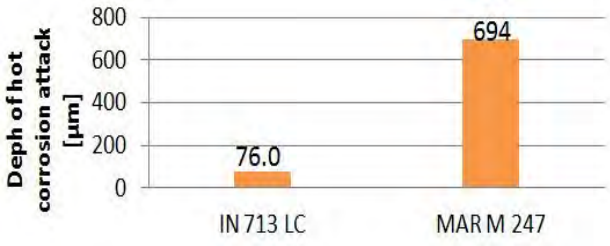

Fig. 5 Comparison of hot corrosion attack for the samples without coating
Obr. 5 Porovnanie vysokoteplotného korózneho napadnutia u vzoriek bez povlaku

Macroscopic comparisons of samples with Al – coating exhibit better resistance against hot corrosion attack in the case of the sample with MAR M 247 (Fig. 1 b, 2 b). The coating thicknesses for both types of samples were measured and compared mutually (Fig. 6). According to

the measurement results, it can be concluded that the sample with IN 713 LC has by 10 [μm] thicker coating than the sample with MAR M 247 but we cannot conclude which one sample is better, because time duration of test was not adequate. Process of delamination was observed for both samples (Fig. 3b, 4b).

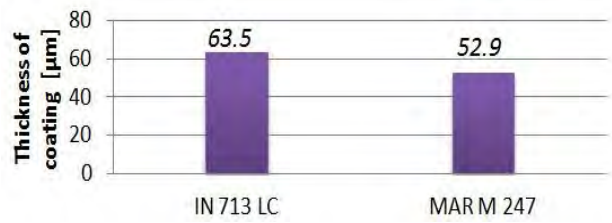

Fig. 6 Thickness of Al – coating after hot corrosion test: + 0.3g Na_2SO_4 after 63 hours at 900 °C
Obr. 6 Hrúbka Al – povlaku po teste na vysokoteplotnú koróziu: + 0.3g Na_2SO_4 after 63 hours at 900 °C

Macroscopic analyses of samples with SiAl – coating exhibit very good hot corrosion resistance for both samples. Process of delamination was higher in the case of IN 713 LC sample (Fig. 3c). The coating thicknesses for both types of samples were measured and compared mutually (Fig. 7). But we cannot conclude which one sample is better, because time duration of test was not adequate and the reason was the same as it was in the case of samples with Al – coating.

Fig. 7 Thickness of SiAl – coating after hot corrosion test: + 0.3g Na_2SO_4 after 63 hours at 900 °C
Obr. 7 Hrúbka SiAl – povlaku po teste na vysokoteplotnú koróziu: + 0.3g Na_2SO_4 after 63 hours at 900 °C

EDS analyses of cross-sections showed the presence of sulphur in IN 713 LC without coating as well as in MAR M 247 without coating (Tab. 1, 2). We can conclude that hot corrosion for the samples without coating is in propagation stage. The presence of sulphur was not confirmed in the case of samples with Al and SiAl – coating (Tab. 1, 2) because TGO (which was made by coating) acted as diffusion barrier which stopped diffusion of sulphur into coating and superalloy. The presence of oxides was observed in the case of samples with Al and SiAl – coating but there was not any presence of sulphur (Fig. 3, 4) and in this case, hot corrosion attack was in initiation stage.

Experiment confirmed the advantages relating to the application of Al and SiAl – diffusion coating in aggressive environment which imitated environmental condition during operation of turbine engine.

Acknowledgement
This experiment was made in cooperation with company PBS Velká Bíteš a. s., Velká Bíteš, Czech Republic and The Silesian University of Technology, Katowice, Poland.

Literature

[1] HETMANCZYK, M., SWADZBA, L., MENDALA, B.: *Advanced materials and protective coatings in aero – engines application*. Journal of Achievements in Materials and Manufacturing Engineering. 2007. vol. 24, no.1, p. 372-381

[2] POKLUDA, J., KIANICOVÁ, M. *Gas Turbines*. Damage and Performance Assessment of Protective Coatings on Turbine Blades. Ed. Gurrappa Injeti. Sciyo. India 2010

[3] BOSE, S. *High temperature Coatings*. Elsevier Science & Technology Books, 2007. 299 p. ISBN 0750682523

[4] SIMS, C.T., STOLOFF, N.S., HAGEL, W.C. (eds.) *Superalloys II*. New York: 1987,John Wiley & Sons. 640 p. ISBN: 0471011479

[5] KIANICOVÁ, M., SLÁMEČKA, K., POKLUDA, J. *Damage of diffusion coatings on turbine blades*. In Metal 2011: 20 mez. metal. konference*:* 18. – 20. 5. 2011. Brno, Hotel Voroněž, Česká republika. Brno: TANGER: Květen, 2011, s. 840 – 847. ISBN 978-80-87294-24-6

Nové zařízení pro tepelné zpracování trub

Evraz North America orders heat treatment system. Metallurgical Plant and Technology 2013, č. 4, s. 8

Firma Evraz North America sídlící v Chicagu objednala zařízení pro tepelné zpracování pro válcovnu trubek ve svém závodě v Calgary v Kanadě. Kapacita tepelného zpracování se tím zvýší o 150 %. Linka je určena pro olejářské trubky. Jde o linku 12 MW TemperLine s ročním výkonem více než 200 kt. Linka umožňuje rychlý přechod na jiný typ trubek. Měla by být uvedena do provozu ve čtvrtém kvartále 2014.

L J

Hutnické listy č.7/2013, roč. LXVI
ISSN 0018-8069

Influence of the Temperature Applied during Annealing/Stretching on a Structure of Polypropylene Film

Vplyv teploty žíhania/dĺženia na štruktúru polypropylenového filmu

doc. Mgr. Ivan Kopal, PhD.[1], **Ing. Leoš Polka**[1], **prof. Ing. Lubomír Lapčík, PhD.**[2]

[1]University of Alexander Dubček in Trenčín, Faculty of Industrial Technologies in Púchov, I. Krasku 491/30, 020 01 Púchov, Slovak Republic
[2]Tomas Bata University in Zlín, Faculty of technology, náměstí T. G. Masaryka 275, 762 72 Zlín, Czech Republic

This study is focused on the influence of the temperature applied during annealing/stretching of bi-axially oriented polypropylene films using Fourier transform infrared spectroscopy (FTIR) method. There are several changes in a structural orientation of polypropylene after exceeding the temperature over glass transition point. The given mentioned changes include the reorganization of polymeric macromolecules in time and decreased defect concentration. Crystallinity degree of polypropylene is changed as a result of these processes and the evaluation and analysis was based on deconvoluted infrared absorption spectra registered in transmission setup of FTIR-8601PC spectrometer at the room temperature of 23°C. It was proven experimentally that there is an increase in crystalline to amorphous phase ratio in a temperature range of 120°C – 170°C with rising temperature of annealing/ stretching of bi-axially oriented polypropylene film.

Keywords: *polypropylene, FTIR, crystallinity of polymers, relaxation transitions*

Polypropylén vďaka svojim fyzikálnym, chemický a mechanickým vlastnostiam nachádza široké uplatnenie v celom rade praktických aplikácií. Tenké filmy mono a biaxiálne orientovaného izotaktického polypropylénu sa napríklad intenzívne využívajú v elektrickom a elektronickom sektore výroby. Pri ich produkcii dochádza vplyvom teploty nad teplotou sklovitého prechodu k pozvoľnému preusporiadavaniu polymérnych makromolekúl, ako aj ku znižovaniu koncentrácie defektov. Výsledkom týchto procesov je zmena stupňa kryštalinity polypropylénu, ktorú identifikujeme prostredníctvom infračervenej spektroskopie s Fourierovou transformáciou. Táto diagnostická metóda predstavuje vysoko efektívny nástroj skúmania štruktúry organických aj anorganických zlúčenín, ktorý je založený na absorpcii infračerveného žiarenia dopadajúceho na vzorku vyšetrovaného materiálu, pričom dochádza k zmenám rotačných a vibračných energetických stavov jeho molekúl v závislosti na zmenách ich dipólového momentu. Zmenu stupňa kryštalinity biaxiálne orientovaného izotaktického polypropylénového filmu v tejto práci kvantifikujeme na základe analýzy dekonvolučných infračervených absorpčných spektier zaregistrovaných v transmisnom usporiadaní na infračervenom spektrometri FTIR-8601PC pri teplote okolitého prostredia 23 °C. Experimentálne bolo preukázané, že v teplotnom intervale 120 – 170 °C s narastajúcou teplotou žíhania/dĺženia skúmaného biaxiálne orientovaného polypropylénového filmu sa podiel obsahu kryštalickej fázy oproti amorfnej fáze v ňom zvyšuje, teda, že stupeň kryštalinity rastie. Na príčine je skutočnosť, že vplyvom temperácie nad teplotou sklovitého prechodu dochádza k pozvoľnému preusporiadaniu polymérnych makromolekúl, ako aj ku znižovaniu koncentrácie defektov. Dá sa predpokladať, že polymérne reťazce amorfnej fázy a kryštalografická os v kryštalickej fáze sa orientujú prednostne v smere dĺženia izotaktického polypropylénu.

Kľúčové slová: *polypropylene, FTIR, kryštalinita polymérov, relaxačné prechody*

Polypropylene (PP) represents one of the most common polymeric materials. It is a representative of stereoregular polymer commonly found in isotactic, syndiotactic, stereoblock, as well as atactic conformation. Isotactic polypropylene (iPP) is one of the earliest stereoregular polymers, synthesized in 1955 using a Ziegler–Natta catalyst. Local isotactic and syndiotactic sequences of polypropylene have a potential to crystallize to generate a stable structure [1]. Due to its very suitable chemical, physical, as well as mechanical properties, which can be varied by customizing the production process or with various additives, it is widely used for in commercial and household applications different spheres of industry. The most frequently used type of PP is isotactic with an intermediate level of crystallinity. Mono and bi-axially oriented iPP films have excellent physical properties making them very suitable for electric and electronic applications which profit mainly from their great moisture, oil and lubricants resistance along with their electrical resistance [2]. The bi-axially oriented PP film, studied by the Fourier transform infrared spectroscopy (FTIR) method, was chosen as an interest of this study. Mechanical testing revealed that mechanical properties are considerably dependent on the temperature applied during annealing/stretching of bi-axially oriented iPP film. FTIR analysis has a very great potential for further investigation of this particular phenomenon.

FTIR spectroscopy is highly efficient diagnostic tool based on the infrared beams absorption which goes through a material specimen. These IR beams cause rotation and vibration energetic state of molecules to change their dipolar momentum by altering [3]. As a result of the FTIR analysis, there is a IR spectra reflecting functional dependency of energy and IR wavelength in graphical representation of relating absorbance with wavenumber [4]. IR spectra analysis allows us to identify organic and inorganic compounds with very high accuracy. It is possible to compare measurements with digitalized libraries of IR spectra and for structural characterization of materials under FTIR investigation [5]. There are 3 main FTIR techniques: transmission, reflectance as well as attenuated total reflectance [6]. The transmission FTIR technique is applied in our study.

Materials and methods

Samples of bi-axially oriented iPP homopolymer were fixed in a horizontal position in a frame towards IR source and IR detector in a spectrometer was used for evaluation by means of FTIR analysis. In a process of manufacturing, the thin iPP film with a thickness of 400μm, the specimens of which were prepared, the extruded sheet was drawn firstly in machine direction and then in transverse direction with draw ratio of 4 x 7. The temperatures of 120, 140, 150, 160, 170°C were applied during annealing/stretching of the material. After stretching the material, there was a considerably greater tensile strength and lower elongation at break in stretching direction and it was proven using dynamic mechanical analysis by help of Perkin Elmer Pyris Diamond Mechanical Analyzer 8000 [7]. IR absorption spectra for iPP films prepared at the room temperature 23°C and relative humidity of 60 % were also registered. The transmission FTIR method by help of FTIR-8601PC Shimadzu spectrometer with a wavenumber range of 4000 – 700 cm^{-1}, step of a 2 cm^{-1} and resolution of 2 cm^{-1} was used for IR spectra analysis of tested specimens. The machine was calibrated by polystyrene calibration foil. IR spectra were processed in SigmaPlot software. Photography of experimental equipment can be found in Fig. 1.

Fig. 1 Shimadzu FTIR-8601PC spectrometer
Obr. 1 Spektrometer FTIR – 8601PC Shimadzu

Results and discussion

Registered IR spectra in a wavenumber range of 2800 – 700 cm^{-1} are listed in Fig. 2. Our samples are labeled in TB x/10_y °C_H pattern, where x – elongation ratio, y – annealing/stretching temperature and H – horizontal arrangement towards IR source and IR detector in the spectrometer.

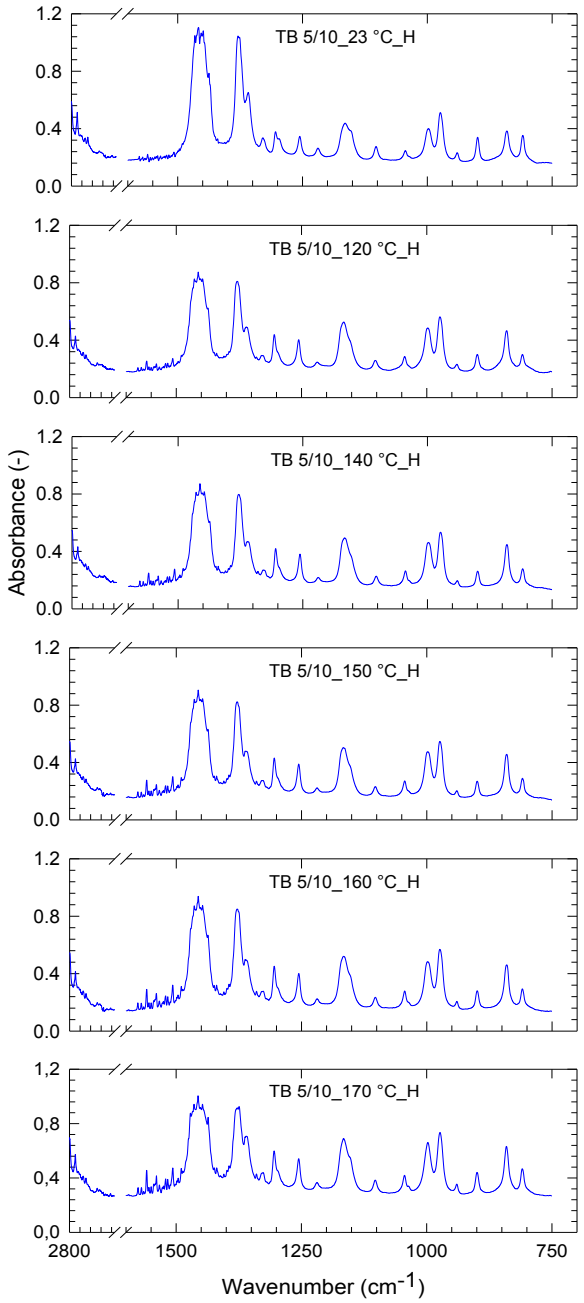

Fig. 2 FTIR spectra of bi-axially oriented polypropylene film
Obr. 2 FTIR spektrá biaxiálne orientovaného PP filmu

In the fingerprint region of IR spectra, it is possible to see absorbance peaks typical for CH_3 rocking and C-C chain stretching vibrations of iPP amorphous phase at wavenumber of 973 cm^{-1} and at 998 cm^{-1} , there are the peaks characteristic for CH_3 rocking, CH_2 wagging and CH bending of the crystalline phase consisting of α-helix short PP chains [8]. Absorbance intensity A_{998} at

Hutnické listy č.7/2013, roč. LXVI
ISSN 0018-8069

998 cm^{-1} of crystalline phase and absorbance intensity A_{973} at 973 cm^{-1} of amorphous phase were used to count the crystalline to amorphous phase ratio for iPP samples as A_{998}/A_{973} [9].

For a purpose of a resolution of enhancement, the registered IR spectra were deconvoluted to single components. This band-narrowing process of IR spectra was done by the Fourier self-deconvolution method [10]. Deconvolution spectra of iPP sample for temperature 23 °C is presented in Fig. 3. Based on the fact that the deconvolution spectra for other temperatures are analogous, they are not listed in this study.

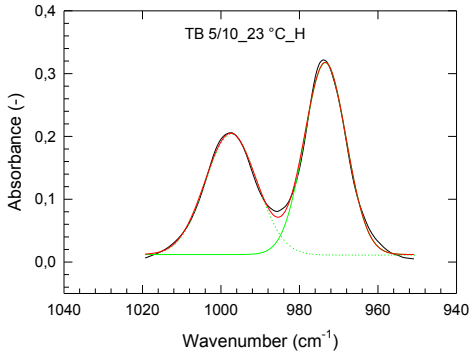

Fig. 3 Deconvolution spectra of iPP film for 23 °C
Obr. 3 Rozklad infračerveného spektra vzorky iPP filmu pri 23°C

Absorbance intensity ratio A_{998}/A_{973} in crystalline and amorphous phase for all applied temperatures during annealing/stretching of examined iPP samples as well as for the temperature of 23°C is presented in Fig. 4 in the form of functional dependency of crystallinity versus temperature.

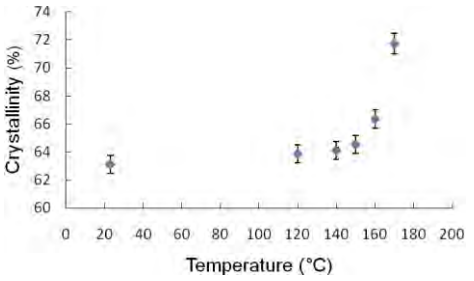

Fig. 4 Temperature dependence of crystallinity for iPP samples
Obr. 4 Závislosť pomeru kryštalickej a amorfnej fázy (kryštalinity) na teplote u vzoriek iPP

In the Fig. 4, there is a noticeable increase in crystallinity with rising temperature applied during the annealing/ stretching of bi-axially oriented iPP film. This can be explained with changes in a structural orientation of polypropylene after exceeding the temperature over the glass transition point as insidious reorganization of polymeric macromolecules as well as decreasing defect concentration. We can assume PP chains to be preferentially oriented in a stretching direction.

Conclusions

On the basis of the study of the bi-axially oriented polypropylene films through transmission FTIR technique, it was proven that the ratio between amorphous and the crystalline phase (crystallinity) can be increased by applying higher temperature during annealing/ stretching of iPP films at the range of 120 °C – 170 °C.

Acknowledgments
Authors consider it a nice obligation to thank to the Institute of Macromolecular Chemistry AV ČR Brno and Ing. M. Hřibová, PhD. and prof. Ing. F. Rybnikář, DrSc. from FT UTB in Zlín for lending us studied material samples.

Literature

[1] NAKAOIKI, T., FUKUI, D. *Single-helix crystal in atactic polypropylene.* Journal of Molecular Structure, vol. 1051, 2013, p 271–275

[2] LEE, S.H., et al. *Rheological and electrical properties of polypropylene/MWCNT composites prepared with MWCNT masterbatch chips*. European Polymer Journal, vol. 44, Issue 6, June 2008, p. 1620-1630, ISSN 0014-3057

[3] TAN, H.P., LING, S.K., CHUAH, C.H. *One- and two-dimensional Fourier transform infrared correlation spectroscopy of Phyllagathis rotundifolia*. Journal of Molecular Structure, vol. 1006, Issues 1–3, 14 December 2011, p. 297-302, ISSN 0022-2860

[4] SUBRAMANIAN, N., et al. *FT-IR, FT-Raman spectra, density functional computations of the vibrational spectra and molecular conformational analysis of 2,5-di-tert-butyl-hydroquinone.* Spectrochimica Acta Part A: Molecular and Biomolecular Spectroscopy, vol. 83, Issue 1, December 2011, p. 165-174, ISSN 1386-1425

[5] LARKIN, P. *Infrared and Raman Spectroscopy - Chapter 7 - General Outline and Strategies for IR and Raman Spectral Interpretation.* Elsevier, Oxford, 2011, p. 117-133, ISBN 9780123869845

[6] SUBRAMANIAN, A., RODRIGUEZ-SAONA, L. *Fourier Transform Infrared (FTIR) Spectroscopy, Infrared Spectroscopy for Food Quality Analysis and Control, Academic Press*, San Diego, 2009, p. 145-178, ISBN 9780123741363

[7] ZHENG, K., et al. *In situ FTIR spectroscopic study of the conformational change of syndiotactic polypropylene during the isothermal crystallization*. Polymer, vol. 50, Issue 24, 16 November 2009, p. 5782-5786, ISSN 0032-3861

[8] KARACAN, I., BENLI, H. *The role of dry and wet isothermal annealing treatment on the structure and the mechanical properties of isotactic polypropylene fibers*. Journal of Applied Polymer Science, vol. 124, p. 3037-3050

[9] ISHIOKA, T., MASAOKA, A. *Normal mode analysis of syndiotactic polypro-pylene (T2G2T6G2)*. Polymer, vol. 43, 2002, p. 4639-4644, ISSN 0032-3861

[10] KAPPERS, A., et al. *Deconvolution and Curve Fitting of IR Spectra for CO Adsorbed on Pt/K-LTL: Potassium Promoter Effect and adsorption Site Distribution*. The Journal of Physical Chemistry, vol. 100, 1996, p. 3227–3236, ISSN: 0022-3654

strojírenské dohotovení hutních výrobků

Graphic Design of Chassis Multi-disc Brake for Unmanned Aerial Vehicle

Grafický návrh podvozkovej lamelovej brzdy pre bezpilotné vzdušné prostriedky

Ing. Lenka Hazuchová[1], **doc. Ing. Jan Krmela, Ph.D.**[1]

[1]University of Alexander Dubček in Trenčín, Faculty of Industrial Technologies, I. Krasku 491/30, 020 01 Púchov, Slovak Republic

This paper deals with the design of multi-disc brakes for unmanned aerial vehicles. Nowadays, these types of brakes are more and more popular because of their properties and they can be used in extremely risk areas. Their advantages exceed conventional brake systems (disc or drum brakes). The reason is the higher number of friction segments and brake performance is higher. Aircraft industry puts requirements for surface materials. This causes the bigger production and use of composite materials with carbon base for its unique properties which improve the brake and brake system properties. The combination of carbon with ceramics decreases requirements for system cooling and the maintenance because this material has lower degree of wear as commonly used brakes. The chosen brake concept is designed for dealing with extremely high operational loads with minimal needs of repairs and maintenance. The use of multi-disc brake concept with electromagnetic control and with chosen brake material gives us reliable braking system fulfilling all requirements for the chosen type of vehicle.

Keywords: *multi-disc brake, composite, unmanned aerial vehicle*

Tento príspevok sa zaoberá grafickým návrhom lamelových bŕzd bezpilotných vzdušných prostriedkov. V dnešnej dobe je tento typ bŕzd čoraz populárnejší z dôvodu svojich vlastností a sú využívané v extrémnych rizikových oblastiach. Ich výhody prevyšujú konvenčné brzdové systémy (kotúčové či bubnové brzdy). Dôvodom je vyšší počet trecích segmentov, brzdný účinok je mnohonásobne vyšší. Letecký priemysel dáva vysoké požiadavky na povrchové materiály, čo zapríčiňuje vyššiu produkciu a použitie kompozitných materiálov na báze uhlíka pre jeho jedinečné vlastnosti, ktoré zlepšujú celkové vlastnosti brzdy a brzdového systému. Kombinácia uhlíka s keramikou nám znižuje požiadavky na chladenie systému a takisto aj na údržbu, pretože tento materiál dosahuje nižšiu mieru opotrebenia v porovnaní s bežne používanými brzdami. Zvolený koncept brzdy je navrhnutý tak, aby brzda bola schopná znášať mimoriadne vysoké prevádzkové zaťaženia s minimálnymi potrebami na údržbu a opravy. Použitie koncepcie lamelovej brzdy s elektromagnetickým ovládaním a so zvoleným materiálom nám umožňuje získať brzdiaci systém spĺňajúci všetky požiadavky pre zvolený typ dopravného prostriedku. Pretože brzdy sú jedným zo základných prvkov bezpečnosti akýchkoľvek dopravných prostriedkov, je potrebné analyzovať sily pôsobiace v kritických fázach použitia lamelových bŕzd. Prioritný význam pri návrhu brzdy zohráva pristávacia rýchlosť. Vzhľadom k tomu, že dopravný prostriedok, pre ktorý bola brzda navrhnutá, nepredpokladá použitie aerodynamických bŕzd, všetku kinetickú energiu dopravného prostriedku pri brzdení musia absorbovať brzdy. Dôvodom zvolenej koncepcie lamelovej brzdy je nielen vysoká účinnosť, nízka hmotnosť, ale najmä vysoká odolnosť voči opotrebeniu a nízke nároky na údržbu. Zvolené materiály použité na lamely brzdy sa vyznačujú mimoriadne nízkou hmotnosťou oproti bežne používaným oceľovým lamelám, či lamelám zo spekaných karbidov. Zároveň tieto bežne používané materiály majú pomerne nízky teplotný prah tepelnej odolnosti, čo môže spôsobiť nebezpečný pokles účinnosti bŕzd. Navrhnutý kompozit s keramickou matricou posúva tepelnú kapacitu až o viac ako 400 % oproti súčasným konštrukčným riešeniam. Napriek tomu, že nadobúdacia cena takejto brzdy môže byť približne trojnásobná, prevádzkové náklady a životnosť brzdy sú na nízkej finančnej úrovni. Výsledným efektom je, že celkové náklady počas celej technickej životnosti brzdy sú výrazne nižšie ako u lacnejších oceľových lamiel, či lamiel zo spekaných karbidov.

Kľúčové slová: *lamelová brzda, kompozit, bezpilotný vzdušný prostriedok*

Hutnické listy č.7/2013, roč. LXVI
ISSN 0018-8069

The most commonly used brakes in the aircraft are multi-disc brakes because of their high braking performance, reliability and low weight. The gradual brakes analyze shows that most effective brakes for Unmanned Aerial Vehicles (UAV) are multi-disc brakes. The second aspect for multi-disc brake selection is connected with the maximum dimensions of UAV. Accordingly, the multi-disc brakes were chosen because of their high effectiveness and brake performance despite its small size.

Multi-disc brake graphic design

The reasons and the benefits of this option are:

- high reliability,
- high efficiency at very low weight,
- significant dimensional space constraint of the brake on the main landing gear,
- the design simplicity,
- easy maintenance and repairs.

The Figure 1 shows the multi-disc brake designed for the UAV´s main landing gear. The wheel disc of the landing gear is standard for this type of UAV. The area of wheel disc is limited due to the UAV size. In the last years, the multi-disc brake has the considerable expansion in almost all airplanes categories. The reason is the high brake efficiency which in combination with aerodynamic brakes provides the significant landing run reduction of the vehicle. In this case, the combination with aerodynamic brakes is not necessary because of the low overall weight and landing weight of UAV. The typical control way of aircraft multi-disc brakes is the hydraulic control. Although this control way of braking system has many advantages, it also has major disadvantages [1]. These disadvantages include:

- relatively high weight (pressure energy source, pipes, brake fluid, etc.),
- considerable vulnerability against the battle damage or operational wear,
- demands for maintenance and repairs (e. g. brake fluid exchange, brake system bleed, etc.).

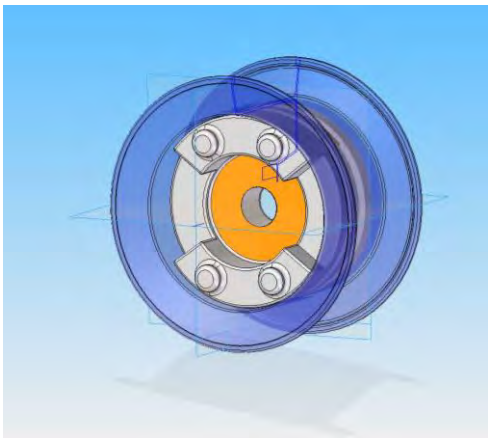

Fig. 1 Multi-disc brake with wheel disc [2]
Obr. 1 Lamelová brzda s diskom kolesa [2]

In this case, the specific requirements for UAV have to be accomplished. These requirements include:

- minimum possible brake system weight,
- the simplicity of technical solutions,
- minimal maintenance and repairs.

Based on these specific requirements, it was decided to solve the braking control system using electromangnetic control. Electronamgnetic control is not space consuming as it is in the case with hydraulic control containing pressure energy source, pressure vessels, pipes, safety valves, filters, etc. Electromagnetic control is more simple and needs less maintenance. The source of power is the motor unit which transfers the energy through the alternator to the other electrical equipment in UAV. There is also the possibility to backup the whole system several times using electrical conductions („fly-by-wire“ system).

In Fig. 2, there is the illustration of the design based on complexity and simple manipulation at brake control and maintenance. The use of UAV is connected with the operational deployment in extreme weather (atmospheric) conditions. For these reasons, it was decided to place electric lines and brake control to the covers and landing gear. The minimized risk of the damage for operating parts of the brake of this location is an advantage. New problem arises due to control elements protection to ensure simple availability to the parts to be repaired. This is related to the possibility of the brake remove [3].

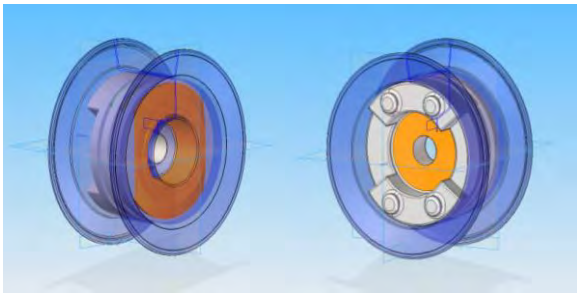

Fig. 2 The place of the brake in wheel disc [2]
Obr. 2 Umiestnenie brzdy v disku [2]

The simple construction of electromagnetic multi-disc brake gives us the opportunity to solve problems simply. The discs are positioned with the pressure cylinders on the brake. It is obvious that removal from the wheel disc can be done as a whole and not separately as the modular structure. We can only remove the pressure cylinders after disconnection the grounding line located under the cover of pressure cylinder [3].

Hutnické listy č.7/2013, roč. LXVI
ISSN 0018-8069

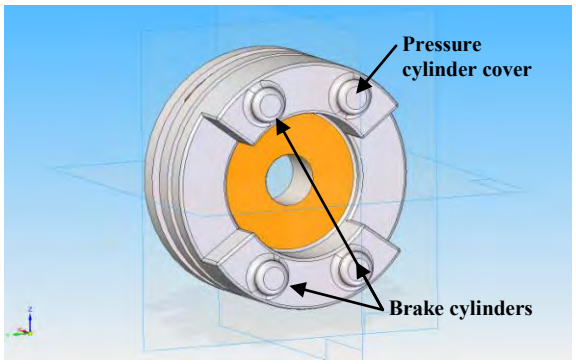

Fig. 3 Multi-disc brake modul after the removal from the landing gear [2]
Obr. 3 Modul lamelovej brzdy po demontáži z podvozkovej nohy [2]

In Fig. 3, there is the whole multi-disc brake after the removal from the main landing gear. The coloured parts show the functional part of the brake, such as brake plates with cylinders in gray colour. Malfunction parts in terms of braking performance are freely positioned and attached discs (orange colour) [2]. The two types of discs are main parts:

1. Rotary discs – with a ceramic matrix composite (CMCs). These have projections on the circumference and they are connected to the rotating part of the wheel in the slots with the possibility of axial movement.
2. Fixed discs – with metal-ceramic material and these have the projections towards the centre and are connected to the fixed part of the wheel in the slots, again with the possibility of axial movement [4].

Main parts of the multi-disc brake are on Fig. 4.

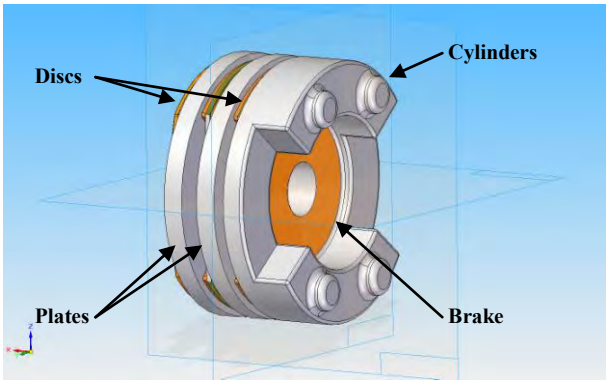

Fig. 4 Main parts of the multi-disc brake [2]
Obr. 4 Hlavné časti lamelovej brzdy [2]

Pressure cylinders operate on the discs from the edge pressing the discs on the plate. Once the brake is active the cylinders are pressing the discs to axial movement against the plate and braking occurs among the plates (Fig. 5). After releasing the pressure, disc returns by expander springs which were pressed by the cylinders. Brakes have a large braking torque and work smoothly. After all, they have bad heat dissipation as the result of brake friction. Automatic adjusters are used to simplify the operation [3].

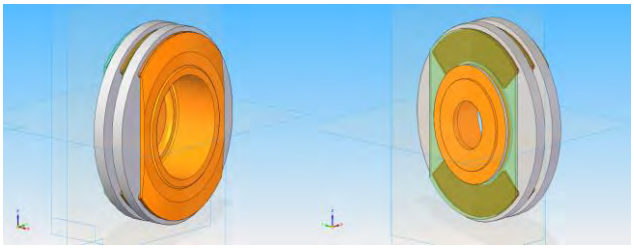

Fig. 5 Brake with pressure middle discs [2]
Obr. 5 Teleso brzdy so strednými prítlačnými lamelami [2]

Conclusions

The increase relating to the braking force of UAV´s brakes and small disc size in the space of main landing gear were main reasons for specification of suitable material with better values than those commonly used for the multi-disc brakes production. The material used for the brake design has to satisfy all the requirements including high braking efficiency conditions even at high temperatures. The material has to be strong enough to avoid cracking during the activity. The reason is the connected with the loose of fitting plates in the brake. The selected material is the ceramic matrix composite (CMCs). This composite will be dealt in terms of computational modeling and material parameters for brake could be used to meet constructionally all the demanding requirements of the aircraft industry.

Literature

[1] HAVELKA, V. Konstrukce a projektování letadel II. University mimeographed. Prague, Czech Republic : ČVUT. 1986 (in Czech)

[2] HAZUCHOVÁ, L. Návrh lamelovej brzdy dopravného prostriedku so zohľadnením na účinnosť, spoľahlivosť a údržbu. Diplomová práca. Trenčín, Slovak Republic : Trenčianska univerzita Alexandra Dubčeka v Trenčíne, Fakulta špeciálnej techniky. 2013. 62 p. (in Slovak)

[3] BREUER, B. BILL, K.-H. Bremsenhandbuch: Grundlagen, Komponenten, Systeme, Fahrdynamik. 1. Aufl. ATZ-MTZ-Fachbuch. Vieweg Verlag. 2003. ISBN 978-3-8348-0064-0

[4] NASLAIN, R. Ceramic matrix composites. Université Bordeaux 1, 33600 Pessac. France

Microlocation of Critical Parts of the Tire Casing

Mikrolokalita kritických častí plášťa pneumatík

Ing. Jozefína Panáčková[1], **Ing. Peter Vido**[1], **doc. Ing. Jan Krmela, Ph.D.**[1]

[1]University of Alexander Dubček in Trenčín, Faculty of Industrial Technologies, I. Krasku 491/30, 020 01 Púchov, Slovak Republic

This paper deals with microlocation of critical parts of the tire casing such as endings of steel cord belts and endings of carcass layers around bead wires. On the road, vehicles, including cars, have to meet more extreme conditions because of the increasing demands during their usage due to the increasing speed. Therefore, the attention is paid to durability and safety. An important safety feature of a car stands also for the tires since they provide contact of the car with the road and have a significant impact on the handling, directional stability of the vehicle and safety indicators. Tires can be characterized as composites with non-linear elastomeric matrix reinforced with textile and steel cords. It is very important to deal with the tire as a whole, but in terms of better understanding of the behavior of the tires it is also important to know the microlocations of critical points in the tire casings. In relation to transverse sections of the tires for trucks, bonds or connections between steel cord and elastomer were studied using light and electron microscopy. These results will be used as a means of input data for the computational modeling of the tire casings.

Keywords: *tire casing, composite, tire bead, degradation, steel cord belt*

Tento príspevok sa zaoberá mikrolokalitou kritických častí plášťa pneumatík ako sú ukončenia oceľokordových nárazníkov a ukončenia kostrovej vložky okolo pätných lán. Na cestné dopravné prostriedky, vrátane automobilov, sú všeobecne kladené čím viac zvýšené požiadavky na ich prevádzku v dôsledku zvyšujúcej sa rýchlosti. Preto je dôraz kladený na životnosť a bezpečnosť. Dôležitým bezpečnostným prvkom automobilu sú tiež pneumatiky, pretože zabezpečujú kontakt automobilu s vozovkou a majú výrazný vplyv na jazdné vlastnosti, smerovú stabilitu automobilu a jeho bezpečnostné ukazovatele. Pneumatiky je možné charakterizovať ako kompozity s nelineárnou elastomérnou matricou, vystuženou textilnými a oceľovými kordmi. Na rozhraní medzi matricou a kordmi môžu nastať rôzne formy degradačných procesov, ktorých iniciácia môže byť daná použitím nekvalitných materiálov pre výrobu autoplášťov, nedodržaním technológie procesu výroby, ale i skladovacích a prevádzkových podmienok. Táto adhézna väzba medzi oceľokordmi a nánosovými zmesami môže byť degradačnými procesmi výrazne narušená. To môže v konečnom dôsledku mať vplyv na kompaktnosť celej pneumatiky, čo môže spôsobiť haváriu automobilu. Je veľmi dôležité sa zaoberať pneumatikami ako celok, ale z hľadiska lepšieho pochopenia správania sa pneumatík je tiež dôležité poznať mikrolokality najmä kritických miest v plášťoch pneumatík. K týmto kritickým miestam patrí oblasť koruny a pätky plášťa. Dnešný trend vo vývoji a výskume ako automobilov, tak aj plášťov pneumatík je smerovaný na využitie výpočtového modelovania ako podporného prostriedku k experimentom. V priečných rezoch plášťov pneumatík pre nákladné automobily boli sledované svetelnou a elektrónovou mikroskópiou mikrolokality z hľadiska väzieb oceľový kord-elastomér. Tieto výsledky budú použité ako podporné prostriedky pre výpočtové modelovanie plášťov pneumatík.

Kľúčové slová: *plášť pneumatiky, kompozit, pätka plášťa, degradácia, oceľokordový nárazník*

Tire casing of the car tire is an important element in terms of safety. It is a car-road contact point. Therefore, increased attention has to be paid to research and manufacturing of casings and to their structural design including entry materials in the production. Function of the casing is to transfer all the forces between the vehicle and the road. These are the longitudinal forces (acceleration, braking), transverse (driving the car in the corners) and vertical (own weight of the car). Furthermore, ca tire has to fulfill other functions, such as participate by its flexibility in relation to automobile movement - to absorb shocks caused by road bumps. The casing is the main component of resistance against rolling, therefore it must be sufficiently rigid and because of the required suspension parameters it also must be flexible at the same time. It is necessary to align these two contradictory requirements.

Tire casing

In terms of a composite material, the tire is a very complex element. It is defined as a casing with or without a tube and an insert which is mounted on the rim and filled with pressure medium. The casing can be defined as a flexible outer part of the tire, which ensures contact of the car with the road and its bead part abuts against the rim. It must also meet a variety of operational and other requirements [1]. The most

difficult structural element is the steel cord belt. It is important because it affects the whole tire strength and it is connected with the effect on deformation characteristics of the casing.

Results and discussion

Example of the structure of a truck tire casing with critical areas of the tire, which contain the reinforcing elements, is shown in Fig.1. Typical violations occur within the casing in place of ending of steel cord belts and endings of the carcass around bead wires in the casing bead area due to poor quality of production or by overloading of the tire casings. These areas belong to the typical areas in the tire casing.

Fig. 1 Typical points of damage of the radial tire casing, A - the ending area of steel cord belts; B - the ending area around the end of carcass which is around bead wires
Obr. 1 Typické miesta poškodzovania radiálneho plášťa pneumatiky, A – oblasť ukončenia oceľokordových nárazníkov; B - oblasť ukončenia kostrovej vložky okolo pätných lán

Publications [2, 3] deal with the critical areas in the tire casings in terms of security and the use of computational modeling. The attention is paid to the interface of the elastomer with the cord. Fig. 2 can be an example of a critical area where there is the area of the casing bead [4].

Fig. 2 The area of the casing bead
Obr. 2 Oblasť pätky plášťa

Fig. 3 shows another example of a critical part of the casing and it is the degraded area of the ending of steel cord belts. These are typical by separation of belt components from each other. It is very dangerous in terms of the car's driving parameters.

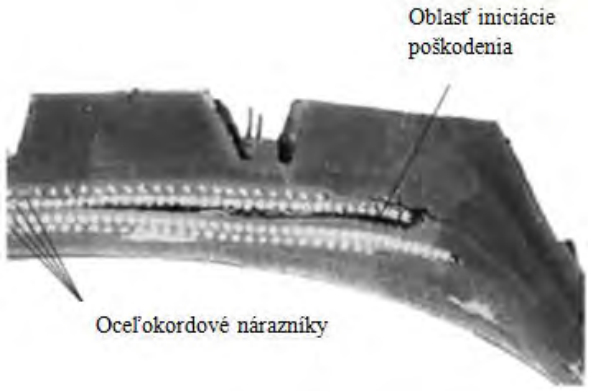

Fig. 3 Rupture area by delamination of steel cord belt in the crown of the tire casing [5]
Obr. 3 Oblasť porušenia delamináciou oceľokordového nárazníka v korune plášťa pneumatiky [5]

In Fig. 4, the detail is focused on the steel cord belts in the radial tire casings for trucks. Separation of elastomer from cords occurs in this area during the manifestation of degradation.

Fig. 4 Ruptured area of the steel cord belt in the crown of the tire casing [5]
Obr. 4 Oblasť porušenia oceľokordového nárazníka v korune plášťa pneumatiky [5]

Cord wire is used to manufacture steel cords for car tires, conveyor belts and pressure hoses. It is made of high-carbon steel with high requirements in relation to quality therefore their continuous testing and inspection must be carried out. Wires with the diameter of 0.15 mm and strength to 4000MPa are obtained by cold drawing [5]. The wire is then processed by heat. Finally, it is metalized in a galvanic way. The given process of galvanization is connected with the process of galvanization with copper and then it is metalized by zinc. The applied brass surface contains 63-70% copper and 37-30% Zn. Brass metallization is a critical factor for the adhesion of elastomer with cord. The final brass layer is about 0.1 to 0.7 microns thick.

In Fig. 5, there is the image of the surface of the reinforcing cords for steel cord belts of truck tire casings. The following EDX surface analysis was focused on the surface of the steel cord. In position #1, we focused on the determination of the chemical composition of the base material. In position #2, we focused on determination of the concentration of chemical elements in the ruptured area of the cord

Hutnické listy č.7/2013, roč. LXVI
ISSN 0018-8069

surface. Determination of the concentration of individual elements in the analyzed area is in Table 1.

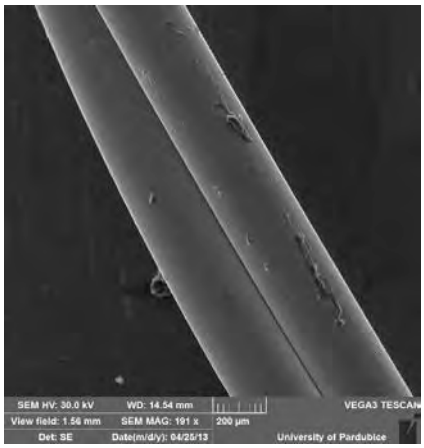

Fig. 5 SEM image of the surface of steel cords
Obr. 5 SEM snímok povrchu oceľových kordov

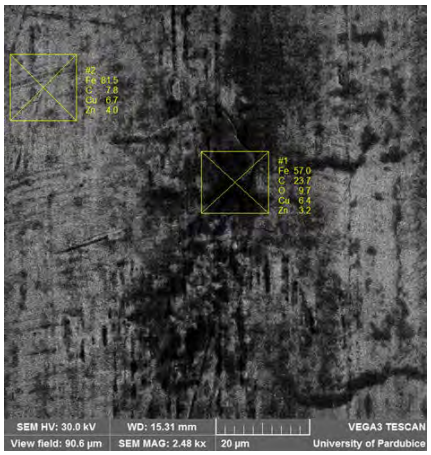

Fig. 6 Application of EDX surface analyses on the surface of the steel cord
Obr. 6 Aplikovanie EDX plošných analýz na povrch oceľového kordu

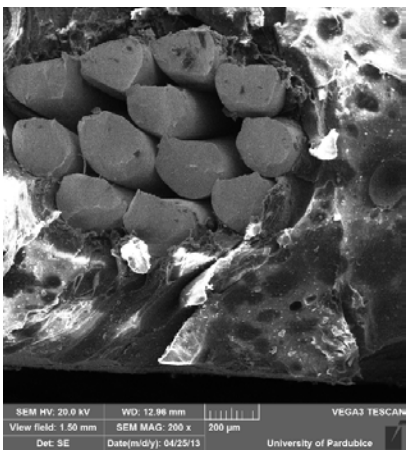

Fig. 7 SEM image of the steel cord belt in transverse section
Obr. 7 SEM snímok oceľokordového nárazníka v priečnom reze

Tab. 1 The results of EDX analysis of the surface of steel cords for tire casings
Tab. 1 Výsledky plošnej EDX analýzy povrchu oceľových kordov pre plášte pneumatiky

position	C	O	Fe	Cu	Zn
#1	23.7	9.7	57.0	6.4	3.2
#2	7.8	-	81.5	6.7	4.0

In Fig. 7, there is a detail of the interface of steel cord and of steel cord belt elastomer in the tire casing where the most common undesired state is connected with insufficient adhesion to the elastomeric cord.

Conclusions

It is necessary to deal further with critical areas in tire casings for better understanding of the mechanisms and processes that can occur in these areas. Separation of the elastomer from cord occurred in a large extent. In the case of occurrence of degradation processes in elastomer-steel cord bonds the compactness of the whole tire may be affected. This can lead to a loss of reliability and functionality of the tires and ultimately to a vehicle accident.

Literature

[1] DRDÁKOVÁ, J., STRUHARŇANSKÁ, M., KRMELA, J. Vybrané fyzikálno – mechanické vlastnosti špecifických kompozitných materiálov s elastomérmi. In Semdok 2013, 18th International of PhD.students´ seminar Slovak Republik, 2013: Univerzity of Žilina in Žilina, p. 104-107, ISBN 978-80-554-0629-9

[2] VIDO, P., DRDÁKOVÁ, J., STRUHARŇANSKÁ, M, KRMELA, J. Vybrané experimentálne skúšky kompozitov s elastomérovou matricou pre overenie výpočtových modelov pneumatík. In TechMat 2012, Pardubice: Univerzita Pardubice, Czech Republic: 2011, p. 90-96, (CD-ROM), ISBN 978-80-7395-537-3

[3] DRDÁKOVÁ, J., STRUHARŇANSKÁ, M, KRMELA, J. Selected physical – mechanical properties of specific composite materials with elastomer. In ARSA 2012– The 1st Virtual International Conference on Advanced Research in Scientific Areas (ARSA-2012) Slovak Republic, Žilina: EDIS, 2012, p. 1785-1788, ISBN 978-80-554-0606-0

[4] KRMELA J., TOMANOVÁ V., DRDÁKOVÁ J., VIDO P. Väzba kord-elastomer v pneumatikách z pohledu charakteru kordu a mikroskopického pozorování. In: Sborník přednášek z konference TechMat '10. Pardubice, Univerzita Pardubice, Czech Republic: 2010, p. 83-86, (CD-ROM). ISBN 978-80-7395-324-9

[5] DRDÁKOVÁ J., KRMELA J., KRMELOVÁ V. Microlocation of the system elastomer – steel cord in the tire after degradation process. In: Sborník přednášek z konference TechMat '11. Pardubice: Univerzita Pardubice, Czech Republic: 2011, p. 130-135, (CD-ROM), ISBN 978-80-7395-431-4

ekologie, recyklace, druhotné zpracování materiálu

The Reinforcing Effect of the Dust from Glass Production in Rubber Compounds

Stužujúci účinok prachu zo sklárskej výroby v kaučukových zmesiach

Ing. Slavomíra Domčeková[1], prof. Ing. Darina Ondrušová[1], PhD., Ing. Lenka Špániková[1], Ing. Zuzana Jankurová, PhD.[1]

[1]University of Alexander Dubček in Trenčín, Faculty of Industrial Technologies in Púchov, I. Krasku 491/30, 020 01 Púchov, Slovak Republic

The presented work deals with the substitution of standard filler - carbon black for the alternative filler - the dust from flue gas filters in glass industry. The dust can be considered as non-black and no-active filler which was prepared by crushing and then by sieving of particles which were less than 0.045 mm. The adapted filler was shuffled to model rubber compounds. Difference of the tested rubber compounds was connected with the type as well as amount of filler. Four different compounds were prepared for this investigation, where one of them was filled with standard filler - carbon black. The other rubber compounds contained combination of carbon black with the alternative filler - dust. The main aim is the verification of the dust influence on the reinforcing effect in rubber compounds by using RPA 2000. The Rubber-Process-Analyzer allows a very reliable and detailed investigation of the dynamic behaviour on a much easier and faster way than the common dynamic analysis of vulcanizates.

Key words: *alternative filler, dust, rubber compound, reinforcing effect, RPA 2000*

Prezentovaná práca je zameraná na využitie odpadu - prachu zo spalinových filtrov zo sklárskej výroby vo funkcii alternatívneho plniva do kaučukových zmesí. Použitý prach pred samotným zamiešaním do gumárenských zmesí bol upravovaný drvením a sitovaním na veľkosť častíc menšiu než 0,045 mm. Takto pripravené plnivo sa zamiešavalo do modelových gumárenských zmesí, za účelom náhrady štandardne používaného plniva - sadzí alternatívnym plnivom - odpadným prachom zo spalinových filtrov zo sklárskej výroby. Rozdiel v zložení zmesí spočíval v použitom type a množstve plniva. Pripravené modelové gumárenské zmesi s označením SP 40/0, SP 30/10, SP 20/20, SP 10/30 dokumentujú obsah plniva v dsk v pomere sadze / prach. Zmesi sa pripravovali dvojstupňovým miešaním v hnetacom stroji Plastograf - Brabender. Podmienky prvého stupňa pozostávali z teploty, ktorá dosahovala 110 °C a v 60 otáčkach za minútu. Podmienky druhého stupňa boli 100 °C pri 50 otáčkach za minútu. Následne po zamiešaní zmesí bol hodnotený Payne effect pomocou prístroja RPA 2000. RPA 2000 je univerzálny prístroj, ktorý slúži na meranie dynamických a viskoelastických vlastností vstupných polymérov, surových zmesí, ale i výsledných vulkanizátov. Skladá sa z dvoch vyhrievaných bikonických hláv, ktoré tvoria dutinu formy do ktorej sa vkladá skúšobná vzorka. Spodná hlava počas merania vzorky osciluje, čo vyvoláva šmykovú deformáciu, pričom sila potrebná ku kmitu spodnej hlavy závisí od tuhosti kaučukovej zmesi. Pre pochopenie stuženia gumy, je potrebné si všimnúť jej mäknutie pod napätím pri veľmi malých dynamických deformáciách, tzv. Payne effect. Na základe získaných výsledkov možno predpokladať využitie prachu hlavne v technickej gume, na ktorú nie sú kladené až také vysoké kvalitatívne nároky. Skúmané alternatívne plnivo - prach zo spalinových filtrov zo sklárskej výroby môže nájsť využitie hlavne kvôli výraznému zlacneniu zmesi recykláciou odpadu.

Kľúčové slová: *alternatívne plnivo, prach, gumárenská zmes, Payne effect, RPA 2000*

Carbon black has been the preferred reinforcing filler for rubber. It is available in a great variety of types and is used in virtually all sorts of rubbers [1].

The particle size is the fundamental property of the filler used in a filled elastomer. This affects the reinforcement of elastomer most strongly. Van Der Waals force attraction is one of the sources of reinforcement between the carbon black surface and the rubber matrix. The rubber chains are also grafted onto the carbon black surface by covalent bonds. The interaction is caused by a reaction between the functional group at the carbon black particle surface and free radicals on polymer chains. The filler-rubber interface is made up of complex physical and chemical interaction [2]. The surface activity is the predominant factor with regard to filler-filler and filler-polymer interaction. In relation to carbon black as filler, Payne-effect was investigated. This investigated effect depends on the basic properties, such as specific surface area, structure and surface activity. The given investigation was performed by help of the Rubber-Process-Analyzer (RPA) [3] which allows a very reliable and detailed investigation of the dynamic behaviour on a much easier and faster way than the common dynamic analysis of vulcanizates [3,4,5].

Experimental

The four model rubber compounds were prepared for the testing procedures (tab.1). These compounds were prepared by mixing in Brabender, the mixer with volume of chamber 70 cm^3 according to norm STN 62 1425 [6]. In the first mixing step, we added natural rubber, activator ZnO, stearic acid, filler and plasticizer. Tested compounds were filled only with carbon black or carbon black as a filer was combined with the dust while the combination of the dust and carbon black was in the various ratios. Temperature 110 °C at the 60 rotations per second was the condition relating to the first mixing step. In the second mixing step, we added curing agent (sulfur) and accelerator to the compound. Temperature 100 °C at the 50 rotations per second was the condition relating to the second mixing step. After mixing process, rubber compounds were left for 24 hours.

Tab. 1 Formulation of rubber compounds
Tab. 1 Zloženie gumárenských zmesi

Ingredients [*phr]	SP 40/0	SP 30/10	SP 20/20	SP 10/30
	I. step			
SMR	100	100	100	100
ZnO	2	2	2	2
Stearic Acid	1	1	1	1
Carbon Black	40	30	20	10
Dust	-	10	20	30
Platicizer	5	5	5	5
	II. step			
Sulphur	1.2	1.2	1.2	1.2
Accelator	1.5	1.5	1.5	1.5

*phr = parts per hundred rubber

Prepared rubber compounds were investigated by using Rubber-Process-Analyzer (RPA 2000). The obtained values of prepared rubber compounds with alternative filler were compared with the values of reference rubber compound with standard filler.

Results and discussion

The Payne effect was measured by Rubber-Process-Analyzer. The given reinforcing effect was evaluated on the basis of the ratio of the storage modulus G´ and amplitude before curing process as well as after curing process. The upper curve shows deformation softening of the sample before relaxation and lower curve shows deformation softening of the sample after relaxation. According to the evaluation, it can be concluded that the higher storage modulus G´ means that the reinforcing effect of the filler is better in rubber matrix. In relation to the storage modulus G´, the distance between upper curve and the lower curve shows destruction of network of rubber compound after relaxation. The measuring conditions include the specification of the frequency (1Hz), amplitude (0.1-1000 %), temperature (70 °C) before curing process and (170 °C) after curing process. The storage modulus G´ before cure (fig. 1) is approx. 225 kPa and after cure, it is approx. 900 kPa for the compound SP 40/0 which was filled only with 40 phr of carbon black. After the relaxation (fig. 2) the storage modulus G´ is decreased and it means that the polymer network is deteriorated.

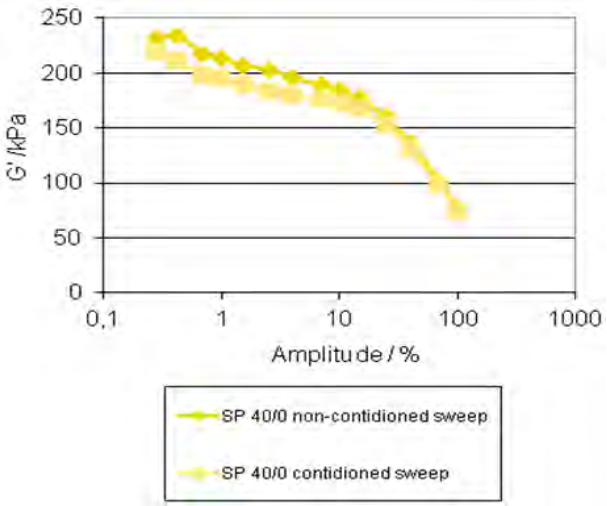

Fig. 1 The ratio of storage modulus G´ and amplitude before cure for compound SP 40/0
Obr. 1 Pomer šmykového modulu G´a amplitúdy pred vulkanizáciou pre zmes SP 40/0

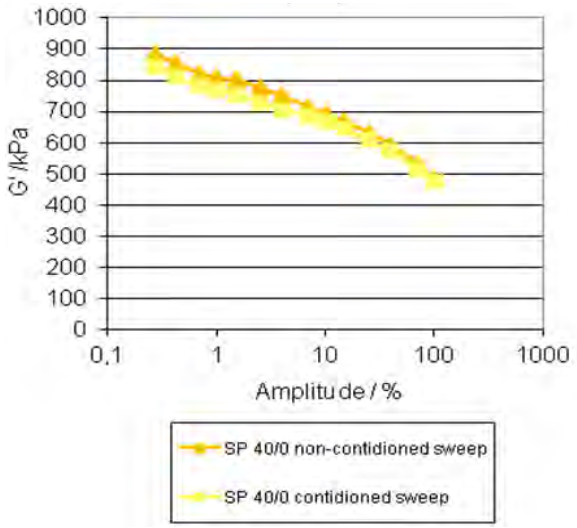

Fig. 2 The ratio of storage modulus G´ and amplitude after cure for compound SP 40/0
Obr. 2 Pomer šmykového modulu G´a amplitúdy po vulkanizácií pre zmes SP 40/0

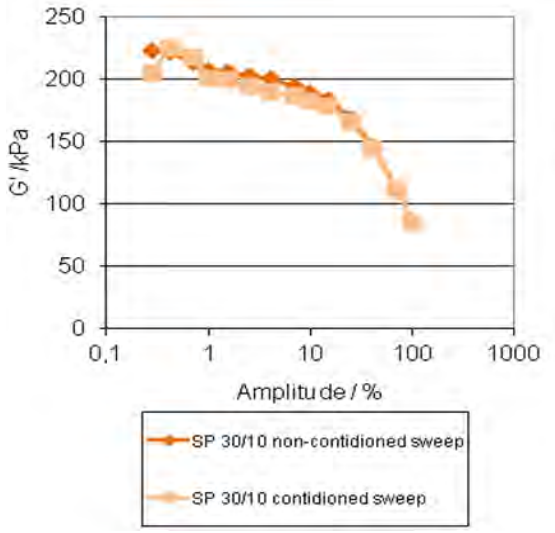

Fig. 3 The ratio of storage modulus G ´and amplitude before cure for compound SP 30/10
Obr. 3 Pomer šmykového modulu G´a amplitúdy pred vulkanizáciou pre zmes SP 30/10

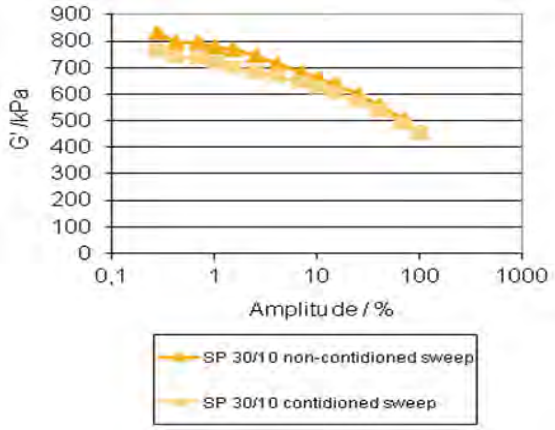

Fig. 4 The ratio of storage modulus G ´and amplitude after cure for compound SP 30/10
Obr. 4 Pomer šmykového modulu G´a amplitúdy po vulkanizácii pre zmes SP 30/10

The graph (fig. 3, 4) shows sample SP 30/10 which was filled with 30 phr of carbon black together with 10 phr of dust. The storage modulus G´ slightly decreases due to decrease of the reinforcing effect of filler in rubber matrix.

Increase of the dust in rubber compound causes decrease of the storage modulus G´. The sample SP 40/0 which was filled only with 40 phr of carbon black shows decrease of the storage modulus G´ approximately by 200 kPa in compare with sample SP 20/20 which was filled with 20 phr of carbon black in combination with 20 phr of dust (fig. 5, 6).

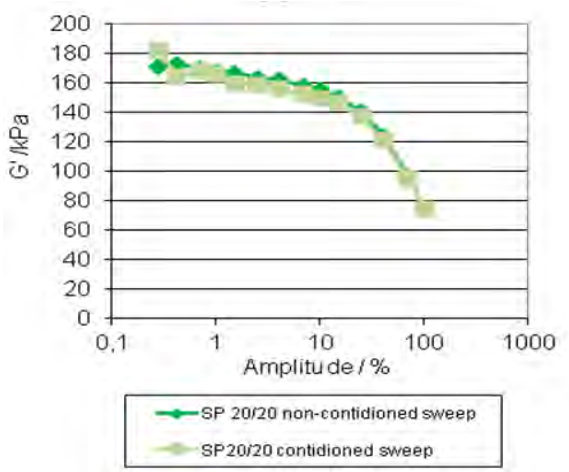

Fig. 5 The ratio of storage modulus G´ and amplitude before cure for compound SP 20/20
Obr. 5 Pomer šmykového modulu G´a amplitúdy pred vulkanizáciou pre zmes SP 20/20

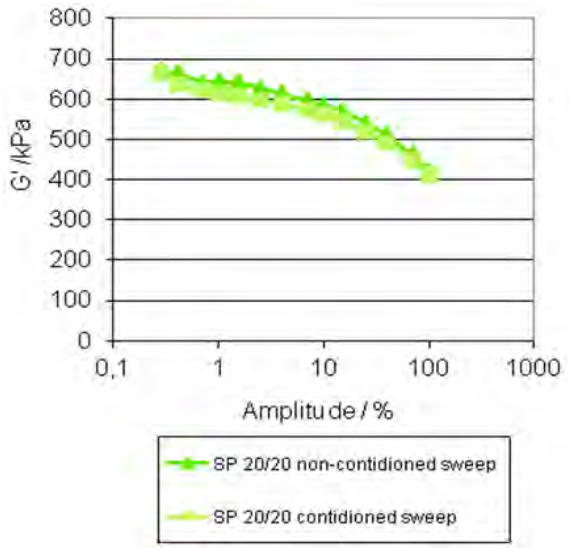

Fig. 6 The ratio of storage modulus G´ and amplitude after cure for compound SP 20/20
Obr. 6 Pomer šmykového modulu G´a amplitúdy po vulkanizácii pre zmes SP 20/20

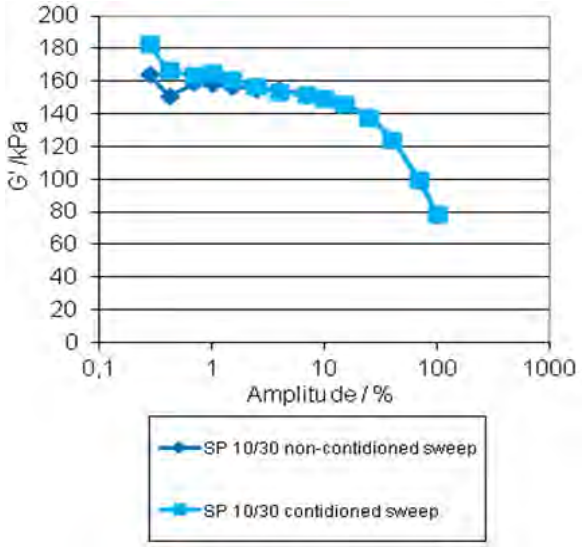

Fig. 7 The ratio of storage modulus G´ and amplitude before cure for compound SP 10/30
Obr. 7 Pomer šmykového modulu G´a amplitúdy pred vulkanizáciou pre zmes SP 10/30

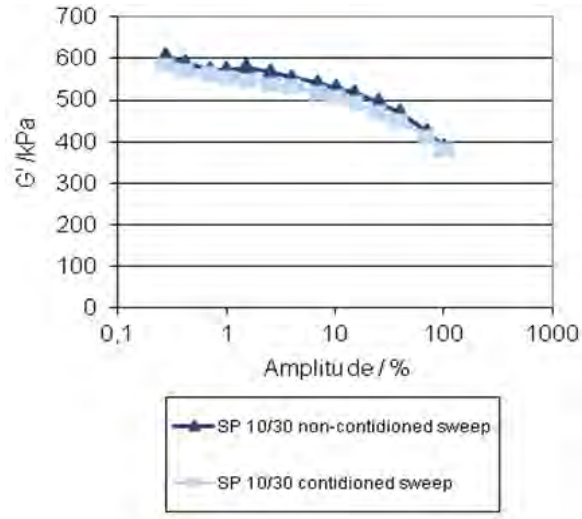

Fig. 8 The ratio of storage modulus G´ and amplitude after cure for compound SP 10/30
Obr. 8 Pomer šmykového modulu G´a amplitúdy po vulkanizácii pre zmes SP 10/30

Increase of the dust in rubber compound leads to decrease of the storage modulus G´ but the rubber compound has better relaxation before cure as well as after curing process (fig. 7, 8). This fact is confirmed on the basis of the ratio of storage modulus G´ and amplitude for compound SP 10/30 which was filled with 10 phr of carbon black together with 30 phr of dust because the lower curve is the approximately the same as the upper curve.

Conclusions

Increase of the dust in rubber compound decreases the storage modulus G´ (it means the decrease of the reinforcing effect) but the rubber compound filled with 30 phr of dust has better relaxation before curing process as well as after curing process in comparison to the compound filled only with 40 phr of carbon black. The dust can be used in the technical rubber because there are not high requirements and this alternative filler does not exhibit the worst result of measurement and the most important fact is that from the economical aspect, the alternative filler is cheaper.

Acknowledgements
This work has been supported by VEGA No. 1/0530/11 and KEGA No. 007 TnUAD – 4/2013.

Literature

[1] NOORDEMMER, J.W.M., DRIERKES, W.K. Silica - Filled Rubber Compounds. In: Technologist´s Handbook. Smithers Rapa Technology. Volume 2. 2009. p 443. ISBN 978-1-84735099-2

[2] FRÖHLICH, J., NIEDERMEIER, W., LUGINSLAND, H.D. The effect of filer-filler and filler-elastomer interaction on rubber reinforcement. In: Composites Part A: Applied Science and Manufacturing , Volume 36, 2005, p.449-460.

[3] NIEDERMEIER, W. - FRÖHLICH, J. - LUGINSLAND, H.D. - Köln. Reinforcement Mechanism in the Rubber Matrix. 2002.

[4] JHA, V. Carbon Black Filler Reinforcement of Elastomers. University of London. October 2008. A thesis for the degree of Doctor of Philosophy Department of Materials Queen Mary [online] Available from: http://www.sems.qmul.ac.uk/research/honours/doc.php?id=335, 7.10.2013

[5] VAVRO, J., HAJSKÁ, H., VAVRO, J.jr., KOVÁČIKOVÁ, P. Analysis of the Defects in Tyres for freight Vehicles at the dynamic Loading. Machine Modelling and Simulations. Poznaň : Politechnika Pozňanska, 2012. p. 193-200, ISBN 978-83-923315-2-0

[6] Príprava gumárenských zmesí STN 62 1425

The Use of the Monoionic Form of Montmorillonite for Removal of Toxic Organic Pollutants

Použitie monoiónovej formy montmorillonitu na odstránenie toxických organických zlúčenín

Ing. Veronika Janíková[1], **Ing. Róbert Janík, PhD.**[1], **prof. Ing. Eugen Jóna, DrSc.**[1]

[1]University of Alexander Dubček in Trenčín, Faculty of Industrial Technologies, I. Krasku 491/30, 020 01 Púchov, Slovak Republic

Montmorillonite is one of the most important clay minerals and it is typical for huge expandability. It is able to accept not only water into the interlayer, but also toxic organic compounds and it has a positive effect in relation to its using in environmnet. Montmorillonite has been used in pharmacy and in industry of buildings and as insulating material. Prepared monoionic form of montmorillonite was Cu^{2+}-MMT and used organic compounds were benzene and phenol. These compounds have variety of utilisations, for example in production of plastic, in rubber industry and in pharmacy and a lot of phenols can be found in nature. For the investigation and acquisition of results, we used an XRD diffraction and IR spectroscopy. After interaction Cu^{2+}-MMT with benzene and phenol, we can see a movement of diffraction peak in comparison to monoionic form. It is proven that benzene and phenol are present into the interlayer space. The application of IR spectroscopy was useful for finding new absorption bands which can be attributed to benzene (vibration of aromatic ring) and phenol (vibration of v(OH) group).

Keywords: *Montmorillonite, benzene, phenol, XRD diffraction analysis, IR spectroscopy*

Montmorillonit je jedným z najvýznamnejších predstaviteľov ílových minerálov, pričom medzi jeho výhody patrí jeho vrstevnatá štruktúra, ktorá pozostáva zo siete tetraédrov a oktaédrov. Montmorillonit sa vyznačuje vysokou expandabilitou štruktúry, čo znamená, že je schopný prijať do svojho medzivrstvia nielen vodu, ale aj toxické organické zlúčeniny, čo dokazuje jeho výhodné využitie najmä z hľadiska životného prostredia. Svoje využitie montmorillonit nachádza aj vo farmaceutickom a stavebnom priemysle. Jednou z pripravených monoiónových foriem montmorillonitu bola meďnatá forma montmorillonitu (Cu^{2+}-MMT), pri ktorej došlo k interkalácii toxických organických zlúčenín do medzivrstvia montmorillonitu. Pre prácu boli vybrané organické látky zo skupiny aromatických zlúčenín, benzén a fenol. Tieto toxické látky majú široké využitie v rôznych odvetviach priemyslu, s čím je spojená aj kontaminácia životného prostredia týmito látkami. Benzén nachádza svoje využitie v oblasti výroby plastov, syntetických vlákien, gumy, farbív ale aj liekov a pesticídov. Využitie fenolu je najmä pri výrobe plastov, syntetických živíc a liečiv, no množstvo fenolov a fenolových éterov sa nachádza aj v prírode. Vhodné analytické metódy, ktoré dokazujú skutočnosť, že montmorillonit dokáže tieto toxické látky prijať do medzivrstvia a tým zabrániť úniku do okolia, boli RTG difrakčná analýza a IČ spektroskopia. Po interakcii Cu^{2+}-MMT s benzénom a fenolom je na RTG difrakčnom zázname viditeľný posun difrakčného píku v porovnaní s Cu^{2+}-MMT, čo dokazuje interkaláciu týchto organických zlúčenín do štruktúry MMT. Na zázname IČ spektra Cu^{2+}-MMT po interakcii s benzénom a fenolom možno pozorovať nové absorpčné pásy, ktoré možno priradiť vibráciám skeletu aromatického kruhu, pričom pri fenole možno pozorovať výrazný absorpčný pás, ktorý možno priradiť pásom v(OH) skupín, zapojených do vodíkovej väzby.

Kľúčové slová: *Montmorillonit, benzén, fenol, RTG difrakčná analýzy, IČ spektroskopia*

Montmorillonite belongs to the smectic clays with layered structure and exhibits a swelling behaviour resulting from the weak attraction between the oxygens on the bottom and top of the tetrahedral sheets [1, 5]. Smectites are expandable clay minerals with the structure 2:1 [2]. Montmorillonite aggregates have three different spaces, i.e. interlayer space, inter-particle space and inter-aggregate space. Therefore, all clay minerals are porous containing pores of varied size and shape [3]. Clay minerals are widely used in a range of many applications in relation to ceramics and refractory materials, foundry binding sands and moreover, they are also used in paper production, as catalysts or additives into polymeric materials. These minerals are especially interesting as barriers in toxic and nuclear waste deposits [4]. Clays which belong to the phyllosilicate groups and they are very interesting materials from the aspect of the adsorption. On the other hand, clay minerals are known to be excellent adsorbents and it could be used for elimination of various organic compounds from water [5]. In the mechanochemical adsorption study of organic compounds by expanding montmorillonite, the clay is ground with excess of the organic compound [6]. Montmorillonites are widely

used in a range of applications because of their high cation exchange capacity, swelling capacity, high surface areas and consequential strong adsorption as well as absorption capacities. They can be even used as reinforcement material in polymer-clay nanocomposites due to the particles with one dimension in the nanometer range [7, 8]. These clay properties can be enhanced by converting the montmorillonite to an organoclay by ion exchange of the cation with a surfactant molecule. The surface properties of these organoclays are changed significantly from hydrophilic to hydrophobic. These clays then have useful properties, for example, the removal of oil from potable water and other toxic chemicals as well as humic materials or substance from water. These modified clay minerals represented by organoclays stand for a family of materials which have many application in a range of key areas, such as adsorbent of organic pollutants, rheological control agents, reinforcing fillers for plastics and electric materials. The influence of montmorillonite surfaces on the chemical and physical properties of adsorbed H_2O molecules has been the subject of a number of recent studies using structural, thermodynamic, spectroscopic, and computational methods [7]. As a result of rapid development of chemical and petrochemical industries, the earth surface and ground waters are polluted by various organic and inorganic chemicals, such as phenolic compounds, dyes and heavy metals [9]. Many organic compounds have been classified as hazardous pollutants because of their potential toxicity to human health [10]. Benzene and phenol or phenolic compounds are very harmful to organisms even at very low concentration due to their toxicity, foul odour and carcinogenic properties. These compounds are present in effluents of the petroleum refining, coke furnaces, batteries, coal gasification plants, ply board manufacturing industries, etc [11]. There are many methods for the removal of organic pollutants from aqueous solutions, such as adsorption, chemical precipitation, ion exchange, membrane processes, biological degradation, chemical oxidation and solvent extraction [10]. One of the main problems in the environmental field is the intrusion of toxic contaminants from waste disposal and other sources into the subsoil and underlying ground water supply [12]. The organic derivatives also found application as rheological control agents in aqueous and nonaqueous dispersions and they have been used as lubricants, drilling fluids, greases, oils, and paints. High chemical and mechanical resistance and low coefficient of frication are attractive features from the aspect of the application of organoclays as commercially used self-lubricating materials. Clay minerals are frequently used in industry [13]. XRD spectral analysis and many other techniques are very useful for materials characterisation. Many authors have used these techniques for various materials characterisation. This article describes only XRD diffraction and IR spectroscopy [14].

Results and discussion

A preparation of Cu^{2+}-montmorillonite

The stock of $CuCl_2$ solution with concentration c = 1 $mol.dm^{-3}$ and water was added to Ca^{2+}-MMT. This prepared suspension was mixed for five hours per day and after 24 hour this process was repeated. After sedimentation, solution of $CuCl_2$ and water was poured but solution of $CuCl_2$ and water was added to the suspension again. This mentioned process was repeated five times. As a result, $CuCl_2$ was washed by water until Cl^- was eliminated completely. A present of Cl^- was investigated by solution of 2% $AgNO_3$. After this process, Cu^{2+}-MMT was dried by heating at 60°C. After drying, this sample was crushed to a powder and prepared for following analysis.

A preparation of Cu^{2+}-MMT with benzene and with phenol

Benzene (0.18 g) was added to 1 g of Cu^{2+}-MMT and this solution was mixed with 100 ml of distilled water. Solution was mixed until MMT was completely solvated and when the reaction was complete. The end of the reaction was indicated by change of colour in relation to original and mixed solution. When sample became sediment, it was removed and the water was evaporated from solution. The preparation of Cu^{2+}-MMT with phenol was performed in the same way as it was in the case of preparation of sample with benzene. Phenol (8.4 g) was added to 1 g of Cu^{2+}-MMT and this solution was mixed with 100 ml of distilled water.

XRD diffraction analysis

In Fig. 1, we can see a movement of peak maximum d_{001} to the 2 Theta (x) and that movement has a direction to the left leading to lower values. It means that there is the interlayer distance for Cu^{2+}-MMT after interaction with benzene and phenol. In relation to Cu^{2+}-MMT with benzene, the size of interlayer space is 0.22 nm and in the case of combination with phenol, the given size is 0.28 nm. This fact is also presented in table 1.

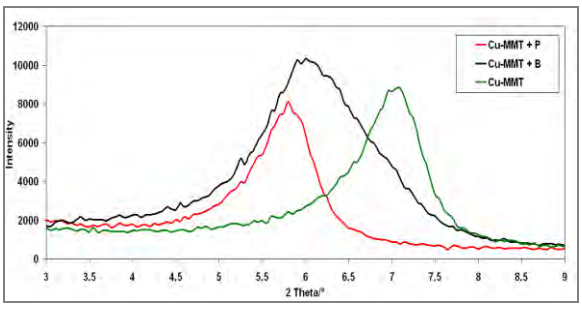

Fig. 1 XRD diffraction of Cu^{2+}- montmorillonites
Obr. 1 RTG difrakčný záznam Cu^{2+}-montmorillonitov

Tab. 1 A values of interlayer distances from XRD diffraction analysis for studied samples of Cu^{2+}-MMT
Tab. 1 Hodnoty medzivrstvia vybraných vzoriek Cu^{2+}-MMT získané pomocou RTG difrakčnej analýzy

sample	2 Theta/[°]	d_{001}/[nm]	Δd_{001}/[nm]
Cu^{2+}-MMT	7.06	1.25	
Cu^{2+}-MMT + B	6.00	1.47	+ 0.22
Cu^{2+}-MMT + P	5.80	1.53	+ 0.28

Infrared spectroscopy

In Fig. 2, we can see IR spectrum of Cu^{2+}-MMT and Cu^{2+}-MMT after interaction with benzene and phenol. The biggest change in spectrum of Cu^{2+}-MMT was after interaction with phenol. New absorption bands are observed at 1317, 1295, 1168 and 1151 cm^{-1} and it can be attributed to stretching vibration of C–O groups and deformational vibrations of C–OH. In relation to IR spectrum, we can see an absorption bands of Cu^{2+}-MMT + phenol at 3230 cm^{-1}. This given fact can be attributed to groups of ν(OH) which are connected to hydrogen bonds and they are more lower than bands of free O–H. After interaction of Cu^{2+}-MMT with benzene, we can see the vibrations of aromatic ring and they are at 1592, 1502 and 1472 cm^{-1}.

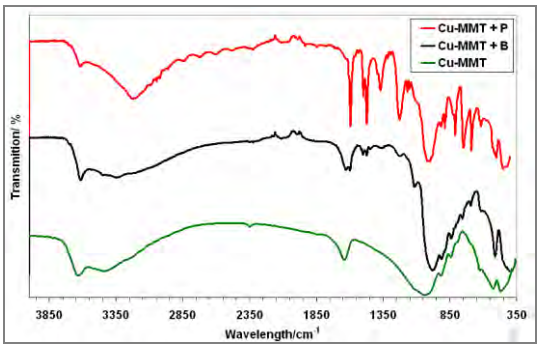

Fig. 2 IR spectra of Cu^{2+}-MMT and its organomontmorillonites
Obr. 2 Infračervené spektrá Cu^{2+}-MMT a jeho organomontmorillonitov

Conclusions

The aim of this measurement was to prove that not only montmorillonite but also its monoionic form Cu^{2+}-MMT is suitable and can be widely used in industry. Toxic organic compounds, such as benzene and phenol which were used in this work are toxic for human and for environment. Properties of MMT are closely connected with the evidence that MMT is able to accept these organic compounds to its interlayer. We can use Cu^{2+}-MMT to remove toxic organic compounds mainly in water but also in soil as well as in the air. After interaction of Cu^{2+}-MMT with toxic organic compounds, benzene and phenol were intercalated. The better intercalation was observed for phenol. This fact is confirmed by help of XRD diffraction and IR spectra. XRD diffraction showed that movement of Cu^{2+}-MMT into the interlayer space was better after interaction with phenol in comparison to interaction of Cu^{2+}-MMT with benzene. IR spectra give evidence that phenol has more evident absorption band in comparison to IR spectra band relating to benzene. The given mentioned facts lead to conclusion that benzene is electroneutral from the aspect of electron charge and its entering into interlayer space is better without orientation to interlayer. On the other side, phenol has an –OH group as well as a dipole moment which causes its orientation.

Literature

[1] YAPAR, S., YILMAZ M. Removal of phenol by using montmorillonite, clinoptilolite and hydrotalcite. *Adsorption*, 2004, vol. 10, p. 287-298

[2] ZHENG, Y., ZAOUI, A. How water and counterions diffuse into the hydrated montmorillonite. *Solid State Ionics,* 2011, vol. 203, p. 80-85

[3] ZHU, J., ZHU, L., ZHU, R., TIAN, S., LI, J. Surface microtopohraphy of surfactant modified montmorillonite. *Applied clay Science*, 2009, vol. 45, p. 70-75

[4] MADEJOVÁ, J., PÁLKOVÁ, H., KOMADEL, P. Behaviour of Li^{+} and Cu^{2+} in heated montmorillonite: Evidence from far-, mid-, and near-IR regions. *Vibrational spectroscopy*, 2006, vol. 40, p. 80-88

[5] JANÍK, R., JÓNA, E., PAVLÍK, V. Montmorillonite as silicate material and its application in rubber industry. *Hutnické listy*, 2011, č. 7, p. 52-56, ISSN 0018-8069

[6] ABRAMOVA, E., LAPIDES, I., YARIV, S. Thermo-XRD investigation of monoionic montmorillonites mechanochemically treated with urea. *Journal of Thermal Analysis and Calorimetry,* 2007, vol. 90, p. 99-106

[7] ZHOU, Q., FROST, R. L., HE, H., XI, Y., ZBIK, M. TEM, XRD and thermal stability of adsorbed paranitrophenol on DDOAB organoclay. *Journal of Colloid and Interface Science,* 2007, vol. 311, p. 24-37

[8] MADEJOVÁ, J., JANKOVIČ, Ľ., PENTRÁK, M., KOMADEL, P. Benefits of near-infrared spectroscopy for characterization of selected organo-montmorillonites. *Vibrational Spectroscopy,* 2011, vol. 57, p. 8-14

[9] SENTURK, H. B., OZDES, D., GUNDOGDU, A., DURAN, C., SOYLAK, M. Removal of phenol from aqueous solutions by adsorption onto organomodified Tirebolu bentonite: Equilibrium, kinetic and thermodynamic study. *Journal of Hazardous Materials*, 2009, vol. 172, p. 353-362

[10] YILDIZ, N., GÖNÜLŞEN, R., KOYUNCU, H., ÇALIMLI, A. Adsorption of benzoic acid and hydroquinone by organically modified bentonites. *Colloids and Surfaces*, 2005, vol. 260, p. 87-54

[11] AGHAV, R. M., KUMAR, S., MUKHERJEE S.N. Artificial neural network modeling in competitive adsorption of pehnol and resorcinol from water environment using some carbonaceus adsorbents. *Journal of Hazardous Materials*, 2011, vol. 188, p. 67-77

[12] ANDREJKOVIČOVÁ, S., ROCHA, S., JANOTKA, I., KOMADEL, P. An investigation into the use of blends of two bentonites for geosynthetic clay liners. *Geotextiles and Geomembranes*, 2008, vol. 26, p. 436-445

[13] HRACHOVÁ, J., MADEJOVÁ, J., BILLIK, P., KOMADEL, P., FAJNOR, V.P. Dry grinding of Ca and octadecyl-trimethylammonium montmorillonite. *Colloid and Interface Science*, 2007, vol. 316, p. 589-595

[14] ŠNIRCOVÁ, S., JÓNA, E., JANÍK, R. Co(II)-exchanged montmorillonite with ethylendiamine, trimethyl-and tetramethyl-ethylenediamine and their thermal decomposition. *Journal of Thermal Analysis and Calorimetry*, 2011, vol. 104, no. 3, p. 937-941

Hutnické listy č.7/2013, roč. LXVI
ISSN 0018-8069

zkušebnictví, měřictví, laboratorní metody

Evaluation of Heat Transfer and Moisture Transfer in the Selected Assortment of Home Fabrics

Hodnotenie prestupu tepla a vlhkosti u vybraného sortimentu bielizňových textílií

Ing. Jela Legerská, PhD.[1]

[1] University of Alexander Dubček in Trenčín, Faculty of Industrial Technologies, I. Krasku 491/30, 020 01 Púchov, Slovak Republic

The paper deals with the information about experimental measurements relating to the heat and water vapor transfer on the available textile materials. We evaluated home fabrics-bed linens. Tested fabrics were made of different material compositions. We selected fabrics with a high thermal resistance value Rct and low-value evaporation resistance Ret as the most suitable material for the production of that range. We can conclude that with increasing content of components in mixed polyester, knitted fabric improves the moisture transfer from the skin through the fabric into the environment. On the other side or on contrary, increasing the content of cellulosic materials in a mixed knitted fabric improves its thermal insulation properties. Significant degree of tightness between the endpoints of the thermal resistance and evaporative resistance has been demonstrated by correlation of dependency (fig. 3).

Keywords: *thermal resistance, evaporative resistance, index of moisture transfer, home fabrics*

V práci sa zaoberáme problematikou experimentálneho merania tepelného odporu a výparného odporu textilných tkanín. Súčasne s uvedenými parametrami boli merané hodnoty teplotnej vodivosti, tepelného ohmatu, prestupu vodných pár a hrúbky. Merania tepelno-izolačných vlastností sa robili na prístroji Alambeta a merania prestupu vodných pár na prístroji Permetest. Hodnotený bol sortiment bytových textílií - tkanín určených na posteľnú bielizeň. Skúšané tkaniny mali plošnú hmotnosť v rozmedzí od 85 do 170 g.m^{-2} a boli vyrobené v plátnovej a atlasovej väzbe s rôznym materiálovým zložením. Ako najvhodnejšia pre výrobu tohto sortimentu bola vybraná tkanina s vysokou hodnotou tepelného odporu R_{ct} a nízkou hodnotou výparného odpor $R_{et.}$ Porovnanie hodnôt tepelného a výparného odporu sa urobilo aj na základe výpočtu tzv. indexu prenosu vlhkosti i_{mt} ktorý predstavuje úroveň komfortu textílií. Vyššia hodnota i_m u vzorky1(balna/polyester) znamenala, že tento materiál bude z hľadiska nosenia najkomfortnejší. Cieľom príspevku bolo aj hodnotenie vplyvu hrúbky tkanín na prestup tepla a vlhkosti. Z porovnania vyplýva, že s rastom hrúbky bude u sledovaného sortimentu stúpať aj hodnota tepelného a výparného odporu. Najlepším izolátorom tepla na základe meraní tepelného odporu boli zvolené vzorky 1, 2, 3 (2,3- 100% bavlny a 1 bavlna/polyester). Na druhej strane vzorky 2,3 budú mať nižšiu schopnosť odvádzať vlhkosť od pokožky do prostredia pretože merané hodnoty výparného odporu sú najvyššie. Z pohľadu najlepšieho transportéra vlhkosti od pokožky do prostredia bude najvhodnejšia vzorka 1 (balna/polyester) a vzorka 5 (100% polyester Micro - metalic). Všeobecne možno konštatovať, že s rastúcim obsahom polyesterovej komponenty v zmesovej pletenine sa zlepšuje transport tejto vlhkosti od pokožky cez textíliu do prostredia. Naopak zvyšovanie obsahu celulózových materiálov v zmesovej pletenine zlepšuje jej tepelno-izolačné vlastnosti. Významná miera tesnosti medzi sledovanými vlastnosťami tepelného odporu a výparného odporu bola dokázaná z korelačnej závislosti (obr. 3).

Kľúčové slová: *tepelný odpor, výparný odpor, index prestupu vlhkosti, bielizňové textílie*

The interdependence of physiology and comfort clothing is closely connected with the dependence between physiological properties of textile materials, the physiological functions of the organism and climatic environmental conditions [1].

Transfer of heat and water vapor are the main physiological properties of textiles. These properties result from the requirements of the usage of clothing textiles and home fabrics and from basic physiological action of the skin [2]. They are influenced by the type of the material, its properties and the form of mutual connection bindings of threads into the surface fabrics. In this paper, the main objective is to give closer information relating to all important aspects standing for measurement of heat transfer and transfer of water vapor. Measurements were performed for the assortment of home fabric used to make linen for the beds. The values for measured characteristics were mutually compared. Based on the obtained experimental results, index of moisture transfer was calculated because the given index of moisture transfer represents the level of comfort of woven fabrics.

Material

The evaluation of the fabrics was made for different types of textile materials. The basic specifying parametres of the tested textile materials are presented in Tab. 1 [3]. Structural arrangement of threads in the fabric is shown by microscopic images in Fig. 1.

Tab. 1 Parameters and material compositions of fabrics
Tab. 1 Parametre a materiálové zloženie tkanín

n.	Material	ρ_s [g.m^{-2}]	Structure
1	50/50% cotton/polyester	170	plain
2	100% cotton	125	satin
3	100% cotton Makro satin	120	satin
4	100% Tencel	130	satin
5	100% polyester Micro Metallic	85	plain
6	100% polyester	120	plain

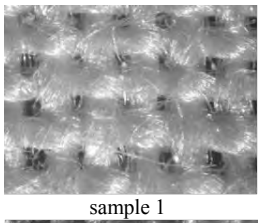
sample 1

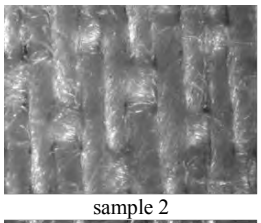
sample 2

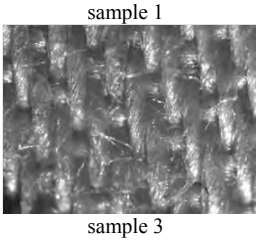
sample 3

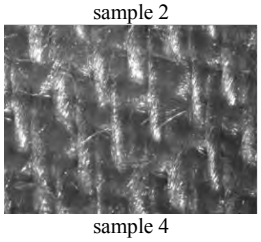
sample 4

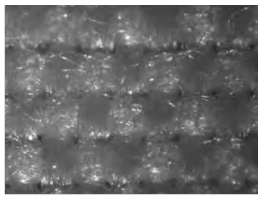
sample 5

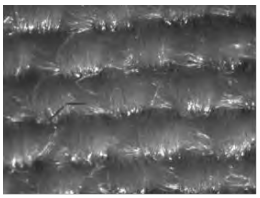
sample 6

Fig. 1 The samples of tested fabrics n. 1, 2, 3, 4, 5, 6
Obr. 1 Skúšobné tkaniny č. 1, 2, 3, 4, 5, 6

Measurement of heat and water vapor transfer

Measurement of the heat transfer

The heat transfer has been measured by help of the special testing device Alambeta (Fig. 2). The special measurement method was selected in order to simulate and objectively evaluate the thermal contact between the skin moisture and dry cloth in relation to short-time contact [4]. Measurement of thermal properties was closely connected with heat flows passing on the basis of conduction from unsteady to steady conditions. The special device was used for measurement of these characteristic parametres (Tab. 2, 3):

- thermal conductivity $\lambda.10^{-3}$ [W.m^{-1}.K^{-1}]
- heat conductivity a [m^2.s^{-1}]
- thermal resistance $R_{ct}.10^{-3}$ [W^{-1}.K.m^2]
- thickness h [mm]
- thermal feel b [W.m^{-2}.s$^{1/2}$.K^{-1}]

Tab. 2 Values of the heat transfer
Tab. 2 Hodnoty prestupu tepla

n.	$\lambda.10^{-3}$ [W.m^{-1}.K^{-1}]	a [m^2.s^{-1}]	$R_{ct}.10^{-3}$ [W^{-1}.K.m^2]	b [W.m^{-2}.s$^{1/2}$.K^{-1}]
1	66.45	0.056	23.32	280.67
2	69.3	0.066	25.40	265.67
3	77.18	0.083	24.62	272.50
4	62.04	0.050	22.73	277.40
5	54.86	0.061	20.05	225.40
6	53.68	0.059	20.86	223.00

Measurement of the water vapor transfer

The basis principle of this test was to measure the transfer of heat flow q [W.m^{-2}] over the surface of the thermal model of human skin – transmittance of fabric towards the environment. Measurement was made by help of the device Permetest (Fig. 2) [5]. The model surface was porous and moistened, thus the cooling function in sweat was simulated. The sample was placed on the surface where the outer side was blown by the conditioned air. Measured data were evaluated with microcomputer device. Using the mentioned device, these given characteristic were measured:

- permeability of water vapor p_r [%]
- water vapor resistance R_{et} [Pa.m^2.W^{-1}].

The Tab. 3 represents the obtained values relating to these mentioned characteristic properties.

Hutnické listy č.7/2013, roč. LXVI
ISSN 0018-8069

Fig. 2 Device Alambeta
Obr. 2 Prístroj Alambeta

Fig. 2 Device Permetest
Obr. 2 Prístroj Permetest

Tab. 3 Values of water vapor transfer
Tab. 3 Hodnoty prestupu vodných pár

n.	h [mm]	p_r [%]	R_{et} [Pa.m^2.W^{-1}]
1	1.55	79.125	1.375
2	1.76	72.85	1.975
3	1.9	75.625	1.75
4	1.41	76.6	1.6
5	1.1	79.475	1.35
6	1.12	77.325	1.575

Results and discussion

Transfers of heat and water vapor were investigated for the purpose of comparison and evaluation of the properties for selected textile materials. Tested fabrics had different material composition. Monitored characteristics are part of the physiological property group. They determine the state of comfort or discomfort of contacted fabrics in relation to skin of human body. Selection of tested samples contained actual range of the most used materials used for linen for bed cloth. Good insulating materials have low thermal conductivity ($\lambda \leq 1$) and high value of thermal resistance R_{ct} [6]. All tested fabrics exhibited good thermal insulation properties because $\lambda \leq 1$. The best insulation ability should be attributed to the samples n. 5, 6, because they show the lowest value of thermal conductivity. However, they exhibited also less thickness and the values presenting their thermal resistance R_{ct} are relatively low. Therefore, Fig. 3 shows the dependence of the thermal resistance R_{ct} and evaporation resistance R_{et} on fabric thickness h. Highest values of thermal resistance were measured for samples n.1, 2, 3 (1 - cotton/polyester 50/50%, 2 - 100% cotton, 3 - 100% cotton Macro satin) and it means that these fabrics isolate more heat between the skin, clothing and environment. The obtained values of heat conductivity – a (Tab. 2) were also compared. The higher values relate to fact that there is the faster compensation of temperature by textile fabric from the aspect of conductivity between the skin and environment. The results show that sample 3 has the fastest dissipation of heat to the environment and thus it compensates the temperature between the skin and environment in a best way. The values of heat feel - b were also interesting. The materials that have greater value of the heat feel – b were cooler by touch in comparison to materials which exhibited the lower values. The lowest value of heat feel - b were obtained in the case of samples 5, 6 and it implies that this material will be felt as warmer and more comfortable by touch. The next measurement values represent the resistance to the transfer of water vapor R_{et} between skin and clothing and thus, there is the creation of discomfort. The smallest resistance to penetration of water vapor was measured for samples n.1, 5 (1 - 100% cotton, 5 - 100% polyester). This implies that the materials will be good in relation to transfer of moisture from the skin to the environment. There also can be the occurrence of such situation when R_{ct} and R_{et} may not be consistent and good textile fabric retents sweat and insulates heat poorly or conversely. In such cases, it is appropriate to calculate the so-called index of moisture transfer which is a measure of comfort and we can calculate it according relation [7]:

$$i_{mt} = S \,.R_{ct} / R_{et} \qquad (1)$$

where S value stands for 60 Pa/K. If the index value of moisture transfers i_m is higher, then the textile fabric is more comfortable in terms of contact with the organism [8]. Calculated values of index i_m are shown in tab. 4.

Tab. 4 Index of moisture transfer i_{mt}
Tab. 4 Index prestupu vlhkosti i_{mt}

n.	1	2	3	4	5	6
i_{mt}	1	0.77	0.84	0.78	0.89	0.79

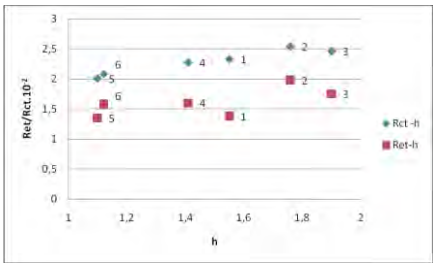

Fig. 3 Dependence of heat resistance R_{ct} and evaporation resistance R_{et} on sample thickness h
Obr. 3 Závislosť tepelného odporu R_{ct} a výparného odporu R_e od hrúbky h

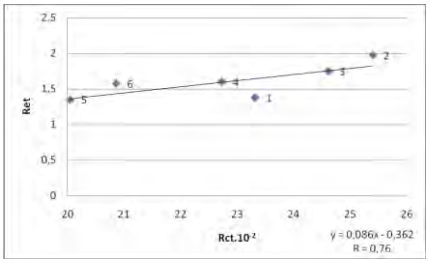

Fig. 4 The correlation dependence of the thermal resistance $R_{ct}.10^{-2}$ to evaporative resistance R_{et} for the woven fabrics
Obr. 4 Korelačná závislosť medzi tepelným a výparným odporom tkanín

Based on results, it can be assessed that the sample 1 (cotton/polyester 50/50%) is the most comfortable. The comparison of the performance characteristics to the thickness was also done (Fig. 3). The values R_{ct} and R_{et} have slightly increasing tendency together with thickness. The correlation dependence was performed for comparison of the measured values of R_{ct} and R_{et}. The solution can be seen in the regression line (Fig. 4). It shows the direct linear correlation relationship between thermal resistance R_{ct} and evaporative resistance R_{et}.

Conclusions

Specific properties including thermal resistance, thermal conductivity and evaporative resistance were investigated. We came to this conclusion by comparing the following characteristics:

1. The results of measurements show that the differences in the values of R_{ct} and λ depend on the thickness and area weight of fabrics. The lowest value of thermal resistance was obtained for sample of woven fabric n. 5.
2. The lowest resistance of water vapor transfer can be noticed for the fabrics represented by sample 5 and 1 (1 - cotton/ polyester and 5 - 100% polyester Metallic).
3. Sample 2, 3 (100% cotton sateen) exhibit the best values from the aspect of the heat insulation. These two samples exhibit the highest resistance in comparison to the transfer of heat towards the environment.
4. In relation to "feel by touch", the best values were observed for the samples 5, 6 because they are made of soft polyester fibers and microfibers.
5. The highest value of moisture transfer index was calculated and specified in the case of sample 1. This fabric is physiologically most comfortable in terms of contact with the organism.
6. The sample 5, made of polyester microfibers, had the best moisture transfer of the in relation to the skin, fabric and ambient environment (in comparison to other materials). In this case, the lowest values were obtained for evaporative resistance R_{et}.
7. In general, we can conclude that with the increasing content of the polyester fabric, the moisture transfer into the environment improves. Increasing content of cellulosic materials in the fabric improves the ability to insulate heat.

Acknowledgement
This work was supported by project of Slovak Grant Agency KEGA: 002 TnUAD 4/2011.

Literature

[1] JAMBRICH, M. et al Fibrois materials based on polypropylene, bamboo and cotton fibres. *Vlákna a textil* 15, 2008, p. 3-12

[2] MURÁROVÁ, A. Fyziológia odievania I. Tepelná regulácia človeka. *Vlákna a textil* 8 (1), 2001, p. 48-49

[3] STN ISO 800845: *Stanovenie hmotnosti na jednotku dĺžky a hmotnosti na jednotku plochy*. SÚTN Bratislava, 1999

[4] VRBOVÁ, V. I.IN 23-304-02 01: *Měření tepelných vlastností na prístroji Alambeta*, TU Liberec, 2002

[5] HES, L. Interná norma č. 23-304-01/01: *Stanovenie termo-fyziologických vlastností vlákien*. TU Liberec, 2002

[6] HAVENITH, G. *Physiological parameters in heat tolerance.* Nederlands Militair Geneeskundig Tihdschrift 40, p. 231-233, STU, Bratislava, 1987

[7] ISO 11092:1993(E*) Textiles-Physiological effects-Measurement of thermal and water - vapour resisitance under steady-state conditions (sweating guarded - hotplate test),* International Organization for Standardization Case Postale 56-CH-1211 Geneve 20-Switzerland

[8] MURÁROVÁ, A., MURÁROVÁ, Z. *Fyziológia a komfort pri odievaní,* elektronická verzia prednášok, Bratislava 2011. s. 42-43. ISBN 978-80-970966-3-2

Výstavba nové širokopásové trati v Číně

Baosteel to build new hot strip mill. Metallurgical Plant and Technology, 2013, č. 4, s. 16

Čínská společnost Baosteel Zhangjiang Iron Steel objednala u firmy SMS Siemag novou širokopásovou trať 2250 mm. Trať bude umístěna v nově budovaném závodě v Zhangjiang v jižní Číně. Je projektována na roční výkon 5,5 mil. t pásu válcovaného za tepla o tloušťce 1,2 až 25,4 mm a šířce 800 až 2100 mm. V sortimentu budou hlubokotažné oceli i vysoce pevné oceli na trubky.

Na vstupní straně válcovací tratě bude postaven lis pro kalibrování šířky. Dvě vratné stolice duo a jedna vratná stolice kvarto budou sloužit pro předválcování. Hotovní spojité pořadí bude mít sedm stolic CVC. Za nimi bude následovat laminární chlazení a dvě hydraulické navíječky. Trať by měla jít do provozu koncem roku 2015.

L J

Evaluation of Total Hand Value of Fabrics

Hodnotenie úplného ohmatu textílií

Ing. Jela Legerská, PhD.[1], **Ing. Matej Drobný**[1]

[1] University of Alexander Dubček in Trenčín, Faculty of Industrial Technologies, I. Krasku 491/30, 020 01 Púchov, Slovak Republic

This paper deals with the objective evaluation of hand values using the KES system - Kawabata evaluation system for fabrics. There is the description of the impact of specific mechanical properties by help of measuring device KES which was utilized for analysis and evaluation of the hand value. The measured mechanical properties are transferred from the mathematic formulation of primary hand HV and total hand value THV. The experiment is taken from men's category suiting fabrics. Assortment of textile laminated membrane was evaluated. The sublimation printing was applied on this material locally at different temperatures. Change of the sublimation properties was also monitored. The measurement results show that sublimation printing reduced the value THV. The value t = 180 ºC was chosen as the most suitable sublimation temperature preserving the selected characteristics.

Keywords: *laminated membrane textile, sublimation printing, hand value, total hand value*

Príspevok sa zaoberá problematikou senzorického komfortu textílií. Tento je možné z určitého hľadiska rozdeliť na zložku komfortu nosenia a ohmatu. Zložka komfort ohmatu sa hodnotí objektívnou a subjektívnou metódou. Cieľom príspevku bolo hodnotenie objektívneho ohmatu. Meranie sa vykonávalo so systémom KES (Kawabata evolution system). Skupina štyroch prístrojov systému KES testovala šesť základných mechanických vlastností textílií súvisiacich s objektívnym hodnotením ohmatu ktorými sú: ťah, šmyk, ohyb, tlak, koeficient trenia a geometrická drsnosť. Experimentálne meraný objektívny ohmat bol potom porovnávaný so subjektívnym ohmatom. Výsledkom bolo stanovenie úplného ohmatu - total hand value THV vychádzajúceho s regresnej závislosti medzi dvoma zložkami ohmatu. Ako základ pre stanovenie závislosti bola z hodnôt zvolená kategória, ktorá vyhovuje mužským odevom. Experimentálne merania sa robili na vybraných druhoch laminovaných membránových textílií. Tieto vrstvené textílie boli z lícnej strany vo forme záťažných pletenín na ktoré boli nanesené neporézne membrány doplnené z rubnej strany spevňujúcou záťažnou alebo osnovnou pleteninou. Na lícnu stranu týchto laminovaných membránových textílií bol urobený experiment počas ktorého boli tieto potlačené sublimačnou potlačou aplikovanou pri teplotách 180, 200 a 220 ºC. Výsledkom výskumu bola voľba optimálnej teploty tlače a sledovanie vplyvu nastavenej hodnoty tlaku a teploty na ohmat materiálov. Z výsledkov meraní vyplýva, že s rastúcou teplotou sublimačnej potlače sa znižuje ohmat u všetkých sledovaných textílií. Najvýraznejší je tento pokles pri najvyššej teplote sublimácie. Preto najvhodnejšia teplota pre sublimačnú potlač pri zachovaní vlastností ohmatu bola zvolená t = 180 ºC. Laminovaná membránová textília WW Karo bola vybraná ako textília s najlepším celkovým ohmatom THV.

Kľúčové slová: *laminovaná membránová textília, sublimačná potlač, ohmat, úplný ohmat*

The purpose of this paper is focused on a system of objective evaluation methods for the characterization of sensory comfort of clothing while the method and device of KES is used and by this way, we can predict the performance of clothing sensory comfort properties of fabrics on the basis of converting natural range of physical, physiological and psychological sensory studies [1]. Sensory comfort represents feelings of the organism skin in contact with the first layer of clothing. From a certain point of view, the sensory comfort can be divided into wearing comfort and hand comfort. Comfort wearing includes surface texture of fabrics, selected mechanical and transport properties. Comfort of hand textiles is defined as a set of characteristics affecting the organoleptic sensation by skin in contact with the fabric [2].It is strongly subjective characteristic based on perceptions through the fingers and palms. Hand value of wearing clothing can be evaluated by subjective and objective methods. Subjective determination of hand value gives expression about feelings that are caused by fabric in contact with the human skin. Subjective hand value can be evaluated by direct or indirect methods. Direct evaluation is done by a group of assessors. The indirect assessment is made by mutual comparison of the fabrics (reference fabric and tested fabric) with the most satisfying hand value. Those methods are mainly influenced by the choice of assessors and therefore they are compared with an objective evaluated hand value. Objective evaluation of the hand value is response and total hand value stimulus in relation to a group of mechanical, thermal and surface properties [2]. The KES-F system (Kawabata's hand evaluation system for fabrics) was developed in Japan by the Hand Evaluation and Standardization Committee

(HESC, established in1972) organized by professor Kawabata [3]. On this basis, the properties of primary hand value - HV has been chosen and descriptive form has been processed as it is shown in tab. 1. Primary hand value - HV was evaluated here and it was in the scale from 0 to 10. The value of 10 means the high influence on characteristic of the fabric and 1 stands for low influence on characteristic of the fabric [3]. The types of clothing were evaluated on the basis of primary hand value and total hand value in relation to these selected terms (tab. 1):

- winter men's clothing fabrics: KOSHI, NUMERI ,FUKURO
- summer men's clothing fabrics: KOSHI, SHARI, HARI ,FUKURAMI
- men's dress: SHINAYKASA, KISHIMI, SOFUTOSA

Finally, in relation to the complex evaluation of the hand value, the determined subjective results were compared to data obtained in an objective way. The result was connected with determination of total hand value THV evaluated in grades from 1 to 5 (tab. 2) where the highest value means the best hand value [4].

Tab. 1 Primary hand value HV [3]
Tab. 1 Primárny ohmat HV [3]

Japanese marking	Characteristic
KO/koshi	stiffness
N/numeri	smoothness
F/fukurami	fullness, softness
S/shari	crispness,
H/hari	anti-drape stiffness
SO/sofutosa	soft feeling
KI/kishimi	scrooping feeling
SHI/shinayakasa	flexibility

Tab. 2 Total Hand Values THV [3]
Tab. 2 Úplný ohmat THV [3]

THV	Evaluation of hand value
0	inconvenient
1	very bad
2	second-rare
3	good
4	very good
5	excellent

Evaluation materials

The tested fabrics were designed for sports garments. These are nowadays decorated by colour printing and it is mainly because of aesthetic reasons as well as promotions. The mentioned printing may change the whole range of properties and in our case, it is especially connected with respect of skin - sensory comfort. The manufacturers, therefore, develop new approaches to harmonize production technology of printing materials in terms of comfort sustainability. The transfer printing is the most common way of the local textile-sublimation. The given sublimation is carried out on the principle of colour transfer from the transfer paper on fabric under the action of pressure, heat and time [5]. The sublimation printing was applied on the tested materials (tab. 3). The tested materials designated as Mission light, Kalas, T-Rex, WW-Karo were manufactured as laminates with non-porous membrane. Non-porous membrane was strongly connected with the face side of jersey knitted fabric and reverse side of knitted lined fabric. Membrane is impermeable to water from outside, but allows the transfer of water vapour from the skin to the environment. Membranes were made of polyester and polyurethane [6]. Technical parameters of following materials are given tab. 3. The given experiment was performed at three different temperatures: 180 °C, 200 °C, 220 °C. The selected samples were exposed to the compression stress with the presence of the sublimation colour and three of samples were stressed without the presence of the sublimation colour.

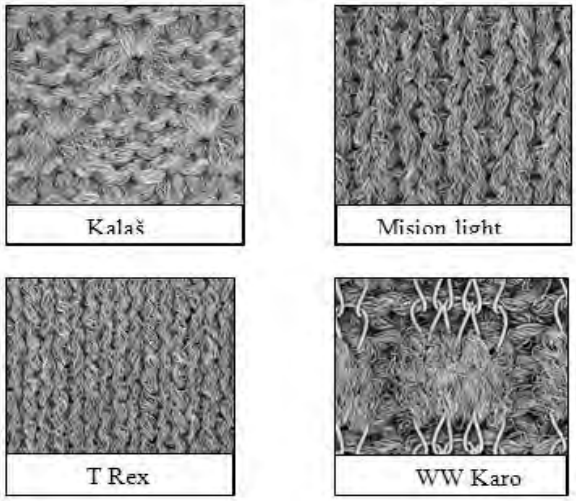

Fig. 1 Face side of laminated membrane textiles
Obr. 1 Lícna strana laminovaných membránových textílií

Tab. 3 Technical parameters of laminated membrane textiles
Tab. 3 Technické parametre laminovaných membranových textílií

Sample	Material composition	ρ_s [g.m^{-2}]
Mission light	100% PL	160
Kalashell	100% PL	160
T-Rex	88% PL, 6% EA, 6% PU	245
W-W Karo	96% PL, 4% PU	275

Research of the monitored textiles is focused on the following goals:

- to select optimum temperature of printing while the given temperature must be suitable for preserving the characteristics from the aspect of hand value;
- to compare the performance of the material in relation to the hand values and choose the most suitable material;
- to compare THV before and after application of sublimation printing.

Methods

In relation to these textiles, objective measurement method and its scientific principles are applied for the instrumental measurement and interpretation of

Hutnické listy č.7/2013, roč. LXVI
ISSN 0018-8069

mechanical stress and surface properties of textile including textile properties, such as shear, bending, compression, surface friction and roughness. The textiles hand value is calculated from measurements of these properties. Empirical equations for calculating of Primary Hand Values and Total Hand Values were put forward by Kawabata and Niwa [3].The characteristic values are calculated from recorded data obtained by each tester. Tensile properties (force-strain curve) and shear properties (force-angle curve) are measured by the same measuring device (FB 1). Bending properties (torque-angle curve) are measured by bending of reverse sides against face sides (FB 2) under the specified angle. Pressure-thickness curves are obtained by compression tester (FB 3).The measurements of surface friction (friction coefficient variation curve) and surface roughness (thickness variation curve) are tested by help of the same apparatus (FB 4) using different detectors. All measured values (except of compression) are performed in the longitudinal (warp) and cross (weft) direction (Fig. 2-5). The measured mechanical properties are plotted in the so-called Snake diagram (Fig. 2-5) which represents the total range of mechanical properties in the horizontal scale [7]. The course of measurement and processing of the results was managed by means of PC software. The samples with the proportions 20 × 20 cm were prepared for all four devices and these samples were without creases and folds as well as they were cut in the longitudinal and transverse directions.

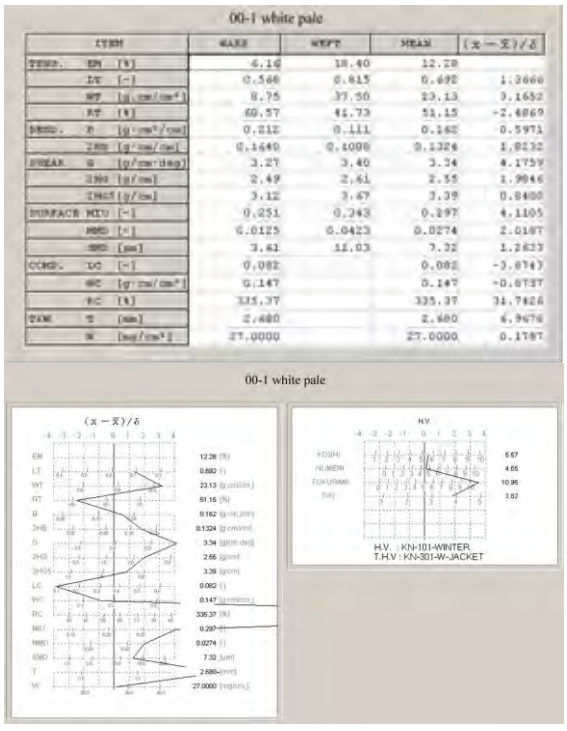

Fig. 2 The values and snake diagram before sublimation (white colour) - sample WW Karo
Obr. 2 Hodnoty hadových grafov pred sublimáciou (biela farba) - vzorka WW Karo

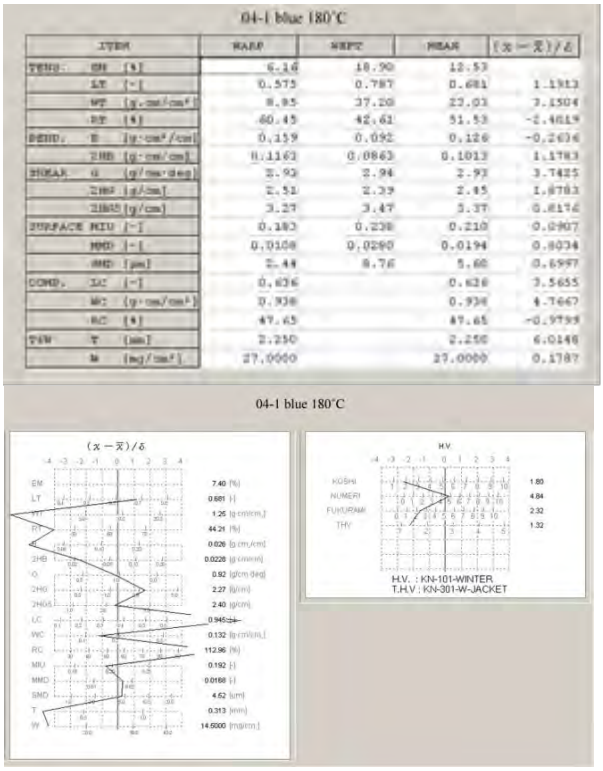

Fig. 3 The values and snake diagram with the use of sublimation temperature 180 °C (blue colour) - sample WW Karo
Obr. 3 Hodnoty hadových grafov pri sublimačnej teplote 180 °C (modrá farba) - vzorka WW Karo

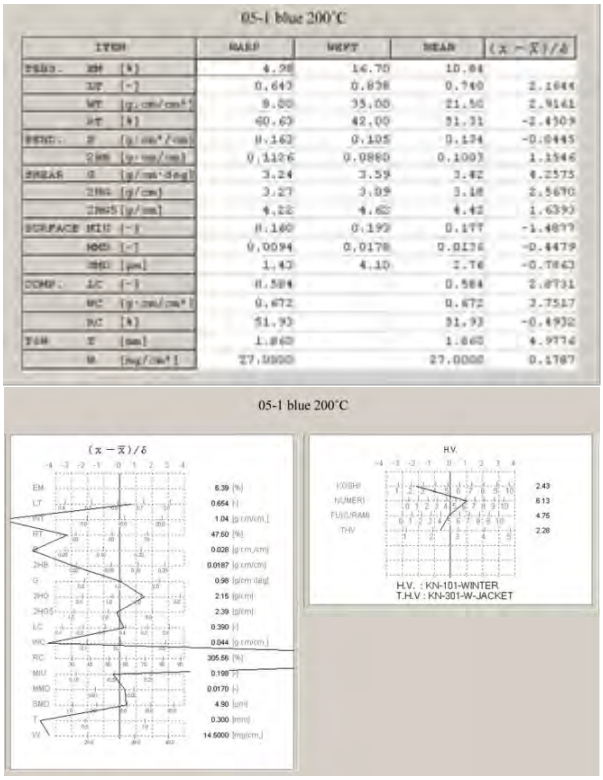

Fig. 4 The values and snake diagram with the use of sublimation temperature 200 °C (blue colour) - sample WW Karo
Obr. 4 Hodnoty hadových grafov pri sublimačnej teplote 200 °C (modrá farba) - vzorka WW Karo

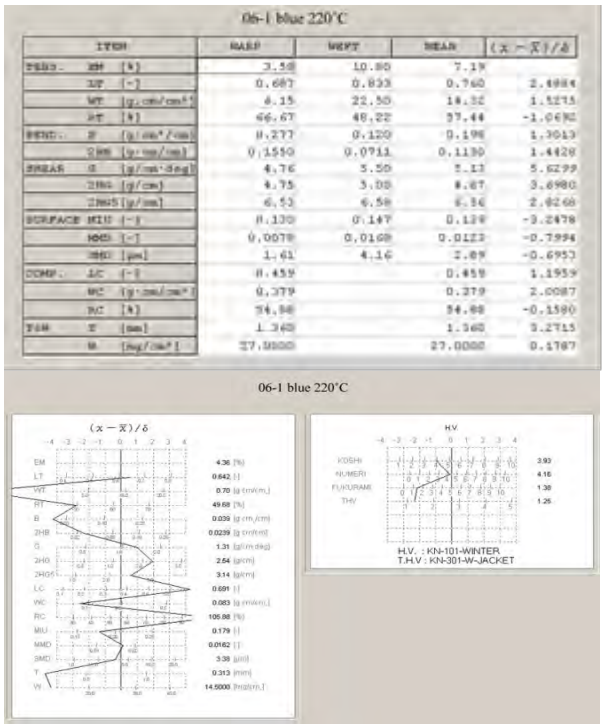

Fig. 5 The values and snake diagram with the use of sublimation temperature 220 °C (blue colour) - sample WW Karo
Obr. 5 Hodnoty hadových grafov pri sublimačnej teplote 220 °C (modrá farba) - vzorka WW Karo

Results and discussion

The total hand value - THV was variable for all materials. It is in the range from the degree 1 - very bad up to the degree 4 - very good .All tested fabrics had the best THV before the sublimation (fig. 6). THV value was decreased due to sublimation printing. The total hand value was worsened with increasing temperature of printing. From the aspect of the used tested temperatures, the best hand value was observed at temperature 180 °C. The highest values of THV (fig. 6) were achieved in relation to the laminated membrane material WW Karo. Suitable sublimation temperature (from the investigated range) should have the value which is characteristic for value before the sublimation procedure or higher value is also acceptable. From this mentioned aspect, the most suitable temperature for sublimation of laminated material was t = 180 ºC.

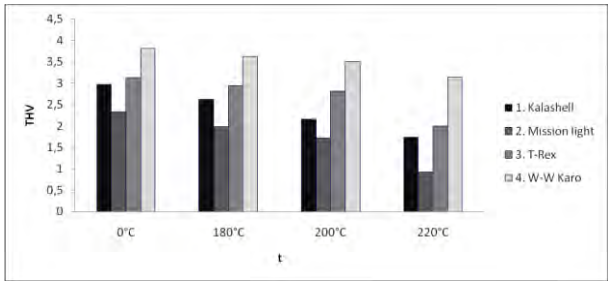

Fig. 6 THV values measured at different sublimation temperatures Note: Values THV 0 ºC is the before sublimation
Obr. 6 Hodnoty THV namerané pri rôznych teplotách sublimácie Poznámka: 0ºC predstavuje hodnoty THV pred sublimáciou

Conclusions

In this paper has been evaluated total hand value properties THV by objective method using Kes FB 1, 2, 3, 4. The assortment of four laminated fabrics with the hydrophobic membrane in the middle was evaluated. The surface of all tested fabrics was modified by sublimation printing. Using the assortment of sports clothing, the common fabrics were evaluated. These conclusions were obtained from measurement results:

1. THV is decreased with increasing temperature of sublimation.
2. Laminated membrane fabric WW Karo were the best and the most suitable in relation to THV.
3. To preserve the required properties, the best temperature for sublimation printing of the laminated membrane textile was t = 180 ºC.
4. During sublimation, pressure reduced the thickness of fabric and it had the impact on other properties.
5. Measured characteristics of textiles with sublimation printing were markedly different in comparison to the textiles without printing.

To predict overall clothing comfort on the basis of these new apparatuses, statistical and neural network models have been developed and the results show that the mean values of sensory comfort factors and the overall comfort are predictable from the physical factors obtained from the measurements with all the instruments developed. In summary, new evaluation methods and instruments with predictive models have been developed to characterize the sensory comfort of clothing and it can be utilized to design and develop textiles and apparel products with superior functional and comfort performances.

Literature

[1] HU, J. *Characterization of sensory comfort of apparel products,* Hong Kong Polytechnic University 2006, p. 6-8 http://repository.lib.poly.edu.hk/jspui/handle/10397/2616

[2] HES, L. SLUKA, P. *Úvod do komfortu*, TU Liberec, Fakulta textilná, 2005, s. 5-8

[3] KAWABATA, S. *The standardization and analysis of hand evaluation* (2nd Edition). The hand evaluation and standardization committee, The Textile Machinery Society of Japan, Osaka, 1980

[4] BOOS, A. „*Concepts and understanding of fabrics hand*“, Australian Wool Inovation Limitec, Australia, Wood head Publishing Limited, 2005

[5] http://kapatex.cz/sluzby/sublimacni-tisk/blog

[6] http://www.czemp.cz/cs/membranoveprocesy/membranove materiály

[7] SHISHOO, R. *Objective measurement of fabric handle: Dream or reality?* In Proceedings of Avantex, International Symposium for High-Tech Apparel Textiles and Fashion Engineering with InnovationForum, p.15, Frankfurt, Germany, 2000

Measurement of Thermal Properties of Car Seat Covers Using Pulse Transient Method

Meranie tepelných vlastností autopoťahov pulznou prechodovou metódou

Ing. Jela Legerská, PhD.[1], **doc. Mgr. Ivan Kopal, PhD.**[1]

[1]University of Alexander Dubček in Trenčín, Faculty of Industrial Technologies, I. Krasku 491/30, 020 01 Púchov, Slovak Republic

This paper is closely connected with study of the thermal parameters for car seat covers. The main aim of the study was to use the pulse transient method for measurement of the thermal parameters in the order to do thermal analysis. Nowadays, the given method is used for the laboratory evaluation of metal and plastic materials. The application of the mentioned method was also tested for textile materials. The measurement results of thermal parameters obtained by the pulse transient method were compared to measurement results of the same parameters while Permetest was used as the measuring device. According to the obtained measurement results, it can be concluded that the pulse transient method is not very suitable for the studied assortment. The basic analysis of the structure for each layer of material was mentioned in work. The given analysis was shown in the images obtained by help the image analysis Nis element. The effect of the structural properties of the surface fabrics on the thermal properties was evaluated.

Keywords: *car set cover, thermal resistance, thermal conductivity, pulse transient method*

Tento článok je určený štúdiu tepelných parametrov autopoťahov. Hlavným cieľom štúdie bolo overenie novej pulznej prechodovej metódy pre meranie tepelných parametrov. V súčasnej dobe je prezentovaná metóda používaná v laboratóriách kovových a plastických materiálov. Táto metóda slúži na meranie tepelných ukazovateľov ako sú: tepelná vodivosť, teplotná vodivosť a tepelná kapacity. Experimentálnymi meraniami bola vyskúšaná možnosť použitia tejto metódy aj pre hodnotenie textilných materiálov. Správnosť výsledkov získaných pulznou prechodovou metódou bola porovnaná s meraniami tepelných parametrov na prístroji Permetest. Permetest je jeden z meracích prístrojov, ktorý sa v súčasnosti používa na merania tepelno-izolačných vlastností v textilných laboratóriách. Z výsledkov experimentálnych meraní vyplynuli nasledujúce závery: s rastúcou hrúbkou textílie stúpala tepelná vodivosť získaná pulznou prechodovou metódou, rovnako stúpal s rastúcou hrúbkou aj tepelný odpor meraný na prístroji Permetest. V závislosti na dosiahnutých rozdielnych výsledkoch meraní, možno dospieť k záveru, že pulzná prechodová metóda nie je vhodná pre skúmaný sortimentu textílií. Súčasná metóda využívajúca prístroj Permetest je vhodnejšia pre meranie tepelného odporu textílií. Simuluje pomerne presne prenos tepla vedením od pokožky cez sedačku do ďalšieho prostredia. Tieto reálne podmienky na overovanej pulznej prechodovej metóde nie je možné zabezpečiť a preto považujeme túto metódu za nevhodnú pre meranie tepelno-izolačných vlastností v textilnom laboratóriu. Vplyv vyššieho tlaku na skúšobné vzorky počas merania nesimuloval ani jeden z použitých prístrojov. Tým sa skúšané metódy nepriblížili reálnym podmienkam praktického používania autopoťahov. Štrukturálne parametre lícnej strany tkaniny (väzba, dostava väzby, zotkanie) nemali vplyv na výsledky meraní tepelného odporu a tepelnej vodivosti. Rast hrúbky skúšaných textílií, bude mať vplyv nie len na tepelno-izolačné vlastnosti, ale aj na stabilitu tvaru, odevné spracovanie a konečnú cenu autopoťahov.

Kľúčové slová: *autopoťahy, tepelný odpor, tepelná vodivosť, pulzná prechodová metóda*

The development of materials for car seat covers is also related to the development and usage of new or better materials in automobile industry. These given textile materials are commonly used for the car seat covers and the car interior facing. The given paper is connected with car seat cover materials. These materials are produced as laminated textile fabrics. Automobile plants pay high attention to the comfort because of continuous increasing requirements for satisfaction of the consumer. From the aspect of the design and expectation of negative influences on the driver's performance during the different seasons. In this paper, functionality, the new material combinations have been looked for. Nowadays, the functionality is increased by the comfort. This fact can be understood as the condition of organism, where the physiological functions of the organism are in the optimum. These conditions also include influences of the surrounding environment while they should not cause undesirable feelings. These feelings can be understood as the subjective comfort [1]. There is not any occurrence of feelings of heat or cold therefore there is not any thermal-insulation parameters were especially measured. The new unconventional method was used

for measurement and it was compared to the current methods used in of the accredited laboratories. The influence of the structure of textile layers on heat transfer was also evaluated.

Experimental procedure

Material

The special assortment of laminated textile fabric for car seat covers has been tested in this paper. The investigated materials are composed of three layers. The first layer is a woven fabric made of polyester fibers (fig. 1a).The middle layer was made of the polyurethane foam which represented the cellular materials with cavities of various shapes and sizes (fig. 1b). The blowing agents will be used as the special additive agents preserving the increase of the volume. These blowing agents release gases or vapours and by the influence of this process, cellular structure of products occurs [2]. Cellular materials have the special structure where cells are interconnected or closed and it has also influence on properties. The jersey knitted fabric made of polyester filaments was used as the reverse side (fig. 1c). The layers were connected into the whole by means of flame (fig. 1d). Basic parameters of the woven fabrics are introduced in Table 1.

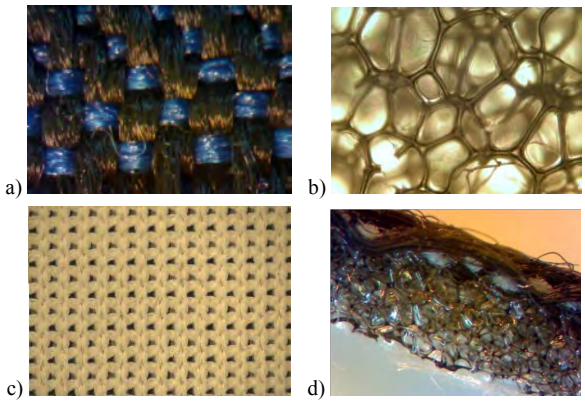

Fig. 1 Microscopic images of laminated textile material
Obr. 1 Mikroskopické snímky laminovaných textílií

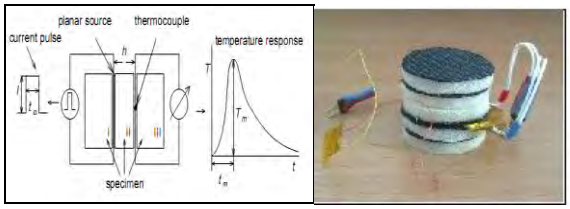

Fig. 2 The principle scheme of the pulse transient method [6] and placement of the tested sample
Obr. 2 Schéma pulznej prechodovej metódy a uloženie skúšobnej vzorky

Tab. 1 Basic data on laminated textile material
Tab. 1 Základné údaje laminovaných textílií

n.	Weave	ρ_s[g.m^{-2}]	ρ_v[g.cm^{-3}]	h[mm]
1	Twill	395	0.2018	1.9
2	Plain	502	0.1115	4.5
3	Fancy satin	441	0.1837	2.4
4	Fancy satin	433	0.2061	2.1
5	Satin	351	0.1671	2.1
6	Plain	507	0.1152	4.4
7	Satin	577	0.0901	6.4
8	Kitted fabric	353	0.1357	2.6
9	Satin	429	0.0932	4.6
10	Twill reinforced	287	0.1304	2.2
11	Struck	395	0.0877	4.5
12	Satin	276	0.138	2
13	Twill	618	0.0824	7.5
14	Twill	489	0.1137	4.3

Pulse transient method

This method can be included into the dynamic methods. Using the given method, these following parameters can be measured and determined from textiles: thermal conductivity λ [W.K^{-1}m^{-1}], thermal diffusivity α [m^2.s^{-1}] and the specific heat capacity c_p [J kg^{-1} K^{-1}]. The tested specimen is composed of three parts I-II-III, see fig. 2. This method is used for measurement of the heat excitation pulse, which generates electric current passing non-point sources of heat 1 [3]. Thermocouple placed between the specimen II and III is used for measurement of the temperature response of the specimen. Three basic thermo physical parameters are calculated from the observed curve standing for temperature response according to the relations [4]. This model is characterized by this temperature function:

$$T(h,t) = \frac{Q}{c_p \rho \sqrt{\pi \alpha t}} \exp\left(\frac{h^2}{4\alpha t}\right) \qquad (1)$$

where $Q=RI^2t_o$ is the amount of heat generated by the heat pulse through the unit area, R is the electrical resistance of the heat source, I is the current supplied at time t_o, ρ is the density and c_p and α are unknown thermo physical parameters (specific heat and thermal diffusivity) [5]. The temperature function is the solution of heat equation with respect to the appropriate boundary and initial conditions.To determine the thermo physical properties, maximum temperature response is used as input. For the calculation of thermo physical parameters, these equations were used: - specific heat c_p and thermal diffusivity α

$$c_p = Q / T_m.h.\rho\sqrt{2\pi.e} \qquad (2)$$

$$\alpha = h^2 / 2t_m \qquad (3)$$

Hutnické listy č. 7/2013, roč. LXVI
ISSN 0018-8069

where T_m is the maximum temperature response at the time t_m and e is Euler's number. The thermal conductivity λ is defined by a well-known formula:

$$\lambda = \alpha.c_p.\rho \quad (4)$$

Specimen with the diameter 30 mm, and with the thickness which is less than 3 mm was heated for time of 1 s while the voltage was 1.4 V and the supplied current was 1A. When the thickness of the specimen was 3 mm, the time of heating process increased to 1.5 seconds.The two variants of heating temperature were chosen: 20 ºC and 32 ºC. The temperature response of the specimen was measured during the 600 s. Stable or steady temperature of specimen was held for 100 minutes [6,7].

Resistance method

The device Permetest represents so called skin model which is covered by the tested specimen during the investigation. The device is utilized for measurement of thermal and evaporation flow which is transferred by convection into the surrounding environment. The computer which is the part of device allows making settings of the tested parameters. The device evaluates the values of the evaporation resistance R_{et} [$m^2.Pa.W^{-1}$], thermal resistance R_{ct} [$m^2.K.W^{-1}$] and the relative permeability of water vapor q [%]. In this case thermal resistance was measured. The given thermal resistance gives information on the density of the heat flow passing trough the specified area as the response to the same temperature degree. The formula for the calculation is [8]:

$$R_{ct} = K.(t_m - t_a).\left(\frac{1}{q_s} - \frac{1}{q_o}\right) \quad (5)$$

where K is the measurement constant, t_m temperature of measuring device head, t_a is the air temperature in the device channel, q_o [$W.m^{-2}$] is the area density of the heat flow passing through the measuring head which is not covered, q_s is the area density of the heat flow passing through the measuring head which is covered. The device constant is determined by the formula:

$$K = \frac{R_{ct}RT}{(t_m - t_k).\left(\frac{1}{q_{RT}} - \frac{1}{q_o}\right)} \quad (6)$$

where R_{ct} RT is value of R_{ct} standards, q_{RT} is the area heat flow density passing through the measuring head which is covered by reference fabric - the reference standard, t_k temperature of reference fabric - the reference standard [8]. Five specimens with dimensions of 120x120 mm were measured under the following conditions: head temperature 32-34 °C; the environmental temperature 22-24 °C; air velocity in the measuring channels v_v = 0.3 $m.s^{-1}$; measurement time 2 min; the relative humidity in the laboratory 50-55 %.

Results of measurements

Thermal parameters were measured for 14 laminated textiles. The results of the thermal conductivity λ [$WK^{-1}m^{-1}$] and the results of thermal resistance R_{ct} [$W^{-1}Km^2$] were used for mutual comparison while the thermal conductivity λ [$WK^{-1}m^{-1}$] was measured by pulse transient method and thermal resistance R_{ct} [$W^{-1}Km^2$] was measured by the device Permetest. The values of thermal conductivity and thermal resistance obtained at two temperatures including 20 ºC and 32 ºC are presented in Table 2. For thermal parameters, the small increase was observed with the increasing temperature. For textile specialists, the term of heat resistance is more suitable than the term of thermal conductivity because it is more used in textile field. Therefore, the values of thermal conductivity were calculated to obtain the values of the thermal resistance and moreover, the values of the thermal resistance were calculated to obtain thermal conductivity (see the grey colour in Table 2). It was done according to the known relationship:

$$R_{ct}=h/\lambda \quad (7)$$

Tab.2 Experimental and calculated (bols font) values
Tab.2 Experimentálne a vypočítané hodnoty

n.	$\lambda_{20°C}$/ $R_{ct\ 20°C}$	$\lambda_{32°C}$/ $R_{ct\ 32°C}$	λ/ $R_{(permetest)}$
1	0.034 / 0.0559	0.0349 / 0.0544	0.0124 / 0.1532
2	0.0467 / 0.0964	0.0487 / 0.0924	0.096 / 0.469
3	0.0405 / 0.0593	0.0416 / 0.0577	0.0100 / 0.241
4	0.0349 / 0.0602	0.0357 / 0.0589	0.0119 / 0.1769
5	0.0323 / 0.065	0.0342 / 0.0614	0.0115 / 0.1829
6	0.0455 / 0.0967	0.0464 / 0.0948	0.0082 / 0.5402
7	0.0971 /0.0659	0.1031 / 0.0621	0.0094 / 0.6778
8	0.0667 / 0.039	0.0705 / 0.0369	0.0120 / 0.2231
9	0.0501 / 0.0918	0.052 / 0.0885	0.0095 / 0.4854
10	0.032 / 0.0688	0.0331 / 0.0665	0.0107 / 0.2062
11	0.0707 / 0.0636	0.0735 / 0.0612	0.0082 / 0.5516
12	0.0285 / 0.0702	0.0293 / 0.0683	0.0096 / 0.2089
13	0.1309 / 0.0573	0.1393 / 0.0538	0.0086 / 0.8757
14	0.0068 / 0.063	0.0717 / 0.058	0.00126 / 0.3421

Results and discussion

The purpose of this work was to verify the possibility relating to usage of this new method by help of which the heat transfer for many thick laminated textiles was measured. For measured values, the great variability is characteristic, therefore they cannot be compared (Table 2). All the values have relative deviation which is lower than 2 %. According to the literature knowledge, the results obtained by the device Permetest are the real values which are more suitable. Obtained data by the new method (pulse transient method) are too low and it corresponds to values for thin textile fabrics but it does not correspond to three-layered thick textiles [9]. The reason of low values of thermal resistance can be hidden in increased air content in the measured area.

The different conditions of measurement can be also reason of unreal results. Pulse transient method does not give correct evidence about conductive heat transfer between the skin and the textile fabric and environment. For a more objective evaluation of the two methods, correlations of dependence were made for obtained values of thermal resistance, thermal conductivity and thickness of laminated textiles (fig. 4, 5). The resolution of this regression is connected with this conclusion:

- thermal conductivity increases with the material thickness in relation to pulse transient method (see fig. 4).
- thermal resistance increases with the thickness of the measured material in relation to the measurements done by device Permetest (fig. 5).

According to these controversial results, the pulse transient method is not suitable for measurement of textile materials. The weave of face side of the textile fabric and its different thickness does not affect the change in thermal resistance. The design and fashionableness of pattern and color play the most important role for the selection of the textile fabrics.

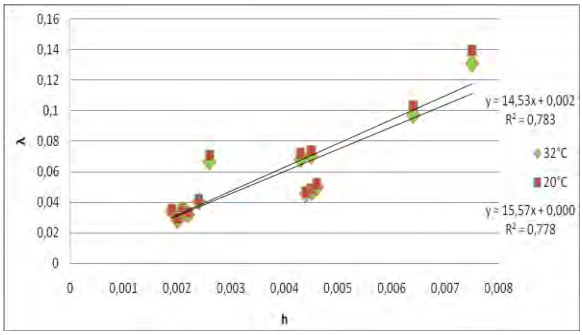

Fig. 4 Correlation between thermal conductivity λ and thickness h - pulse transients method

Obr. 4 Korelačná závislosť medzi tepelnou vodivosťou λ a hrúbkou h meraná pulznou prechodovou metódou

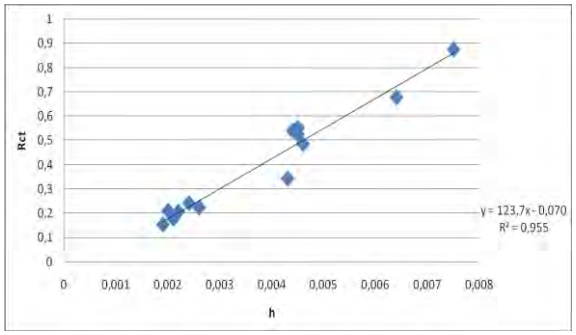

Fig. 5 Correlation between thermal resistance R_{ct} and thickness h - device Permetest

Obr. 5 Korelačná závislosť medzi tepelným odporom R_{ct} a hrúbkou h meraná na prístroji Permetest

Conclusions

In this paper, the study of thermo-physical parameters of car seat covers is presented. Presented figures demonstrate that thermal resistance has increasing character in dependency on increasing thickness (fig. 5). This increasing character is the most important in relation to sample 13 and 7 which have the maximum thickness. The thickness of the middle layer has the significant influence on the results of thermal resistance. The increasing thickness of laminated fabric will have influence on the shape stability, the garment processing and final price. Using two measurement methods, the results relating to thermal resistance confirmed the variability of measurements. The results obtained by pulse transient method were not suitable for measurement of some specific properties relating to textile materials.The method utilizing the device Permetest has been still the most effective method for measurement of the thermal resistance. This method is suitable for simulation of the heat transfer by conduction from the skin through the car seat and further environment. The device Permetest is designed for measurement of the common sorts of textiles. During the measurements of thermal indicators for the car seat covers, it is necessary to take in account the higher pressure acting on the laminated fabric. The thickness of the measured specimen is significantly pressured. From the aspect of the both measurement method, the mentioned pressure can not be simulated by any of the mentioned devices. Structural parameters of the face side of the woven fabrics did not have any influence on the measurement results of the thermal resistance.

Literature

[1] HESS, L., SLUKA, P. *Introductio tu komfortable fabric*, TU Liberec 2005

[2] SKOČOVSKÝ, P., PALČEK, P., KONEČNÁ, R., VÁRKOLY, L. *Construction materials*, University of Žilina, 2000, ISBN 80-7100-608

[3] OPATOVÁ, V. *Investigation of temperature dependence of thermal properties of hardened polyurethane Carbon nanotubes,* Dissertation thesis, FPT Púchov, 2012, p. 36-38

[4] KUBIČÁR, Ľ. Pulse Method Of Measuring Basic Thermophysical Parameters. *Comprehensive Analytical Chemistry*, 1990, Vol. XII, p. 350, ISSN 0069-8024

[5] WIGGINS, K.G., ALLARD, J.E. The Evidential Value Of Fabric Car Seats And Car Seat Covers. *Journal of the Forensic science society,* 1987, 27 (2), p. 93-102

[6] KUBIČÁR, L., ET ALL. *Thermophysical Parameters Measurement By Classic And Transient Methods*. CPU Nitra, 2000, ISBN 80-8050-361-3

[7] KOPAL I., KOVÁČ K., URÍČOVÁ S. *The thermophysical parameters study of car seat covers of different thickness,* Metallic sheets, Ostrava 2012

[8] SLUKA, P. *Evaporative and hydraulic resistance of multilayer fabrics thesis*. Dissertation thesis, TU Liberec 2006, p. 56

[9] HES, L. *Evaluation of thermal comfort of outdoor clothing*, Cultex TU Liberec, 2009, p. 47-51

Hutnické listy č. 7/2013, roč. LXVI
ISSN 0018-8069

Determination of Dynamic and Static Material Characteristics for Tire Casing Treads with their Various Time of Aging

Stanovenie dynamických a statických materiálových parametrov rôzne starých behúňov plášťov pneumatík

Ing. Michal Pastorek[1], **doc. Ing. Jan Krmela, Ph.D.**[1]

[1]University of Alexander Dubček in Trenčín, Faculty of Industrial Technologies, I. Krasku 491/30, 020 01 Púchov, Slovak Republic

The paper is focused on determination of dynamic and static material characteristics of variously old treads for passenger tires casings. These characteristics serve as the input data for computational modeling of tire casings. To obtain these material characteristics for the purpose of calculations, it was necessary to carry out experiments, especially dynamic tests using DMA and static tensile tests. In the paper, the selected results from DMA tests and static tensile tests of treads which were aged variously are presented. Based on the experimental results, it is can be possible to determine the Mooney-Rivlin parameters which are necessary input data into computational models of tire casings and their parts. Computational models will be designed to be able to include the effect of aging of individual tire casing parts. Research of degradation processes can lead to design and material changes to increase the resistance of casings against certain forms of degradation (aging) and by this way it would be possible to improve their safety indicators and lifetime.

Keywords: *tire casing, degradation, tensile test, dynamic-mechanical analysis, tread*

Článok sa zaoberá stanovením dynamických a statických materiálových charakteristík behúňov rozlične starých plášťov na pneumatikách osobných automobilov. Tieto charakteristiky slúžia ako vstupné dáta pre počítačové modelovanie plášťov pneumatík. Pre získanie týchto materiálových charakteristík na účely výpočtov bolo nutné vykonať experimenty, najmä dynamické skúšky pomocou metódy DMA a statické skúšky v ťahu. V článku sú prezentované vybrané výsledky z DMA testov a statických skúšok v ťahu behúňov rôzne starých plášťov pneumatík. Zo získaných experimentálnych výsledkov je potom možné určiť Mooney-Rivlinove parametre, ktoré patria medzi potrebné vstupné dáta do výpočtových modelov plášťov pneumatík a ich častí. Výpočtové modely budú navrhnuté tak, aby bolo možné zahrnúť vplyv starnutia jednotlivých častí plášťa. Výskum je zameraný na vybrané rôzne staré plášte pneumatík výrobcu Continental. Skúšobné vzorky pre statické ťahové skúšky boli vyrezané z behúňov vybraných troch rôzne starých plášťov pneumatík. Statické skúšobné zariadenie pre skúšku ťahom Hounsfield H20K-W bolo použité pre mechanické statické ťahové skúšky v jednoosovom silovom pôsobení zaťažujúcej sily až do pretrhnutia. Rýchlosť zaťažovania bola 20 mm / min a počiatočná vzdialenosť medzi čeľusťami bola 20 mm. Testovacie zariadenie PYRIS Diamond od firmy Perkin Elmer bolo použité pre merania pomocou dynamicko-mechanickej analýzy. Toto zariadenie bolo použité na meranie modulu pružnosti E', stratového modulu E'' a tangensu stratového uhla δ v teplotnom rozsahu -70 až 110 °C. Z oboch dynamických a statických skúšok možno konštatovať, že najstarší behúň je výrazne zdegradovaný a preto môže byť jeho použitie potenciálne nebezpečné. Výskum degradačných procesov môže viesť k dizajnovým a materiálovým zmenám na zvýšenie odolnosti plášťov proti niektorým formám degradácie (starnutie), zlepšenie ich bezpečnostných indikátorov a životnosti.

Kľúčové slová: *plášť pneumatiky, degradácia, skúška v ťahu, dynamicko-mechanická analýza, behúň*

Nowadays, tires are one of the most important products in the market. Therefore, it is important to determine all the fundamentals relating to degradation caused by aging because the influence of ozone is considered to have the negative effect on mechanical properties and behavior of tires after several years. The tire casing is a very complicated composite part of the car. Tires are the only point of contact between the car and the road and therefore, they have to perform a variety of functions such as: direction keeping, load carrying and the shock absorbing from road roughness.

For the input parameters in computational models of tires and tire parts, as well as for verification and comparison of the the results of calculations with experimental data, it is necessary to perform dynamic and static experiments of tire casings and their parts. Tire casings are in research and development and verification of loading and stress-strain states is closely connected with the finite element method which is the most often used method. Therefore, it is necessary to determine the material characteristics of the individual casing parts accurately [1].

Research is focused on chosen selected old tire casings provided by the manufacturer Continental. The article is focused on the experimental determination of dynamic and static material characteristics of treads of these tire casings. These data are important material inputs into computational models of the natural degradation of tire casings.

Performed experiments

Experimental tests were performed in order to obtain material characteristics and parameters of the selected parts of the tire casing as important material inputs into the calculations for verification and analysis of computer models with experimental data.

Division of experimental tests that were needed to obtain material characteristics of individual components of the tire casing is shown schematically in Fig. 1.

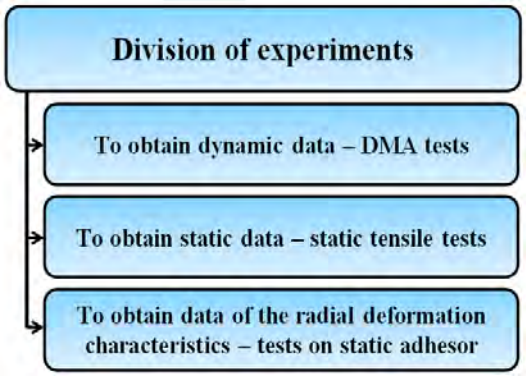

Fig. 1 Division of experiments
Obr. 1 Rozdelenie experimentov

This paper is focused on static tests in uniaxial stress and dynamic tests using the DMA method. These tests are important not only for the evaluation of material characteristics of finished rubber products, but they have a high explanatory ability even about the quality of preparation of rubber compounds and they also helps to wind the answer a whether the individual mixtures are selected correctly for the given application. The determination of mechanical characteristics of the tire casing parts has its irreplaceable role and it is also important in research and development, where the various properties are compared and evaluated among themselves [2].

The results from dynamic tests and tensile tests in uniaxial stress can be used to determine the Mooney-Rivlin parameters which are important inputs into the computational models of the tire casings. Tests of the given experimental samples from tire treads were performed with respect to the parameters of the test equipment and test conditions.

Static tensile tests

Test samples for static tensile tests were cut from treads of three selected tire casings which were old in a different way. Static test device for tensile testing Hounsfield H20K-W was used for the mechanical static tensile test in uniaxial force influence of the load force until the breakage. Detail of the clamping of the test samples from tire treads in the test equipment is shown on Fig. 2. Loading rate was 20 mm / min and initial distance between the clamps was 20 mm [3].

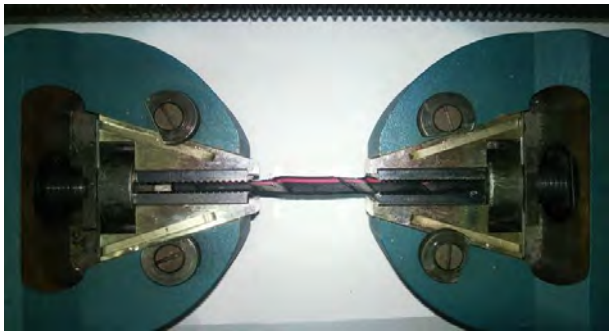

Fig. 2 Detail of a clamped sample
Obr. 2 Detail vzorky upevnenej v čeľustiach

In Fig. 3, there are shown the dependencies of load force from elongation of tire tread samples which were aged differently. From the dependencies, we can see that the middle aged (5 year old) and the new tire treads have significantly higher values in the dependency of load force from elongation than the oldest (17 year old) tire tread.

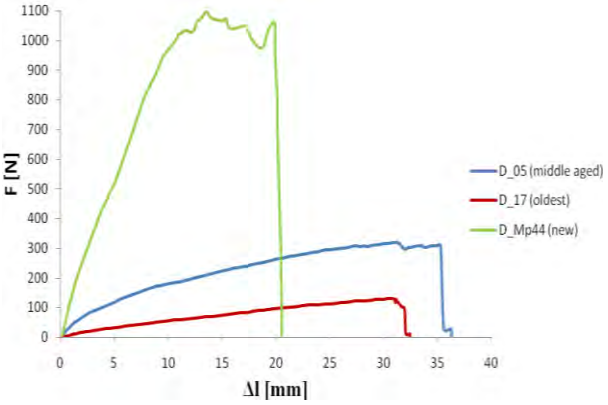

Fig. 3 Dependencies of load force from elongation of tire treads
Obr. 3 Závislosti zaťažujúcej sily od predĺženia pre behúne pneumatiky

Fig. 4 shows the dependencies of stress from elongation of the same samples.

Comparison of results of tire treads is shown in Table 1.

Tab. 1 Comparison of results of tread samples
Tab. 1 Porovnanie výsledkov pre vzorky behúňov

Tread	F [N]	σ [MPa]	ε [mm]	ε [%]
Middle aged	319.47	5.06	31.27	156.34
Oldest	129.37	3.18	30.59	152.95
New	1095.63	13.44	13.5	67.48

Hutnické listy č. 7/2013, roč. LXVI
ISSN 0018-8069

Rubber of the oldest (17 years old) tire tread is significantly degraded as can be seen from the dependencies of force and stress from elongation.

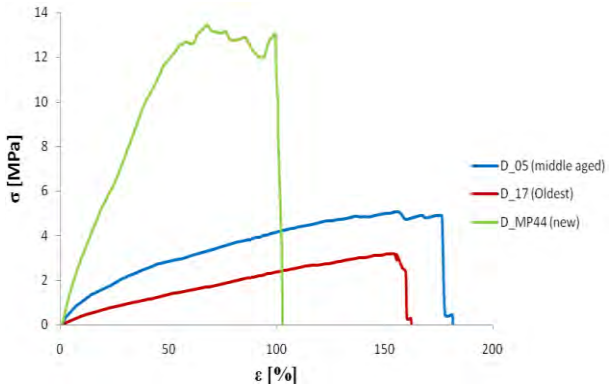

Fig. 4 Dependencies of stress from elongation
Obr. 4 Závislosti napätia od pomerného predĺženia

Dynamic DMA tests

Dynamic-mechanical analysis is a sensitive technique able to characterize and interpret the mechanical behavior of the material. Principle of the DMA method is based on monitoring of the viscoelastic response of materials subjected to small oscillating strain. The method separates the viscoelastic response of material into two components of the modulus (E *): the real part, which is represented by the elastic modulus (E ') and the imaginary part representing the damping or viscosity component (E"). The total modulus called Complex modulus is calculated as E * = E '+ iE " [4, 5].

PYRIS Diamond test device from Perkin Elmer was used for dynamic-mechanical analysis measurements (Fig. 5).

Fig. 5 Pyris Diamond DMA device in laboratory at FIT
Obr. 5 Zariadenie Pyris Diamond DMA v laboratóriu na FPT

The article presents the results for the modules of elasticity of samples from treads of tire casings with their different aging. Figures 6, 7 and 8 show the results from measurements of elastic modulus E ', loss modulus E" and the tangent of loss angle δ for a temperature range from -70 to 110 ° C at frequency 1 Hz.

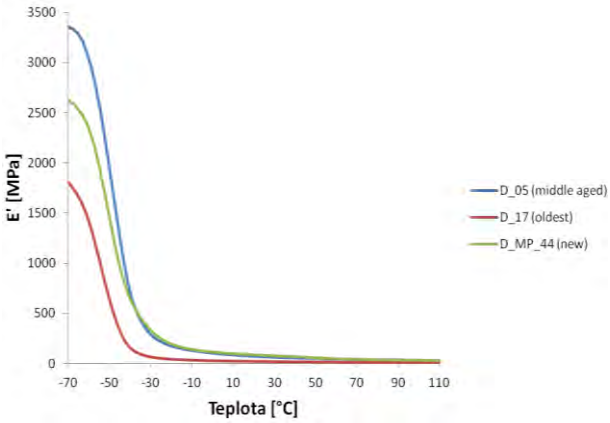

Fig. 6 Dependency of elastic modulus E' from temperature
Obr. 6 Závislosť elastického modulu E' od teploty

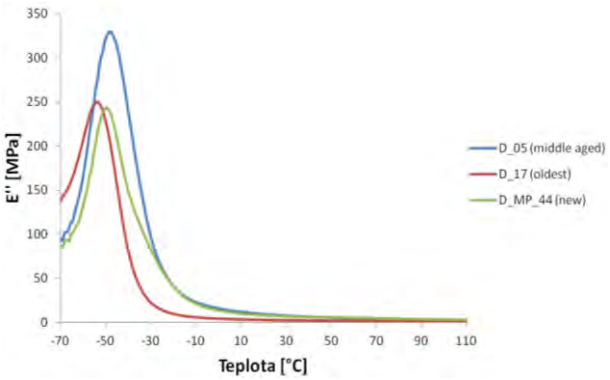

Fig. 7 Dependency of loss modulus E" from temperature
Obr. 7 Závislosť elastického modulu E" od teploty

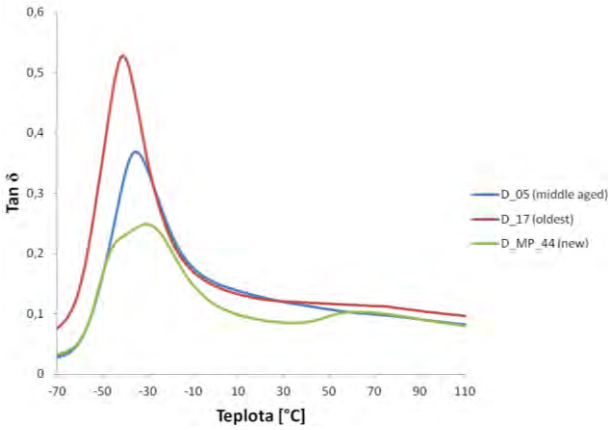

Fig. 8 Dependency of tan δ from temperature
Obr. 8 Závislosť tan δ od teploty

Tread samples were prepared from 17 years old and 5 years old Matador 165 R13 tires and a new Matador 185/55 R15 tires. Samples were rectangular with the height of 40 mm, the width of 4 mm and thickness of 2.5 mm.

From the results can be seen that the tread from the oldest casing has considerably degraded material characteristics compared to the other treads and it results in significantly lower values of the elastic modulus E 'and also in the higher values of the tangent of the loss angle δ.

The dependency of the tangent of loss angle δ of the given treads from elongation (Fig. 9) is also shown in this article.

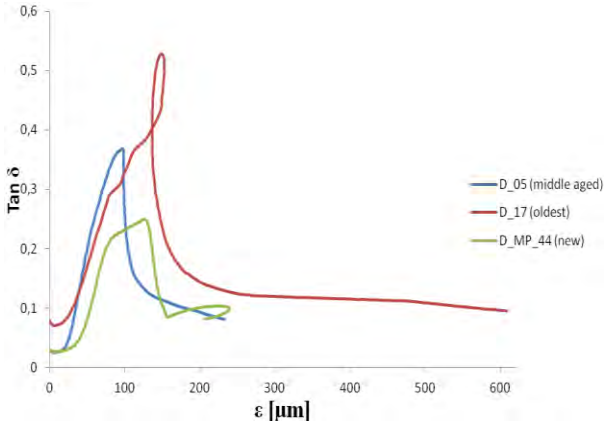

Fig. 9 Dependency of tan δ from elongation
Obr. 9 Závislosť tan δ od predĺženia

From the dependency of tan δ from the elongation can be seen that the values of tan δ increase in dependency from elongation are highest for the oldest tread. The progress of the dependency of the oldest tread is quite different in comparison to the newer treads. In the rubber of the oldest tread a slight shrinkage occurs near the glass transition point. This is probably due to structural changes inside of its structure.

Values of complex modulus E* for three different temperatures and the temperature of glass transition are shown in Table 2.

Tab. 2 Values of *E** and the glass transition temperature *Tg*
Tab. 2 Hodnoty E* a teploty skelného prechodu *Tg*

Tread	E* [MPa] - 70°C	E* [MPa] 0°C	E* [MPa] + 110°C	Tg [°C]
5 year old	3356.80	103.95	31.35	-36.26
17 y. old	1800.41	25.19	7.49	-41.18
New	2618.57	115.76	31.35	-31.29

From both dynamic and static tests, it can be concluded that the oldest tire tread is significantly degraded and therefore its usage could be potentially dangerous.

Conclusions

Dynamic and static experiments were used in the article in order to acquire the material characteristics of differently aged tire casing treads. These characteristics are important material inputs into calculations and they are important for verification analysis of computational models with experimental data.

The tread samples were first subjected to static tests in uniaxial stress. The experimental results were processed and evaluated in the form of graphical dependencies between stress and elongation. Then the DMA method was used to determine the elastic modulus E ', loss modulus E" and tangent of the loss angle δ.

From both dynamic and static tests, it can be concluded that the oldest tire tread is significantly degraded and therefore its usage could be potentially dangerous.

Research of degradation processes can lead to possible design and material changes which can lead to an increase of the durability and safety indicators of tire casings as well as against some forms of degradation.

Literature

[1] KRMELA, J. *Systémový přístup k výpočtovému modelování pneumatik I*., 1. vyd., Czech Republic 2008, ISBN 978-80-7399-365-8, 102 p.

[2] PASTOREK, M., VIDO, P., KRMELA, J. Selected experiments of composites with elastomers for computational modelling of a tire. In: ARSA2012: Proceedings in advanced research in scientific areas, The 1st virtual international conference. Slovak Republic, Žilina: EDIS, 2012, p.1554-1559, ISBN 978-80-554-0606-0

[3] VIDO, P., PASTOREK, M., KRMELA, J. Vybrané experimentálne skúšky kompozitov s elastomérovou matricou pre overenie výpočtových modelov pneumatík. In: SEMDOK 2013 : 18th International of PhD. student´s seminar, Slovak Republic, Žilina, 2013, p. 152-155, ISBN 978-80-554-0629-9

[4] PASTOREK, M., KRMELA, J., KOVÁČ, K. Určenie modulu pružnosti osobných plášťov pneumatík. In: TechMat´12 : Prespektivní technologie a materiály pro technické aplikace. Conference proceedings. Czech Republic, Pardubice: Univerzita Pardubice, 2012, p. 83-89, ISBN 978-80-7395-537-3

[5] VIDO, P., PASTOREK, M., DRDÁKOVÁ, J., STRUHARŇANSKÁ, M., KRMELA, J. Determination of material characteristics for verification of computational models of tires. In: Interdisciplinární mezinárodní vědecká konference doktorandů a odborných asistentů QUAERE 2013. Czech Republic, Hradec Králové: MAGNANIMITAS, 3. vyd., 2013, p. 2611-2616, ISBN 978-80-905243-7-8

Hutnické listy č. 7/2013, roč. LXVI
ISSN 0018-8069

Experimental and Numerical Modal Analysis of the Plate of Carbon Composite

Experimentálna a numerická modálna analýza dosky uhlíkového kompozitu

Ing. Ján Vavro, jr., PhD.[1], prof. Ing. Ján Vavro, PhD.[1], Ing. Alena Vavrová[1], Ing. Petra Kováčiková[1], Ing. Radka Bezdedová[1]

[1]University of Alexander Dubček in Trenčín, Faculty of Industrial Technologies, I. Krasku 491/30, 020 01 Púchov, Slovak Republic

The given paper is closely connected with the experimental modal analysis of eigenfrequences of carbon composite material. In relation to the tested carbon composite, modal analysis was performed by help of special measuring device Pulse 12. The mentioned device was supplied by company Brüel & Kjear and the experimental measurements were carried out using damaged and undamaged plate sample which were prepared from the mentioned material hereinbefore. The investigated and analyzed plates of carbon composite were made of six layers of carbon fibres and they were arranged under the angle 90º (it is like fabric material made off carbon fibres). The layers arranged in the given way were joined by epoxide resin MGS 285. The experimental measurement of eigenfrequencies of carbon composite plates was carried out using the undamaged and damaged sample with proportions 78 mm x 78 mm while ten measurements were performed for each one specified site of the sample. In relation to the damaged plate sample, there was the circular cutout with the diameter 6 mm in the centre. The finite element method in the software system ADINA v.8.6.2 was used for numerical analysis of the eigenfrequencies. According to the comparison of frequency response for undamaged and damaged sample, it can be concluded that the eigenfrequency of the damaged sample is less than the eigenfrequency of the undamaged sample. The measurement range for frequencies was up to 14 000 Hz.

Keywords: *experimental modal analysis, numerical analysis, finite element method, Pulse 12, carbon composite material.*

Článok sa zaoberá experimentálnou modálnou analýzou vlastných frekvencií uhlíkového kompozitného materiálu, pričom sa vytvoril výpočtový model a hodnotili sa vlastné tvary frekvencií pre nepoškodenú a poškodenú vzorku. V súčasnosti je experimentálna modálna analýza (EMA) neoddeliteľnou súčasťou odboru dynamiky, pretože pomocou danej analýzy možno overovať, prípadne dopĺňať výsledky, ktoré boli získané na základe analytickej metódy. Experimentálne meranie bolo vykonané na aparatúre PULSE 12 poskytnutou firmou Brüel & Kjear a ako skúšobné vzorky boli použité dosky, zhotovené z uhlíkového kompozitného materiálu. Uvedené uhlíkové kompozitné vzorky boli vyrobené zo šiestich vrstiev uhlíkových vlákien, uložených pod uhlom 90° (tkanina z uhlíkových vlákien) a následne zaliatych epoxidom typu MGS 285. Experimentálne meranie vlastných frekvencií uhlíkového kompozitu sa uskutočnilo na nepoškodenej a poškodenej vzorke s rozmermi 78mm x 78 mm. Poškodená vzorka mala v strede vyrezaný kruhový otvor s priemerom 6 mm. V každom meranom mieste vzorky sa zaznamenávali frekvencie zo stanoveného počtu úderov(v našom prípade to bolo 10 úderov), ktoré systém Pulse spriemeroval, vyhodnotil a graficky zobrazil v grafoch frekvenčnej odozvy a koherencie. Numerická analýza bola vykonaná pomocou metódy konečných prvkov v programovom prostredí ADINA v. 2.8.6. a pre výpočtový model v spomínanom programovom prostredí sa použila metóda Subspace iteration. Pre epoxidovú matricu L 285 a uhlíkové vlákna boli použité materiálové konštanty, ktoré sú udané výrobcom. Vzorky, pripravené z uhlíkového kompozitného materiálu, boli uchytené po celom svojom obvode v špeciálnom prípravku medzi dvomi oceľovými doskami, ktoré boli spojené štyrmi skrutkami. Samotná analýza a porovnanie vlastných frekvencií sa vykonali za účelom diagnostiky poruchy kompozitného materiálu na základe využitia kombinácie modálnej experimentálnej analýzy a numerickej analýzy založenej na metóde konečných prvkov.

Kľúčové slová: *experimentálna modálna analýza, ,numerická analýza, metóda konečných prvkov, Pulse 12, uhlíkový kompozitný materiál*

The experimental modal analysis belongs to Dynamics that is the special scientific field where so-called modal parameters of the object (e.g. eigenfrequencies, own shapes of the vibrations, absorption or damping parameters) are investigated. These mentioned parameters can be obtained in an analytical way by help of finite element analysis (FEM) or they can be determined on the basis of the experimental analysis.

The experimental analysis is connected with verification or completing of those results which were acquired on the basis of the analytical method. The given analysis is

based on the principle which involves the usage of the process where the complex vibration process is divided into the simple modal constituent vibrations or parts. Each one of these constituent parts can be characterized by its natural frequency or eigenfrequency as well as it has its own shape of the vibration [1].

The sixties of last century can be understood as the beginning of the modern era of the experimental modal analysis (EMA) because of the introduction of Fourier transformation and development and progress relating to the computer technologies. Nowadays, experimental modal analysis (EMA) represents the scientific field which stands for some connecting point between signal adjustment and computational technology, theory of mechanics, vibrations, acoustics and signals processing [2, 3, 4].

EMA can be also used for verification of the mathematical models and nowadays, it can help us to solve various technical problems including:

a) the determination of eigenfrequencies for any objects because if the excitation frequencies correspond to eigenfrequencies, it can lead to excessive vibrations of the construction (resonance) and it means the decrease of lifetime and reliability,

b) the determination of the own or natural shapes of the vibration and control them by exciting actions of the system with the aim to find the critical site of the construction where the vibration is the highest,

c) the verification of the authenticity relating to the mathematical models which were made by help of finite element methods and moreover, the change of models parameters can be done by help of experiments and measurements in order to obtain the mutual accordance (modal tuning),

d) the modification and the change of construction geometry with the aim to eliminate the intervals or zones of in-service exciting actions (structural modification).

Experimental measurement of the eigenfrequencies

The experimental measurements were performed by help of special device PULSE 12 from company Brüel & Kjear. The samples obtained from carbon composite material were used for measurement process. The mentioned composites were made of six layers of carbon fibres and they were arranged under the angle 90º (it is like fabric material composed of carbon fibres). Then, the layers arranged in the given way were joined by epoxide resin MGS 285.

The experimental measurement of eigenfrequencies for carbon composite was carried out using the undamaged and damaged samples with proportions 78 mm x 78 mm. In relation to the damaged sample, there was the circular cutout with the diameter 6 mm in the centre. The samples were held around the whole circumference in special fixture and moreover, they were between two plates which were fastened by four screws. The testing equipment for experimental measurement can be seen in Fig 1. For each one site, the frequencies obtained on the basis of ten hammer impacts were recorded and they were subsequently averaged, evaluated and displayed in the graphical way by Pulse system in graphs of the frequency response and coherency. The software which is supplied together with the measurement device is used for settings, controlling, and collection of obtained measurement data. The given software contains everything which is needed for measurement. The measurement process as well as setting of the required conditions is done by help of organizers and the user can make settings of software according to own requirements. The given settings can be saved and used as some pattern again during any other measurement. As can be seen in Fig. 1, the position of the accelerometer for the undamaged sample was in the centre and hammer impacts were performed for four sites – in the corners of the sample. In relation to the damaged sample with the 6 mm circular cutout, the position of the accelerometer was in the corner of the sample. The obtained eigenfrequencies for both types of samples are shown in Tab. 1.

Fig. 1 Testing equipment for experimental measurements
Obr. 1 Zostava experimentálneho merania

Tab. 1 Obtained values of eigenfrequencies for damaged and undamaged sample of the carbon composite
Tab. 1 Namerané hodnoty vlastných frekvencií poškodenej a nepoškodenej vzorky uhlíkového kompozitu

Obtained values of eigenfrequencies (Hz)		
Number of frequency	**Undamaged sample**	**Damaged sample**
1	5030.89	4501.43
2	6160.26	5619.97
3	8550.60	8486.66
4	9902.33	9401.92
5	10942.10	10732.40

Numerical analysis of the eigenfrequencies

The specific method, called “Subspace iteration“ method was used for creation of the computational model in the program system ADINA 2.8.6. The material constant parametres were used for epoxide matrix L285 as well as for carbon fibres and these constant parametres, shown in Tab. 2, were specified by the producer.

Hutnické listy č.7/2013, roč. LXVI
ISSN 0018-8069

Tab. 2 Material constant parameters which were used for computational model
Tab. 2 Materiálové konštanty použité pri výpočtovom modeli

Material constant parameter	Epoxide matrix L 285	Carbon fibre
Young's modulus E [GPa]	3.45	380
Poisson's number μ	0.3	0.33
Density ρ [kg/m^3]	1200	1950

Numerical analysis was solved for two computational models:

a) for undamaged sample with the proportions 78 mm x 78 mm and it was reinforced with six layers of carbon fibres while the fibres were arranged under angle 90°;

b) for damaged sample with the circular cutout in the centre of the sample and the diameter of the cutout was 6 mm.

Tab. 3 Computational model of the carbon composite undamaged sample and eigenfrequencies of its first five shapes
Tab. 3 Výpočtový model nepoškodenej vzorky uhlíkového kompozitu a jej prvých päť tvarov vlastných frekvencií

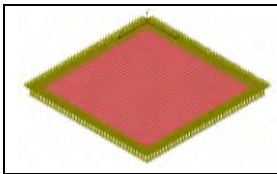	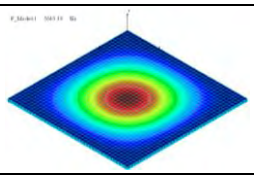
Computational model of the undamaged carbon fibre sample	The first shape of the eigenfrequency
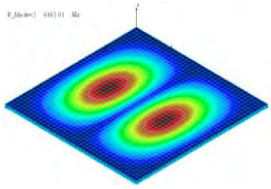	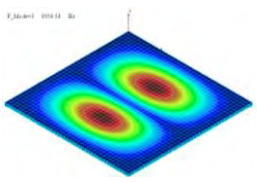
The second shape of the eigenfrequency	The third shape of the eigenfrequency
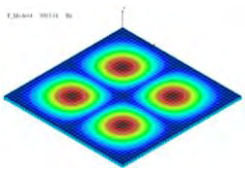	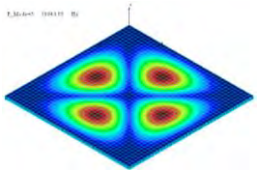
The fourth shape of the eigenfrequency	The fifth shape of the eigenfrequency

The computational model of the undamaged composite as well as its first five shapes of eigenfrequencies can be seen in the Tab. 3. The computational model of the damaged composite sample with the circular cutout in the centre as well as its first five shapes of eigenfrequencies can be seen in the Tab. 4. The given own or natural shapes represent the dynamic behaviour of the model or possible movement of the system vibrations and they are ordered from the lowest frequency to the highest one. In relation to the individual models, the own or natural shapes of the eigenfrequencies depend on the way of removal of the degrees of freedom and they also depend on size and shape of the defect as well as the location or site of the defect on the model. The first one shape represents the lowest frequency and the fifth shape represents the highest frequency. The calculated results of eigenfrequencies for the damaged and undamaged samples are introduced in Tab. 5.

Tab. 4 Computational model of the carbon composite damaged sample and eigenfrequencies of its first five shapes
Tab. 4 Výpočtový model poškodenej vzorky uhlíkového kompozitu a jej prvých päť tvarov vlastných frekvencií

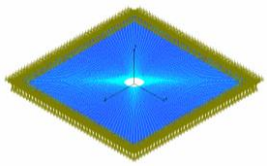	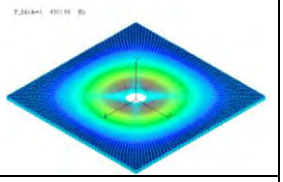
Computational model of the damaged carbon fibre sample	The first shape of the eigenfrequency
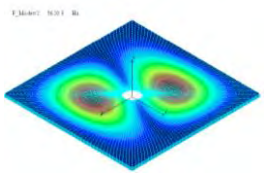	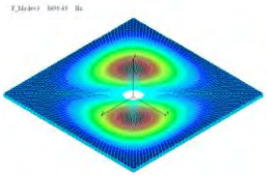
The second shape of the eigenfrequency	The third shape of the eigenfrequency
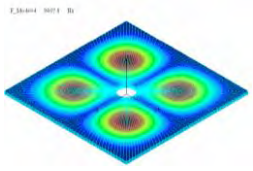	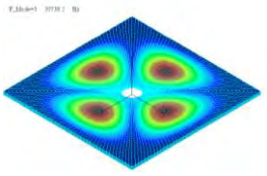
The fourth shape of the eigenfrequency	The fifth shape of the eigenfrequency

Tab. 5 Calculation of the eigenfrequencies for damaged and undamaged sample
Tab. 5 Vypočítané vlastné frekvencie nepoškodenej a poškodenej vzorky

Calculation values of eigenfrequencies (Hz)		
Number of frequency	**Undamaged sample**	**Damaged sample**
1	5040.39	4502.98
2	6162.01	5620.30
3	8558.54	8490.49
4	9905.06	9407.80
5	10945.05	10739.20

Conclusions

As mentioned above, ten measurements were performed for the each one tested site of the sample. Tab. 1 shows the average value resulting from all ten measurements which were performed for four specified sites of the sample. According to the obtained results based on measurement, it can be concluded that the frequencies of the damaged sample are less than the frequencies of the undamaged sample. The same results were obtained in the case of the numerical analysis which was based on the finite element method and it is shown in Tab. 5. The measurement range of the frequencies was given up to 14 000 Hz. According to results which were obtained on the basis of measurement of frequencies (Tab. 1) and results which were obtained on the basis of the calculation of the frequencies (Tab. 5), it can be assessed that increase of the frequency leads to the higher value of the shift in relation to the comparison of the damaged and undamaged sample – the difference of the frequencies is noticeable.

Acknowledgement
The work presented in this paper was supported by VEGA grant No. 1/0530/11 and KEGA grant No.007 TnUAD-4/2013.

Literature

[1] ALLEMANG, R.J. Analytical and Experimental Modal Analysis, UC-SDRLCN. 1994

[2] AMABILIM, M., PAGNANELI, F., PELLEGRINI, M. Experimental modal analysis ofa water-filled circular cylindrical tank, 2001

[3] AVITABILE, P. Exerimental modal Analysis. A simple non-mathematical presentation. Universityof Massachusetts, January 2001

[4] TREBUŇA, F., ŠIMČÁK, F., HUŇADY, R. Kmitanie a modálna analýza mechanických sústav. 1. vyd. Košice, 2012. 236 s. ISBN 978-80-553-1206-4

[5] TREBUŇA, F., et al. An Application of High-speed Digital Image Correlation in Determination of Modal Parameters. *Acta Mechanica Slovaca*, 2011, roč. 15, č. 4, p. 6-12, ISSN 1335-2393

[6] TREBUŇA, F., et al. Modal analysis of transport complex and drop tests of container for transport ofspent nuclear fuel. In: EAN 2012: proceedings of the 50-th Annual Conference on Experimental Stress Analysis: Tábor, Czech Republic, 4.6-7.6.2012. Praha: ČVUT 2012, p. 1-8, ISSN 978-80-01-05060-6

Experimental and Numerical Modal Analysis of the Plate of Glass Composite

Experimentálna a numerická modálna analýza dosky skleneného kompozitu

Ing. Ján Vavro, jr., PhD.[1], **prof. Ing. Ján Vavro, PhD.**[1], **Ing. Alena Vavrová**[1], **Ing. Petra Kováčiková**[1], **Ing. Radka Bezdedová**[1]

[1]University of Alexander Dubček in Trenčín, Faculty of Industrial Technologies, I. Krasku 491/30, 020 01 Púchov, Slovak Republic

The given paper is closely connected with the experimental modal analysis of eigenfrequences of glass composite material. In relation to the tested glass composite, modal analysis was performed by help of special measuring device Pulse 12. The mentioned device was supplied by company Brüel & Kjear and the experimental measurements were carried out using damaged and undamaged plate sample which were prepared from the mentioned material hereinbefore. The investigated and analyzed plates of glass composite were made of six layers of glass fibres and they were arranged under the angle 90° (it is like fabric material made off glass fibres). The layers arranged in the given way were joined by epoxide resin MGS 285. The experimental measurement of eigenfrequencies of glass composite plates was carried out using the undamaged and damaged sample with proportions 78 mm x 78 mm while ten measurements were performed for each one specified site of the sample. In relation to the damaged plate sample, there was the circular cutout with the diameter 6 mm in the centre. The finite element method in the software system ADINA v.8.6.2 was used for numerical analysis of the eigenfrequencies. According to the comparison of frequency response for undamaged and damaged sample, it can be concluded that the eigenfrequency of the damaged sample is less than the eigenfrequency of the undamaged sample. The measurement range for frequencies was up to 14 000 Hz.

Keywords: *experimental modal analysis, numerical analysis, finite element method, Pulse 12, glass composite material.*

Článok sa zaoberá experimentálnou modálnou analýzou vlastných frekvencií skleneného kompozitného materiálu, pričom sa vytvoril výpočtový model a hodnotili sa vlastné tvary frekvencií pre nepoškodenú a poškodenú vzorku. V súčasnosti je experimentálna modálna analýza (EMA) neoddeliteľnou súčasťou odboru dynamiky, pretože pomocou danej analýzy možno overovať, prípadne dopĺňať výsledky, ktoré boli získané na základe analytickej metódy. Experimentálne meranie bolo vykonané na aparatúre PULSE 12, poskytnutej firmou Brüel & Kjear a ako skúšobné vzorky boli použité dosky, zhotovené zo skleneného kompozitného materiálu. Uvedené sklenené kompozitné vzorky boli vyrobené zo šiestich vrstiev sklenených vlákien, uložených pod uhlom 90° (tkanina zo sklenených vlákien) a následne zaliatych epoxidom typu MGS 285. Experimentálne meranie vlastných frekvencií skleneného kompozitu sa uskutočnilo na nepoškodenej a poškodenej vzorke s rozmermi 78mm x 78 mm. Poškodená vzorka mala v strede vyrezaný kruhový otvor s priemerom 6 mm. V každom meranom mieste vzorky sa zaznamenávali frekvencie zo stanoveného počtu úderov (v našom prípade to bolo 10 úderov), ktoré systém Pulse spriemeroval, vyhodnotil a graficky zobrazil v grafoch frekvenčnej odozvy a koherencie. Numerická analýza bola vykonaná pomocou metódy konečných prvkov v programovom prostredí ADINA v. 2.8.6. a pre výpočtový model v spomínanom programovom prostredí sa použila metóda Subspace iteration. Pre epoxidovú matricu L 285 a sklenené vlákna boli použité materiálové konštanty, ktoré sú udané výrobcom. Vzorky, pripravené zo skleneného kompozitného materiálu, boli uchytené po celom svojom obvode v špeciálnom prípravku medzi dvomi oceľovými doskami, ktoré boli spojené štyrmi skrutkami. Samotná analýza a porovnanie vlastných frekvencií sa vykonali za účelom diagnostiky poruchy kompozitného materiálu na základe využitia kombinácie modálnej experimentálnej analýzy a numerickej analýzy založenej na metóde konečných prvkov.

Kľúčové slová: *experimentálna modálna analýza, ,numerická analýza, metóda konečných prvkov, Pulse 12, sklenený kompozitný materiál*

The experimental modal analysis belongs to the dynamics that is the special scientific field where so-called modal parameters of the object (e.g. eigenfrequencies, own shapes of the vibrations, absorption or damping parameters) are investigated. These mentioned parameters can be obtained in an the basis of the analytical method. The given analysis involves the usage of the process including the principle analytical way by help of finite element analysis (FEM) or they can be determined on the basis of the experimental analysis.

The experimental analysis is connected with verification or completing of those results which were acquired on where the complex vibration process is divided into the simple modal constituent vibrations or parts. Each one

of these constituent parts can be characterized by its natural frequency or eigenfrequency as well as it has its own shape of the vibration [1].

The sixties of last century can be understood as the beginning of the modern era of the experimental modal analysis (EMA) because of the introduction of Fourier transformation and development and progress relating to the computer technologies. Nowadays, experimental modal analysis (EMA) represents the scientific field which stands for some connecting point between signal adjustment and computational technology, theory of mechanics, vibrations, acoustics and signals processing [2, 3, 4].

EMA can be also used for verification of the mathematical models and nowadays, it can help us to solve various technical problems including:

a) the determination of eigenfrequencies for any objects because if the excitation frequencies correspond to eigenfrequencies, it can lead to excessive vibrations of the construction (resonance) and it means the decrease of lifetime and reliability,

b) the determination of the own or natural shapes of the vibration and control them by exciting actions of the system with the aim to find the critical site of the construction where the vibration is the highest,

c) the verification of the authenticity relating to the mathematical models which were made by help of finite element methods and moreover, the change of models parameters can be done by help of experiments and measurements in order to obtain the mutual accordance (modal tuning),

d) the modification and the change of construction geometry with the aim to eliminate the intervals or zones of in-service exciting actions (structural modification).

Experimental measurement of the eigenfrequencies

The experimental measurements were performed by help of special device PULSE 12 from company Brüel & Kjear. The samples obtained from glass composite material were used for measurement process. The mentioned composites were made of six layers of glass fibres and they were arranged under the angle 90º (it is like fabric material composed of glass fibres). The layers arranged in the given way were joined by epoxide resin MGS 285.

The experimental measurement of eigenfrequencies for glass composite was carried out using the undamaged and damaged samples with proportions 78 mm x 78 mm. In relation to the damaged sample, there was the circular cutout with the diameter 6 mm in the centre. The samples were held around the whole circumference in special fixture and moreover, they were between two material constant parametres were used for epoxide matrix L285 as well as for glass fibres and these plates which were fastened by four screws. The testing equipment for experimental measurement can be seen in Fig 1. For each one site, the frequencies obtained on the basis of ten hammer impacts were recorded and they were subsequently averaged, evaluated and displayed in the graphical way by Pulse system in graphs of the frequency response and coherency. The software which is supplied together with the measurement device is used for settings, controlling, and collection of obtained measurement data. The given software contains everything which is needed for measurement. The measurement process as well as setting of the required conditions is done by help of organizers and the user can make settings of software according to own requirements. The given settings can be saved and used as some pattern again during any other measurement. As can be seen in Fig. 1, the position of the accelerometer for the undamaged sample was in the centre and hammer impacts were performed for four sites – in the corners of the sample. In relation to the damaged sample with the 6 mm circular cutout, the position of the accelerometer was in the corner of the sample. The obtained eigenfrequencies for both types of samples are shown in Tab. 1.

Fig. 1 Testing equipment for experimental measurements
Obr. 1 Zostava experimentálneho merania

Tab. 1 Obtained values of eigenfrequencies for damaged and undamaged sample of the glass composite
Tab. 1 Namerané hodnoty vlastných frekvencií poškodenej a nepoškodenej vzorky skleneného kompozitu

Obtained values of eigenfrequencies (Hz)		
Number of frequency	**Undamaged sample**	**Damaged sample**
1	3795.71	3707.69
2	6111.82	5602.43
3	8459.74	7221.23
4	9284.23	8582.75
5	11062.7	10342.10

Numerical analysis of the eigenfrequencies

The specific method, called "Subspace iteration" method was used for creation of the computational model in the program system ADINA 2.8.6. The constant parametres, shown in Tab. 2, were specified by the producer.

Hutnické listy č.7/2013, roč. LXVI
ISSN 0018-8069

Tab. 2 Material constant parameters which were used for computational model
Tab. 2 Materiálové konštanty použité pri výpočtovom modeli

Material constant parameter	Epoxide matrix L 285	Glass fibre
Young's modulus E [GPa]	3.45	73
Poisson's number μ	0.3	0.22
Density ρ [kg/m^3]	1200	2600

Numerical analysis was solved for two computational models:

a) for undamaged sample with the proportions 78 mm x 78 mm and it was reinforced with six layers of glass fibres while the fibres were arranged under angle 90°;

b) for damaged sample with the circular cutout in the centre of the sample and the diameter of the cutout was 6 mm.

c)

Tab. 3 Computational model of the glass composite undamaged sample and eigenfrequencies of its first five shapes
Tab. 3 Výpočtový model nepoškodenej vzorky skleneného kompozitu a jej prvých päť tvarov vlastných frekvencií

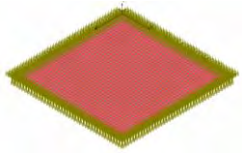	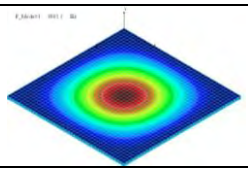
Computational model of the undamaged glass fibre sample	The first shape of the eigenfrequency
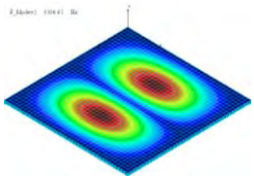	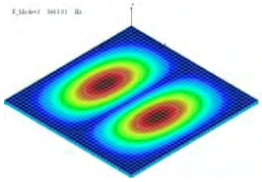
The second shape of the eigenfrequency	The third shape of the eigenfrequency
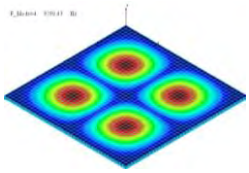	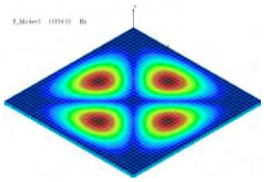
The fourth shape of the eigenfrequency	The fifth shape of the eigenfrequency

The computational model of the undamaged composite as well as its first five shapes of eigenfrequencies can be seen in the Tab. 3. The computational model of the damaged composite sample with the circular cutout in the centre as well as its first five shapes of eigenfrequencies can be seen in the Tab. 4. The given own or natural shapes represent the dynamic behaviour of the model or possible movement of the system vibrations and they are ordered from the lowest frequency to the highest one. In relation to the individual models, the own or natural shapes of the eigenfrequencies depend on the way of removal of the degrees of freedom and they also depend on size and shape of the defect as well as the location or site of the defect on the model. The first one shape represents the lowest frequency and the fifth shape represents the highest frequency. The calculated results of eigenfrequencies for the damaged and undamaged samples are introduced in Tab. 5.

Tab. 4 Computational model of the glass composite damaged sample and eigenfrequencies of its first five shapes
Tab. 4 Výpočtový model poškodenej vzorky skleneného kompozitu a jej prvých päť tvarov vlastných frekvencií

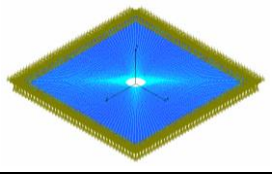	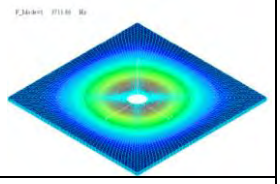
Computational model of the damaged glass fibre sample	The first shape of the eigenfrequency
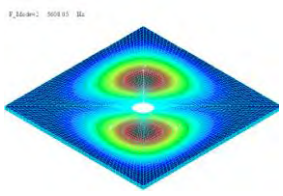	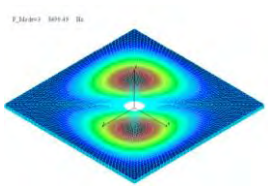
The second shape of the eigenfrequency	The third shape of the eigenfrequency
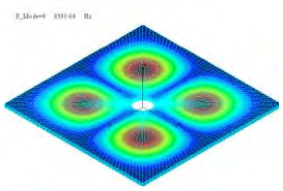	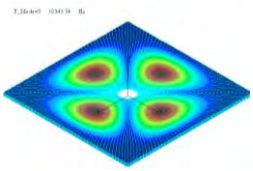
The fourth shape of the eigenfrequency	The fifth shape of the eigenfrequency

Tab. 5 Calculation of the eigenfrequencies for damaged and undamaged sample
Tab. 5 Vypočítané vlastné frekvencie nepoškodenej a poškodenej vzorky

Calculation values of eigenfrequencies (Hz)		
Number of frequency	**Undamaged sample**	**Damaged sample**
1	3802.20	3711.86
2	6106.62	5608.05
3	8463.01	7226.58
4	9290.43	8590.64
5	11054.01	10349.34

Conclusions

As mentioned above, ten measurements were performed for the each one tested site of the sample. Tab. 1 shows the average value resulting from all ten measurements which were performed for four specified sites of the sample. According to the obtained results based on measurement, it can be concluded that the frequencies of the damaged sample are less than the frequencies of the undamaged sample. The same results were obtained in the case of the numerical analysis which was based on the finite element method and it is shown in Tab. 5. The measurement range of the frequencies was given up to 14 000 Hz. According to results which were obtained on the basis of measurement of frequencies (Tab. 1) and results which were obtained on the basis of the calculation of the frequencies (Tab. 5), it can be assessed that increase of the frequency leads to the higher value of the shift in relation to the comparison of the damaged and undamaged sample – the difference of the frequencies is noticeable.

Acknowledgement
The work presented in this paper was supported by VEGA grant No. 1/0530/11 and KEGA grant No.007 TnUAD-4/2013.

Literature

[1] ALLEMANG, R.J. Analytical and Experimental Modal Analysis, UC-SDRLCN. 1994

[2] AMABILIM, M., PAGNANELI, F., PELLEGRINI, M. Experimental modal analysis ofa water-filled circular cylindrical tank, 2001

[3] AVITABILE, P. Exerimental modal Analysis. A simple non-mathematical presentation. Universityof Massachusetts, January 2001

[4] TREBUŇA, F., ŠIMČÁK, F., HUŇADY, R. Kmitanie a modálna analýza mechanických sústav. 1. vyd. Košice, 2012. 236 s. ISBN 978-80-553-1206-4

[5] TREBUŇA, F., et al. An Application of High-speed Digital Image Correlation in Determination of Modal Parameters. *Acta Mechanica Slovaca*, 2011, roč. 15, č. 4, p. 6-12, ISSN 1335-2393

[6] TREBUŇA, F., et al. Modal analysis of transport complex and drop tests of container for transport ofspent nuclear fuel. In: EAN 2012: proceedings of the 50-th Annual Conference on Experimental Stress Analysis: Tábor, Czech Republic, 4.6-7.6.2012. Praha: ČVUT 2012, p. 1-8, ISSN 978-80-01-05060-6

Nový závod na výrobu nerezavějící oceli

Liquid steel production at Outokumpu Stainless in Calvert, Alabama, USA. Metallurgical Plant and Technology, 2013, č. 4, s. 38

Nový závod na výrobu plechů z nerezavějící oceli uvedla do provozu firma Outokumpu Stainless v Calvert blízko přístavu Mobile ve státě Alabama v USA. Tvoří ho nově vybudovaná ocelárna a stávající válcovna.

V ocelárně je elektrická oblouková pec 160 t. Dále je zde zařízení AOD (argon oxygen decarburization) o kapacitě 180 t a pánvová pec. Oblouková pec a zařízení AOD mají odprašování.

Ocel se odlévá do bram na jednoproudém zařízení pro plynulé odlévání. Má rovný krystalizátor. Odlitá brama se ohýbá s radiusem 9 m. Bramy mají šířku 800 až 1900 mm a tloušťku 180 až 240 mm. Rychlost lití je 1,3 m/min. Vibrace kokily jsou vyvozovány hydraulicky. Sekundární chlazení je typu Dynacs, tažné válce mají vnitřní chlazení. Vyrábějí se zde nerezavějící oceli řady 200, 300 a 400 podle AISI.

Bramy se válcují za tepla na pásy ve stávající válcovně. Pás se pak převáží do závodu Outokumpu v Mexiku k dalšímu zpracování.

L J

Hutnické listy č. 7/2013, roč. LXVI
ISSN 0018-8069

Experimental and Numerical Modal Analysis of the Plate of Glass Composite with Delamination Damage

Experimentálna a numerická modálna analýza dosky skleneného kompozitu poškodeného delamináciou

Ing. Ján Vavro, jr., PhD.[1], **prof. Ing. Ján Vavro, PhD.**[1], **Ing. Alena Vavrová**[1], **Ing. Petra Kováčiková**[1], **Ing. Radka Bezdedová**[1]

[1]University of Alexander Dubček in Trenčín, Faculty of Industrial Technologies, I. Krasku 491/30, 020 01 Púchov, Slovak Republic

The given paper is closely connected with the experimental modal analysis of eigenfrequences and own or natural shapes of glass composite material, the damage of which was caused on the basis of delamination. In relation to the tested glass composite, modal analysis was performed by help of special measuring device Pulse 12. The mentioned device was supplied by company Brüel & Kjear and the experimental measurements were carried out using damaged and undamaged plate sample which were prepared from the mentioned material hereinbefore. The investigated and analyzed plates of glass composite were made of six layers of glass fibres and they were arranged under the angle 90° (it is like fabric material made off glass fibres). The layers arranged in the given way were joined by epoxide resin MGS 285. The experimental measurement of eigenfrequencies of glass composite plates was carried out using the undamaged and damaged sample with proportions 78 mm x 78 mm while ten measurements were performed for each one specified site of the sample. In relation to the damaged plate sample, the given sample was damaged on the base of delemination. The damage was simulated by help of special foil which was placed between the3rd and4thlayer in order to avoid the mutual connection of the mentioned layers on the area with proportions 25mm x25 mm. The finite element method in the software system ADINA v.8.6.2 was used for numerical analysis of the eigenfrequencies. According to the comparison of frequency response for undamaged and damaged sample, it can be concluded that the eigenfrequency of the damaged sample is less than the eigenfrequency of the undamaged sample. The measurement range for frequencies was up to 14 000 Hz.

Keywords: *experimental modal analysis, numerical analysis, finite element method, Pulse 12, glass composite material*

Článok sa zaoberá experimentálnou a numerickou modálnou analýzou vlastných frekvencií a vlastných tvarov kmitania dosky skleneného kompozitného materiálu poškodeného delamináciou. V súčasnosti je experimentálna modálna analýza (EMA) neoddeliteľnou súčasťou odboru dynamiky, pretože pomocou danej analýzy možno overovať, prípadne dopĺňať výsledky, ktoré boli získané na základe analytickej metódy. Experimentálne meranie bolo vykonané na aparatúre PULSE 12, poskytnutej firmou Brüel & Kjear a ako skúšobné vzorky boli použité dosky, zhotovené zo skleneného kompozitného materiálu. Uvedené sklenené kompozitné vzorky boli vyrobené zo šiestich vrstiev sklenených vlákien, uložených pod uhlom 90° (tkanina zo sklenených vlákien) a následne zaliatych epoxidom typu MGS 285. Experimentálne meranie vlastných frekvencií skleneného kompozitu sa uskutočnilo na poškodenej vzorke s rozmermi 78mm x 78 mm. Poškodenie vzorky bolo medzi treťou a štvrtou vrstvou špeciálnou fóliou, aby nedošlo ku spojeniu jednotlivých vrstiev sklenených vlákien na ploche 25 x 25 mm. V každom meranom mieste vzorky sa zaznamenávali frekvencie zo stanoveného počtu úderov (v našom prípade to bolo 10 úderov), ktoré systém Pulse spriemeroval, vyhodnotil a graficky zobrazil v grafoch frekvenčnej odozvy a koherencie. Numerická analýza bola vykonaná pomocou metódy konečných prvkov v programovom prostredí ADINA v. 2.8.6. a pre výpočtový model v spomínanom programovom prostredí sa použila metóda Subspace iteration. Pre epoxidovú matricu L 285 a sklenené vlákna boli použité materiálové konštanty, ktoré sú udané výrobcom. Vzorky, pripravené zo skleneného kompozitného materiálu, boli uchytené po celom svojom obvode v špeciálnom prípravku medzi dvomi oceľovými doskami, ktoré boli spojené štyrmi skrutkami. Samotná analýza a porovnanie vlastných frekvencií sa vykonali za účelom diagnostiky poruchy kompozitného materiálu na základe využitia kombinácie modálnej experimentálnej analýzy a numerickej analýzy založenej na metóde konečných prvkov.

Kľúčové slová: *experimentálna modálna analýza, numerická analýza, metóda konečných prvkov, Pulse 12, sklenený kompozitný materiál*

The experimental modal analysis belongs to the dynamics that is the special scientific field where so-called modal parameters of the object (e.g. eigenfrequencies, own shapes of the vibrations, absorption or damping parameters) are investigated. These mentioned parameters can be obtained in an

analytical way by help of finite element analysis (FEM) or they can be determined on the basis of the experimental analysis.

The experimental analysis is connected with verification or completing of those results which were acquired on the basis of the analytical method. The given analysis involves the usage of the process including the principle where the complex vibration process is divided into the simple modal constituent vibrations or parts. Each one of these constituent parts can be characterized by its natural frequency or eigenfrequency as well as it has its own shape of the vibration [1].

The sixties of last century can be understood as the beginning of the modern era of the experimental modal analysis (EMA) because of the introduction of Fourier transformation and development and progress relating to the computer technologies. Nowadays, experimental modal analysis (EMA) represents the scientific field which stands for some connecting point between signal adjustment and computational technology, theory of mechanics, vibrations, acoustics and signals processing [2, 3, 4].

EMA can be also used for verification of the mathematical models and nowadays, it can help us to solve various technical problems including:

a) the determination of eigenfrequencies for any objects because if the excitation frequencies correspond to eigenfrequencies, it can lead to excessive vibrations of the construction (resonance) and it means the decrease of lifetime and reliability,

b) the determination of the own or natural shapes of the vibration and control them by exciting actions of the system with the aim to find the critical site of the construction where the vibration is the highest,

c) the verification of the authenticity relating to the mathematical models which were made by help of finite element methods and moreover, the change of models parameters can be done by help of experiments and measurements in order to obtain the mutual accordance (modal tuning),

d) the modification and the change of construction geometry with the aim to eliminate the intervals or zones of in-service exciting actions (structural modification).

Experimental measurement of the eigenfrequencies

The experimental measurements were performed by help of special device PULSE 12 from company Brüel & Kjear. The samples obtained from glass composite material were used for measurement process. The mentioned composites were made of six layers of glass fibres and they were arranged under the angle 90º (it is like fabric material composed of glass fibres). The layers arranged in the given way were joined by epoxide resin MGS 285.

The experimental measurement of eigenfrequencies for glass composite was carried out using the undamaged and damaged samples with proportions 78 mm x 78 mm. The samples were held around the whole circumference in special fixture and moreover, they were between two plates which were fastened by four screws. In relation to the damaged sample, the given sample was damaged on the base of delemination and the damage was simulated by help of special foil which was placed between the3rd and4thlayer in order to avoid the mutual connection of the mentioned layers on the area with proportions 25mm x25 mm. The testing equipment for experimental measurement can be seen in Fig 1. For each one site, the frequencies obtained on the basis of ten hammer impacts were recorded and they were subsequently averaged, evaluated and displayed in the graphical way by Pulse system in graphs of the frequency response and coherency. The software which is supplied together with the measurement device is used for settings, controlling, and collection of obtained measurement data. The given software contains everything which is needed for measurement. The measurement process as well as setting of the required conditions is done by help of organizers and the user can make settings of software according to own requirements. The given settings can be saved and used as some pattern again during any other measurement. As can be seen in Fig. 1, the position of the accelerometer for the undamaged sample was in the centre and hammer impacts were performed for four sites – in the corners of the sample. In relation to the damaged sample with the 6 mm circular cutout, the position of the accelerometer was in the corner of the sample. The obtained eigenfrequencies for both types of samples are shown in Tab. 1.

Fig. 1 Testing equipment for experimental measurements
Obr. 1 Zostava experimentálneho merania

Hutnické listy č. 7/2013, roč. LXVI
ISSN 0018-8069

Tab. 1 Obtained values of eigenfrequencies for damaged and undamaged sample of the glass composite
Tab. 1 Namerané hodnoty vlastných frekvencií poškodenej a nepoškodenej vzorky skleneného kompozitu

Obtained values of eigenfrequencies (Hz)		
Number of Frequency	**Undamaged sample**	**Damaged sample**
1	3795.71	1872.68
2	6111.82	4242.25
3	8459.74	6380.05
4	9284.23	8145.04
5	11062.7	9361.76

Numerical analysis of the eigenfrequencies

The specific method, called "Subspace iteration" method was used for creation of the computational model in the program system ADINA 2.8.6. The material constant parametres were used for epoxide matrix L285 as well as for glass fibres and these constant parametres, shown in Tab. 2, were specified by the producer.

Tab. 2 Material constant parameters which were used for computational model
Tab. 2 Materiálové konštanty použité pri výpočtovom modeli

Material constant parameter	**Epoxide matrix L 285**	**Glass fibre**
Young's modulus E [GPa]	3.45	73
Poisson's number μ	0.3	0.22
Density ρ [kg/m^3]	1200	2600

Numerical analysis was solved for two computational models:

a) for undamaged sample with the proportions 78 mm x 78 mm and it was reinforced with six layers of glass fibres while the fibres were arranged under angle 90°;

b) for damaged sample, the damage of which was based on delamination which was simulated by help of special foil which was placed between the3rd and4thlayer in order to avoid the mutual connection of the mentioned layers on the area with the determined proportions 25mm x25 mm.

The computational model of the undamaged composite as well as its first five shapes of eigenfrequencies can be seen in the Tab. 3. The computational model of the damaged composite sample with the circular cutout in the centre as well as its first five shapes of eigenfrequencies can be seen in the Tab. 4. The given own or natural shapes represent the dynamic behaviour of the model or possible movement of the system vibrations and they are ordered from the lowest frequency to the highest one. In relation to the individual models, the own or natural shapes of the eigenfrequencies depend on the way of removal of the degrees of freedom and they also depend on size and shape of the defect as well as the location or site of the defect on the model. The first one shape represents the lowest frequency and the fifth shape represents the highest frequency. The calculated results of eigenfrequencies for the damaged and undamaged samples are introduced in Tab. 5.

Tab. 3 Computational model of the glass composite undamaged sample and eigenfrequencies of its first five shapes
Tab. 3 Výpočtový model nepoškodenej vzorky skleneného kompozitu a jej prvých päť tvarov vlastných frekvencií

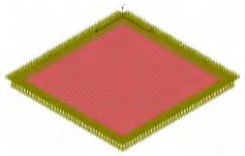	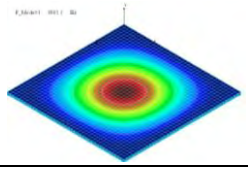
Computational model of the undamaged glass fibre sample	The first shape of the eigenfrequency
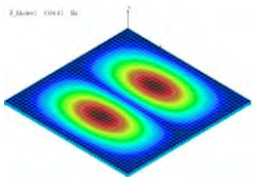	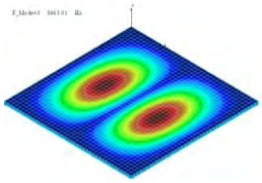
The second shape of the eigenfrequency	The third shape of the eigenfrequency
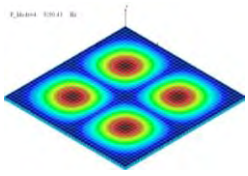	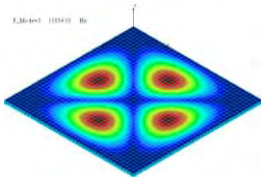
The fourth shape of the eigenfrequency	The fifth shape of the eigenfrequency

Tab. 4 Computational model of the glass composite damaged sample and eigenfrequencies of its first five shapes
Tab. 4 Výpočtový model poškodenej vzorky skleneného kompozitu a jej prvých päť tvarov vlastných frekvencií

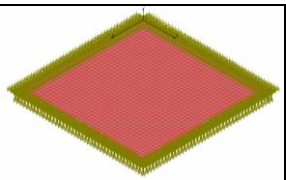	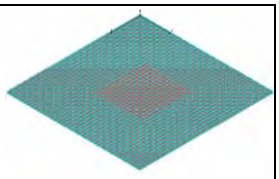
Computational model of the damaged glass fibre sample	The first shape of the eigenfrequency
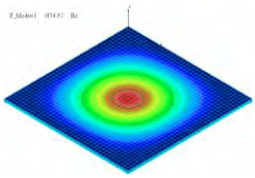	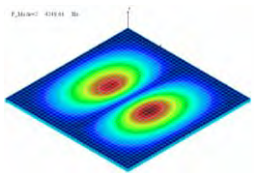
The second shape of the eigenfrequency	The third shape of the eigenfrequency
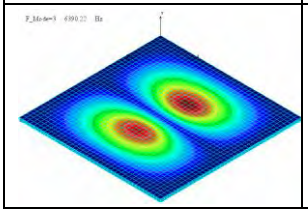	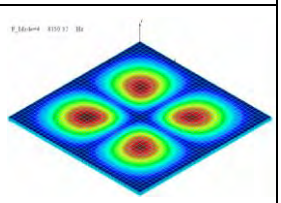
The fourth shape of the eigenfrequency	The fifth shape of the eigenfrequency

Tab. 5 Calculation of the eigenfrequencies for damaged and undamaged sample
Tab. 5 Vypočítané vlastné frekvencie nepoškodenej a poškodenej vzorky

Calculation values of eigenfrequencies (Hz)		
Number of frequency	**Undamaged sample**	**Damaged sample**
1	3802.20	1874.93
2	6106.62	4248.66
3	8463.01	6390.22
4	9290.43	9369.34
5	11054.01	10868.02

Conclusions

As mentioned above, ten measurements were performed for the each one specified site of the sample. Tab. 1 shows the average value resulting from all ten measurements which were performed for four specified sites of the sample. According to the obtained results based on measurement, it can be concluded that the frequencies of the damaged sample are less than the frequencies of the undamaged sample. The same results were obtained in the case of the numerical analysis which was based on the finite element method and it is shown in Tab. 5. The measurement range of the frequencies was determined up to 14 000 Hz. According to results which were obtained on the basis of measurement of frequencies (Tab. 1) and results which were obtained on the basis of the calculation of the frequencies (Tab. 5), it can be assessed that increase of the frequency leads to the higher value of the shift in relation to the comparison of the damaged and undamaged sample – the difference of the frequencies is noticeable.

Acknowledgement
The work presented in this paper was supported by VEGA grant No. 1/0530/11 and KEGA grant No.007 TnUAD-4/2013.

Literature

[1] ALLEMANG, R.J. Analytical and Experimental Modal Analysis, UC-SDRLCN. 1994

[2] AMABILIM, M., PAGNANELI, F., PELLEGRINI, M. Experimental modal analysis ofa water-filled circular cylindrical tank, 2001

[3] AVITABILE, P. Exerimental modal Analysis. A simple non-mathematical presentation. Universityof Massachusetts, January 2001

[4] TREBUŇA, F., ŠIMČÁK, F., HUŇADY, R. Kmitanie a modálna analýza mechanických sústav. 1. vyd. Košice, 2012. 236 s. ISBN 978-80-553-1206-4

[5] TREBUŇA, F., et al. An Application of High-speed Digital Image Correlation in Determination of Modal Parameters. *Acta Mechanica Slovaca*, 2011, roč. 15, č. 4, p. 6-12, ISSN 1335-2393

[6] TREBUŇA, F., et al. Modal analysis of transport complex and drop tests of container for transport ofspent nuclear fuel. In: EAN 2012: proceedings of the 50-th Annual Conference on Experimental Stress Analysis: Tábor, Czech Republic, 4.6-7.6.2012. Praha: ČVUT 2012, p. 1-8, ISSN 978-80-01-05060-6

Hutnické listy č.7/2013, roč. LXVI
ISSN 0018-8069

Investigation of Mechanical Properties of Composite System Cord-elastomer for Use of Computational Modeling of Tire Casing

Vyšetrovanie mechanických vlastností kompozitného systému kord-elastomér pre potreby výpočtového modelovania plášťov pneumatík

Ing. Peter Vido[1], **Ing. Jozefína Panáčková**[1], **doc. Ing. Jan Krmela, Ph.D.**[1], **Ing. Rudolf Valášek**[1]

[1]University of Alexander Dubček in Trenčín, Faculty of Industrial Technologies, I. Krasku 491/30, 020 01 Púchov, Slovak Republic

The article deals with determination of mechanical properties of specific composites with elastomeric matrix and steel reinforcement, forming steel cord belts, as input material parameters into the computational models of car tires. A finite element method (FEM) will be applied for computational modeling of tires. For stress-strain analysis of tires, it is necessary to determine individual material parameters for steel reinforcement as well as elastomeric matrix experimentally,. These parameters will be determined from the aspect of material characteristics of the individual components constituting the composite. In the article, there are presented partial results of experiments used to obtain the material characteristics of cord-elastomer composites which are necessary for verification of computational models in comparison to experiments and they can be also used as input data in the calculations.

Keywords: *composites, tire casing, steel cord, elastomeric matrix, computational modeling*

Článok sa zaoberá stanovením mechanických vlastností kompozitného systému oceľový kord–elastomér ako vstupných údajov do výpočtových modelov plášťov pneumatík. Tieto kompozity tvoria oceľokordové nárazníky ako aj kostru plášťa pneumatiky pre osobné automobily. Jednotlivé konštrukčné časti plášťov pneumatík sú reprezentované špecifickými experimentálnymi vzorkami v zastúpení od nánosových zmesí až po vzorky, kde sa vyskytujú v interakcii oceľové kordy, textilné kordy a elastomérové matrice. Statické skúšky v ťahu sú dôležité pre hodnotenie nielen mechanických vlastností hotových gumárenských výrobkov, ale majú vysokú vypovedaciu schopnosť aj o kvalite prípravy gumárenských zmesí a oceľových výstuží tiež, či boli jednotlivé komponenty pre danú aplikáciu správne zvolené. Výpočtové modelovanie plášťov pneumatík bude realizované s využitím metódy konečných prvkov. Pri vytváraní výpočtových modelov je dôraz kladený na materiálové charakteristiky a parametre jednotlivých častí pneumatík ako dôležitých vstupných materiálových údajov do modelov. Pomocou vybraných experimentov možno stanoviť mechanické vlastnosti jednotlivých konštrukčných častí plášťov pneumatiky. Pre deformačno-napäťové analýzy plášťov pneumatík je potrebné experimentálne stanoviť materiálové parametre ako pre oceľové výstuže, tak pre elastomérovú matricu. Tieto parametre budú získané z materiálových charakteristík jednotlivých komponentov tvoriacich plášť pneumatiky. Dôležitými faktormi, ktoré môžu značne ovplyvniť presnosť výpočtov vybraných častí plášťov pneumatík, sú počiatočné a okrajové podmienky, reflektujúce zaťaženie, geometriu a materiálové parametre pre každú konštrukčnú a materiálovú časť plášťa. V článku sú prezentované vybrané výsledky z experimentov potrebných na získanie materiálových charakteristík kordovo-elastomérových kompozitov, ktoré sú nevyhnutné aj pre verifikáciu výpočtových modelov s experimentmi.

Kľúčové slová: *kompozit, plášť pneumatiky, oceľový kord, elastomér, výpočtové modelovanie*

To determine the input parameters into the computational models of the tire for passenger cars and their parts, it is necessary to perform a whole range of experiments. In relation to creation of computational models of tires, the emphasis is on the mechanical properties and characteristics of the various parts of the tire as important input material data for these models. Using selected experiments, we can determine the mechanical properties of individual components of the tire.

Determination of material parameters of individual parts of the tire casing

Individual construction parts of tire for passenger car are represented by specific experimental samples from alluvial mixtures of samples and it is connected with the interaction of steel, textile, polymer cords and elastomeric matrix. Static tensile tests are important for the evaluation of material parameters of finished rubber products and they also give evidence whether the individual mixtures for the application were selected correctly. Division of experimental tests needed for material characteristics of individual components of the tire casing is shown schematically in Fig. 1.

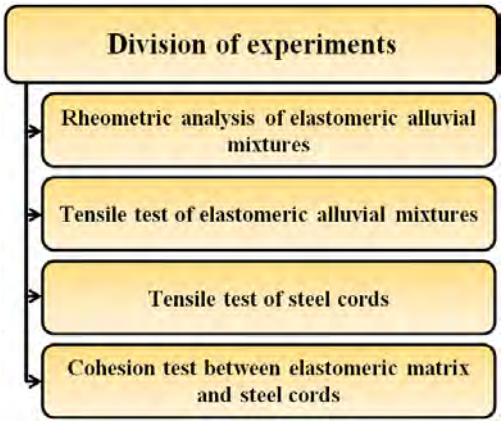

Fig. 1 Division of experiments
Obr. 1 Rozdelenie experimentov

Experiments with alluvial mixtures

The determination of the mechanical properties of vulcanizates has important role in the research and development of specific composites with elastomeric matrix and steel or textile reinforcement. Before the vulcanisation of elastomer mixtures, it is necessary to determinate the vulcanisation characteristics of the alluvial mixtures by using rheometric analysis, performed in accordance to ISO 3417 [1]. Torque curve acting on the vulcanization mixture is shown in Fig. 2.

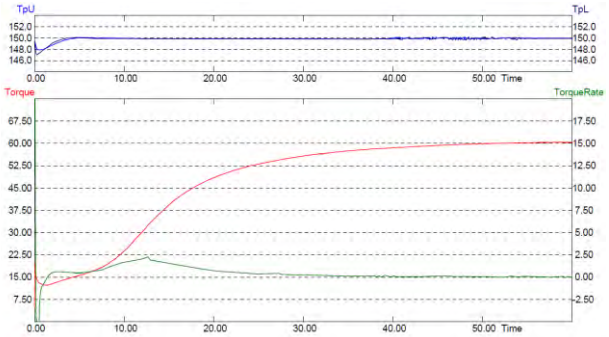

Fig. 2 Diagram from rheometric analysis
Obr. 2 Záznam z reometrickej analýzy

From the results of rheometric analysis of given rubber mixture, the most important data including the time of vulcanization (30 minutes), temperature (150 °C) and pressure of vulcanizing press (20 MPa) are specified. Vulcanisation of mixtures was performed in laboratory at Faculty of industrial technologies in Puchov.

The static universal testing machine Hounsfield H20K-W was used for the static tensile test with uniaxial load. Loading rate was set for 25 mm / minute and the initial distance between the clamps was set for 80 mm [2, 3]. Graphical dependency of loading force from elongation was transformed into diagram of dependence of tension from elongation which is shown in Fig. 3.

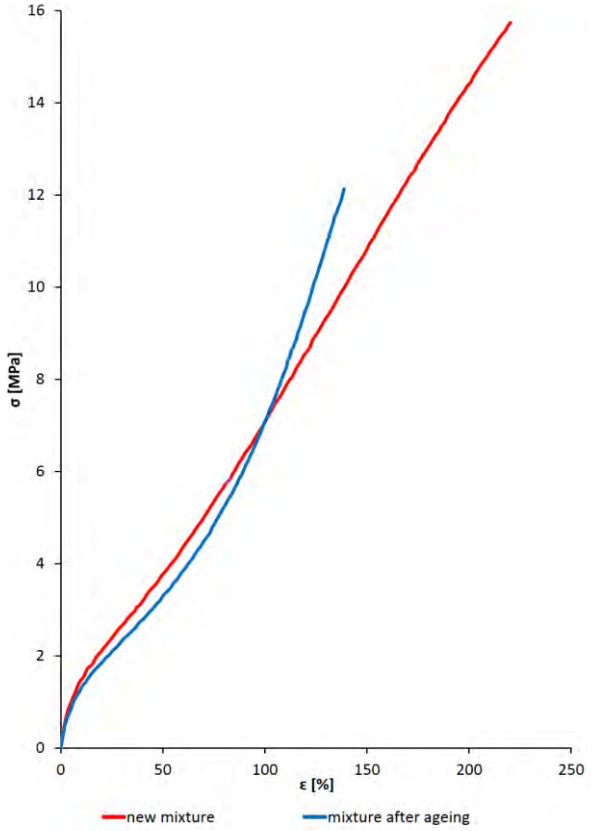

Fig. 3 Dependency of tension from elongation for alluvial mixtures
Obr. 3 Závislosť napätia od pomerného predĺženia pre nánosov zmesí

Examination of steel cords

The steel cords in form of wire with construction 2x0.30 serving as steel reinforcements in the buffers of tire casings for passenger cars were examined by a static tensile test. Loading rate was set for 5 mm / minute and the initial distance between the clamps was 200 mm. Dependences of tension from the elongation for the steel cords are shown in Fig. 4.

Hatched area of graph in Fig. 4 represents the area that limits the curves of dependency of tension from elongation for the steel cords with construction 2x0.30. On the basis of comparison of the values of maximum force to rupture for same type of cord, we can conclude that between the maximum and minimum measured value of the force is the difference 12% (relative to maximal force).

Cohesion test between steel cords and elastomeric matrix

For the cohesion test between the elastomeric matrix and steel cords, preparations were designed and manufactured allowing performing this test by the device Hounsfield H20K-W which has not been primarily adapted to perform such a test [4].

Hutnické listy č.7/2013, roč. LXVI
ISSN 0018-8069

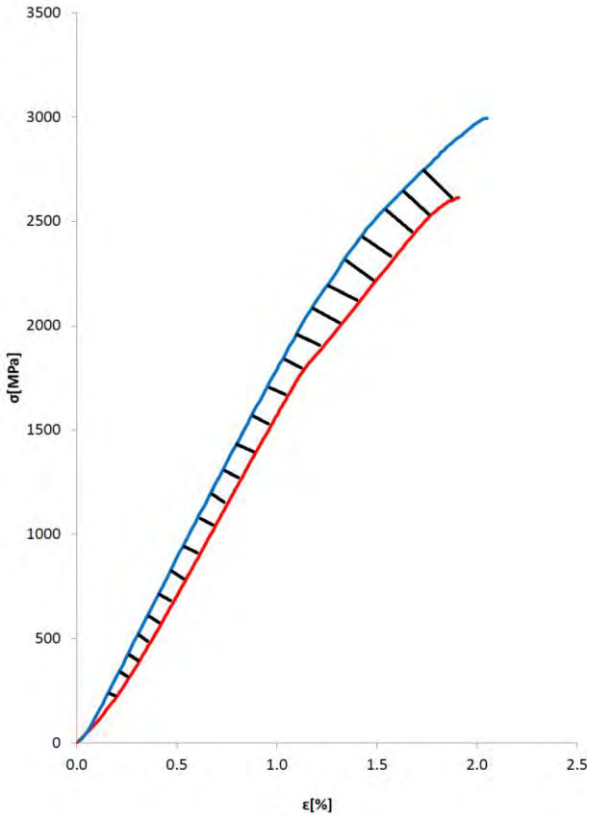

Fig. 4 Dependency of tension from elongation for steel cords
Obr. 4 Závislosť napätia od pomerného predĺženia pre oceľové kordy

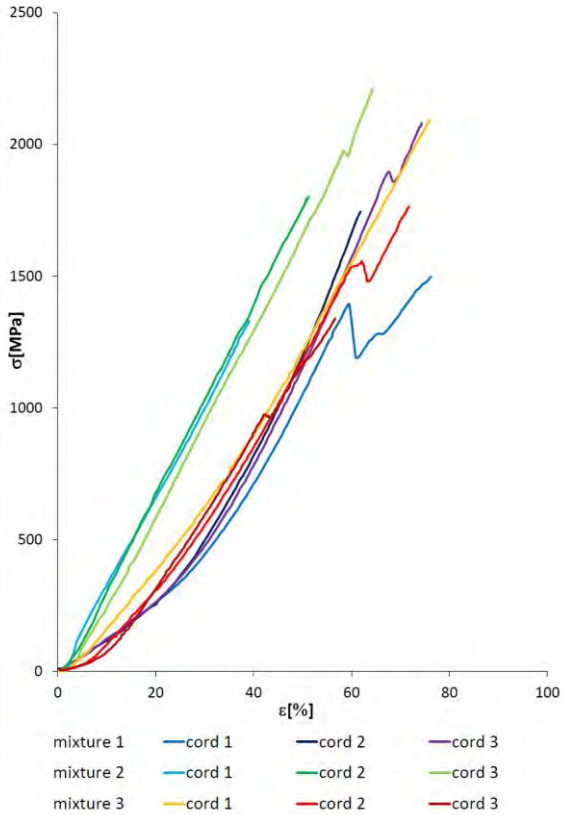

Fig. 5 Dependency of tension from elongation from cohesion test between steel cords and elastomeric matrix
Obr. 5 Závislosť napätia od pomerného predĺženia zo skúšky súdržnosti medzi elastomérom a oceľovým kordom

A new alluvial mixture and alluvial mixtures degraded due to air ozone (called oxidative aging) were used for the cohesion test. Fig. 5 shows the dependence of tension from elongation for steel cords and elastomeric compounds, when the length of steel cord pressed in the elastomer matrix was 10 mm.

Results from tests of cohesion between elastomeric matrix and steel cords in the form of dependency of load torque on the elongation has been processed and compared for various constructions of reinforcement and for different types of alluvial mixtures [5]. The new alluvial mixture (mixture 1) has approximately the same course of dependency of tension from elongation as a mixture of the same composition (mixture 3) which was exposed to air ozone for a period of one year. The influencing factor may be the different chemical composition than was declared by the manufacturer. Due to better knowledge of the behavior of system cord-elastomer, the samples with a length of steel cord pressed in a matrix of 20 mm and 50 mm were also subjected to a static test of cohesion.

Comparison of dependency of the force from elongation for chosen elastomeric samples with length 10, 20 and 50 mm of steel cord which was pressed into matrix is shown in Fig. 6. Curve "a" represent the cords pressed 10 mm into matrix, curve "b" represent cords pressed 20 mm into matrix and curve "c" represent cords pressed 50 mm into matrix.

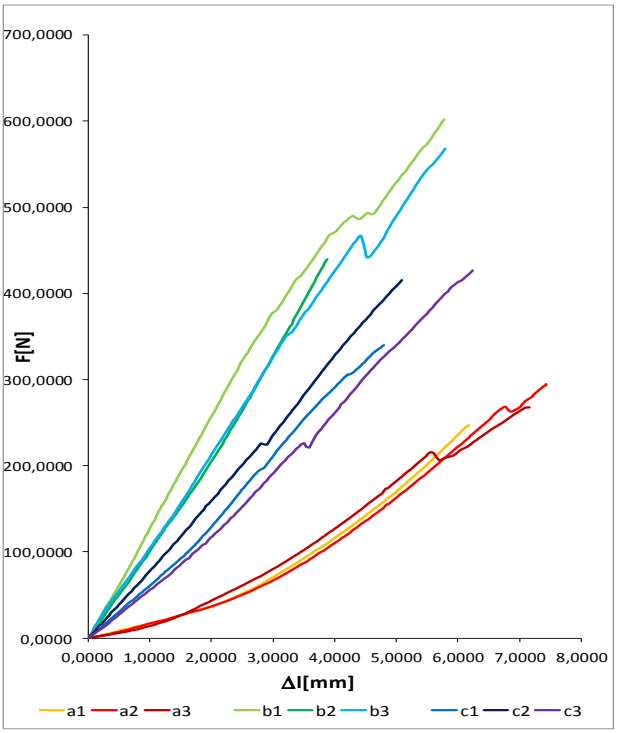

Fig. 6 Dependency of tension from elongation from cohesion test for various length of molding
Obr. 6 Závislosť napätia od pomerného predĺženia zo skúšky súdržnosti pre rôzne dĺžky zálisu

According to the manufacturers who specified parameters and following the results of the experiments, spatial model of steel cord (Fig. 7) and an elastomeric

matrix was modeled in order to simulate the specific conditions.

Fig. 7 Spatial model of steel cord 2x0.30
Obr. 7 Model oceľového lanka 2x0.30

Conclusions

The tensile tests of elastomeric blends and composites with elastomeric matrix as well as the degradation tests lead to an acquisition of the whole range of material parameters used as inputs into the calculations and they can be also used for verification analysis. Selected elastomeric samples represent the alluvial mixtures for rubberizing of steel cords that are used in the production of steel cord belts in car tire casings for passenger cars.

From the results of static tensile tests with uniaxial tension in the form of dependency of tension from elongation, it can be concluded that course of dependency of the samples of the new elastomeric compound has "more linear" character in comparison to the same mixture after aging.

Tensile strength tests of steel cords were used to verify the material characteristics declared by the manufacturer and data reported by the manufacturer correspond to the achieved results.

For the test of cohesion between the elastomeric matrix and steel reinforcement, it is necessary to know the tensile strength of steel cords so that we know whether there is the destruction of the adhesive bond in the system cord-Elastomer or reinforcement rupture.

For samples with 20 and 50 millimeter matrix, the bond of the system cord-elastomer was stronger than the tensile strength of steel cords and cord rupture occurred.

The results mentioned in the article are part of research of computational modeling relating to pulling of cords and they are also connected with verification with the respect of the experiments. Therefore, the obtained results will be used as verification parameters for the calculation of car tire casings or specific parts of tires – steel cord buffers and they will be compared to the data obtained experimentally.

Literature

[1] International standard ISO 3417, Rubber – Measurement of vulcanization characteristics with the oscillating disc curemeter

[2] DRDÁKOVÁ, J., KRMELA, J. Mikrolokalita degradovaných oceľokordových nárazníkov v plášti radiálnych pneumatík. In: Preveda - interaktívna konferencia mladých vedcov, Slovak Republic, 2012 [cited 10.9.2012], http://www.preveda.sk/conference/viewer/id=518/presentation/, p. 75, ISBN 978-80-970712-3-3

[3] STRUHARŇANSKÁ, M., PAJTÁŠOVÁ, M., KRMELA, J. Vybrané fyzikálno-mechanické vlastnosti polymérnych materiálov s plnivami na báze kremičitanov. In: Preveda - interaktívna konferencia mladých vedcov, Slovak Republic, 2012 [cited 4.4.2012] <http://www.preveda.sk/conference/article/id=456/>, p. 76, ISBN 978-80-970712-3-3

[4] VIDO, P. Systém kord – elastomér pri výrobe plášťa a jeho vplyv na životnosť pneumatiky. [diploma work]. University of Alexander Dubček in Trenčín, Faculty of Industrial Technologies, Slovak Republic, 2011, 68 p., (in Slovak)

[5] VIDO, P., PASTOREK, M., KRMELA, J. Vybrané experimentálne skúšky kompozitov s elastomérovou matricou pre overenie výpočtových modelov pneumatík. In: Zborník príspevkov: SEMDOK 2013: 18th International of PhD. students´ seminar, Slovak Republic, 2013, pp.152-155, ISBN 978-80-554-0629-9

Hutnické listy č.7/2013, roč. LXVI
ISSN 0018-8069

výpočetní metody

Finding Inflection Points of the Function Given by Experimental Data

Hľadanie inflexných bodov funkcie zadanej prostredníctvom experimentálnych dát

doc. Mgr. Ivan Kopal, Ph.D.[1], **doc. RNDr. Ladislav Matejíčka, CSc.**[1]

[1]University of Alexander Dubček in Trenčín, Faculty of Industrial Technologies in Púchov, I. Krasku 491/30, 020 01 Púchov, Slovak Republic

The solution of many scientific and engineering problems requires finding local and global extremes as well as inflection points of functions that have been obtained as experimental dependence among various physical quantities in the final set of elements. The aim of our work is to present an efficient algorithm for identifying the inflection points of functions given by experimental data set based on the substitution of appropriate functions describing experimental data representing acceptable analytical approach by approximations. In the paper we also mention a program code that implements the described algorithm in the working environment of the software package MATLAB® which also includes brief author's comments and is considered to be a freeware for any non-commercial use.

Key words: *inflection points, extremes of function, Dynamic Mechanical Analysis, relaxation transitions*

Riešenie mnohých vedeckých a inžinierskych problémov vyžaduje hľadanie lokálnych a globálnych extrémov, ako aj inflexných bodov funkcií, ktoré boli získané ako experimentálne závislosti medzi rôznymi fyzikálnymi veličinami na konečnej množine prvkov. Tieto signifikantné body experimentálnych funkcií totiž obvykle indikujú rozličné procesy prebiehajúce v skúmaných štruktúrach a často umožňujú identifikovať neznáme parametre, ktoré v týchto procesoch figurujú, prípadne ich ovplyvňujú. Ako príklad je možné uviesť experimentálne funkčné závislosti dynamických mechanických modulov od teploty, získané dynamickou mechanickou analýzou polymérnych materiálov, body extrémov a inflexné body ktorých určujú oblasti primárnych aj sekundárnych relaxačných prechodov. Hľadanie lokálnych a globálnych extrémov funkcií pritom zvyčajne nepredstavuje žiaden závažnejší praktický problém, na vyriešenie ktorého postačuje zistiť minimálne, ako aj maximálne hodnoty vhodným spôsobom vyhladenej krivky experimentálnych dát v príslušných intervaloch nezávislých premenných. Naproti tomu, identifikácia inflexných bodov predstavuje pomerne vysoko sofistikovaný proces, ktorý už vyžaduje výpočtovú techniku a efektívne algoritmy riešenia. Experimentálne funkcie sú totiž obvykle nespojité, takže neexistujú ich derivácie, čo nedovoľuje na ich analýzu použiť žiadne metódy klasickej matematickej analýzy. Je preto nevyhnutné hľadať iné, dostatočne výkonné spôsoby. Cieľom tejto práce je predstaviť efektívny algoritmus identifikácie inflexných bodov funkcií zadaných prostredníctvom experimentálnych údajov založený na substitúcii vhodných funkcií popisujúcich experimentálne dáta aproximáciami predstavujúcimi ich akceptovateľné analytické priblíženie. V práci tiež uvádzame programový kód implementujúci popísaný algoritmus v pracovnom prostredí softvérového balíka MATLAB®, ktorý uvádzame so stručným autorským komentárom a považujeme ho za voľne šíriteľný pre akékoľvek nekomerčné použitie.

Kľúčové slová: *inflexné body, extrémy funkcií, dynamická mechanická analýza, relaxačné prechody*

The solution of a number of scientific and engineering problems leads to finding local and global extremes and inflection points of functional dependencies between different physical quantities that have been obtained by measurements in the final set of elements, or in the final set of discrete variables. These significant points of functions usually indicate various processes occurring in the studied structures and they often can determine unknown parameters that figure in this processes or that affect them. The aim of our research is to present an efficient algorithm for identifying inflection points of functions given by using discrete experimental data and moreover, it is connected with the program code implementing of this algorithm in relation to the various practical applications.

An example of the function given by experimental data set is shown in figure Fig. 1. The function shown in this

figure represents the experimental dependence of loss odulus E" on temperature T for amorphous polymer, specifically for hardened polyurethane, in temperature range from - 126 °C to 250 °C that has been obtained by measurements of dynamic viscoelastic properties of the above mentioned material. The investigation is based on the method of dynamic mechanical analysis (DMA) using the experimental device PYRIS Diamond Perkin Elmer 8000 Dynamic Mechanical Analyzer [1]. As one can see, this experimental function given by a set of discrete experimental data shows several extremes as well as several inflection points. The experimental device used for DMA measurements of hardened polyurethane is shown in figure Fig. 2. The more detailed description of DMA experiment is presented in work [2].

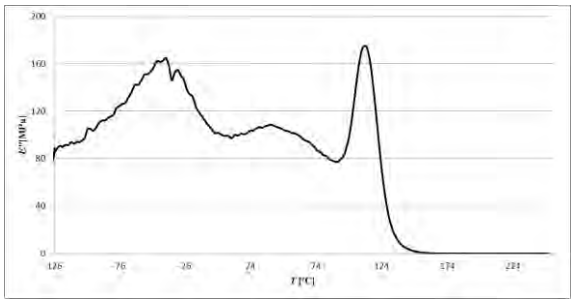

Fig. 1 Experimental functional dependence of dynamic loss modulus E'' on temperature T for hardened polyurethane as an example of function given by discrete experimental data
Obr. 1 Experimentálna funkčná závislosť dynamického stratového modulu E'' od teploty T pre tvrdený polyuretán ako príklad funkcie zadanej pomocou diskrétnych dát

Identification of inflection points of this function allows identifying temperatures of primary as well as secondary relaxation transitions in the studied material, which are essential for its successful implementation in practical applications [3-5]. While the primary or α-transition in polymers is the glass transition at temperature T_g, or at T_α, the secondary transitions are sub-T_g relaxations at temperatures T_β, T_γ and T_δ, which are lower than the glass transition temperature. Individual relaxations in polymers are determined by different conformational changes in polymer chains at different temperatures and it determines their structure

Fig. 2 Experimental device Pyris Diamond Perkin Elmer Dynamic Mechanical Analyzer 8000
Obr. 2 Experimentálna aparatúra Pyris Diamond Perkin Elmer DMA Dynamic Mechanical Analyzer 8000

and virtually affects practically all properties of polymeric materials [6]. We would like to point out that the glass transition occurs when large segments of polymer chains start moving, β-transition is related to either localized movement in the main chain or very large side movement, γ-transition relates to the movements occurring in the side chain of polymers and δ-transition is related to very small motions within polymer macromolecule [7].

Dynamic mechanical analysis principles

Dynamic mechanical analysis is an effective technique to investigate temperature effects on material stiffness. It represents one of the most sensitive methods which can be used to characterize mechanical behavior of materials. The DMA principle is based on monitoring the viscoelastic response of material sample which is loaded by a small oscillation strain. DMA distribute viscoelastic response of material on two components of the complex dynamic modulus

$$E^* = E' + iE'', \tag{1}$$

on real component, which represents elastic modulus E', and on the imaginary component, which represents loss modulus E''. The ratio

$$\tan\delta = E''/E' \tag{2}$$

represents the damping factor tan δ. This separation of E^* into E' and E'' describes two independent processes: elasticity (reversible component) and viscosity (loss or dissipation energy) in materials.

In DMA test, the mechanical response of a viscoelastic material is studied as a function of temperature and time while it is subjected to a small sinusoidal strain. DMA determines storage modulus, loss modulus, damping factor and other material characteristics as a function of time, frequency, stress, temperature, and atmosphere or as a combination of these parameters. By the investigations of dynamic mechanical properties of polymer materials, the results are typically provided as a graphical plot of E', E'' and tan δ versus temperature or time [8-10].

Searching for significant points of functions

Searching for local and global extremes of functions does not usually mean a serious practical problem. To determine the minimum and maximum values properly, a smoothed curve of experimental data on the basis of independent variables is sufficient to its resolution [11]. Identification of inflection points of functions is quite highly sophisticated process that requires computing and efficient solution algorithms. In fact, experimental functions are usually not continuous and therefore there are not their derivatives, so it is not able to apply any classical methods of mathematical analysis to analyze them. But there are several effective ways to identify significant points of experimental functions including their points of inflection [12]. The measurements can be replaced by appropriate functions and subsequently can be examined by the methods of classical mathematical

Hutnické listy č.7/2013, roč. LXVI
ISSN 0018-8069

analysis. In another way the substitution of formulas for obtaining experimental data of derivable functions by convergence formulas that are their equally acceptable analytical approximation can be used [13]. In this way, it is possible to obtain a good compensation of formulas commonly used in classical mathematical analysis for given data set [14]. To solve the problem of identifying the inflection points of functions given by experimental points in this paper, we used the second method. This allowed us to develop a highly efficient algorithm and to write its simple program code implemented in the software package MATLAB® and it also related to the possibilities of practical application demonstrated on the particular example in engineering practice.

Theoretical background

As a theoretical basis for identifying inflection points of functions given by a set of experimental data we use the following classical results of mathematical analysis.
If a function $f(x)$ has the second derivative $f''(x)$ on an interval, then the point x_0 is called the point of inflection if $f''(x) = 0$ and function is changed from convex to concave or vice versa. We recall that $f(x)$ is a convex function if $f''(x) > 0$ and it is a concave function just then if $f''(x) < 0$.

The derivative $f'(x)$ is defined as

$$f'(x) = \lim_{h \to 0} \frac{f(x+h) - f(x)}{h}. \quad (1)$$

Let $(x_1, y_1),..., (x_n, y_n)$ be a set of measures. Suppose that $x_{i+1} - x_i$ are positive very small numbers for $i = 1, ... , n$, where n is a number of experimental points. Then we can substitute

$$f_i' = \frac{f(x_i + 1) - f(x_i)}{x_{i+1} - x_i} \quad (3)$$

for $i = 1, ..., n - 1$ with small errors.

Similarly,

$$f''(x_i) = 2\frac{f_i' - f_{i-1}'}{x_{i+1} - x_{i-1}} \quad (4)$$

for $i = 2, ... , n -1$. Now it is evident that the inflexion points can be found as the points for which

$$f''(x_i) = 0, \quad (5)$$

and

$$f''(x_{i-1}) f''(x_{i+1}) < 0, \quad (6)$$

or the points

$$x_k = (x_{i+1} + x_{i+2})/2, \quad (7)$$

and

$$y_k = (f(x_{i+1}) + f(x_{i+2}))/2 \quad (8)$$

if

$$f''(x_i) f''(x_{i+1}) < 0. \quad (9)$$

Matlab® code

yib

A short but the very efficient computer program, which also includes brief author's comments, was created in the environment of the software package for technical computing, modelling and simulations MATLAB® and it was in relation to the above described algorithm for identifying inflection points of functions given by using experimental data set. The program is considered to be a freeware for any non-commercial use.

```
% Identification of inflection points

% data of the independent variable x
x=-2:0.001:2*pi;

% size of variable x
m=size(x);

% number of data
n=m(1,2);

% data of the dependent variable y
for i=1:n
    y(i)=x(i).*sin(x(i));
end
y;

% subroutine for calculation dy of the first derivative
% of variable y
for i=1:n-1
    dy(i)=(y(i+1)-y(i))./(x(i+1)-x(i));
end
dy;

% subroutine for calculation ddy of the second
% derivative of variable y
for i=1:n-2
    ddy(i)=2.*(dy(i+1)-dy(i))./(x(i+2)-x(i));
end
ddy;

% subroutine for finding of inflection points of the
function given by experimental data x, y
k=1;
for i=2:n-3
ab=ddy(i).*ddy(i+1);
    if ab<0
        xib(k)=(x(i+1)+x(i+2))/2;
        yib(k)=(y(i+1)+y(i+2))/2;
        k=k+1
    end
end
j=1;
for i=2:n-3
    if ddy(i)==0 & (ddy(i+1).*ddy(i-1)<0)
        xibn(j)=x(i+1);
        yibn(j)=y(i+1);
        j=j+1;
    end
end
xib
% subroutine for plotting of data together with
```

```
% inflection points
if (k>1) & (j>1)
    plot(x,y,'m',xib,yib,'dk',xibn,yibn,'dr')
end
if k>1 & j==1
   plot (x,y,'m',xib,yib,'dk')
end
if j>1 & k==1
   plot (x,y,'m',xibn,yibn,'dk')
end
poinb=k+j-2

title('the function with inflection points')
text(xib(1)-1,yib(1)-1,'the first inf.p.=(-1.0765,0.9476)')
text(xib(2)-1,yib(2)-0.5,'the second inf. p.
=(1.0765,0.9476)')
text(xib(3)-1,yib(3)-1,'the third inf. p. =(3.6435,-
1.7529)')
xlabel('data x')
ylabel('data y')
```

Practical use

The possibilities of practical use of described algorithm as well as program code listed in the previous paragraph are demonstrated in finding inflection points of function given by a set of experimental data, which have been obtained by simulating in the working environment of the software package MATLAB®. Discrete variables x_i and y_i are given by the functions

$$x_i = -2*\pi + (i-1)*0.001 \tag{10}$$

and

$$y_i = x_i \sin(x_i), \tag{11}$$

for

$$i = 1,\ldots,8284. \tag{12}$$

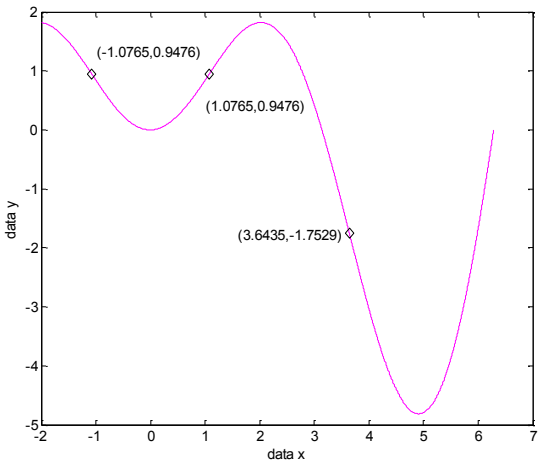

Fig. 3 Experimental function with found inflection points
Obr. 3 Experimentálna funkcia s nájdenými inflexnými bodmi

Experimental function $y = y(x)$ together with found inflection points ib1 = (-1.0765, 0.9476), ib2 = (1.0765, 0.9476) and ib3 = (3.6435, -1.7529) is shown in figure Fig. 3.

Conclusions

An efficient algorithm for identifying inflection points of experimental functions given by a set of discrete data that is based on the substitution of derivable functions describing experimental data representing acceptable analytical approach by approximations was described in this paper. Also a program code that implements the described algorithm in the working environment of the software package MATLAB® is included.

Literature

[1] PASTOREK, M., KRMELA, J., KOVÁČ, K. *Určenie modulu pružnosti osobných plášťov pneumatík.* In: TechMat´12. Pardubice: Univerzita Pardubice, 2012, ISBN 978-80-7395-537-3. p. 83-89

[2] UHERKOVÁ, S., SLALKOVÁ, P., JÓNA, E., KOVÁČ, K., PAVLÍK, V. *Preparation of PVA/SO Blends and Study of their thermo.mechanical Properties.* Polyméry 2012. Bratislava: SAV, 2012, ISBN 978-80-970923-0, p. 54-55

[3] KOPAL, I., BAČÍKOVÁ, M., KOVÁČ, K. *Dynamic mechanical analysis (DMA) of natural rubber/styrene-butadiene rubber (NR/SBR) blends with different content of carbon black & N-isopropyl-N'-phenyl-p-phenylenediamine antidegradant.* Technológ, 2013, vol. 4, ISSN 1337-8996, p. 11-14

[4] KOPAL, I., KOVÁČ, K. *Dynamic mechanical analysis of hardened polyurethane.* Technológ, 2013, vol. 4, ISSN 1337-8996, p. 83-86

[5] KOVÁČ, I. *Vyšetrovanie vybraných fyzikálnych vlastností polymérnych materiálov*: projekt dizertačnej práce. Púchov: FPT TnUAD, 2013, 73 s.

[6] KREVELEN, V., NIJENHUIS, A. *Properties of Polymers.* Elsevier Science, 2009, ISBN 9780080548197, p. 1032

[7] KOMALAN, C. et al. *Dynamic mechanical analysis of binary and ternary polymer blends based on nylon copolymer/EPDM rubber and EPM grafted maleic anhydride compatibilizer.* eXPRESS Polymer Letters, 2007, vol.1, No. 10, ISSN 1788-618X, p. 641-653

[8] MENARD, K. *Dynamic Mechanical Analysis: A Practical Introduction*. 2nd ed., CRC Press, 1999, ISBN-10 1420053124

[9] SEPE, M. *Dynamic Mechanical Analysis for Plastics Engineering*. Plastics Design LIbrar, 1997, ISBN 1-884207-64-2

[10] MANZUR, A., HERNANDEZ-SANCHEZ, F. *Activation Energy for the Glass Transition of a Confined Elastomer in HDPE/PP Blends*. Journal of Macromolecular Sciencew, Part B: Physics, 2006, vol. 45, ISSN 0022-2348, p. 139-152

[11] MATEJIDES, M. *Diferenciálny počet funkcií jednej premennej*. Matcentrum, 2001, ISBN 80-89077-01-3, p. 207

[12] DUBOVSKÁ, R., KVASNICA P., KVASNICA, I. *Perspective of Parallel Simulation in Mechatronic Systems - Metal Cutting*. In: Proceeding 2013 International scientific conference on „MEMS and Mechanics 2013“, 2013, Wuhan, China, In Print

[13] KVASNICA P., KVASNICA, I. *Parallel Modelling of Fault/Tolerant Software Systems*. International Review on Computers and Software (IRECOS), 2012, vol. 7, No. 2, ISSN 1828-6003, p. 621 – 625

[14] POBOCIKOVA I. *Better confidence intervals for a binomial proportion.* Communications : scientific letters of the University of Žilina, 2010, vol. 12, No. 1(2010), ISSN 1335-4205, p. 31-37

hutnictví ve světě

Nové zařízení pro plynulé odlévání bram v Číně

Hebei Puyanng orders slab caster. Metallurgical Plant and Technology, 2013, č. 4, s. 10

Čínská firma Hebei Puyang Iron and Steel objednala u čínské pobočky firmy SMS Siemag Technology dodávku zařízení pro plynulé odlévání bram střední velikosti. Zařízení je určeno pro závod ve Wuan City v provincii Hebei. Závod chce rozšířit svůj sortiment o plechy pro svařované trubky, tlakové nádoby a vysoce pevné lodní plechy. Nové jednoproudé zařízení pro plynulé odlévání je určeno pro bramy o tloušťce 150 až 180 mm při šířce 1000 až 2300 mm. Roční výrobnost je plánována na 1,2 mil. t. Projekt počítá s budoucí úpravou na současné odlévání dvou úzkých bram v jednom krystalizátoru.

L J

Nové kapacity pro válcování za studena v Číně

Benxi to install cold rolling and strip processing lines. Metallurgical Plant and Technology, 2013, č. 4, s. 10 a 12
SMS Siemag to supply record strip width cold rolling lines to Benxi. Iron and Steel Technoloby, August 2013, s. 13
Tangshan places order for cold rolling complex. Metallurgical Plant and Technology, 2013, č. 4, s. 12
Anshan to receive slitting line. Metallurgical Plant and Technology, 2013 č. 4, s. 13.
Behai Chengde to install stainless steel tandem cold mill. Metallurgical Plant and Technology, 2013, č. 4, s. 14

Čínská firma Bengagng Steel Plates (Benxi) objednala u německé firmy SMS Siemag mořicí linku, tandem pro válcování za studena a dvě spojité žíhací linky. Válcovací tandem bude mít pět šestiválcových stolic vybavený kombinovanou technologií CVC/ESS. Budou se válcovat pásy o šířce 1000 až 2150 mm. Jde tedy o rekordní šířku válcovanou za studena. Vstupní tloušťka bude 1,2 až 6 mm, výstupní tloušťka se bude pohybovat v rozmezí 0,3 až 2,5 mm. Jedna žíhací linka bude zpracovávat pásy do šířky 1630 mm, druhá až do šířky až 2150 mm.

Budovaná linka je součástí válcovny za studena č. 3 v severní čínské provincii Liaoning. Vyrábět se budou hlavně plechy pro automobilky včetně vysoce pevných ocelí DP a TRIP. Válcovat se budou i martenzitické oceli. Válcovna bude mít kapacitu 2,3 mil. t/r a měla by začít pracovat v létě 2015.

Další linku vybuduje firma Tangshan Iron and Steel Group v provincii Hebei. Zařízení dodá Siemens Metal Technologies. Hlavní výrobní zařízení bude obsahovat mořicí linku, tandem pro válcování za studena, žíhací linku a pozinkovací linku. Budou se zpracovávat vysoce pevné oceli pro automobilky. Roční výrobnost bude činit 1,6 mil./t. Pozinkovací linku dodává firma Andritz, bude mít výrobnost 415 kt/r. Rovněž dodá žíhací linku s kapacitou 770 kt/r. Budou se zde vyrábět pásy o tloušťce 0,2 až 2,5 mm při šířce 700 až 1600 mm. Výroba má být zahájena na počátku r. 2015.

Firma Anshan Iron and Steel Group objednala u firmy Siemens Metals Technologies linku pro podélné dělení pásů válcovaných za studena. Maximální šířka dělených pásů bude 1850 mm, tloušťka od 0,3 do 2 mm při pevnosti až 800 MPa. Maximální počet pásků, které lze získat dělením z jednoho širokého pásu, je 30. Linka je vybavena zařízením vyvozujícím zpětný tah. Měla by jít do provozu ve 2. kvartále r. 2014.

Firma Beihai Chengde Stainless Steel objednala u firmy Siemens Metal Technologies na dodávku pětistolicového tandemu typu Power X-HI a laserového svařovacího zařízení pro svůj závod v provincii Guangxi. Trať bude mít roční výkon 600 kt pásů z nerezavějící oceli řady 200 a 300 podle ASTM. Vstupním polotovarem budou žíhané a mořené pásy o tloušťce 1,0 až 5,0 mm a šířce 800 až 1300 mm. Budou se válcovat rychlostí 400 m/min na výstupní tloušťku 0,3 až 3,0 mm. Tandem bude vybaven letmou výměnou válců, při níž není nutné přerušovat pracovní proces. Trať by měla jít do provozu v polovině roku 2014.

L J

Širokopásová válcovna hliníku v Číně

Nanshan Aluminium to build wide plate mill. Metallurgical Plant and Technology, 2013, č. 4, s. 13

Válcovnu hliníkových pásů buduje čínská firma Nanshan. Hlavním dodavatelem technologického zařízení je firma SMS Siemag, která dodává mechanickou část vyrobenou převážně v Německu, a firma ABB, která dodává elektrickou část a automatizovaný systém řízení. Na trati se budou válcovat pásy široké až 2650 mm. Trať by měla jít do provozu koncem roku 2014.

L J

Profil a uplatnenie absolventov jednotlivých študijných programov na FPT TnU AD v Púchove:

POČÍTAČOVÁ PODPORA MATERIÁLOVÉHO INŽINIERSTVA (bakalársky študijný program)

Absolventi nájdu uplatnenie v priemyselných podnikoch v oblasti výroby technických materiálov, ich technologického spracovania na polotovary a výrobky, ako aj v oblasti kontroly ich kvality, nákupu a predaja materiálov. Môžu sa uplatniť tiež na miestach odborných pracovníkov v konštrukčných kanceláriách. Sú schopní pracovať ako členovia vývojových tímov, samostatne riešiť technické problémy a vedia udržiavať kontakt s neustálym technickým vývojom v oblasti technických materiálov. Ich znalosti z manažérskych a ekonomických predmetov ich predurčujú aj na vedenie menších špecializovaných operatívnych technických tímov, kde sa vyžaduje samostatné a operatívne rozhodovanie. Sú pripravení pokračovať vo vlastnom profesionálnom raste.

MATERIÁLOVÉ INŽINIERSTVO (bakalársky študijný program)

Absolventi bakalárskeho štúdia majú základné vedomosti z oblasti výroby, technologického spracovania degradácie a experimentálneho hodnotenia vlastností rôznych druhov technických materiálov. Získajú základné vedomosti o chemickom zložení a štruktúre v technickej praxi používaných kovových, nekovových a moderných kompozitných materiálov. Dokážu hodnotiť vlastnosti technických materiálov a materiálových technológií z environmentálneho hľadiska. Získajú schopnosti a zručnosti v testovaní mechanických vlastností materiálov, vedia pracovať so skúšobnými zariadeniami, dokážu hodnotiť štruktúru materiálov, získajú tiež základné vedomosti z výpočtového modelovania a simulácie zaťaženia materiálov a ich optimálneho návrhu z pohľadu prevádzkového zaťaženia. Absolventi daného študijného programu získajú tiež základné vedomosti z oblasti skúmania vplyvov technologických procesov výroby materiálov na zložky životného prostredia, s dôrazom na procesy vývoja nových progresívnych technológií a materiálov, recyklačných a remediačných technológií hlavných druhov priemyselných odpadov a zavádzanie málo- a bezodpadových technológií do praxe. Sú pripravení najmä na pôsobenie v priemyselnom podniku v oblasti výroby technických materiálov, ich technologického spracovania na polotovary a výrobky, ako aj v oblasti kontroly ich kvality, nákupu a predaja materiálov. Sú schopní riadiť chod technologických výrobných celkov a zariadení, vrátane ekologických, navrhovať technológie na ochranu ovzdušia, vody a pôdy a posudzovať vplyv odpadov na životné prostredie.

MATERIÁLOVÁ TECHNOLÓGIA (bakalársky študijný program)

Absolventi sú pripravení najmä na pôsobenie v priemyselnom podniku v oblasti výroby technických materiálov, ich technologického spracovania na polotovary a výrobky, ako aj v oblasti kontroly ich kvality, nákupu a predaja materiálov, servisu a údržby. Získajú schopnosti a zručnosti v zisťovaní mechanických vlastností materiálov, vedia pracovať so skúšobnými zariadeniami, vedia hodnotiť štruktúru materiálov. Sú schopní pracovať ako členovia vývojových tímov, samostatne riešiť technické problémy a vedia udržiavať kontakt s neustálym technickým vývojom v oblasti technických materiálov. Sú pripravení pokračovať vo vlastnom profesionálnom raste.

TEXTILNÁ TECHNOLÓGIA A NÁVRHÁRSTVO (bakalársky študijný program)

Absolventi získajú vedomosti z priemyselných, gumárenských, textilných a sklárskych technológií v spojitosti s návrhom dizajnu finálneho výrobku. Nájdu uplatnenie vo všetkých sférach textilného a priemyselného dizajnu, ako i v oblasti základných technológií, návrhárstva, vývoja a výskumu.

MATERIÁLOVÉ INŽINIERSTVO (inžiniersky študijný program)

Absolventi inžinierskeho štúdia nájdu uplatnenie vo výskume a vývoji v oblasti materiálového inžinierstva, priemyselného inžinierstva, aplikácie experimentálnych metód štúdia štruktúry a vlastností materiálov. V základnom výskume pri vývoji nových materiálov, výskume fyzikálnych vlastností materiálov a vývoji nových diagnostických metód, inovačných procesoch, riešení trvalo udržateľných technológií s minimálnou spotrebou surovín, energie a bezodpadových procesov (komplexné spracovávanie vstupných surovín a materiálov). Vo výrobnom procese ako technológ výroby alebo riadiaci pracovník, pri navrhovaní a riadení environmentálne akceptovateľných priemyselných technologických procesov, techniky prostredia, environmentálnych materiálov, spotrebných výrobkov a technických služieb. V riadiacej sfére v oblasti riešenia problémov pri výrobe, spracovaní, zabezpečovaní kvality, využitia a recyklácie materiálov, dokážu viesť tímy pracovníkov pri zabezpečovaní ekonomickej prosperity podniku. Vo verejnej správe v oblasti odborov životného prostredia a trvalo udržateľného rozvoja regiónov, miest a obcí, ako špecialisti na odborných útvaroch. V podnikateľskej sfére vo všetkých oblastiach výrobno-technologických procesov, riadiacich procesov a procesov zabezpečujúcich ekonomický rozvoj firmy a jej prosperitu.

MATERIÁLY (doktorandský študijný program)

Cieľom vzdelávania v treťom stupni štúdia je výchova odborníkov s hlbokými vedomosťami z oblastí fyzikálnych a chemických vlastností materiálov, ich diagnostiky a počítačovej simulácie ich fyzikálnych vlastností. Absolvent doktorandského štúdia vie samostatne riešiť problémy z oblastí širokého spektra konštrukčných materiálov a na základe hlbokých teoretických vedomostí a praktických zručností predikovať ich úžitkové vlastnosti. Je pripravený samostatne pracovať vo vedeckom tíme a po zapracovaní tiež riadiť prácu riešiteľského kolektívu. Jeho uplatnenie bude vo výskumných ústavoch, na vysokých školách, ako aj vo vrcholových riadiacich funkciách podnikov s orientáciou na kovové a nekovové materiály, tenké vrstvy, diagnostiku a skúšobníctvo.